Introduction to Meteorology

Richard Bernatz
Luther College

April 20, 2026

Contents

List of Figures

List of Tables

Introduction/Prologue

> "Never, no matter what progress of science, will honest scientific men (women) who have regard for their professional reputations venture to predict the weather."
>
> –Dominique Francois Arago

0.1 Units

Units used throughout this text will be the **International System of Units** or SI (French - Système International). Table 1 lists these units.

Table 1 includes some "derived" SI measures for force and energy.

- The newton (N), as a unit of force, is defined as mass times acceleration. With mass given in kg and acceleration as meters per second squared, one N = kg ·meter ·s^{-2}.
- Pressure is defined as force per unit area. Therefore, pressure has SI units of N ·m^{-2} = kg ·meter ·s^{-2} ·m^{-2} = kg ·m^{-1} ·s^{-2}, and is known as a Pascal (Pa).

Symbol	Name	Quantity
m	meter	length
kg	kilogram	mass
K	kelvin	temperature
s	second	time
N	newton	force
Pa	pascal	pressure
J	joule	energy
A	ampere	electrical current

Table 1: International System of Units and derived measures.

- The joule (J), as a unit of energy, is defined as force times distance, or a newton ·meter = kg $\cdot m^2$ $\cdot s^{-2}$

Chapter 1

Atmospheric Composition & Variables

1.1 Overview

This chapter provides an introduction to the Earth's atmosphere by describing its constituents and introducing some of the principle (or primitive) variables that determine the state of the atmosphere as a function of time and space. The atmosphere is one of several components, or "sub-systems," that make up what some environmental scientists call the **Earth System**. It comprises the area, and all of its constituents, from the surface of the Earth "upwards" to an elevation of about 10,000 meters. (Why this elevation will be explained later in this chapter.) The sub-systems are segregated in order to study the structure and workings of the individual component in a somewhat more simplistic way. However, the systems are very much interdependent as they exchange mass and energy and influences across the "boundaries" that separate them. Other components include the **biosphere** (plant and animal life), the **hydrosphere** (the combined mass of water contained in the oceans, lakes, rivers atmosphere and soil), the **cryosphere** (the frozen water makeup of the Earth's surface), the **pedosphere** (the outermost layer of the Earth, essentially the soil). The chapter begins by providing a brief evolutionary history of the Earth's atmosphere.

1.2 Evolving Earth Atmosphere

The history of the slowly changing makeup and characteristics of the Earth's atmosphere is typically separated into three general periods distinguished by actions, either external or internal, that bring about atmospheric composition changes that differentiate the periods. A simplified evolutionary time line for the Earth's atmosphere is depicted in Figure 1.1. Important evolutionary mechanisms and distinctive periods are briefly explained in this

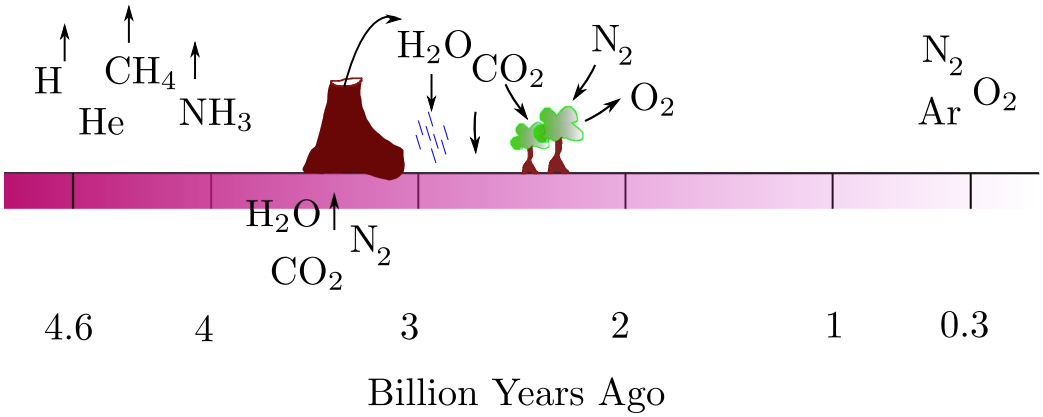

Figure 1.1: Atmosphere evolutionary time line.

section.

1.2.1 Initial Period

The initial period begins about 4.6 billion years ago. The most abundant gases in the universe, atomic hydrogen (H) and helium (He), were the primary atmospheric constituents of this period. Other gases include methane (CH_4) and ammonia (NH_3) molecules. The mass of atoms and molecules (combinations of atoms) is determined, roughly, by the number of protons and neutrons they have. Hydrogen and helium are, respectively, the first and second lightest atoms in the universe. The carbon (C) and nitrogen (N) atoms that combine with hydrogen to form methane and ammonia are sixth and seventh lightest atoms, respectively. Consequently, all four primary constituents of the "first" atmosphere were light and had sufficient energy relative to mass to escape from the Earth's warm surface and atmosphere.

1.2.2 Out-Gassing

The Earth's surface cooled as it aged and the cooling lead to the process known as **out-gassing** where volcanoes spewed massive amounts of subsurface gas into the evolving atmosphere. The gases consisted mostly of water vapor (H_2O), carbon dioxide (CO_2) and diatomic nitrogen (N_2). The percentage makeup of the out-gassing was, approximately, 80%, 10% and 3%, respectively. The cooling surface and atmosphere caused almost all of the water vapor to rain out to form the oceans. A good portion of the carbon dioxide dissolved in the oceans and eventually formed the sedimentary rocks. Unlike water vapor and carbon dioxide, nitrogen had no significant removal mechanism in the evolving atmosphere so the atmospheric nitrogen mass remained relatively unchanged.

1.2.3 Photosynthesis

Plant life developed approximately 2 to 3 billion years ago. Growing plants use carbon dioxide, water and energy from the sun in a plant-building process known as **photosynthesis**.

$$6CO_2 + 12H_2O \underset{\text{plant enzymes}}{\overset{\text{energy}}{\rightarrow}} C_6H_{12}O_6 + 6O_2 + 6H_2O$$

Photosynthetic process by-products include glucose ($C_6H_{12}O_6$) for the plants and diatomic oxygen (O_2) released to the air. The significant scale of the photosynthetic process signaled the beginning of another period in the history of the Earth's atmosphere.

1.2.4 Current Atmosphere

Scientific evidence suggests the Earth's current atmosphere dates back about 300 million (0.3 billion) years. The present atmospheric state is much older than the history of humans on the Earth. Recent archaeological digs east of Tel Aviv, Israel provide evidence that humans inhabited the region as much as 400,000 years ago.

1.3 Atmospheric Parcels

In order to talk more specifically about the composition and characteristics of the atmosphere, we need to introduce the extremely useful concept of an **atmospheric parcel**. Our current atmosphere is comprised of individual atoms, molecules, and other constituents that have their own identity and significant independent motion defined by their speed and direction. Yet, there are many instances where a conglomeration of atmospheric constituents "stay together" to form a macro identity for extended periods of time.

An analogy of a parcel would be a group of people walking through a crowded region. Each individual in the group has their own identity and may be walking at slightly different speed or direction than others in the group. However, on the whole, the group has an average speed and a common direction (or agreed upon destination). An observer is able to identify the group and assign specific characteristics to the amalgam.

These notions are depicted in Figure 1.2. The longer black vectors[1] shown in the figure represent the parcel's motion (magnitude and direction) which is the average motion of the parcel's constituents.

The closed curve in Figure 1.2 represents the invisible "boundary" of an air parcel. In reality, the parcel is a three-dimensional object that occupies a defined volume. In this two-dimensional depiction, the boundary of the parcel differentiates atmospheric constituents inside the parcel from those that are outside. Notice that the boundary shape and the space

[1] Vectors associated with motion may be thought of as an *arrow* that points in the direction of the motion and whose length represents the magnitude of the speed (a non-negative value).

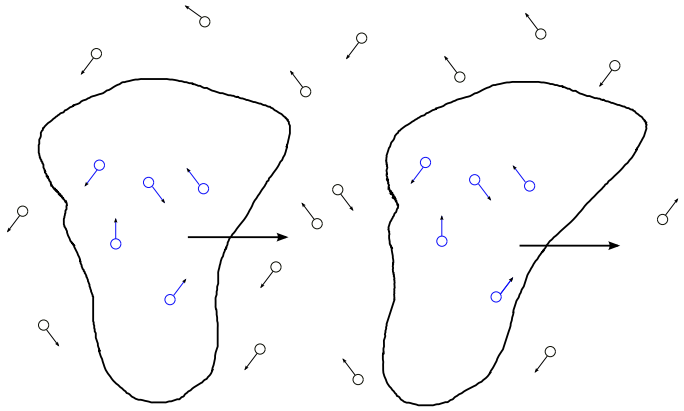

Figure 1.2: Atmosphere parcel made up of individual atoms and molecules.

within the boundary may change as time goes by. However, the makeup of the parcel does not change. That is, the **mass** of the parcel is constant over time.

Parcels have various sizes. However, the magnitude of a parcel's physical dimension (length, or width, or height, for example) is longer than the mean free path length[2] of any parcel constituent. For example, the mean free path length of a typical parcel molecule at standard atmospheric pressure is 68 nanometers (68×10^{-9} meters), which is short relative to the length it must traverse to leave the parcel.

Another way to think of an air parcel is that it must be big enough to contain a very large number of constituents (atoms, molecules, etc.), but small enough so that parcel properties, such as temperature and pressure, are uniform throughout the parcel.

1.3.1 Permanent Constituents

The makeup of the atmosphere is described using an arbitrary atmospheric parcel as a basis. A portion of its total volume is occupied by each of the parcel's constituents. A **permanent constituent** is one whose portion of the parcel does not change over time (from one day or year to the next) nor space (its portion in the atmosphere over Decorah is the same as that over Beijing, for example.) The arbitrary nature of the parcel implies that the portion is the same for every atmospheric parcel regardless of its size, location or time. Table 1.1 lists the six permanent gases with the largest portions.

Nitrogen and oxygen are the two most abundant gases in our atmosphere. Any other permanent constituent occupies less than 1 percent of the volume of any atmospheric parcel. The **atomic mass unit** (AMU) of a atom or molecule is the sum of the protons and neutrons

[2]The distance an atom or molecule will travel between collisions with other particles in the parcel.

Gas	Symbol	AMU*	Volume Percentage
Nitrogen	N_2	28	78.08
Oxygen	O_2	32	20.95
Argon	Ar	40	0.93
Neon	Ne	10	0.0018
Helium	He_2	4	0.0005
Hydrogen	H_2	2	0.00006
Xenon	Xe	131	0.000009

Table 1.1: The permanent gases in the Earth's atmosphere. The permanent gases in the Earth's atmosphere. * - AMU stands for the **atomic mass unit** of the gas. It is the sum of the protons and neutrons of the atom or molecule.

within the atom or molecule. The AMU of an air parcel is

$$\text{AMU} \approx 0.7808 \times 28 + 0.2095 \times 32 + 0.0093 \times 40 = 28.9$$

slightly greater than that of nitrogen due to the greater AMU of oxygen and argon. The percentage of the air parcel's total mass due to oxygen is greater than 20.95% because of its larger AMU. However, for percentages based on volume and mass are "close enough" to regard them as the same. Therefore, a 10 kilogram air parcel contains approximately $10 \times 0.7808 = 7.808$ kilograms of nitrogen, $10 \times 0.2095 = 2.095$ kilograms of oxygen and $10 \times 0.0093 = 0.093$ kilograms of argon.

1.3.2 Variable Constituents

Variable constituents are those whose portions may be different from one atmospheric parcel to the next, or whose portion may change over time within a given parcel. The primary variable constituents are shown in Table 1.2.

Except for water vapor, the variable constituents represent extremely small volume portions of an atmospheric parcel. Their portion are so small, in fact, that they are often measured in parts per million (PPM). That is, if 1 million air parcel constituents are randomly collected, 385 would be carbon dioxide. Ironically, some small-portion constituents play over-sized roles in their effect on daily weather (water vapor) and climate (water vapor, carbon dioxide and methane).

Arguably, water vapor is the most important variable constituent in our atmosphere. There would be no agriculture as we know it without water vapor being transported by atmospheric winds from ocean sources. Water is the only substance that can exist in all three phases (gas, liquid and solid) in our atmosphere. The lack of water vapor results

Constituent	Symbol	AMU*	Volume Percentage	PPM**
Water Vapor	H_2O	18	0 - 4	0 - 40,000
Carbon Dioxide	CO_2	32	0.0385	385
Methane	CH_4	16	0.00017	1.7
Nitrous Oxide	N_2O	44	0.00003	0.3
Ozone	O_3	48	0.000004	0.04
Particles			0.000001	0.01 - 0.15
CFCs			0.00000002	0.0002

Table 1.2: Variable atmospheric constituents. Variable atmospheric constituents. * - AMU = atomic mass unit. ** - PPM = parts per million.

in dry spells and drought. Significant water vapor results in higher relative humidities (increased heat index) and the potential of flooding downpours. Increases in atmospheric concentrations of H_2O, CO_2 and CH_4 concentrations result in an increase in surface average temperature through the enhanced greenhouse effect. For this reason they are referred to as **greenhouse gases**.

The variable nature of a constituent implies that individual constituents do not remain in the atmosphere forever. Each of the greenhouse gases have means by which they enter and leave the atmosphere. Entering and leaving the atmosphere results in a molecule completing a "cycle." The length of stay is the **residency** of the molecule. Residency lengths are typically different for different molecules, even of the same type of molecule. However, each greenhouse gas type has an average atmospheric residency. Water vapor is the shortest with an average of seven days. Next is methane with an average residency of approximately 20 years, followed by carbon dioxide with a 100-year average residency. Although carbon dioxide has received more attention as a greenhouse gas, the warming effect of methane (CH_4) is 86 times more than carbon dioxide over a common time interval[3]. Of course, this is countered by carbon dioxide's much greater atmospheric concentration and residency.

Ozone (O_3) plays a very important role of absorbing high-energy ultraviolet solar energy in the atmospheric region known as the **stratosphere** and a process know as **photodissociation**. The reaction equation is

$$O_3 + h\nu \rightarrow O_2 + O$$

where the term $h\nu$ represents the energy input from solar radiation. Human exposure to this energy is linked to increases in skin cancers. However, ozone concentrations in lower regions of our atmosphere can also have negative influences on human health. Heavy populated, poorly-ventilated regions of the Earth may have increased frequency and severity

[3]Intergovernmental Panel on Climate Change

of smog due, in part, to an ozone concentration increase. Ozone is formed when nitrogen oxides (NO_x)[4], volatile organic compounds (VOCs) and carbon monoxide (CO) react in the presence of sunlight. These precursor chemicals to ozone creation are by-products of automobile and industrial exhaust as well as some chemical solvents.

The significance of particulate matter in the atmosphere cannot be overlooked. Quite simply, there would be no precipitation if not for the presence of particles, or **aerosols**, in our atmosphere. Aerosols are tiny solid or liquid particles that are suspended in the atmosphere. Natural sources include dust, sea salt, smoke from forest fires and volcanic ash. Anthropogenic sources include automobile exhaust (NO_2 - nitrogen dioxide) and the burning of sulfur-containing fuels (SO_2 - sulfur dioxide). Precipitation begins with the formation of cloud droplets on condensation nuclei know as Aitken[5] particles. These particles, with radii less than 0.2 micrometers (μm) can number as many as 10,000 per cubic centimeter (cm^3) of atmospheric air. Aerosols larger than Aitken particles (radii between 0.2 and 1.0 μm) can number as many as 1,000 per cm^3 of air. Giant nuclei, with radii greater than 1.0 μm, can number as many as 10 per cm^3.

Chlorofluorocarbons (CFCs) are included (even though their atmospheric concentration is extremely small) because they are part of an important chapter in our atmospheric environmental history. As their name suggests, CFCs are derived from carbon, chlorine and fluorine. They were commonly used as a refrigerant under the brand name of Freon manufactured by the DuPont corporation. They were scientifically linked to the depletion of stratospheric ozone. Their manufacture has been phased out under the Montreal Protocol of 1987. Use of ozone-depleting CFCs has been banned since 1989. Stratospheric ozone levels soon stabilized in the 1990s and have begun to recover in the 2000s. Levels are projected to return to pre-1980 levels by 2075. This case is an example of how scientifically based, and internationally agreed upon policy, can lead to what appears to be a successful environmental outcome.

1.4 Atmospheric Variables

The concept of an atmospheric parcel supplies the means for defining important primary, or primitive, atmospheric variables. Through the course of the text, we will be defining other variables, some of which will be primary and others will be derived or defined using the primary variables. We begin with the most significant (perhaps) primary variable, temperature.

[4]The subscript x is used to indicate the number of oxygen atoms are in the various form of nitrogen oxides.

[5]John Aitken (1839 - 1919) was a Scottish meteorologist and one of the founders and leading researchers in the area of cloud physics.

1.4.1 Temperature - T

An atmospheric parcel is a finite conglomeration of many constituents. Molecules within the parcel move with varying speeds. Let $\bar{v}$ represent the average speed of the parcels molecules. Energy takes on many forms, and the one associated with motion is know as **kinetic** energy. The (thermodynamic) temperature T of the parcel is given by the following formula

$$T = \alpha \cdot m_W \cdot \bar{v}^2 \tag{1.1}$$

where the average speed $\bar{v}$ is given in units of m·sec^{-1}, m_W is the molecular mass (AMU) of the air parcels ($m_W = 28.9$) and α is a constant of proportionality equal to 4.0×10^{-5} K sec^2 m^{-2}. The resulting temperature has units of **Kelvin (K)**, the **absolute temperature** scale. The Kelvin temperature of the parcel is greater than or equal to zero (never negative). Its lowest possible value of zero results when the average speed its molecules is zero. Speed (the magnitude of velocity) is never negative, so an average speed of zero means *every* atom and molecule of the parcel is motionless.

Example 1.4.1. Calculate the temperature of an air parcel whose molecules have an average speed of 100 m·s^{-1}.

Solution: Simply use the formula as given in Equation (1.1)

$$T = \alpha \cdot m_W \cdot \bar{v}^2 = 4.0 \times 10^{-5} \times 28.9 \times 100^2 = 11.56\text{K}$$

Temperature Scales

An unfortunate aspect of atmospheric science is the use of multiple temperature scales. The Kelvin scale, as we saw above, is associated with the definition of a parcel's thermodynamic temperature. The **Celsius** scale simply moves the Kelvin zero to the location of -273. Therefore, C = K - 273, and K = C + 273. As we shall see later in the course, atmospheric observations recorded at elevations above ground level are typically recorded in either K or C scales. Surface temperature observations made in the United States are recorded in the **Fahrenheit** scale F. The conversions between C and F are: F = $\frac{9}{5}$C + 32 and C = $\frac{5}{9}$(F - 32). The conversions between K and F are: F = $\frac{9}{5}$(K - 273) + 32 and K = $\frac{5}{9}$(F - 32) + 273

Example 1.4.2. The global annual average surface temperature for the Earth is approximately 15 C. Determine the average speed of the molecules in an air parcel having this average temperature.

Solution:

First, convert the temperature to K, T = 273 + 15 = 288 K. Next, use the equation $T = \alpha m_W v^2$ and solve for speed v:

$$v^2 = \frac{T}{\alpha m_W} \Rightarrow v = \sqrt{\frac{T}{\alpha m_W}} = \sqrt{\frac{288}{4.0 \times 10^{-5} \cdot 28.9}} = 499.1 \text{ m/sec}$$

Temperature versus Elevation

The Earth's atmosphere is, for the most part, warmed from the surface of the Earth (This will be explained in detail in Chapter 2.) Consequently, atmospheric temperature, on average, decreases with increasing altitude. The rate of decrease is know as the atmospheric **lapse rate**. The average lapse rate, where the average is calculated for the entire atmosphere "around the globe" over an annual time interval (365 days), is approximately $\frac{6.5}{1000}$ C/m. Note that a minus sign is not used because it is a *lapse* (falling or decreasing) rate. The rate, or slope, can be used in a linear formula to express the temperature T as a function of elevation z, as shown in Equation 1.2

$$\begin{aligned} \frac{T(z) - T_0}{z - z_0} &= \frac{\Delta T}{\Delta z} \\ \Rightarrow T(z) &= T_0 + \left(\frac{\Delta T}{\Delta z}\right)(z - z_0) \\ \Rightarrow T(z) &= T_0 - \frac{6.5}{1000}(z - z_0) \end{aligned} \tag{1.2}$$

where T_0 and z_0 are the starting initial temperature and height, respectively, and the average lapse rate is used.

It must be emphasized that the rate used so far is an average rate. Typically, the lapse rate changes from one segment of the atmosphere to another, or over time for the same segment of the atmosphere. In fact, there are common instances where the atmospheric temperature *increases* with increasing elevation. Such situations are know as temperature **inversions**.

Example 1.4.3. Suppose the surface temperature is 25 C, and the lapse rate within the first 2000 m is 5 °C/1000 m, while the lapse rate in the interval between 2000 m and 5000 m is 4 °C/1000 m. Determine the temperature at (a)

1000 m and (b) 4000 m.

Solution:

(a) $T(1000) = 25 - \frac{5}{1000} \times 1000 = 20$ C

(b) $T(4000) = 25 - \underbrace{\frac{5}{1000} \times 2000}_{\text{step 1 drop}} - \underbrace{\frac{4}{1000} \times 2000}_{\text{step 2 drop}} = 25 - 10 - 8 = 7$ C

In part (b) of Example 1.4.3, the total change in temperature is calculated using to separate steps because the lapse rate changes as the change in altitude goes from the surface to the 4000 m level.

The average lapse rate remains relatively constant through the first 10,000 meters of the atmosphere. Near an elevation of approximately 10,000 m, the temperature does not appreciably change with height, thus demarcating the atmospheric layer know as the **stratosphere** as shown in Figure 1.3. The atmospheric layer starting at the surface of the Earth and extending upwards to the stratosphere is known as the **troposphere**. It is within the troposphere where weather "happens." This atmosphere layer will be the focus of this course. Other atmospheric layers include the mesosphere and the thermosphere where the temperature decreases and increases with altitude, respectively.

Well-Mixed Atmosphere

Example 1.4.2 indicates how fast molecules are moving within a parcel of air near the surface of the Earth. The atmospheric temperature profile shown in Figure 1.3 indicates a parcel at the "top" of the troposphere has an approximate temperature of -50 C. This translates to an average molecular speed of approximately 439 m/sec. Molecular speeds of theses magnitudes through the depth of the troposphere means the atmosphere is **well-mixed**. That is, the atmosphere is not stratified with the heavier (greater AMU) molecules near the bottom and lighter near the top. Consequently, any atmospheric parcel anywhere at any time has the same proportional makeup for permanent gases as outline in Table 1.1.

1.4.2 Density - ρ

The density of a parcel of air, represented by the Greek symbol ρ (rho), is the quotient of its mass and volume. The mass of an object is a measure of the amount of substance is contains. Basic units of mass are the kilogram (kg) and gram (gm), where 1 kg = 1000 gm. The volume of the object measures how much three-dimensional space the object occupies.

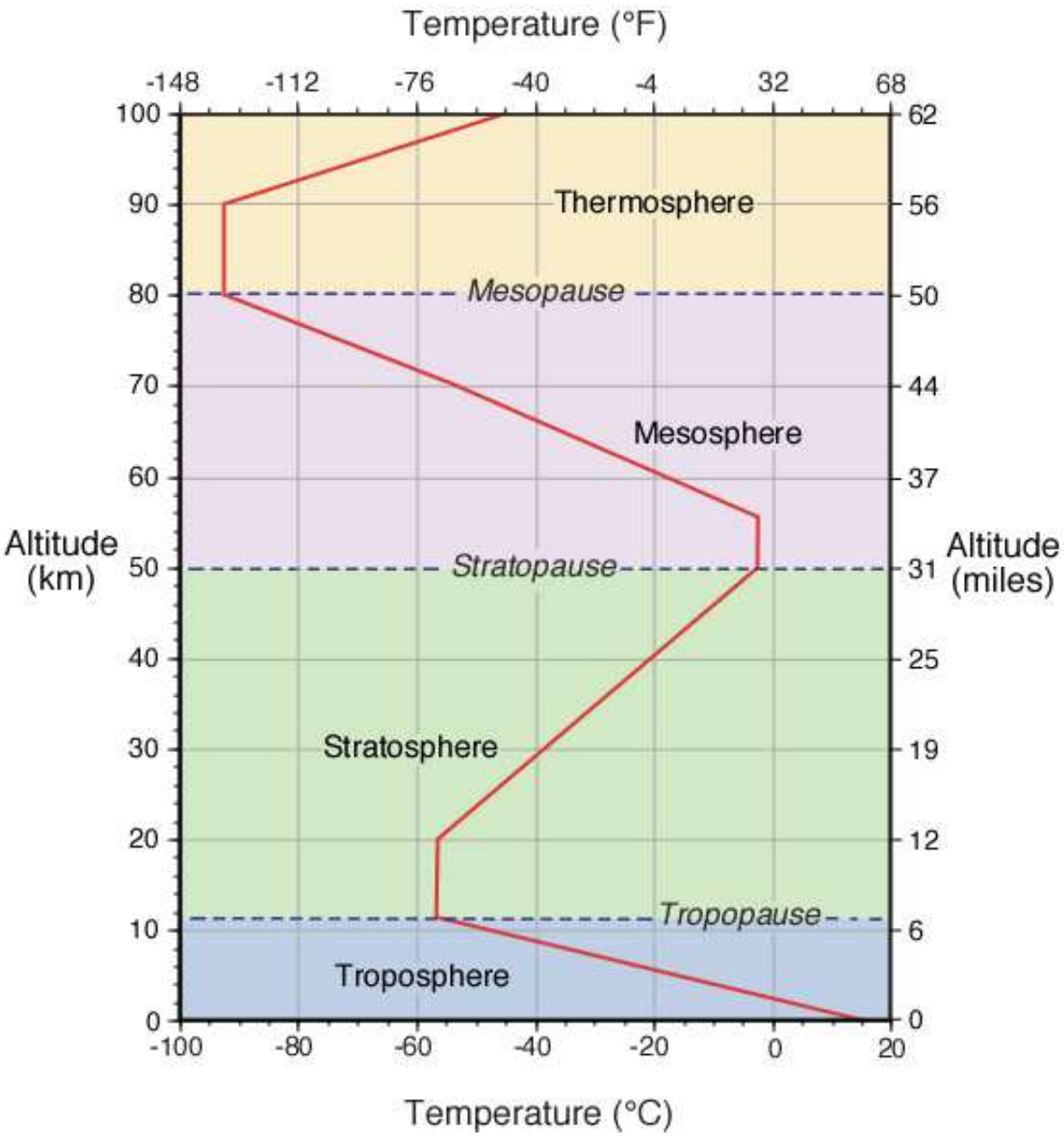

Figure 1.3: Atmospheric temperature as a function of altitude.

The basic units of volume are a cubic meter (m^3) and a liter (L), where 1 m^3 = 1000 L. The average density of an air parcel at the surface of the Earth is 1.22 kg / m^3. This equivalent to 1.22 gm / L because

$$1.22 \text{ kg/m}^3 = 1.22 \times 1000 \text{ gm}/(1000 \text{ L}) \text{ cm}^3 = 1.22 \text{ gm / L}$$

Parcel density decreases exponentially with height. The formula for ρ at elevation z is

$$\rho(z) = \rho_s e^{-z/8000} \tag{1.3}$$

where ρ_s is the surface density and elevation z is measured in meters. The formula is derived by using the Ideal Gas Law (see Section 1.5), applied to the makeup of a typical atmospheric parcel, and assuming a balance between the forces of atmospheric pressure (upwards) and gravity (downwards). This balance of forces is explained in Section 4.4.4.

Example 1.4.4. Determine the mass of oxygen in a two-liter parcel of air at an elevation of 2000 m. Assume a standard atmosphere with a surface density of 1.22 g/L.

Solution:
Determine the mass, in grams, of a one-liter parcel by determining its density at an elevation of 2000 m: $\rho(2000) = 1.22e^{-2000/8000} = 0.95$ g/L. The percentage of mass for oxygen is similar to the percentage of volume of oxygen for a random parcel. Therefore 21% of the mass is oxygen (assuming, correctly, a well-mixed atmosphere), so in the case of a two-liter parcel we have $2 \times 0.21 \times 0.95 =$ $\boxed{0.399\text{g of oxygen}}$.

1.4.3 Pressure - P

Something that causes a change in the motion of an object is considered to be a **force** by scientists. The an object's motion is defined by its direction and speed. The acceleration of an object is the time rate of change of its motion, the magnitude has units of speed divided by time. In the SI system, speed has units of m/s, so acceleration has units of $\frac{\text{m/s}}{\text{s}} = \text{m} \cdot \text{s}^{-2}$. The SI unit of mass is kilogram (kg), so force has units of kg $\cdot$ m $\cdot$ s^{-2} or Newtons (N) in the SI system.

Pressure is defined as force per area. In terms of atmospheric pressure, the force is that due to gravity. The magnitude of the gravitational force F_g on an object of mass m (measured in kg) is given by the formula

$$F_g = m \times g$$

where g is the acceleration due to gravity with magnitude of 9.8 $\text{m}\cdot\text{s}^{-2}$.

One measure of pressure is the **Pascal** (Pa), equivalent to one Newton per square meter $\text{N}\cdot\text{m}^{-2}$. The **bar** is another measure of pressure with 1 bar = 100,000 Pa. The millibar (mb) is one-thousands of a bar, making it equivalent to 100 Pa, or one hectopascal (hPa). One hPa = 0.1 kilopascal (kPa).

The global and time-averaged surface pressure is 1013 mb = 1013 hPa = 101.3 kPa. The atmospheric pressure a parcel "senses" can be thought of as a measure of the weight (weight = mass × acceleration = force) of the air "above" the parcel.

Figure 1.4 depicts an atmospheric column situated above a one-meter square area. An area of one square meter at the surface of the Earth has an average pressure of 1013 mb, the equivalent of 1013 × 100 = 101,300 Pa. The mass in the air column above the one square meter area is determined by dividing the number of Pascals by the acceleration of gravity in the SI system. Specifically,

$$\text{mass} = 101,300/9.8 \approx 10,337 \text{ kg}$$

Is there a difference between the pressure *on* the parcel and the pressure *of* the parcel? In a word, "no." As we saw above, the pressure on a parcel can be understood to be the weight (force) of the mass of air in the column above the parcel. A force, like motion, is a vector so it has both a direction of action and magnitude. The direction of the force of the air in the column is downward, towards the surface of the Earth.

Suppose an arbitrary parcel is in the column and above the surface of the Earth. If pressure were the only force (action) acting on the parcel, it would be pushed to the surface of the Earth. However, as this and more parcels are pushed towards the surface of the Earth, a resulting upwards pressure develops. This pressure increases until it is equal in magnitude (opposite in direction) to the weight of the column of air above the parcel. That is, the pressure "inside" the parcel increases until it balances the "outside" pressure. Consequently, the pressure of the parcel (inside) is equal to the pressure on (outside) the parcel.

Not surprisingly, pressure decreases exponentially with altitude in the same way as density. That is,

$$P(z) = P_s e^{-z/8000} \tag{1.4}$$

where P_s is the surface pressure and elevation z is measured in meters. The functional relationship between pressure P and altitude z can be inverted using the natural log function,

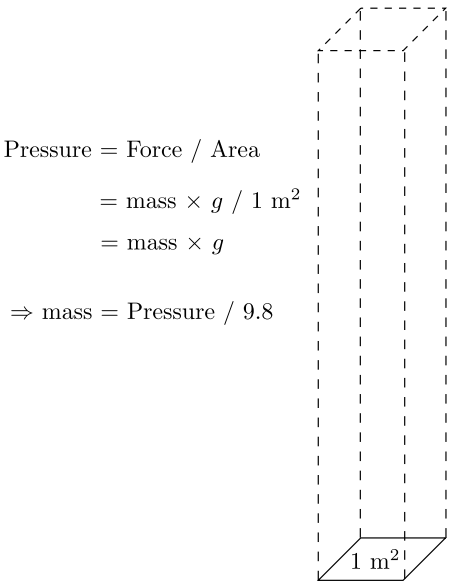

Figure 1.4: Pressure related to the mass of the column of air above.

the inverse function of the natural exponential function. Example 1.4.5 demonstrates this process.

Example 1.4.5. Suppose the surface pressure is $P_s = 1000$ mb. Determine the elevation at which the pressure is 500 mb.

Solution:
Begin with the formula for pressure P as a function of elevation z: $P(z) = P_s e^{-z/8000}$. In this example we are solving for elevation z. Therefore $500 = 1000e^{-z/8000}$ which means $e^{-z/8000} = 0.5$. Take the natural log (ln() of both sides of the equation to get $-z/8000 = \ln 0.5$, so that $z = -8000 \times -0.6931 = \boxed{5545 \text{ m.}}$

The result of Example 1.4.5 is important because it identifies the average elevation at which half of the air mass in a column is below the elevation, and the other half is above. That is, it is the atmospheric mass midpoint in the vertical direction. The next example shows how one may determine the mass in a column of air between two different pressure levels.

A plot of pressure (in kPa) as a function of altitude (in m) is shown in Figure 1.5.

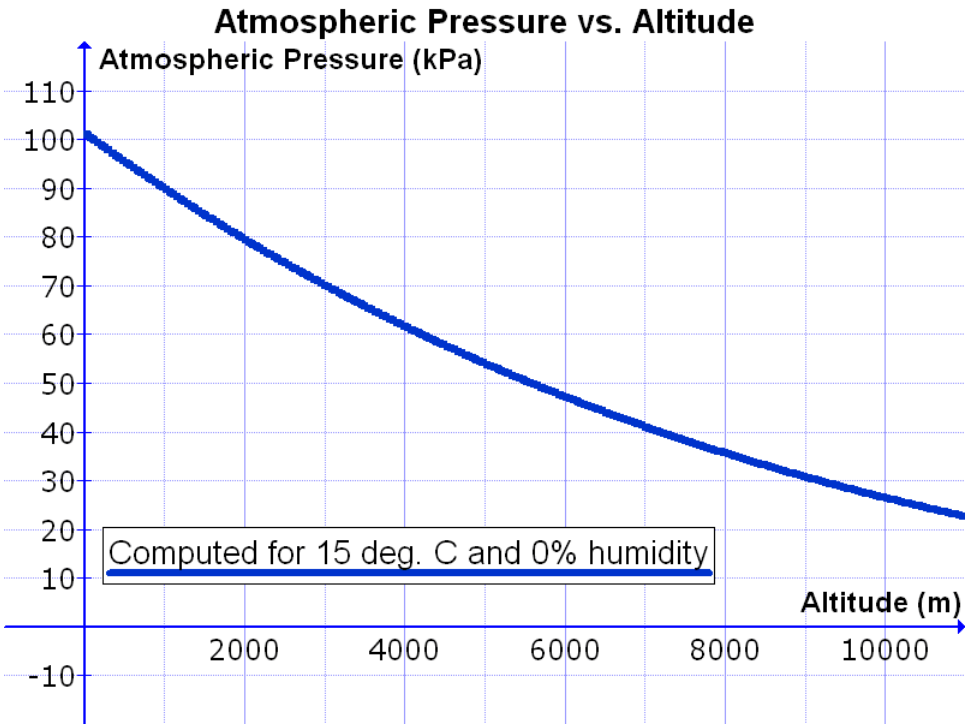

Figure 1.5: Atmospheric Pressure as a function of altitude.

Example 1.4.6. Determine the mass in a one-meter square column between the pressure levels of 850 and 500 mb.

Solution:
The 850 mb level is lower than the 500 mb level (pressure always decreases as you go up in elevation). The increase of 350 mb of pressure between these levels is due to the mass between these levels. Therefore,

$$\text{mass between} = \frac{\text{pressure difference between (in Pa)}}{9.8} = \frac{350 \times 100}{9.8} \approx \boxed{3571 \ \text{ kg}}$$

The exponential decay of pressure with height results in an exponential decay of mass with height because of the relationship of pressure, mass and the acceleration of gravity g in the Earth's atmosphere. The mass above (ma) a certain elevation z is given by

$$ma(z) = 10,337e^{-z/8000} \tag{1.5}$$

where the 10,337 term is the kilogram mass in the entire (surface to the "top" of the atmosphere) one meter-squared column. Consequently, this exponential relationship may be used to determine the mass of a column of air between to levels when they are specified by elevation z.

Example 1.4.7. Determine the mass in a one-meter square column between the elevations of 700m and 1000m.

Solution:
The mass between these elevations is equal to the mass above the 700m level after subtracting the mass above to 1000m level. That is,

$$\begin{aligned}
\text{mass between} &= \text{mass above 700m - mass above 1000m} \\
&= \text{ma}(700) - \text{ma}(1000) \\
&= 10377e^{-700/8000} - 10377e^{-1000/8000} \\
&= 10377(e^{-7/80} - e^{-1/8}) \\
&= 10377(0.9162 - 0.8825) = 10377 \times 0.0337 \approx \boxed{350 \text{ kg}}
\end{aligned}$$

1.5 Ideal Gas Law

The ideal gas law is a relationship between the pressure P, the volume V, and temperature T of a gas. The equation is

$$PV = nRT \tag{1.6}$$

where n is the amount of substance of the system measured in moles (mol), and R is the universal gas constant[6] of 8.314472 J$\cdot$ K$^{-1}\cdot$ mol^{-1}.

A mole of gas contains as many elementary entities (e.g., atoms, molecules, ions, electrons) as 12 grams of carbon 12. Consequently, one mole of carbon has a mass of 12 grams. Avogadro's number is the number of elementary entities. That value is 6.022×10^{23}.

It turns out that the mass in grams of a mole of a gas is roughly its atomic mass unit (AMU). Because the Earth's atmosphere is predominantly N_2 (AMU = 28) and O_2 (AMU = 32), the mass of a mole of atmosphere is approximately 28.9 grams or 0.0289 kg. So, to determine the mass m (in kg) in a n moles of air, multiply n times 0.0289. That is, $m = 0.0289 * n$ or $n = \frac{m}{0.0289}$.

Equation 1.6 can be adjusted using these facts to give a gas law, specifically for the Earth's atmosphere, based on mass. That is

$$\begin{aligned} PV &= \frac{m}{0.0289}(8.314472)T \\ \Rightarrow PV &= \frac{8.314472}{0.0289}mT \\ \Rightarrow PV &= 287mT \\ \Rightarrow P &= 287\frac{m}{V}T \\ \Rightarrow P &= 287\rho T \end{aligned} \tag{1.7}$$

The pressure P in the Equation 1.7 is measured in Pascals. Recall that 1 millibar (mb) is 100 Pascals. Consequently, the last Equation 1.7 can be changed to give the pressure P in mb

$$P = 2.87\rho T \tag{1.8}$$

Constant Density

The form of the Ideal Gas Law shown in Equation 1.8 states that if density ρ is constant, then the temperature and the pressure of the system rise and fall proportionally. Simply stated, we say that temperature and pressure are *directly proportional*.

[6]The letter "J" in the units for R stands for an energy measurement known as a Joule that will be introduced in Chapter 2

Constant Pressure

Solving Equation 1.8 for density ρ in terms of pressure and temperature gives

$$\rho = \frac{P}{2.87T} \tag{1.9}$$

Equation 1.9 indicates that if the pressure of the system remains constant, and the temperature increases, then the density ρ must decrease. If the temperature decreases, the density must increase.

Equation 1.9 may be rearranged to give

$$T = \frac{P}{2.87\rho} \tag{1.10}$$

The last two equations establish the general relationship between temperature and density when pressure is held constant. That is, density and temperature are *inversely proportional*.

Constant Temperature

If temperature T is held constant in Equation 1.8, then one can see that pressure and density are *directly proportional*.

1.6 More Atmospheric Variables

1.6.1 Potential Temperature - Θ

The temperature T of an air parcel is sometimes referred to as the **sensible** temperature because it is the temperature we would "sense" if we put our uncovered hand into the parcel. Also, it is the temperature a thermometer would give if it were placed in the parcel.

As we will see, the temperature of a parcel may change significantly if the pressure of the parcel changes, and we know pressure changes dramatically through the depth of the troposphere. Some vertical motions in the atmosphere are a result of different parcels having different temperatures. However, comparing parcel temperatures for parcels at different pressure levels requires making an adjustment to the sensible temperatures due to the pressure difference. The resulting "comparison" temperature is the **potential temperature**. It is the temperature the parcel would have if its pressure were changed to that of a reference pressure. The exact formula is

$$\Theta = T\left(\frac{P_r}{P}\right)^{R/c_p} = T\left(\frac{P_r}{P}\right)^{0.2859} \tag{1.11}$$

where T and P are the parcel's (sensible) temperature (measured in K) and pressure, respectively, R is a universal gas constant($R = 287\ \mathrm{J{\cdot}K^{-1}{\cdot}kg^{-1}}$), and c_p is heat capacity for

dry air ($c_p = 1004$ J·K^{-1}·kg^{-1}). The term P_r is the reference pressure, and is usually taken to be the surface pressure (≈1013 mb).

The potential temperature defined by Equation 1.11 is valid only if the there is no heat transfer to or from the parcel. Such a restriction is called **adiabatic**. This restriction does not hold, for example, if a parcel mixes with surrounding parcels as it moves, or if it gains or loses heat through radiation. In Chapter 2, various forms of energy and energy transfer mechanisms are introduced, and the concept of an adiabatic process is explicitly defined.

Potential temperature explains why the warmer surface air does not rise to the top of the atmosphere as one might expect because everyone knows that "warm air rises." The following example will aid in our understanding of why the parcel with the warmer sensible temperature does not rise above a parcel under lower pressure with a lower sensible temperature.

Example 1.6.1. A parcel of air, at an elevation of 1500m, has a pressure of 850 mb and a temperature of 5C. Determine its potential temperature for the pressure reference of 1013 mb.

Solution:

$$\Theta = (273+5)\left(\frac{1013}{850}\right)^{0.2859} = 278 \cdot 1.192^{0.2859} = 268 \cdot 1.0514 = 281.8K \approx \boxed{19.3°\text{C}}$$

The result of Example 1.6.1 indicates that if a surface parcel with pressure 1013 mb has a temperature less than 19.3°C, it will not rise because its potential temperature is *less* than the parcel sitting at 850 mb with a temperature of 5°C. Another take away is that a parcel's "natural" elevation level is where it has the same potential temperature as other parcels at that level, and parcels above have greater potential temperatures. In a *stable* atmosphere, potential temperature increases with height.

The next example demonstrates how the sensible temperature can be determined knowing the parcel potential temperature and pressure.

Example 1.6.2. A parcel of air at the 500 mb pressure level has a potential temperature of 315K. Determine the parcel's sensible temperature.

Solution:

$$\Theta = T\left(\frac{1000}{P}\right)^{0.2859} \Rightarrow 315 = T\left(\frac{1000}{500}\right)^{0.2859} = T \cdot 2^{0.2859} = T * 1.219$$

Solving for T gives:

$$T = 315/1.219 = 258.4K = \boxed{\text{-14.6°C}}$$

1.6.2 Mixing Ratio - W

The important role of atmospheric moisture means we need some way of measuring, or quantifying, its presence in the atmosphere. There are various ways to measure atmospheric water vapor. The different measures serve some purposes better than others. That is, the purpose of the measurement may dictate how the measurement is defined. The first one we will use is known as the atmospheric **mixing ratio** (W). As its name suggests, it is the ratio of two numbers. The numerator is the mass of water vapor, usually measured in grams (gm) in a given air parcel. The denominator is the mass of the dry (non-water vapor) constituents of the air parcel usually measured in kilograms (kg) because this mass is considerably larger than that of the water vapor. Therefore, the mixing ratio is given by

$$W = \frac{\text{mass of water vapor (gm)}}{\text{mass of dry constituents (kg)}} \tag{1.12}$$

We know from Table 1.2 that atmospheric water vapor may range from 0 to 4% of the volume of an air parcel. Also, volume and mass ratios of an atmospheric parcel are approximately equivalent, so if an air parcel has 1 kg of dry constituent mass, then the water vapor mass may range from 0 to 0.04 $\times$ 1000 gm = 40 gm. Therefore, atmospheric mixing ratios generally vary between 0 to 40 grams per kilogram. Sometimes, but very rarely, mixing ratios exceed 40 gm per kg.

Example 1.6.3. A 2 cubic meter air parcel has a temperature of 10°C, a pressure of 925 mb and a mixing ratio of 25 gm per kg. Calculate the mass of water vapor in the parcel.

Solution:
First, determine the mass of the parcel. The mass is given by its volume V times its density ρ. The density can be determined using the Ideal Gas Law:

$$P = 2.87\rho T \Rightarrow \rho = \frac{P}{2.87T} = \frac{950}{(2.87 \times (273 + 10))} = 1.17 \text{ kg} \cdot \text{m}^{-3}$$

Next, calculate the dry mass of the parcel:

$$\text{dry mass} = V \times \rho = 2 \text{ m}^3 \times 1.17 \text{ kg} \cdot \text{m}^{-3} = 2.34 \text{ kg}$$

Now, use the mixing ratio to determine the vapor mass in grams:

$$\text{vapor mass} = W \times \text{ dry mass} = 25 \text{ gm per kg} \times 2.34 \text{ kg} = \boxed{58.5 \text{ gm}}$$

Chapter 1 Exercises

1.1 An air parcel has a temperature of 90°F. Determine its temperature in (a) Celsius, (b) Kelvin.

1.2 The temperature of an air parcel is -10°C. Determine its temperature in (a) Kelvin, (b) Fahrenheit.

1.3 If the temperature of an air parcel is 298K, what is the parcel's temperature in (a) Celsius, (b) Fahrenheit.

1.4 Determine the average velocity of the molecules within a parcel of air that has a temperature of 0°C.

1.5 The average speed of the molecules in a parcel of air is 600 m/sec. Calculate the temperature of the parcel in degrees C.

1.6 Determine the density of an air parcel given it has a temperature of 70°F and a pressure of 1000 mb.

1.7 An air parcel has a density of 1.2 kg·m^{-3} and a temperature of 10°C. Determine the air pressure of the parcel.

1.8 Determine the density in g/L of the standard atmosphere (assume a surface density of 1.22 g/L) at an elevation of (a) 1000 m, (b) two miles.

1.9 A parcel at 700 mb has a temperature of -5°C. Calculate the potential temperature of the parcel.

1.10 A parcel has a temperature of 2°C and a potential temperature of 283K. Calculate the approximate elevation of the parcel. Assume a surface pressure of 1000 mb.

1.11 The potential temperature of a parcel at 500 mb is 288K. Determine the parcel's temperature in degrees Celsius.

1.12 At what elevation (in meters), does the standard atmosphere have the following densities? Assume a surface density of 1.22 g/L. (a) 1.0 g/L, (b) 0.5 kg/m^3, (c) 0.1 g/L

1.13 For a standard atmosphere (use surface pressure of 1000 mb), determine the elevation z, in meters, at which (a) 10% of the atmosphere is below z, (b) 50% of the atmosphere is below z, (c) 90% of the atmosphere is below z.

1.14 A classroom in Olin Hall has dimensions 10 m by 12 m by 3 m. Determine (a) the total mass, in kg, of the air in the room, (b) the mass, in kg, of oxygen in the room.

1.15 On a summer day the surface temperature is 72°F. What temperature, in degrees F, would you expect to find at the top of a one-mile high mountain? Assume a standard temperature lapse rate.

1.16 The temperature at an elevation of 8000m is -25°C, while the temperature at an elevation of 2000m is 5°C. Calculate the average lapse rate for this interval in °C / 1000 m.

1.17 Given the temperature at the surface is 72°F and the temperature at the 700 mb pressure level is 10°C, calculate the average lapse rate for this segment of the atmosphere in °C / 1000 m. Assume a surface pressure of 1000 mb.

1.18 The table of data given below gives the measured lapse rates for the atmosphere broken into six intervals. The surface temperature is 75°F. Use these data to determine the atmospheric temperature at (a) 3000m, (b) 5000m, (c) 6000m, and (d) 7500m

Interval (meters agl)	Lapse Rate (°C/ 1000 m)
7000 - 8000	6
5000 - 7000	8
3500 - 5000	7
2000 - 3500	3
1500 - 2000	1
0000 - 1500	4

1.19 The surface temperature at Decorah is 0°C and the surface density is 1.30 g/L. The surface temperature at Tallahassee, Fl is 20°C and the surface density is 1.22 g/L. Assuming a standard lapse rate for temperature over both cities (which means a standard exponential decrease of pressure with elevation), calculate the elevation of the 500 mb pressure surface over each city.

1.20 You are able to determine the atmospheric pressure outside your airplane is 600 mb. If the surface temperature is 20°C, what is the elevation (in meters) of the airplane? Assume a standard atmospheric temperature lapse rate (so pressure decreases exponentially with elevation) and $\rho_s = 1.22$ g/L.

1.21 Consider a column of air that is above a horizontal area of 1 square meter with a surface pressure of 1000 mb. Calculate the mass, in kg, of the air (a) between the pressure levels of 1000 mb and 850 mb, (b) within the first kilometer closest to the earth's surface, and (c) between the elevations of 1 km and 2 km.

1.22 Use the tabular data given below to estimate the precipitable water (depth of water in cm) in a column of air that has a base of one square meter and extends from the surface of the earth to the 500 mb pressure elevation.

Pressure (mb)	Mixing Ratio (g/kg)
1000	20
850	15
700	10
500	5

1.23 An Olin classroom has dimensions 20m by 15m by 3m. If the mixing ratio of the air in the classroom is 30g/kg, determine (a) the mass of the water vapor in the air, (b) the depth of the water if all of the vapor precipitates out of the air.

1.24 A summer thunderstorm over Decorah results in a rainfall depth of 1.5 inches. Estimate the average mixing ratio of the thunderstorm atmosphere assuming 50% of the water vapor in the atmosphere precipitated and the precipitation column extended to an elevation of 6000 m.

1.25 Thunderstorms "mop up" a great volume of moisture-laden air and wring out the water vapor. Suppose a thunderstorm precipitates 100 mm of water (approximately 4 inches) over an area of 1 km^2. Assume the average mixing ratio in any column of air between the surface and 400 mb, and available for precipitation, is 20 g/kg. Additionally, assume the storm's "precipitation efficiency" (what percentage of the precipitable moisture actually precipitates) is 60% for the each column. Estimate the area, in km^2, that the storm must draw from to provide enough precipitable water for the storm. Begin by using Example 1.4.6 to determine the mass in a column of air, between the 1000 mb and 400 mb levels, with a base area of 1 km^2. Use the MR of the air to determine the mass of water, in gm, in the column. Recall that 1 gm of water = 1 cc in volume.

Chapter 2

Energy Types & Transfers

2.1 Overview

Energy provides the ability or capacity to do work on matter. Energy is required to lift an air parcel to a higher elevation. Energy is required to raise the temperature of an air parcel. This chapter describes the various forms of energy pertinent to the Earth's atmosphere and the means by which energy is transferred from one object to another, and from one form to another. The chapter concludes with a summary of the Earth's global, annual energy budget. This latitudinal dependency of this budget is the genesis of the general circulation patterns of the Earth's atmosphere.

2.2 Energy Measures

Energy has various units of measurement, similar to other atmospheric variable or quantities we looked at in Chapter 1. The two primary measures used in this text will are the joule[1] (J) and the calorie (cal).

The joule is defined in terms of energy associated with a force of one newton acting on an object over the distance of one meter. That is, a joule = N $\cdot$ m (newton meter). This definition of a Joule as a measure of energy gives rise to the saying that "work equals force times distance." Another form of energy is related to an electrical circuit where the joule represents the energy dissipated when an electrical current of one ampere passes through a resister of one ohm for one second.

The calorie measurement of energy is defined as the energy required to raise one gram of water one degree C at an atmospheric pressure of 1013 mb and initial temperature of 3.98C. The relationship a calorie and a joule is

$$1 \text{ cal} = 4.186 \text{ J}$$

[1]The joule is named after the English physicist James Prescott Joule (1818 - 1889)

This calorie energy measure is sometimes referred to as the *small* calorie. The large calorie, or *kilogram calorie* (kcal), is the energy required to raise the temperature of a kilogram of water one degree C. Not surprisingly, 1 kcal = 1000 cal. The large calorie is equivalent to what is known as a "food" calorie.

2.3 Atmospheric Energy Forms

Three import forms of energy associated with the Earth's atmosphere are introduced in this section. We will do so through their association with atmospheric parcels. The first is potential energy.

2.3.1 Potential Energy - PE

Atmospheric parcels have an associated mass and an average elevation. The product of its mass and elevation with the acceleration of gravity gives the *potential energy* of the parcel. That is,

$$PE = m \cdot z \cdot g \tag{2.1}$$

where mass m is measured in kilograms, elevation z in meters, and g has the value of 9.8 $\text{m}\cdot\text{s}^{-1}$.

Example 2.3.1. Calculate the potential energy associated with a 5 kg parcel and elevation 1000 feet.

Solution:

First, determine the parcel's elevation in meters. The conversion of feet (ft) to meters (m) is

$$\text{m} = \text{ft}/3.28 \Rightarrow \text{m} = 1000/3.28 \approx 304.9\text{m}$$

Then, find the potential energy:

$$\text{PE} = \text{mass} \times z \times g = 5 \times 304.9 \times 9.8 = \boxed{14{,}940 \text{ J}}$$

2.3.2 Kinetic Energy - KE

Kinetic energy is energy associated with motion. The formula for calculating the kinetic energy of an object in motion is

$$\text{KE} = \frac{1}{2} \cdot m \cdot v^2 \tag{2.2}$$

where m is the mass of the object (in kg) and v is the speed of the object in $\text{m}\cdot\text{s}^{-1}$. The result is the kinetic energy measured in joules.

Example 2.3.2. A 2-liter parcel of dry air is, initially, stationary at 1500m. It falls to the surface of the earth within the downdraft of a thunderstorm. Calculate the parcel's speed at the earth's surface assuming all PE is converted to KE. Take ρ_s =1.22 g/L.

Solution:

First, determine the potential energy (PE) of the parcel. For that, we need the mass of the parcel. The mass is determined from the volume and density. The density is given by $\rho(1500) = 1.22e^{-1500/8000} = 1.01$ g/L. The 2-liter parcel has a mass of 2×1.01 gm $= 2.02$ gm $= 2.02/1000 = 0.00202$ kg. Then, PE $= 0.00202 \times 9.8 \times 1500 = 29.4$ J. Assuming all of the 29.4 J of PE is converted to kinetic energy (KE), we have $\frac{1}{2}mv^2 = 29.4$. Solving for v gives $v = \sqrt{\frac{2\times 29.4}{0.002}}$ $= \boxed{171 \text{ m}\cdot\text{s}^{-1}} \approx \boxed{377 \text{ mi/hr}}$

2.3.3 Thermal Energy - TE

A parcel's **internal energy** is that energy not attributable to its kinetic energy or potential energy. The **thermal energy** of an atmospheric parcel, on the atomic scale, is the portion of the parcel's internal energy that results in the parcel's temperature. The thermal energy has a kinetic component and a potential component. The potential portion is related to atomic-scale vibrations. The kinetic portion of the thermal energy gives rise to the parcel's temperature, defined using the average speed $\bar{v}$ of the atoms and molecules. The specific formula, introduced in Chapter 1, is

$$T = \alpha \cdot m_w \cdot \bar{v}^2$$

where m_w is the molecular mass of the parcel and α is a constant with value 4.0×10^{-5} $\text{K}\cdot\text{m}^2\cdot\text{sec}^{-2}$.

	Specific Heat	
Substance	cal· gm^{-1}· C^{-1}	J· kg^{-1}· C^{-1}
Water	1.00	4186
Mud	0.60	2512
Ice (0 C)	0.50	2093
Sandy Clay	0.33	1381
Dry Air (sea level)	0.24	1005
Quartz Sand	0.19	795
Granite	0.19	794

Table 2.1: Specific heat for various substances.

2.3.4 Parcel Energy

An atmospheric parcel has a measure of energy denoted by the letter "Q." Using the three forms of energy defined above, a parcel's energy may be expressed as

$$Q = PE + KE + TE \tag{2.3}$$

where the three form of energy on the right-hand-side of Equation 2.3 have a common unit of energy measure such as joules or calories. If a process on the parcel, such as its motion in the atmosphere, does not change its energy, that is $\Delta Q = 0$, the process is known as **adiabatic**.

Change in Energy, Change in Temperature

Temperature is related to the kinetic energy of the parcel's molecules and atoms. Therefore, a change in temperature (ΔT) is related to a change in energy (ΔQ). This relationship is derived using the First Law of Thermodynamics, and is shown in Equation 2.4

$$\Delta Q = C \cdot m \cdot \Delta T \tag{2.4}$$

where m is the mass of the object and C is the specific heat (or heat capacity) of the object. The specific heat of the object varies. Those for common materials associated with atmospheric considerations are shown in Table 2.1

Example 2.3.3. A 4-liter parcel of air at the surface of the Earth experiences a 5 C increase in temperature. Calculate the energy required to create this increase in temperature.

Solution:
First, determine the mass of the air. Assume the density is 1.22 gm/L (because it is at the surface of the Earth), so the mass is $m = 4$ L $\times$ 1.22 gm/L $= 4.88$ gm. Then,

$$\Delta Q = m \times C \times \Delta T = 4.88 \times 0.24 \times 5 = \boxed{5.865 \text{ cal}}$$

2.4 Energy of Phase Change

The importance of water in the atmospheric system is due, in part, to its ability to exist in all three phases: solid, liquid and gaseous. Additionally, when water undergoes a change in phase, energy is involved. The six different phase change possibilities are shown in Figure 2.1.

As one might expect, the solid (ice) phase of water is associated with the least energy. One gram of ice requires 80 calories to transition to its water phase. This energy is call the **heat of fusion**. The energy source for such a transition comes from the environment (external to the ice). The reverse transition is freezing, with 80 calories given up to the environment for each gram of water that freezes.

When water vaporizes (transforms from liquid to vapor state), the energy is supplied (lost) by the environment and gained by the water molecules. The **heat of vaporization** is 600 calories per gram. The opposite is true when water condenses. The loss of 600 calories per gram of water is born by the water, and the environment is the beneficiary. A somewhat surprising transition is that from solid to gaseous state and vice versa.

Sublimation occurs when an ice crystal transforms to its vapor state. The **heat of sublimation** is 680 calories per gram, the sum of energies required to go from solid to liquid, and then liquid to the gaseous state. **Deposition** is the reverse transition. Water vapor transforms directly to its solid ice state and liberates 680 calories to the environment for each gram of water vapor.

Example 2.4.1. Suppose 0.01 gram of water condenses and the heat of condensation warms the dry mass of a three-liter parcel of air near the surface of the earth. Determine the temperature increase of the dry parcel.

Solution:
The 0.01 gram of water gives up $0.01 \times 600 = 6$ cal in condensation. The mass of the dry parcel is 3×1.22 g/l $= 3.66$ g. Use $\Delta Q = Cm\Delta T$ to give $6 \text{ cal} = 0.24 \times 3.66 \times \Delta T$. Solving for ΔT gives a $\boxed{6.83 \text{ C}^\circ}$ increase in temperature.

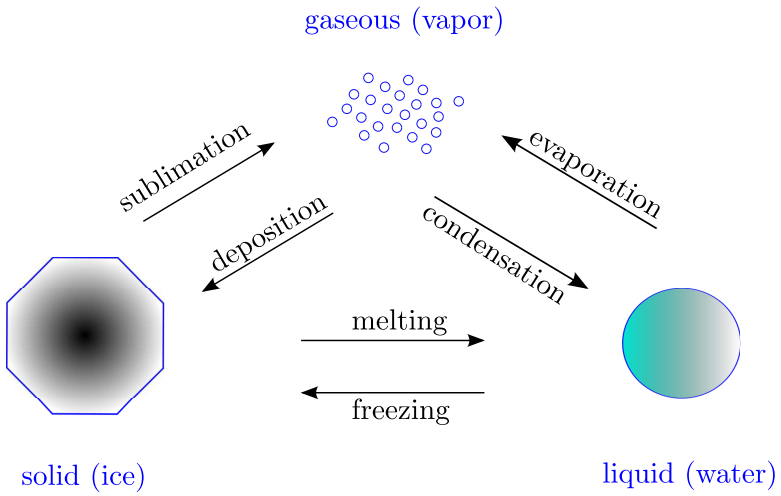

Figure 2.1: The six phase-change processes.

2.5 Energy Transfer Mechanisms

Now that we know what forms of energy there are in the atmospheric system, we turn our attention to the mechanism that transfer energy from one location to another or one object to another. The three prominent mechanisms in operating within the Earth's atmosphere are conduction, convection, and radiation. All three are depicted in Figure 2.2. The transfer of energy, or heat, is frequently measured by how many units of energy (joules or calories) are transferred in a given time interval (a second) over a given area (one square meter), $J \cdot sec^{-1} \cdot m^{-2}$. A watt is equivalent to a joule per second, and it sometimes referred to as power (the time rate of change of work or energy). Quantifying heat transfer includes an area measure (m^2) because energy is perceived to be "flowing" into or out of an object through its surface.

2.5.1 Conduction

The surface of the Earth is warmed by electromagnetic radiation from the sun. The molecules of the surface substance absorb some of the solar energy and begin moving faster due the increase in energy, thus resulting in a warmer surface layer. This warm top layer of the surface is depicted by the red dots in Figure 2.2. The warm surface layer is in contact with the air parcels that sit on the surface of the Earth. These faster moving surface molecules collide with the cooler air-parcel molecules at the surface boundary. The collisions cause the slower moving air-parcel molecules to speed up. The faster moving air-parcel molecules result in a greater average molecular velocity resulting in warmer atmospheric parcels at the surface of the Earth.

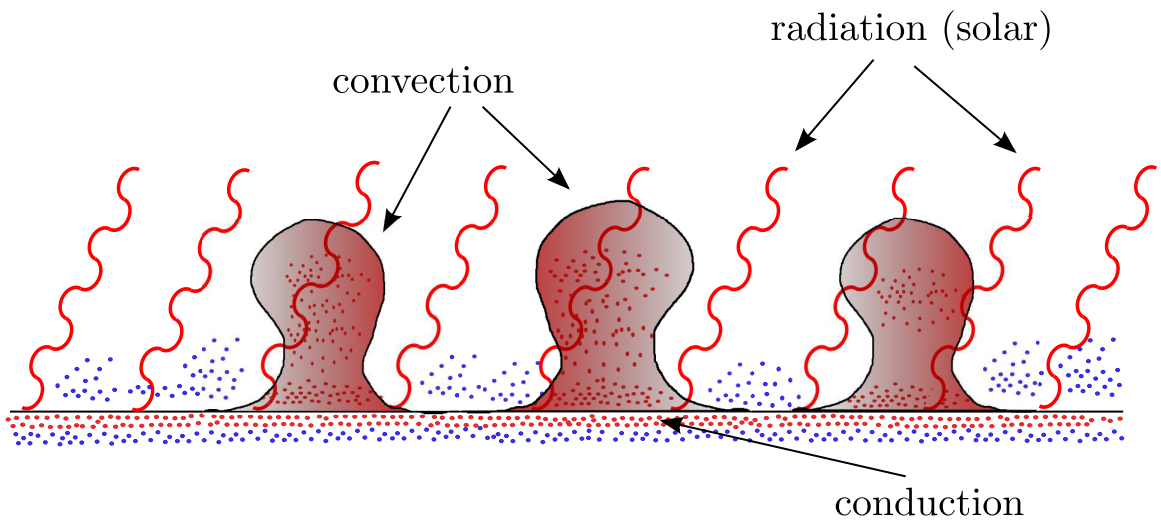

Figure 2.2: Primary atmospheric energy transfer mechanisms.

The efficiency, or effectiveness, of conductive heat transfer depends on the materials involved and a related parameter known as the coefficient of heat conductivity. Table 2.2 list values for various substances. The units for the coefficient are watts per meter per degree C, where the degree C term represents the difference in temperature between adjacent regions. The large the difference, the greater the heat transfer rate. If the difference is zero, then no energy is transferred.

The coefficient of heat conductivity varies greatly between the substances listed in Table 2.2. Still air is the least conductive. This is the primary consideration in house insulation practice. The primary purpose if most insulating material is to prevent the movement of air in the space between the outside and inside walls, as well as the attic region. The highly efficient heat conductivities of certain metals is seen in the table. Another factor to consider is the relationship between material density and heat conductivity. The more dense the material, the closer the molecules. The closer the molecules, the easier it is for them to collide and transfer energy.

2.5.2 Convection

The process of heat convection is represented in Figure 2.2 by the hot air "bubbles" that develop near the surface of the Earth. These result as the effects of conduction create warm "pockets" of air parcels near the surface of the Earth. The heating at the surface, and the resulting conductive heat transfer, are not uniform due to variations in the Earth's surface makeup as well as topography. For example, land surfaces warm fast than water surfaces due to the difference in heat capacities. Also, sloping surfaces that "face" the sun warm

Substance	Conductivity (Watts per meter per °C)
Still air	0.023 (at 20 °C)
Wood	0.08
Dry soil	0.25
Water	0.60 (at 20 °C)
Snow	0.63
Wet soil	2.1
Ice	2.1
Granite	2.7
Iron	80
Silver	427

Table 2.2: The coefficient of heat conductivity for various substances.

more than flat surfaces and those that slope away from the sun's rays. Consequently, certain regions of the surface warm faster, or to greater magnitudes, than others.

These warm bubbles of parcels have a lesser density than the cooler surrounding parcels. This is established through the Ideal Gas Law for atmospheric parcels, $P = 2.87\rho T$. Both warm and cool parcels are at the same elevation (at the surface, actually), so both have the same pressure P. Solving for density gives

$$\rho = \frac{P}{2.87 \cdot T}$$

and it is clear that a higher temperature T results in a lower density ρ for the warmer parcels. The warm bubbles of parcels rise through the atmosphere much like a hot-air balloon rises. The rising motion is transferring heat to the higher elevations in the atmosphere. The significance of convective heat transfer will be quantified in Section 2.7 where we consider a detailed look at the Earth's energy budget.

Convective heat transfer is not limited to vertical motions or vertical transfer of energy. Horizontal convection (frequently referred to as **temperature advection**) is an extremely important phenomenon in the Earth's atmosphere. It develops where horizontal winds blow in a direction that is non-parallel to temperature contours. Figure 2.3 depicts a case where this is true. Surface temperature generally increase from south to north. When a southerly wind develops, as indicated in the figure, then warm air is moved northward creating a situation of heat transfer known as **temperature advection**. If warm air is replacing cold air, it is **warm advection**, as is the case in Figure 2.3. **Cold advection** occurs when cold air is replacing warm air.

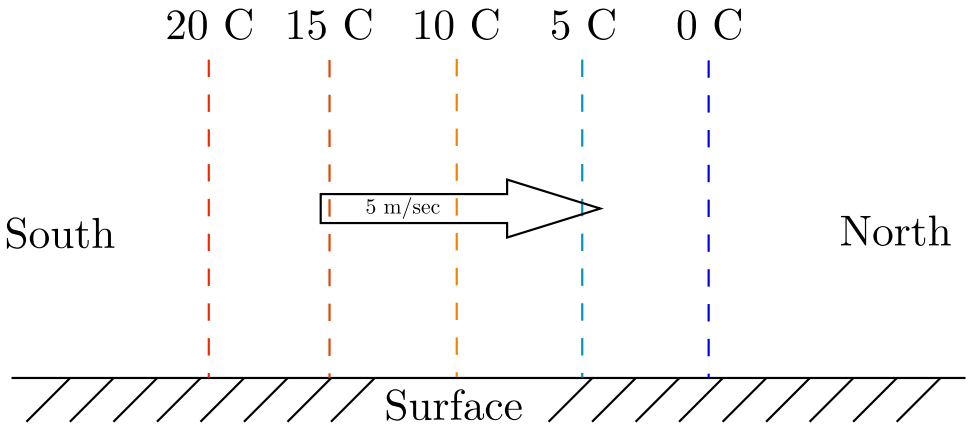

Figure 2.3: An example of temperature advection.

2.5.3 Latent Heat

Latent heat transfer is another form of energy transfer and might be thought of as a "cousin" of convection. This form requires the presence of water vapor in the parcels that are transported in the atmosphere by convection or other means. Additionally, the water vapor must undergo condensation or deposition resulting in the release of the respective heat of phase change. It is common for this process to accompany convection process as depicted in Figure 2.4. Parcels near the surface of the Earth usually have a positive mixing ratio. The vapor form of water is "invisible." As the parcel rises due to convection or some other process, it cools due to the decrease in pressure on the parcel (this process will be explained more fully in Chapter 9). The cooling of the parcel may be sufficient enough to cause the water vapor to condense (if the parcel's temperature is above freezing) or sublimate (if the parcel's temperature drops below freezing). In either case, the change of phase is from the more energetic vapor phase to a less energetic phase, resulting in the release of the heat of condensation or sublimation. This energy release results in a warming of the dry mass of the parcel.

2.5.4 Radiative Transfer

Radiative heat transfer is the most important form of energy transfer because of its magnitude and comprehensive nature. Examination of the Earth's energy budget in Section 2.7 will establish the dominant magnitude of radiative transfer. Additionally, all objects with temperature greater than absolute zero radiate *thermal* electromagnetic energy, so it is pervasive throughout the atmospheric system.

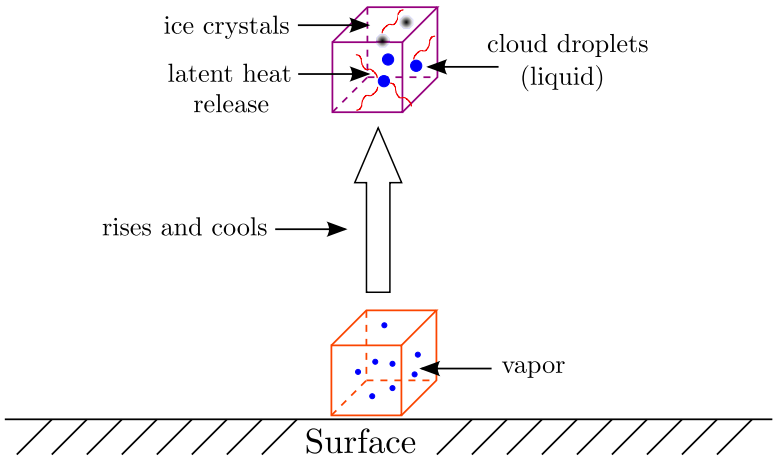

Figure 2.4: Latent heat transfer associated with convective motion.

Electromagnetic Radiation - EMR

Electromagnetic radiation (EMR) is created by accelerating charged particles. A charged particle, for example, is an atom or molecule that has an unequal number of protons (positively charged) and electrons (negatively charged). Atoms and molecules in a substance with positive absolute temperature have an average velocity greater than zero. The interatomic collisions result in a transfer of kinetic energy. This transfer results in acceleration of charged particles and the creation of EMR. The wide range of atomic and molecular speeds (kinetic energy) results in EMR having a range of energies as well.

Electromagnetic radiation (EMR) is characterized in a "classical" way as electric and magnetic fields (EM fields) that oscillate in perpendicular planes. The direction of the EMR propagation is perpendicular to both of these electric and magnetic planes. The initial "near-field" wave interacts with those of other charged particles and create the "far-field" wave that is the EM wave. These waves move outward from the source in all directions at the speed of light.

A wave is characterized by such features as its **wavelength** (λ = the distance between successive peaks). The time required for the wave to complete one oscillation is the wave **period**, measured in seconds. Wave frequency (ν) is the reciprocal of the period, so it has units of s^{-1}. The speed of the wave is given by

$$\text{speed} = \text{wave length} \times \text{frequency} = \lambda \times \nu$$

If two waves have the same speed, but one wave has a shorter wavelength, then its frequency must be greater. All EMR waves travel at the speed of light, so the shorter the wavelength, the greater the frequency of the EMR wave.

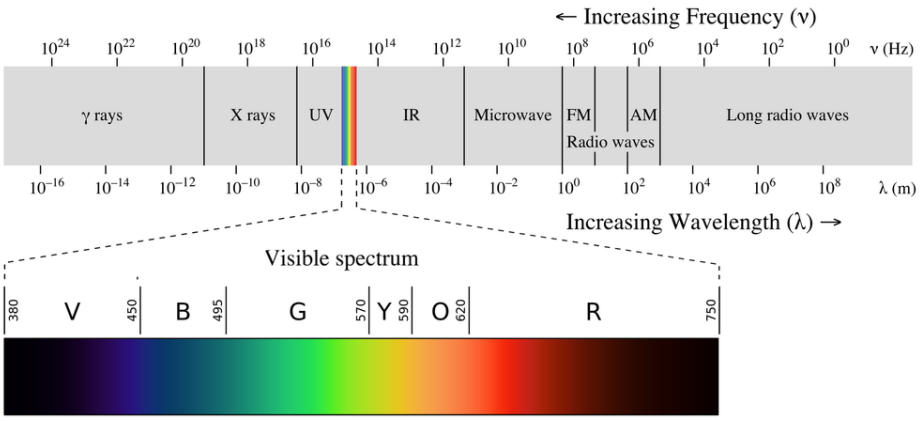

Figure 2.5: Solar radiation spectrum as part of the overall frequency and wavelength spectrum[2].

The EMR from the sun emanates outward, eventually reaching the Earth. The solar radiation spectrum is the distribution of wavelengths and frequencies associated with the sun's EMR, as shown in Figure 2.5. Wavelengths range from a minimum of 10^{-16} m for gamma rays, to a maximum of 10^{8} m for long radio waves. The portion of the spectrum visible to the human eye ranges from 0.380×10^{-6} m (violet or near ultraviolet) to 0.750×10^{-6} m (red or near infrared).

Electromagnetic radiation is mysterious in that it seems to have a "dual identity." It has characteristics that make it similar to other wave phenomena such as water waves. Yet, EMR waves travel through the vacuous regions of our solar system (and beyond), so they do not depend on a medium for transfer as other wave phenomena. This transfer process, and other characteristics of EMR, suggest EMR behaves like a "particle." EMR particles are called a **photons**. The energy E of a photon is given by the formula

$$E = \frac{hc}{\lambda}$$

where h is Planck's constant, c is the speed of light and λ is the wavelength of the EMR. The shorter the wavelength, the more energetic the photon. The frequency of the wave is inversely proportional to its wavelength (as mentioned above). So higher frequency EMR photons have greater energy.

[2]By Philip Ronan, Gringer - File:EM spectrum.svg and File:Linear visible spectrum.svg, CC BY-SA 3.0, https://commons.wikimedia.org/w/index.php?curid=24746679

EMR Emissivity

How effectively a surface emits thermal EMR is measured by its **emissivity** ϵ. Values of ϵrange from 0.0 to 1.0. A surface with emissivity of 1.0 is said to be a perfect **blackbody** radiator. That is, a blackbody radiator emits all of the EMR it generates. Materials with low emissivity (non-blackbody like) include aluminum foil with ϵ= 0.03, and polished copper with ϵ= 0.04. Those with high emissivities include smooth glass with ϵ= 0.95, ice with ϵ= 0.97, and asphalt with ϵ= 0.88. The high emissivity of glass explains why "low E" glass (low ϵ) is an important feature of energy efficient windows. The high emissivity of "regular" glass results in significant energy loss through glass that is heated from the inside of the house by conduction, convection, or radiation from internal sources.

The radiation spectrum and intensity[3] from a blackbody radiator depends only on its temperature. The intensity of the radiation from a blackbody is a function of the wave frequency ν. The formula for B, the blackbody **irradiance**, as a function of ν is known as **Planck's Law** of blackbody radiation, and is given in Equation 2.5

$$B_\nu = \frac{2h\nu^3}{c^2}\frac{1}{e^{\frac{h\nu}{kT}} - 1} \tag{2.5}$$

where h is Planck's constant, c is the speed of light, k is **Boltzmann's** constant, ν is the frequency of the radiation and T is the absolute temperature of the blackbody.

Figure 2.6 shows the sun's irradiance curve as a function of the radiation wavelength measured in μm. There is a certain wavelength (λ_{max}) for which the irradiance is a maximum, and it may be calculated using **Wien's Law** and the temperature of the body, as shown in Equation 2.6,

$$\lambda_{max} = \frac{b}{T} \tag{2.6}$$

where T is the Kelvin temperature and b is Wien's displacement constant with value 2.897×10^{-3} K ·m. The resulting wavelength maximum is in meters. For example, the sun's temperature is calculated to be 6000 K, the wavelength of maximum solar EMR is

$$\lambda_{max} = \frac{2.897 \times 10^{-3}}{5780} = 0.5012 \times 10^{-6}\text{m}$$

that places it in the blue-green region of the visible portion of the solar spectrum. The wavelength of maximum irradiance in the Earth's EMR spectrum is 10.06×10^{-6} m, placing it in the infrared (IR) segment of the EMR spectrum.

Example 2.5.1. A toaster surface heats up to a temperature of 140°F while moderately toasting two slices of bread. Use Wien's Law to determine the wavelength of the radiation spectrum maximum.

[3]Intensity is measured as watts per square meter per μm.

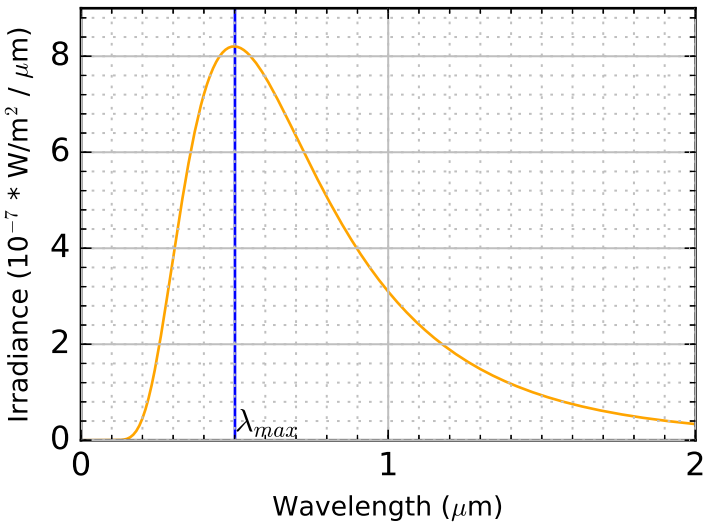

Figure 2.6: Solar irradiance as a function of radiation wavelength.

Solution:

$\lambda_{max} = \dfrac{2.897 \times 10^{-3}}{T}$ where the temperature T in this case is $T = \frac{5}{9}(140 - 32) + 273 = 333$ K. The radiation spectrum maximum has a wavelength

$$\lambda_{max} = \frac{2.897 \times 10^{-3}}{333} = 8.7 \times 10^{-6}\text{m} = 8.7\mu\text{m}$$

Therefore, this places the radiation coming from the toaster in the infrared range (IR) on the spectrum shown in Figure 2.5.

The **total irradiance** E associated with a blackbody's radiation spectrum is given by the area under the spectrum curve, as shown in Figure 2.6. The resulting **Stefan-Boltzmann formula** for E, shown in Equation 2.7, is a function of the blackbody's temperature measured in K.

$$E = \sigma \cdot T^4 \tag{2.7}$$

The term σ in Equation 2.7 is the Stefan-Boltzmann constant with value 5.67 $\times$ 10^{-8} W $\cdot$m^2 $\cdot$K^{-4}.

Example 2.5.2. Suppose a toaster has a surface area of 0.1 square meter, and it takes 2 minutes to toast two slices of bread. Determine the total radiative energy emitted from the toaster in joules.

Solution:

Use the Stefan-Boltzmann formula to first determine the number of watts per meter squared that were emitted from the toaster's surface. E = 5.67 $\times 10^{-8} \times 333^4 = 697.2$ watts per meter squared. Multiply this result by 0.1 to determine the wattage: $697.2 \times 0.1 = 69.72$ watts.

One watt is a joule per second, so the total energy in joules is 69.72 J/sec $\times$ 120 seconds = $\boxed{8{,}366 \text{ J}}$.

NOTE: This number is an over-estimation because we are assuming the toaster's surface temperature is a constant 140°F. The reality is that it will take a good portion of the 120 seconds for the toaster's surface to reach the temp of 140°.

EMR Absorption

EMR is absorbed by varying degrees that depends on the object. The object's absorption coefficient indicates what fraction of the EMR is absorbed. The coefficient is 0.0 if none is absorbed, and 1.0 all is absorbed. Lower energy EMR (waves with longer wavelengths) usually warm the object without changing the nature of its composition. Higher energy EMR, when absorbed, may result in chemical changes (ultraviolet light absorbed by ozone to create O and O_2) or ionization (creating a charged particle).

Selective Absorption

When an photon is absorbed by an atom, an electron of the atom moves to a more energized orbit. Atom electron orbits, and their associated energy levels, do not have a continuous distribution between their minimum and maximum energy levels. Instead, the energy levels and orbits have a few discrete values. Consequently, only photons of a certain energy levels, those with energy that match the difference in energy levels of the atom's electron orbits, are absorbed by an atom. This theory involves the **quantum** theory of EMR. Figure 2.7 shows how a photon with an appropriate energy level is absorbed by an electron orbiting the nucleus of an atom. The newly excited electron is now orbiting the atom at one of the discrete energy levels that are possible with the particular atom.

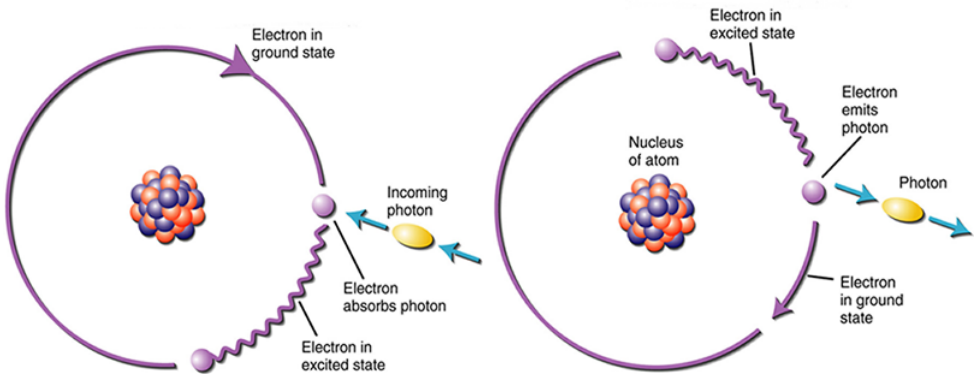

Figure 2.7: Photon absorption and emission.

The absorbing atom may eventually emit a photon when the electron in its "excited" orbit returns to its original orbit. The decrease in energy results in the atom emitting a photon with energy equal to the energy decrease. Therefore, a photon depicted in figure 2.7 will be emitted with the same energy and frequency as that absorbed.

2.6 Greenhouse Effect

Varying acceleration of charged particle create a continuous wavelength spectrum of radiation. The wavelength of maximum emissivity and the "spread" of radiation depend on the average surface temperature of the body. These facts, along with the selective absorption of EMR form the basis of the terrestrial **greenhouse effect**.

The top panel of Figure 2.8 shows the solar (solid red) and terrestrial (solid blue) radiation curves side-by-side. The wavelength of maximum solar emissivity is considerable shorter than that of the earth because of the significant difference in average surface temperatures. The next panel down shows the total absorption and scattering of the earth's atmospheric constituents as a function of wavelength. EMR scattering is also wavelength dependent. However, our focus will be on the EMR absorption when concerning the greenhouse effect.

Referring to the second panel, the gray regions indicate the wavelength intervals over which the atmospheric constituents absorb EMR. The major atmospheric constituents that cause the greenhouse effect, known as **greenhouse gases**, are shown in the bottom (third) panel. Most of the UV portion of the spectrum is absorbed by oxygen and ozone or undergoes **Rayleigh scattering**. However, the earth's atmosphere is rather transparent for the visible portion of the solar spectrum. This is the **atmospheric window** of solar radiation.

[4]https://www.google.com/search?q=solar+spectrum+figure

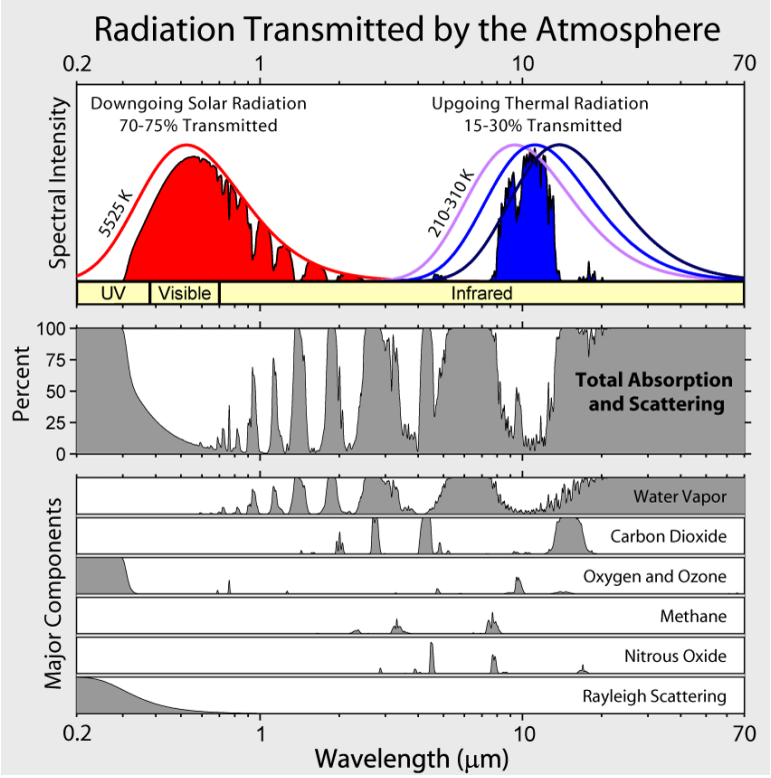

Figure 2.8: Absorption and scattering of the solar and terrestrial EMR spectrums.[4]

EMR in this wavelength range makes it through the atmosphere and is absorbed by the earth's surface.

The surface of the earth is warmed by the solar radiation. However, the average temperature of the earth's surface is much cooler than the solar surface, so the resulting EMR spectrum of the earths exist over longer wavelengths (lower energy). There is a narrower atmospheric window available for the terrestrial EMR. However, water vapor and carbon dioxide absorb a larger portion of the earth's EMR.

2.6.1 Energy Balance Models

Straight-forward and simple calculation using geometry and simplifying assumptions can be used to estimate the average surface temperature of the earth. The unifying principle for a number of similar models is the concept of **energy balance**; the rate of energy onto the earth's surface must equal the rate of energy leaving the surface when the earth's surface

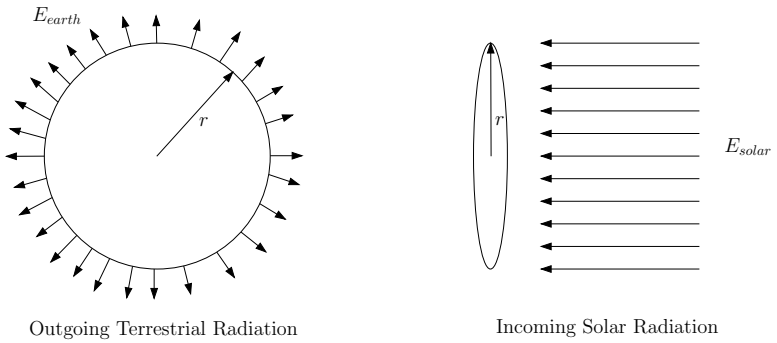

Figure 2.9: Energy flux for the no atmosphere model.

temperature is in equilibrium. That is

$$F_{out} = F_{in} \tag{2.8}$$

where F represents the flux of energy in watts. (Recall that a watt is a joule (energy) per second. The expression of energy per time is the same as "power.") Two initial cases will be considered in this section. The first will be for the case of no earth atmosphere and the second will assume the earth's atmosphere can be taken to be a single uniform "slab" of air.

No Atmosphere Model

The Stefan-Boltzmann formula relates the flux radiance, or emittance E (in watts per square meter), to the temperature T of the body by

$$E = \epsilon \sigma T^4 \tag{2.9}$$

where ϵ is the emissivity of the body (the value is between zero for nothing like a blackbody and 1.0 for an object that is truly a blackbody radiator), and σ is the **Stefan-Boltzmann constant** ($5.67 \times 10^{-8} \frac{W}{m^2 K^4}$).

The total outgoing terrestrial radiation F_{out} is given by the product of E and the surface area of the earth ($4\pi r^2$) where r is the earth's radius. The incoming solar radiation F_{in} is given by the product of the solar emittance magnitude of the solar emittance E and the effective surface area of the earth in the flow of solar radiation as it emanates from the sun. The former magnitude is measured at the top of the earth's atmosphere and is taken to be a constant equal to 1367 $\frac{W}{m^2}$. The effective surface is that of a disc of radius r, where r is the earth's radius. The effective surface is what the sun would "see" when looking at the earth, much like what the moon looks like to us when we view it from the surface of the earth. Another factor in estimating the incoming flux is the earth's average albedo α,

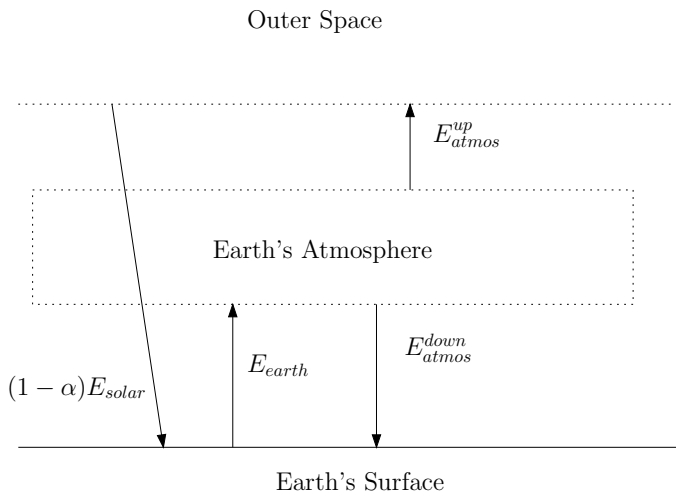

Figure 2.10: The single layer model for the earth's atmosphere.

the portion of the incoming solar radiation that is reflected (not absorbed) by the earth's surface. The value is taken to be 0.33. The resulting balance equation using these formulas becomes

$$4\pi r^2 \epsilon \sigma T^4_{earth} = \pi r^2 (1-\alpha) E_{solar} \tag{2.10}$$

Solving for T_{earth} gives

$$T_{earth} = \left(\frac{(1-\alpha)E_{solar}}{4\epsilon\sigma} \right)^{1/4} \tag{2.11}$$

Substituting values for α, ϵ and E_{solar}, the resulting estimates for the earth's average surface temperature is approximately 253K, or -20°C. This is approximately 35°cooler than the observed average of 15°.

Single Layer Model

In a one-layer model, the earth's atmosphere is considered to be a single "slab" that selectively absorbs and emits energy. Recall the selectivity is due to the atmosphere not being a good blackbody radiator because of its gaseous nature. Figure 2.10 shows the various components in the simple model as well as the various emittances. The principle of balanced fluxes at each of the component boundaries, along with the Stefan-Boltzmann formula, will be used to determine the temperature of the atmosphere and the earth's surface. Working from the top down, at the atmosphere-outer space boundary we have

$$F_{In} = F_{Out} \tag{2.12}$$

which translates to the equation

$$\pi r^2(1-\alpha)E_{solar} = 4\pi r^2 \epsilon \sigma T_{atmos}^4 \tag{2.13}$$

where the incoming surface is the disk and the outgoing surface is the sphere, each with radius r of the earth. Note that this equation is identical to the Earth temperature equation without an atmosphere. The result gives an atmospheric temperature of 255 K. This may be considered to be the "skin" temperature of the earth, or the temperature that would be sensed by a probe stationed just outside the earth's atmosphere.

We continue downward in order to determine the earth's surface temperature. The next constituent boundary to consider is that of the atmosphere. Using the principle of equilibrium again, we have

$$F_{In} = F_{Out}^{down} + F_{Out}^{up} \tag{2.14}$$

giving rise to

$$4\pi r^2 \epsilon \sigma T_{earth}^4 = 4\pi r^2 \epsilon \sigma T_{atmosphere}^4 + 4\pi r^2 \epsilon \sigma T_{atmosphere}^4 \tag{2.15}$$

The surface for both components is the sphere with radius r equal to the earth's radius. The common factors of 4π, r^2, ϵ, and σ may be divided out to give

$$\begin{aligned} T_{earth}^4 &= T_{atmosphere}^4 + T_{atmosphere}^4 \\ T_{earth}^4 &= 2T_{atmosphere}^4 \\ T_{earth} &= 2^{1/4} T_{atmosphere} \end{aligned} \tag{2.16}$$

The last equation gives the surface temperature of the earth to be $2^{1/4}$ (= 1.189) times the temperature of the atmosphere. This results in a value of approximately 303^o Kelvin, or roughly 26^o C. Although this is warmer than the observed average of about 15^o C, it is closer than the temperature determined using the no atmosphere scenario.

2.7 Energy Budget

Next we will consider a more comprehensive view of energy considerations involving the incoming solar radiation, the earth's atmosphere, and the earth's surface. Referring to Figure 2.11, we begin by supposing 100 units of energy (joules) are passing through an area of, say, one square meter at the very "top" of the earth's atmosphere every second. In actuality, the earth receives something like 1367 W/m^2 on average (over time) at the "top" of the atmosphere, but we will use "100" because it is a better number for sake of accounting. Further, we will assume that the system is in equilibrium which means the average temperature of the atmosphere and the average temperature of the earth are constant in time.

The first consideration is the "albedo, " or reflectivity, of the atmosphere and earth's surface. This is the amount of incoming energy that is simply reflected back to outer space.

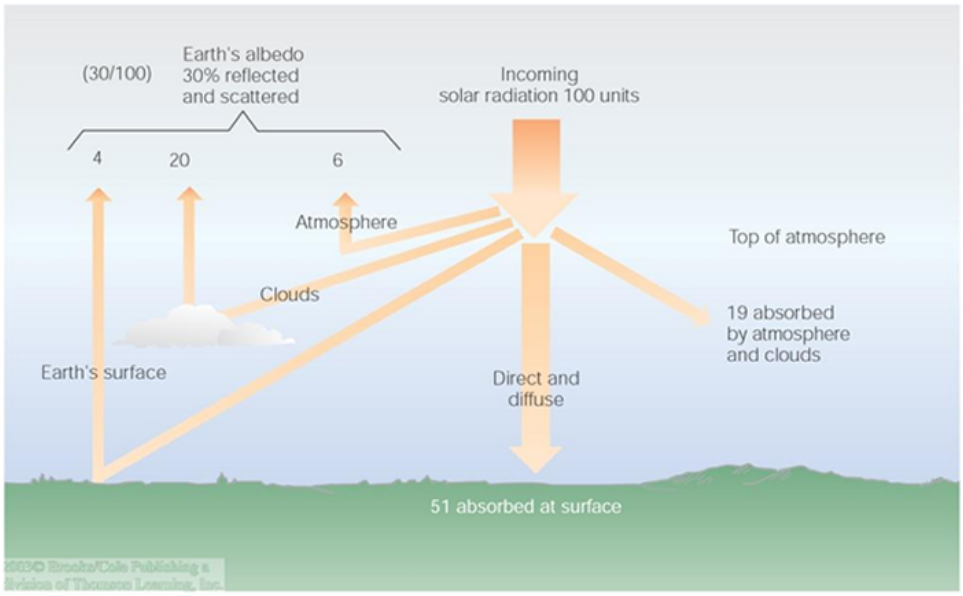

Figure 2.11: Earth's albedo.

Because it is not absorbed, no warming occurs, and no additional consideration is necessary. Reflection is caused by the atmosphere itself, white clouds (high, cold, ice-crystal clouds) by light-colored surface components (ice and snow). The respective amounts of reflection for each of these features are shown in Figure 2.11. All told, about 30% of the incident solar radiation is reflected back to outer space.

The remaining 70 units, shown near the top of Figure 2.12, are absorbed by either the atmosphere (19 units) or the earth (51 units). This means that about 27% of the incoming solar radiation is directly absorbed by the atmosphere. The other 73% passes through the atmosphere, absorbed and unreflected, to be absorbed by the surface of the earth. It may be helpful to think of the atmosphere and the earth's surface as separate "stores" of energy. The energy absorbed these stores translates directly to the temperature of the component. If these component temperatures are constant over an interval of time, then the rate of energy absorption must be balanced by an equal rate of blackbody energy emission.

In addition to the 51 units of energy the surface receives directly from the sun, the natural greenhouse effect due to the atmosphere's greenhouse gases transmits 96 units of radiant to the surface store. Consequently, the surface receives a total of 147 units of energy as shown in Figure 2.12.

Under the assumption of constant temperature, the earth must "give up" 147 units of energy to equal the inflow. We already know one such mechanism for energy transfer is radiation. Through the use of satellite measurements and assumptions of equilibrium, the

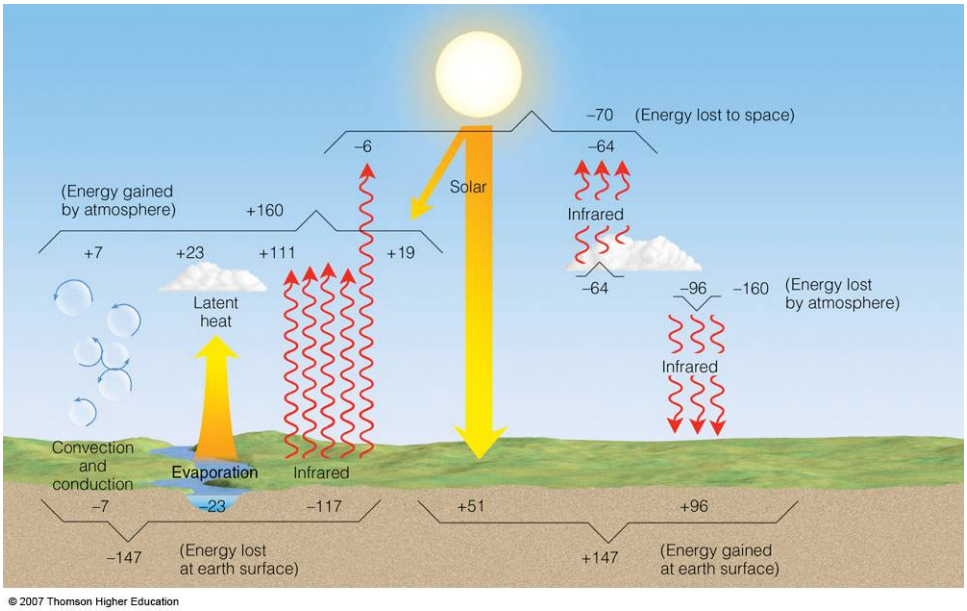

Figure 2.12: Earth's energy budget.

net radiation loss from the earth's surface is 117 units. Radiation off the surface of the earth either escapes to outer space (6 units) or is absorbed by the atmosphere (111 units) as shown in Figure 2.12. Another 23 units is lost from the surface through evaporation (latent heat transfer), the entirety of which is absorbed by the atmosphere. Conduction and convection account for the remaining 7 units that must be lost from the earth's surface to assure an energy balance at that interface.

Considering the atmospheric store of energy, the incoming energy total is 160 units, with all but 19 coming from the surface of the earth. Recall that the earth's atmosphere has a relatively small terrestrial radiation window compared to the solar window, so the majority of the incoming energy is terrestrial radiation. Latent heat transfer, conduction and convection make of the remaining 160 units absorbed by the atmosphere. The assumption of a stable atmospheric average temperature implies that the atmosphere must emit 160 units. Of those, 96 units are "returned" to the earth's surface, while the other 64 are lost to space. These 64 units and the 6 units lost directly to space when emitted from the surface combine to equal the 70 units solar units originally absorbed by the either the atmosphere or the surface.

Now that we have developed an understanding of energy, energy measurements, energy transfer mechanisms, the natural greenhouse effect and the earth-atmosphere average energy transfer budget, we move to the next chapter to understand the primary spatial and temporal controls (influences) of temperature.

Chapter 2 Exercises

2.1 A single 100-watt bulb is lit for 1 hour.

(a) Determine the amount of energy, in joules, consumed by the bulb in one hour.

(b) Calculate the vertical distance, in meters, this amount of energy would lift a 150-pound person.

2.2 A motionless (so KE = 0) two-liter parcel of dry air starts at an elevation of 1200 meters.

(a) Calculate the mass of the air parcel. Assume $\rho_s = 1.22$ g/L.

(b) Calculate the potential energy (PE) of the parcel.

(c) The parcel falls to the surface (where its PE is zero) and its vertical speed reaches 20 $\text{m}\cdot\text{s}^{-1}$. Calculate the kinetic energy (KE) of the parcel.

(d) Note that the gain in KE of the parcel is less than the loss in PE of the parcel. How would you account for (explain) the difference in these numbers? Consider the other form of energy the parcel has, as well as possible mechanisms that may cause a net loss of energy of the parcel.

2.3 A 100 L parcel of air has an initial horizontal speed of 10 $\text{m}\cdot\text{s}^{-1}$. As it moves along the surface of the earth, friction slows the parcel to 5 $\text{m}\cdot\text{s}^{-1}$. If half of the KE lost by the parcel heats the parcel, determine the temperature rise of the parcel in °C. Assume the parcel's density is 1.22 g/L.

2.4 Suppose 500 g of water vapor condenses to make a cloud about the size of an average room.

(a) Assuming the latent heat of condensation is 600 cal/g, how much energy would be released to the dry air in the room?

(b) If the total mass of dry air is 100 kg, calculate the change in temperature (ΔT) of the dry air in degrees C.

2.5 A summer thunderstorm dumps a uniform 1 inch of rain on the area within the city limits of Decorah.

(a) Calculate the volume of water (in cubic centimeters) in this rainfall. (NOTE: The area within the city limits of Decorah is roughly 6.4 square miles.)

(b) Estimate the amount of latent heat (in joules) released into the atmosphere during such an event. Assume all of the rainfall mass began as water vapor and condensed into raindrops.

(c) The atomic bomb that destroyed Hiroshima near the end of World War II is estimated to be equivalent to 20 kilotons of TNT. Calculate the ratio of energies (thunderstorm energy /bomb energy) of these events given that a kiloton of TNT is equivalent to 4.2×10^{12} joules.

2.6 The average surface temperature for Decorah on June 21 is 65°F.

(a) Use the Stefan-Boltzmann formula to determine the total energy, in Joules, that earth's surface will radiate from a one-meter square area over a 24-hour period.

(b) The U.S. Energy Information Administration reports that the average daily electricity use by an American household is approximately 30 kilowatt-hours (kWh). Converting this to the number Joules is done by multiplying by 1000 (kilowatts to watts) and then by 3600 (watt = J/sec times 3600 sec per hour) resulting in an energy use of 108 million Joules. What percentage of this number could be supplied by the Earth's long wave radiation assuming perfect efficiency in capturing and converting the energy for household use?

2.7 Planet A and planet B belong to a distant solar system.

(a) A astrophysicist determines the wavelength of maximum energy emission is 7.2425 μm for planet A. Determine the surface temperature of the planet A in Kelvins.

(b) The total power emitted from the surface of planet B is 459,279 watts. The surface temperature of the planet is 300K. Determine the surface area of the planet B in m^2

.

2.8 The purpose of this exercise is to determine the net thermal radiation loss or gain of the human body on a daily basis. The skin surface of a human body is a boundary between two objects that emit thermal EMR throughout the day. One object, of course, is the human body. The other is the atmosphere that surrounds the human. The surface area of these two objects is just the surface area of the human because the atmosphere surrounds the human. Suppose the surface temperature of a human body averages 90°F, and the atmospheric temperature surrounding the human is a constant 70°F. Use the Stefan-Boltzmann formula to calculate the total net radiation, in large calories, for the human body on a 24-hour basis. Assume a total body surface area of 1.7 m^2 (The average is 1.8 for males and 1.6 for females[5].)

2.9 If you were to design a thermal imaging device for the detection of human bodies, for what approximate range of wavelengths, in μm, should the device be most able to detect?

2.10 A very simple energy balance model for estimating the Earth's average global annual temperature is

$$I_{in} = I_{out} \Rightarrow \pi r^2 (1 - \alpha) E_{solar} = 4\pi r^2 \epsilon \sigma T_{earth}^4$$

[5]Bender, Arnold E. & David A. Bender. Body Surface Area. A Dictionary of Food and Nutrition. New York: Oxford University Press, 1995.

where r is the Earth's radius, $\alpha = 0.33$ is the Earth's albedo, $\sigma = 5.67 \times 10^{-8}$ is the Stefan-Boltzmann constant, $E_{solar} = 1367$ is the solar constant and ϵ is the Earth's emissivity.

(a) T_{earth} is known to be 15°C. Determine the Earth's emissivity.

(b) Data suggest that since 1972, Arctic ice has been decreasing at an average rate of about 3 percent per decade, while Antarctic ice has increased by about 0.8 percent per decade[6]. The net loss of polar ice results in a decrease in the Earth's albedo. Using the value for ϵ found in part (a), estimate the Earth's average surface temperature if the earth's average albedo decreased to 30%.

[6]National Snow and Ice Data Center (https://nsidc.org/)

Chapter 3

Temperature Controls

3.1 Overview

Temperature is, arguably, the most important atmospheric variable. The controls on temperature are explored in this chapter. The controls, or influencers, are cyclic phenomena defined by their period length and magnitude. The various influencers are described in a sequence of decreasing period length. The longest term controls are known as Milankovitch cycles, named after the Serbian geophysicist and astronomer Milutin Milankovitch who first hypothesized the theory in the 1920s. Proxy data constructed from ice, rock and deep ocean cores have support the projected Earth and atmospheric responses due to the **Milankovitch cycles**.

The chapter closes with discussion about the features that control variations in temperatures on annual, seasonal and daily intervals. The annual and seasonal periods align with climatological observations. The causes of temperature fluctuations on the daily time scale include weather or meteorological phenomena.

3.2 Milankovitch Cycles

Temperature is the measure of the average kinetic energy of molecules in motion that make up and object. The single source of energy that eventually translates to the molecular kinetic energy is the sun. Changes in the Earth's orbit around the sun cause variation in the magnitude and distribution of solar radiation absorbed by the Earth's atmosphere and surface. Additionally, the orientation of the Earth's axis of rotation controls the distribution of solar radiation absorbed by the Earth. Milankovitch postulated the existence of three cyclic variations; two related to the Earth's orbit and one associated with the orientation of the Earth's axis of rotation.

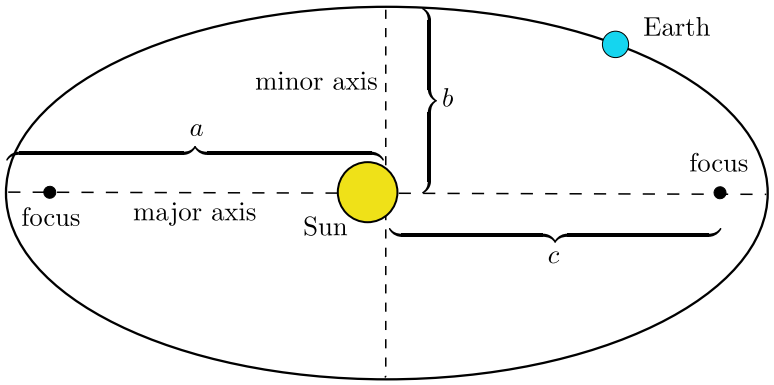

Figure 3.1: The Earth's orbit around the sun with major and minor axes.

3.2.1 Eccentricity (e)

The path traced about by the Earth as it completes its orbit is elliptical as shown in Figure 3.1. The Earth makes a complete orbit around the sun every 365.25 days. The time required to complete one orbit is know as the **period**. The elliptical orbit means the distance between the Earth and the sun is not constant. Additionally, the sun is not at the center of the ellipse, resulting in a single minimum distance, know as the **perihelion**, and a unique maximum distance, known as the **aphelion**. The former occurs on January 3rd, and the later on July 4. The amount of solar radiation at perihelion is about 6.8% more than that received at aphelion even though the decrease in distance is approximately 3.4% (5.1 million km).

An ellipse has a semi-major axis, with a length designated as a and a semi-minor axis, with a length designated as b. Since $a > b$ for an ellipse, the values c, defined by $c^2 = a^2 - b^2$, are locations of the ellipse's **foci** on the semi-major axis, as shown in Figure 3.1. The magnitude of **eccentricity** e is defined by the ratio

$$e = \frac{c}{a} \tag{3.1}$$

An e value of 0 implies a perfectly circular orbit because $e = 0 \Rightarrow b^2 - a^2 = 0 \Rightarrow b = a$. The range for the Earth's eccentricity is $0.000055 \leq e \leq 0.0679$. Therefore, the Earth's orbit is never a perfect circle, and at its greatest eccentricity, the major axis is 0.16% longer than the minor axis. Throughout the entire cycle of eccentricity change, the major axis length remains constant and the minor axis undergoes a change in length. As the minor axis shortens, the magnitude of seasonal differences in temperature increases.

The eccentricity magnitude time-series has multiple components which drive a more complicated relationship of e as a function of time, as shown in Figure 3.2. A simpler cyclic plot would have an amplitude with uniform temporal spacing between the peak and

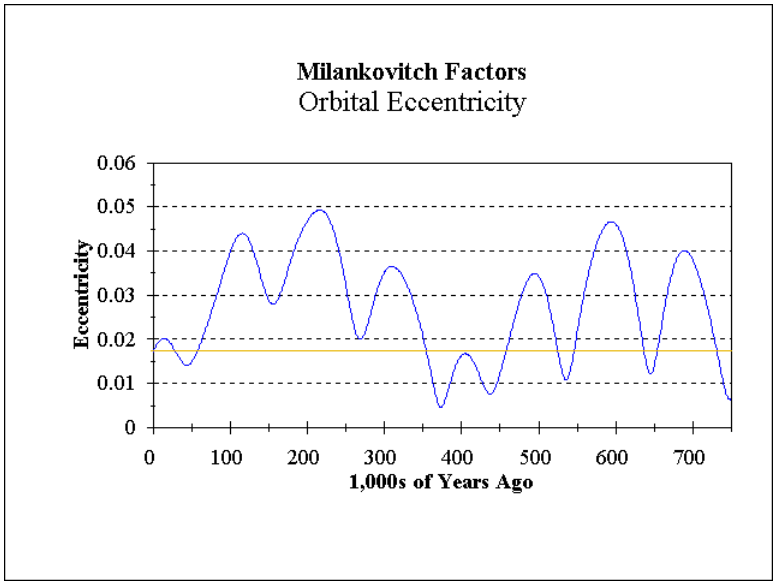

Figure 3.2: Orbital eccentricity versus time in years.

valleys, such as the plot of the sine function. The predominant period for the e curve is approximately 413,000 years, roughly the temporal spacing between the two highest peaks in the figure. Local extrema in the amplitude are caused by portions of the e signal with periods of approximately 125,000 and 95,000 years.

The change in orbital eccentricity is due to the gravitational pull of the planets Jupiter and Saturn. Knowing the the change in orbit is due to the interaction gravitational pulls of the three planets as well as that of the sun gives insight into why the e response as multiple embedded cycles.

Figure 3.3 depicts the average daily solar flux at the top of the atmosphere as a function of Julian day number ($1 \leq$ day number ≤ 365) and latitude ($-90° \leq \phi \leq 90°$). The northern hemisphere maximum is approximately 525 Wm^{-2} at the north pole on summer solstice in late June. This is less than the southern hemisphere "summer" maximum of 563 Wm^{-2}. The Earth is closer to the sun on the winter solstice. The daily average flux at the equator varies much less so, with an approximate range of 425 - 440 Wm^{-2}.

Figure 3.4 shows the percentage difference in daily flux, as a function of day and latitude, between the most eccentric orbit ($e_2 \approx 0.06$) and the current orbit ($e_1 = 0.017$). The obliquity (tilt of the Earth's axis of rotation) is the same (obliquity = 23.45°) for both cases. The greatest percentage change is just over 10% of the maximum of 563 Wm^{-2}, giving a change in magnitude of 56.3 Wm^{-2}. The biggest change occurs at the poles with the NH summer receiving 7% less, but then rapidly transitioning to receiving 10% more at the autumnal equinox. It is important to note that Figure 3.4 depicts a change mostly in

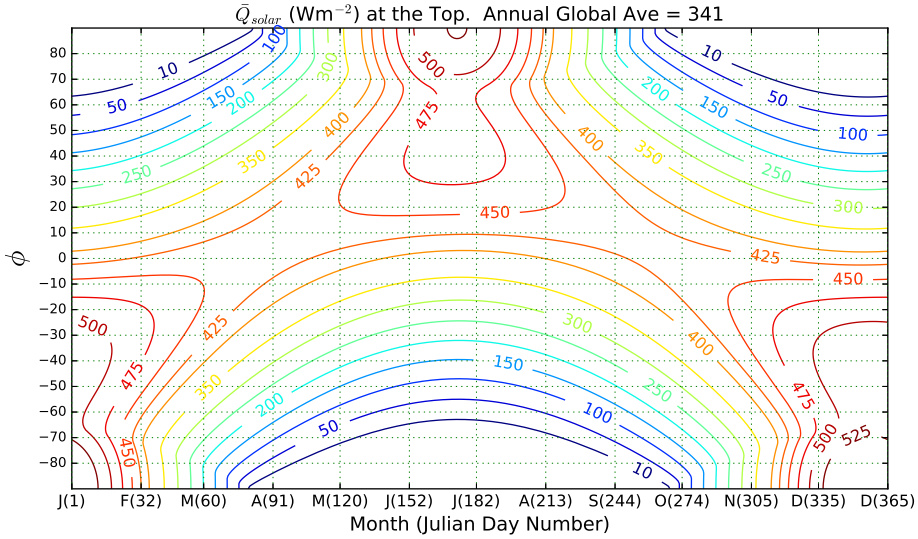

Figure 3.3: Solar flux at the top of the atmosphere with $e = 0.017$.

flux *distribution* because the global annual average of solar flux at the top of the Earth's atmosphere differs by less than 1 Wm^{-2}. That is, the flux deficit over some regions of the earth is almost matched by the flux gain in other areas.

3.2.2 Orbital Inclination (ϵ)

The Earth's elliptical orbit defines a plane in three-dimensional space. The sun's equatorial circle defines another three-dimensional plane. The orbital axes are vectors perpendicular to the respective planes as shown in Figure 3.5. The angle between theses vectors defines the angle of inclination ϵ of the Earth's orbit. Its current value, relative to the plane defined by the solar equator, is approximately 7.2°. The inclination angle drifts up and down and is known as **planetary precession**. The period length is approximately 100,000 years and it, as well as the 100,000 year component of the eccentricity cycle, correlates closely with the 100,000 year period in of Earth's ice ages.

3.2.3 Obliquity (o) and Axial Precession

The Earth revolves around the sun and rotates on its axis, the imaginary line in three dimensional space that passes through the Earth's north and south poles. The rotation axis is not perpendicular to the Earth's orbital plane. It tilts 23.44°off the perpendicular, as indicated in Figure 3.6. The obliquity (o) ranges from a minimum of 22.1° and a maximum of

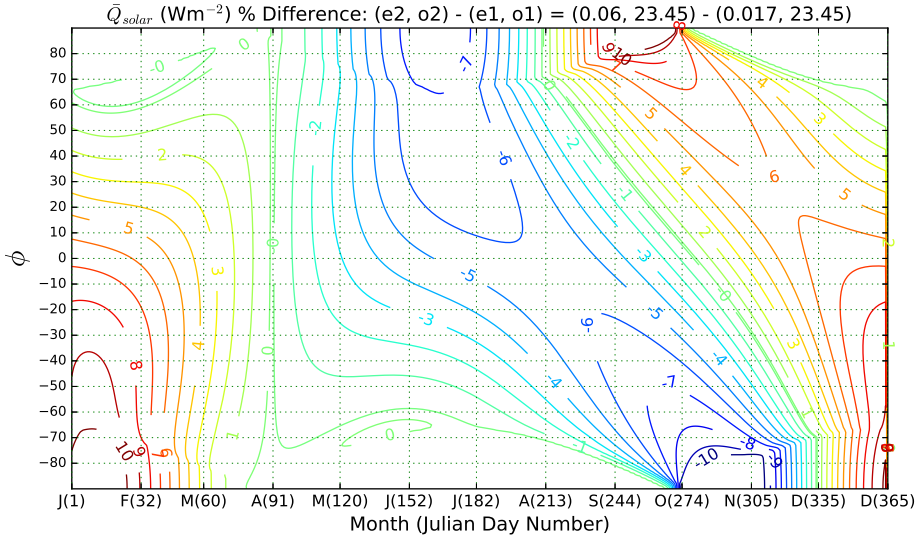

Figure 3.4: Solar flux percentage difference for eccentricities of $e_2 = 0.06$ and $e_1 = 0.017$.

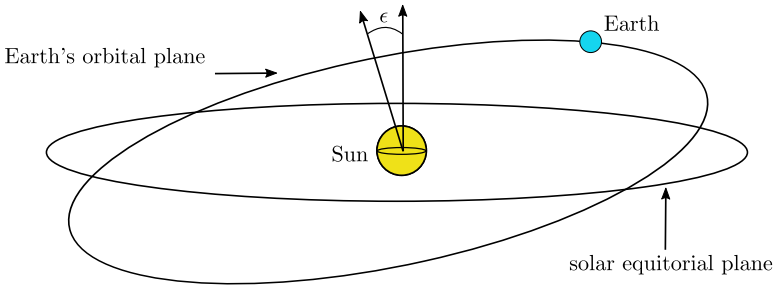

Figure 3.5: The Earth's orbital inclination angle ϵ.

24.5° over a period of approximately 41,000 years. The Earth's axial obliquity is responsible for the seasonal temperature differences. The northern hemisphere winter occurs when the northern "end" of the axis is tipping away from the sun as shown in Figure 3.6. Further, the greater the obliquity, the greater the difference in seasonal temperatures.

Figure 3.7 graphs the percentage difference in daily solar flux for obliquity values of 22.1° and 23.45° for an orbital eccentricity value of e = 0.017.

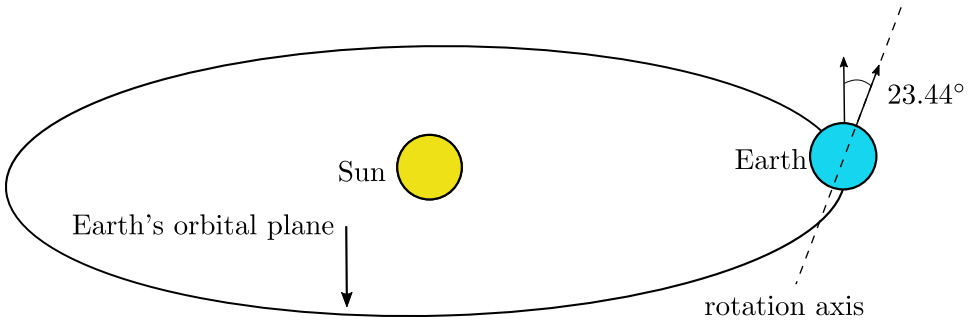

Figure 3.6: Earth's angle of obliquity is currently 23.44°.

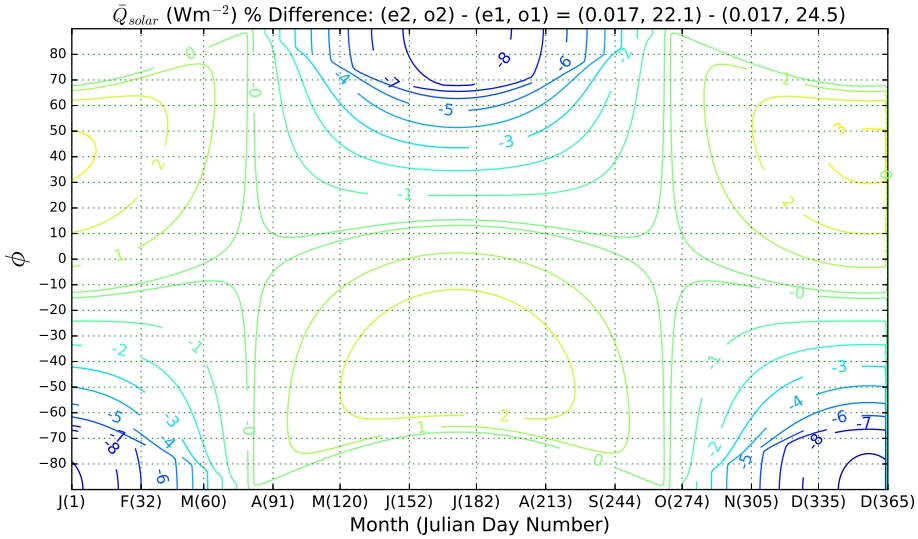

Figure 3.7: Solar flux percentage difference for obliquity values of 22.1° and 23.45°. The orbital eccentricity value is e = 0.017 for both obliquities.

3.3 Apsidal Precession

The is another variation in the Earth's elliptical orbit known as the **Apsidal precession**. In this case, the orbit remains in its *original* plane, but the orientation of it semi-major and semi-minor axes change as shown in Figure 3.8. This cycle is a relatively *new* discovery. It has a period of 112,000 years.

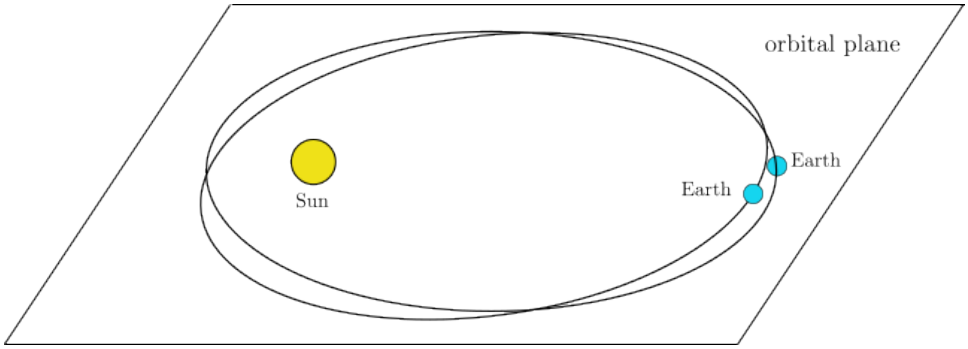

Figure 3.8: Apsidal precession. Both orbits are in the same plane. The difference between the orbits is the orientation of the major and minor axes.

3.4 Annual and Seasonal Controls

The periodic controls of temperature experienced in a personal life time are much shorter in time than those associated with changes in the Earth's orbital shape, orbital plane angle, and the tilt of the Earth's axis. The shorter control cycles are created by the 365.25-day period of the earth's orbit around the sun, and the 24-hour period of the earth's rotation on its axis.

Season temperature control is the result of the tilt of the earth on its axis of rotation as the earth orbits the sun. As the earth orbits the sun, the axis tilts away from the sun in the winter, and toward the sun in the summer as depicted in Figures 3.9 and Figure 3.10, respectively.

The sun's radiation waves travel a sufficient distance to reach the earth so that they may be taken to be directed in a "stack" of parallel lines.

In the winter, the earth's axis tilts away from the sun creating an earth actual surface area that tilts away from the perpendicular orientation with an angle measure of α_w. The surface area of a mid-latitude location is shown on the surface of the earth. An enlarged view is shown as well in the figure to the left of the earth's image.

The solar radiational irradiation is measured in watts per square meter per time. If the area the parallel lines of solar radiation strike has a face that is perpendicular to the wave direction, the area receiving the fixed amount of radiation is as small as possible, so the energy per area per time is a maximum. This perpendicular face has length L_p in figure 3.9.

In the case of the mid-latitude area, the solar radiation "stack" does not strike an area with a face perpendicular the the radiation path. Instead, the actual area this fixed amount of energy strikes is greater because length L_w is greater than that of a perpendicular face, L_p. Consequently, the earth's surface area receives less energy per area per time. Additionally,

the greater the angle α, the greater the surface area for the fixed amount of radiation, so the lesser the energy amount per area (Watts per square meter).

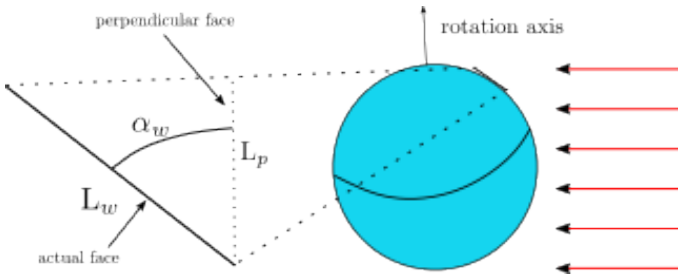

Figure 3.9: Earth axis tilting away from the sun in the northern hemisphere winter.

In the northern hemisphere summer, to earth axis is oriented in a way that tips the northern hemisphere towards the sun. Now, the parallel ray strike a surface that is slanted less than that in the winter, but still by angle $\alpha_s > 0$. However, $\alpha_s < \alpha_w$, so $L_s < L_w$. Consequently, this same mid-latitudinal area receives more energy per meter squared in the summer than it does in the winter.

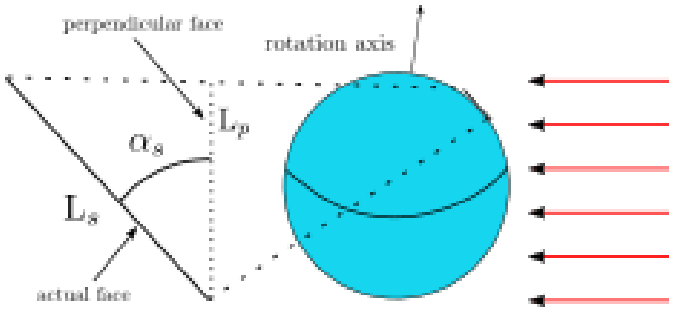

Figure 3.10: Earth axis tilting towards the sun during the northern hemisphere summer.

The annual incoming solar radiation for a midlatitude location such as Decorah, Iowa (43.3° N) is shown in Figure 3.11. The figure shows how dramatic a change in incoming solar radiation is in response to the tilt and the associated change in the energy per area.The maximum value is 486.7 Watts $\cdot$ m^{-2} on June 21st and the minimum value is 133.3 $\cdot$ m^{-2} on December 21st.

If the earth's axis of rotation was not tilted, then the solar radiation input at a given latitude would be constant. consequently, the plot of solar input for Decorah would be a straight, flat line instead of the wavy plot shown in figure 3.11.

However, if the tilt of the earth's axis of rotation were greater, the mid-latitude solar insolation curve would have greater variance over the year. That would mean the plot

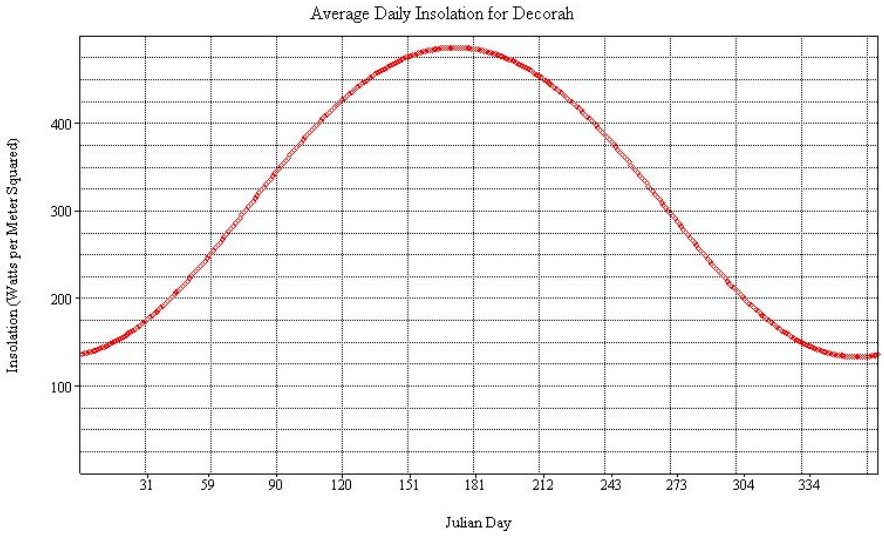

Figure 3.11: Daily incoming solar radiation at the "top" of the atmosphere for Decorah, Iowa, latitude 43.3° N.

would have great peaks and lesser valleys that that shown in Figure3.11. Consequently, there would be a greater difference in seasonal temperatures as well with colder winters and warmer summers than those the current tilt creates.

One might expect there is a latitude at which the insolation curve is 'flat" throughout the year. Although, a good guess would be that it occurs at the 23.5° N latitude, the same degree as the axis tilt, it actually occurs at 37.0° N latitude.

Figure 3.12 depicts the temperature response to seasonal and daily controls for Decorah, Iowa. The seasonal cycle lasting the course of a year is plotted in the smoother, dark-colored curves. The values on these two curves represent the historical daily average high and low temperature. The jagged red and blue curves show the daily high and low for each day for the calendar year of 2025. Successive peak or valleys in these curves are roughly separated by 24 hours in time.

The smoother curves of average temperatures in Figure 3.12 depict *climate* values, while the daily observed maximum and minimum curves represent *weather* readings.

It is interesting to compare the times when the incoming solar radiation is at a maximum and minimum to when the average daily temperature reaches a maximum and minimum value. The solar minimum occurs on December 21 while the daily maximum temperature minimum occurs near the end of January - about a 30 day "lag." A similar lags is seen between the solar maximum on June 21 and the average temperature maximum near the end of July.

The reason for the lag in the time it takes for the earth's surface temperature to either

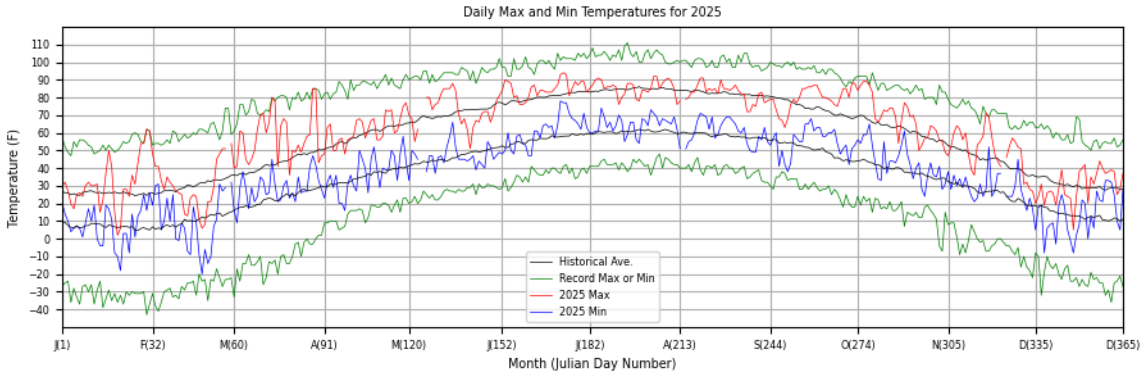

Figure 3.12: Daily high and low temperatures compared to averages for calendar year 2025.

rise or fall in response to the solar radiation and the consequential change in terrestrial radiation. The magnitude of terrestrial long wave radiation is directly related to the earth's temperature T_e ($E = \sigma T_e^4$). The eventual increase in loss due to terrestrial radiation eventually matches the magnitude of the incoming solar radiation at the time of the temperature maximum. As the sun's radiation becomes less, the net energy becomes negative, and the surface temperature begins to decrease.

In terms of the temperature minimum, the increase in solar radiation by the end of January is sufficient to match the terrestrial radiation loss. The temperature "bottoms out" near the end of January when the net energy is zero, and then begins to increase when the net energy is positive - more energy from the sun than energy lost by terrestrial radiation.

3.5 Daily Controls

Daily temperatures are influenced by a number of factors including the type of air mass that is sitting over a given location, the extend (vertically and time-wise) of cloud cover, and the depth and speed of horizontal winds.

3.5.1 Cloud Cover and Radiative Transfer

Shorter wavelength incoming solar radiation during the day time is reflected by high altitude light-colored clouds (ice-based) and impeded by low, darker and thicker water-based clouds as shown in Figure 3.13. Consequently, the day time maximum temperature will be lower than it would be if clouds were not present.

The night time scenario is depicted in Figure 3.13 as well. In this instance, terrestrial radiation is sourced from the earth's surface.

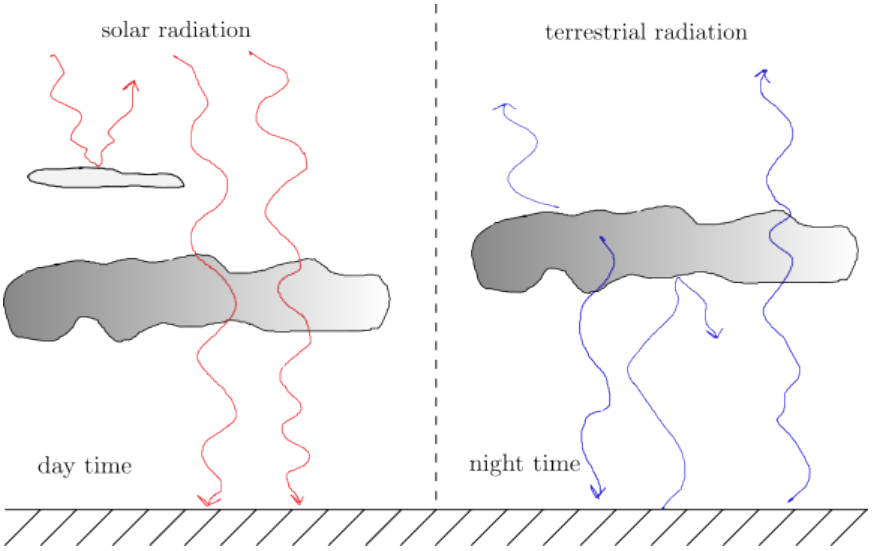

Figure 3.13: Clouds and radiation during the day and night times.

The longer wavelength of the radiation means some of the radiation is absorbed by the water-based clouds and re-radiated back the the surface. The result is warmer overnight temperatures.

3.5.2 Vertical Wind Shear and Mixing

Strong change in vertical winds, known as **vertical wind shear** can result in a rotational effect that moves parcels vertically as depicted in Figure 3.14. Figure 3.14a pertains to the day time case.

A normal daytime temperature profile includes a typical lapse rate of 6°C per 1000 meters. The lapse rate is indicated in Figure 3.14a by the dotted line that slopes to the left from the warmer surface parcels to the cooler near-surface parcels.

Wind speed generally increase with height, especially near the surface where friction effects slow winds to zero at location $z = 0$. When wind speeds at 1500 meters are very strong, the change in wind speed with elevation is intense enough to create a rotation in the vertical plane. This rotation, or mixing, lift the warmer parcels near the surface to higher elevations. Recall that the warmer surface parcels will not rise on their own due to buoyancy because their potential temperature is less than the parcels above them. The mass lost due to rising surface parcels is replaced by the sinking colder parcels from the higher elevation. The ultimate result is to cool the surface region and lessen the lapse rate.

The case for a strong night time vertical wind shear is shown in Figure 3.14b. Solar radiation loss at the surface of the earth as the sun sets causes the surface temperature to

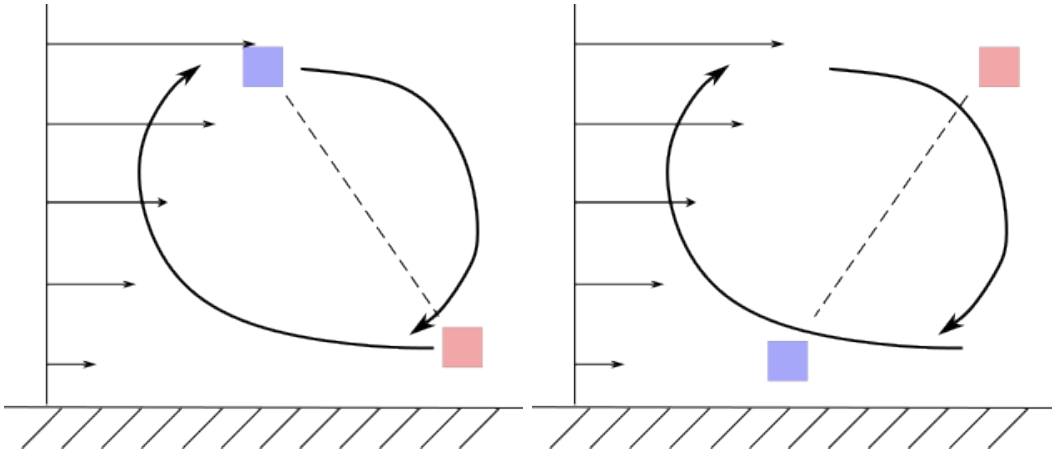

(a) Daytime mixing that cools the surface. (b) Nighttime mixing that warms the surface.

Figure 3.14: Near-surface mixing caused by steep vertical wind shear.

drop, significantly enough to create a temperature inversion - where temperature actually increases with elevation. The temperature inversion is indicated by the dashed line that slants to the right in Figure 3.14b.

The strong vertical wind shear creates a rotational circulation, or mixing, that brings warmer parcels to the surface and colder parcels to the higher elevation. The surface warming is enhanced by the fact that parcels warm as they drop in elevation. The rising parcels cool, so the temperature inversion can be lessened by a significant amount.

In terms of weather forecasting, the take away from the presence of strong vertical wind shear is that the daytime maximum temperature is less than it would, and the over-night minimum temperature is warmer than it would be without the strong increase of wind with elevation.

On clear calm evenings, the surface parcels cool greatly because net terrestrial radiation loss is greater, and the lack of winds means vertical mixing of parcels does not exist to warm the surface region. Under these conditions, a temperature inversion is apt to develop, mean the parcels above the surface are warmer than thos at the surface.

Daily maximum and minimum temperatures occurrence relative to daily radiation maximum and minimums follow a pattern similar;at to the seasonal case. The day time maximum temperature usually lags the time of maximum solar input by about four hours. It occurs at the time the incoming solar radiation magnitude is matched by the outgoing terrestrial radiation magnitude.

A lag with a shorter time length occurs for the 24-hour minimum temperature. It does not occur just at sunrise, as one would expect. Rather, there is a time lag due to the need for the solar input magnitude to match the terrestrial radiation loss. Once this occurs,

perhaps within an hour or so of the sunrise, the surface temperature begins to increase.

3.5.3 Parcel Moisture Content

The heat capacity of water, and water vapor, is greater than that for dry air. Consequently, dry air masses will experience a greater temperature swing during the day than moist air masses.

This effect is most prominent in desert regions of the earth where the air parcels may have close to a mixing ration of 0 grams per kilogram. Daytime highs may reach into the 80°F range, while overnight lows may fall into the 40 - 50°F range. In more humid areas of the world, temperature swings between the maximum and minimum will typically be 20-30°F.

A mathematical understanding of this phenomena is realized through the equation

$$\Delta Q = mC_p\Delta T \tag{3.2}$$

where ΔQ is the change in energy, m is the mass of the substance, C_p is the heat capacity, and ΔT is the change in temperature. If m and ΔQ are fixed but the heat capacity varies between the substance, the one with the lesser capacity C_p will have a greater change in temperature ΔT related to the same change in energy ΔQ.

The difference in heat capacities of water and dry land result in lesser temperature swings of water masses compared to land masses. As a result, coastal areas associated with large lakes (the Great Lakes, for example) and seas experience significant temperature differences between land and water areas. As a result breezes may form (Chicago is the 'windy city") that cool the land areas during the day. Overall, these coastal regions have temperature ranges that less than those at the same latitude that are completely land-based.

3.6 Radiation Energy Imbalance

Solar radiational energy input to the earth-atmosphere system is not equal in the vertical and horizontal (surface) directions. Vertically, the earth's surface receives a surplus of solar energy, and the atmosphere a relative deficit. In terms of the surface distribution, the equatorial region receives a surplus of solar radiation, while the polar regions are in a relative deficit.

If this were the "end of the story," the regions of surplus would continue to warm and the deficit regions would become cooler. However, the earth-atmosphere system has a fixed average annual temperature, so the "rest of the story" includes the means by which these energy imbalances are rectified.

These mechanisms work on long and short length and time scales. Long time and length mechanisms are the ocean circulations and planetary-scale atmospheric circulations that move energy pole-ward from the equatorial region. They are the predominant mechanisms

for balancing horizontal energy inequities. These are, essentially, the "climate" features. The shorter scale features are what might be considered the "weather" phenomena. They are responsible for rectifying both vertical and horizontal imbalances.

The next chapter introduces the forces that develop, for the most part, in response to the temperature imbalances. These forces create and characterize the winds that make up the circulations and storms that work to keep the earth-atmosphere system in a steady average temperature state.

Chapter 3 Exercises

3.1 Confirm that at its greatest eccentricity, the major axis is 0.16% longer than the minor axis as stated in Section 3.2.1.

Chapter 4

Forces & Winds

4.1 Overview

Atmospheric winds are parcels in motion. Understanding motion is predicated by a knowledge of a few principles, or laws, of motion defined by Sir Isaac Newton. These laws relate motion and forces. Coordinate systems provide a framework on which these laws are are written. There are two primary coordinate systems important to the description of atmospheric motion: Cartesian and polar-cylindrical. Next, the fundamental atmospheric forces from which winds are born are identified. Forces in balance sustain winds. Imbalanced forces cause changing winds. Various atmospheric forces are dominant in certain scenarios and distinguish the most important winds.

4.2 Coordinate Systems

Coordinate systems are extremely important tools in describing and understanding physical phenomena. Importantly, they provide the ability to describe the location and motion of an object in a given *space*. Space has dimension. In the meteorological realm, objects and their motion occur in one, two or three dimensions. Two-dimensional motion is usually thought of a *horizontal* motion, such as air parcels moving along a path that is parallel to the ground. Three-dimensional motion includes a vertical component along with the two-dimensional horizontal motion. Air parcels rising in the circulating updraft of a super cellular thunderstorm is an example of three-dimensional motion.

4.2.1 Cartesian Coordinates

The three coordinates in a three-dimensional Cartesian coordinate system are denoted using the letters x, y, and z. That is, the location of a point P is described exactly using the ordered triple (x, y, z).

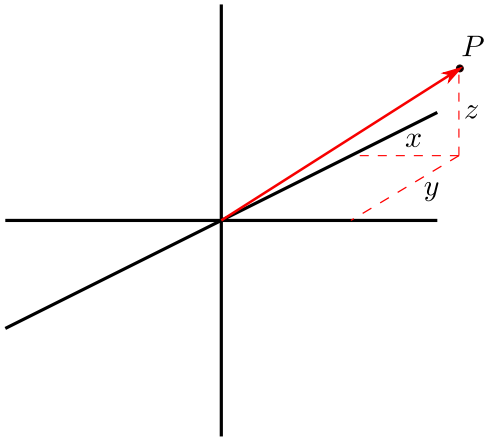

Figure 4.1: Three-dimensional Cartesian coordinate system.

4.2.2 Polar coordinates

In the three-dimensional polar coordinate system, the location of a point p is given by the radial distance r from the origin of the system to the point, the counter-clockwise angular measure θ from the positive x-axis to the radial line, and the elevation z from the reference xy-plane and the point. That is, $P = (r, \theta, z)$.

4.2.3 Vectors

The coordinate triples associated with a point in three-dimensional space are examples of the general concept of a **vector**. The line segment that begins at the coordinate system origin (the segment's *tail*) and ends at the point P (the segment's *tip*) in the space creates a natural arrow, a common way to think of a vector. It has a length, known as its *magnitude*, and a *direction*. Vectors in a physical domain such as the Earth's atmosphere have components that are numbers, or *scalars*. As opposed to vectors, scalars have magnitude only (So no little arrow is drawn above the scalar). The scalar component makeup of vectors allows definitions of vector operations such as vector addition by extending scalar addition (addition of numbers) to each component of the vector. If vector $\vec{v}$ = (3,7) and vector $\vec{u}$ = (-5,2), then

$$\vec{v} + \vec{u} = (3, 7) + (-5, 2) = (3 + -5, 7 + 2) = (-2, 9) \tag{4.1}$$

This process is visualized in Figure 4.3, where the addition of $\vec{u}$ ot $\vec{v}$ is seen as the result of moving $\vec{v}$ so that its tail is positioned at the tip of $\vec{u}$. The result of moving $\vec{v}$ is shown as a dotted vector in Figure 4.3. The new vector is the blue arrow that has its tail at the origin and its tip at the point (-2,9) in the two-dimensional Cartesian coordinate system.

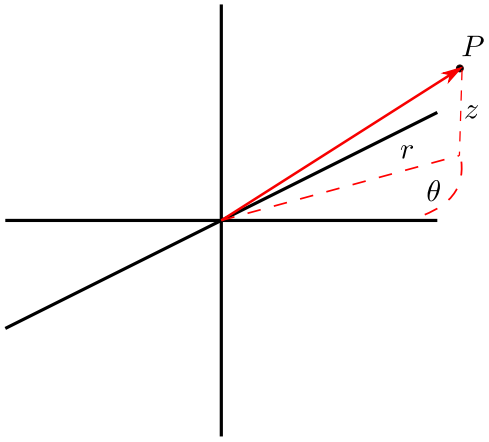

Figure 4.2: Three-dimensional polar-cylindrical coordinate system.

Scalar-vector multiplication of a vector $\vec{v}$ is defined as

$$a\vec{v} = a(v_1, v_2) = (av_1, av_2) \tag{4.2}$$

where a is a scalar and v_1, v_2 are the two scalar components of the two-dimensional vector $\vec{v}$.

When a = -1, the process results in a new vector with the same magnitude as the original vector but a direction that is opposite the original. This concept can be used to define vector subtraction in the following way Scalar-vector multiplication of a vector $\vec{v}$ is defined as

$$\begin{aligned} \vec{u} - \vec{v} &= \vec{u} + -1\vec{v} && (4.3)\\ &= (u_1, u_2) + -1(v_1, v_2) && (4.4)\\ &= (u_1, u_2) + (-v_1, -v_2) && (4.5)\\ &= (u_1 - v_1, u_2 - v_2) && (4.6) \end{aligned}$$

An example of the subtraction of one vector from another is visualized in Figure 4.4. Vectors $\vec{u}$ = (-5, 2) and $\vec{v}$ = (3, 7). Then $\vec{u}$ - $\vec{v}$ is shown with $-\vec{v}$ as a dotted arrow. The result of the subtraction is the red vector with coordinate pair (-8, -5).

The definition of vector addition based on scalar addition, the definition of scalar-vector multiplication, the definition of the *zero vector* ($\vec{0} = (0, 0)$) and the definition of the *negative vector* ($-\vec{v} = -1(v_1, v_2) = (-v_1, -v_2)$) means that vector addition *inherits* the following

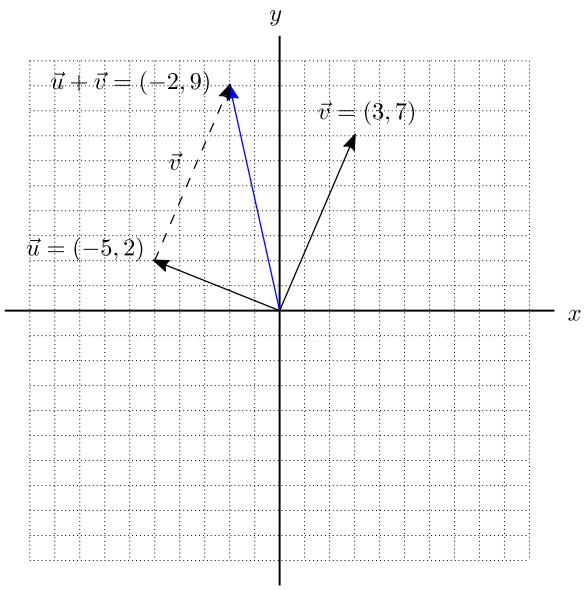

Figure 4.3: Two-dimensional vector addition.

useful properties of scalar addition

$$\vec{u} + \vec{v} = \vec{v} + \vec{u} \tag{4.7}$$

$$\vec{u} - \vec{v} = \vec{u} + -\vec{v} \tag{4.8}$$

$$(\vec{u} + \vec{v}) + \vec{w} = \vec{u} + (\vec{v} + \vec{w}) \tag{4.9}$$

$$\vec{v} + \vec{0} = \vec{v} \tag{4.10}$$

$$\vec{v} - \vec{v} = \vec{0} \tag{4.11}$$

4.2.4 Inertial Frames

A coordinate system can be thought of as a *frame* in which the position and motion of objects may be identified and tracked. An **inertial** or **Newtonian** frame is one that is not accelerating. This means that the frame is fixed (not moving), or if it is moving, its speed and direction of motion are not changing. A frame that is not motionless is non-inertial or non-Newtonian.

The difference in frame of reference is particularly important in planetary-scale atmospheric motions. Figure 4.5 shows the earth situated within a Newtonian framework. The coordinate system in this case is fixed and the earth is revolving on its axis of rotation, shown as a vector protruding through the north pole. Consequently, a object, such as an atmospheric parcel, sitting at rest on the earth's surface is seen to be moving by an observer

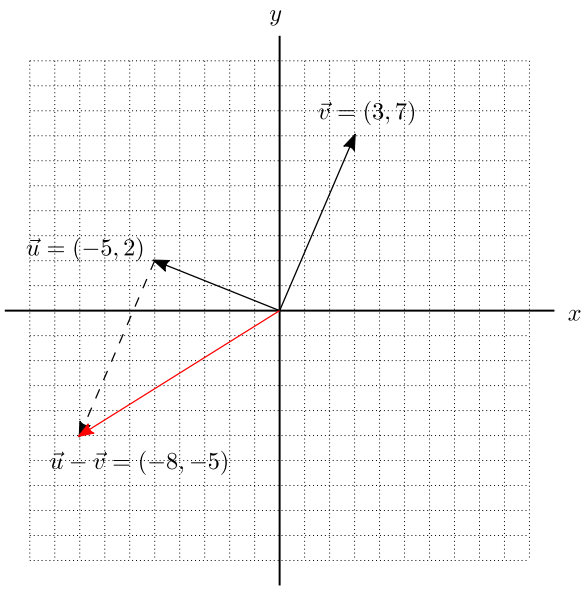

Figure 4.4: Two-dimensional vector subtraction.

who is stationary at any location in the frame of reference. This situation is in contrast to the framework shown in Figure 4.6. In this instance, the coordinate system is rotating in the same direction (counter clockwise) and speed as the earth. Consequently, the stationary air parcel on the surface of the earth is *stationary* in the rotating frame as well.

4.3 Newton's Laws of Motion

Wind, or motion of air parcels, is described by its magnitude (speed = distance/time) and direction (a southerly wind is one that comes from the south). Magnitude and direction define a **vector**. In the case of wind, it is the velocity vector. Vectors are denoted with a little arrow over the top of the letter symbol. So wind velocity is expressed as $\vec{v}$.

The dynamic nature of the earth's atmosphere means that velocity is not constant. The change in velocity with respect to time defines the wind **acceleration** and is denoted as $\overrightarrow{a}$. Formally,

$$\overrightarrow{a} = \frac{\Delta \overrightarrow{v}}{\Delta t} \tag{4.12}$$

where the Greek symbol Δ denotes the "change in" the quantity that follows the symbol.

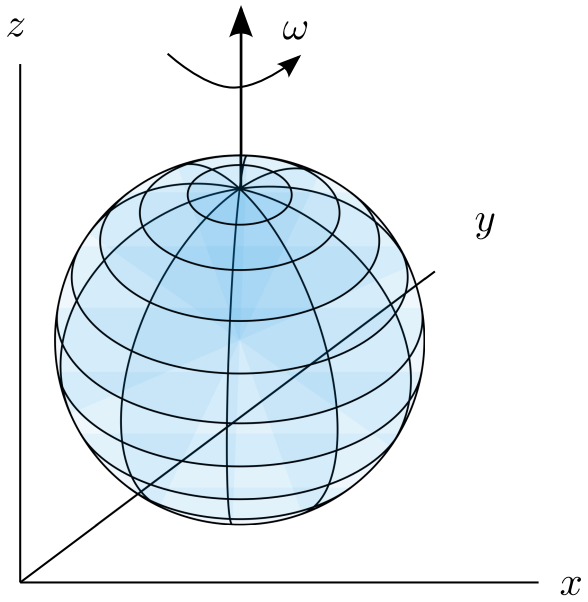

Figure 4.5: Earth within an inertial frame.

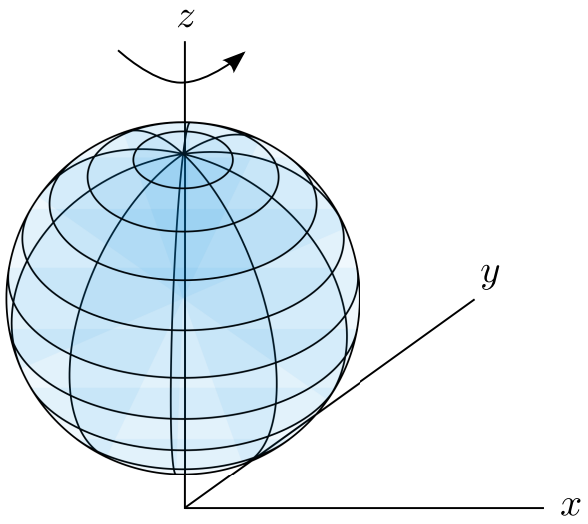

Figure 4.6: Earth within a rotating frame.

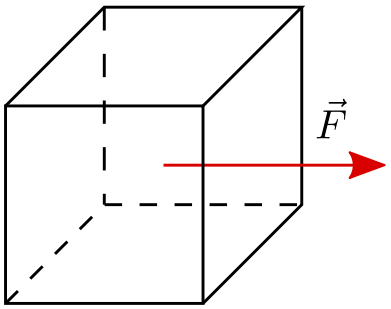

Figure 4.7: An atmospheric parcel with an applied force.

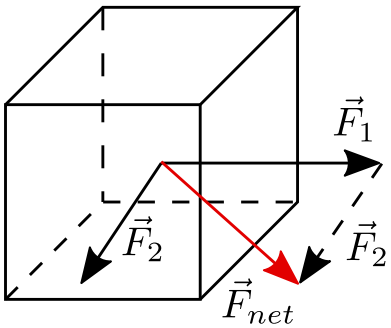

Figure 4.8: An atmospheric parcel with a non-zero net force resulting from the combination of two separate forces, $\vec{F}_1$ and $\vec{F}_2$.

4.3.1 Forces

A change in the velocity vector of an air parcel is caused by an imbalance of forces. A **force** in the physical world is an external cause or action such as a push or pull on an object. Force is a vector defined by its magnitude and direction. The force vector is usually shown as an arrow with its beginning point at the center (or center of mass) of the object, as shown in Figure 4.7.

A parcel often has multiple forces acting on it at once. In this case, it is important to identify the *net* force as the vector sum of the individual forces, that is $\vec{F}_1 + \vec{F}_2 = \vec{F}_{net}$. This process is visualized in Figure 4.8, where the net force is shown in red. The dotted arrow shown is the parallel "translation" of force $\vec{F}_2$ so that its tail is positioned at the tip of $\vec{F}_1$. Now that the concept of a net force has been introduced, Newton's laws of classical motion may be expressed and understood. Initially, the laws will be introduced for the one-dimensional case. That is, the case where parcel motion is limited to a single dimension.

4.3.2 Newton's First Law

Newton's first law states that if no net force is exerted on an object (a net force of magnitude zero), then

- an object at rest will remain at rest
- an object in motion will remain in motion without a change in velocity (there is no acceleration)

It is important to emphasize that this law does NOT state that an object with zero net force acting on it will not move. Rather, if it is moving, it is not accelerating (point 2). If it is not moving, it will not begin to move (point 1).

Parcels, or systems of parcels, on which the net force is zero are sometimes said to be in *equilibrium*. The parcel, or parcels, all have constant velocity vectors. That is, their vectors do not change over a given interval of time. Therefore, all parcels are standing still and remain standing, or all parcels are moving in a *straight* line with a constant speed (the magnitude of their velocity is constant).

4.3.3 Newton's Second Law in One Dimension

Newton's second law pertains, mostly, to cases where the net force on a parcel is not zero. It does hold in the trivial case where the net force is zero. With non-zero net force, the parcel's velocity vector will change in magnitude or direction. (This is an inclusive "or," so both magnitude and direction could change.) If F_{net} is the magnitude of the net force, v is the magnitude of the parcel velocity, and m is the constant mass of the parcel, then

$$m\frac{\Delta v}{\Delta t} = F_{net} \tag{4.13}$$

The law establishes that the magnitude of the rate-of-change of the velocity, $\Delta v/\Delta t$ times the mass of the parcel (m) is equal to the magnitude of the net force. Stated in a slightly different manner, the magnitude of the rate-of-change of the velocity, $\Delta v/\Delta t$, is proportional to the magnitude of the net force with the constant of proportionality being the reciprocal of the mass m, as shown in Equation 4.14. That is, for the same net force, the rate of change of the parcel's velocity will be less for a more massive (heavier) parcel. Think about how much faster you can get a bicycle to move compared to a car by you applying the same magnitude of force to either.

$$\frac{\Delta v}{\Delta t} = \frac{1}{m}F_{net} \tag{4.14}$$

The units on force in the MKS system (SI) are determined by examining Equation 4.13. The left-hand side of the equation has three components. Mass m is measured in kilograms,

velocity v (actually change in velocity) measured in meters per second, and change in time measured in seconds. Consequently, the units on F are

$$F \overset{units}{=} \text{kg} \cdot \text{m} \cdot \text{sec}^{-2} \tag{4.15}$$

A $\text{kg} \cdot \text{m} \cdot \text{sec}^{-2}$ is known as a **Newton**, abbreviated as "N."

4.3.4 Newton's Second Law in Vector Form

Atmospheric parcels do not always travel in a single straight line. Therefore, the velocity vector has multiple components. In the Cartesian coordinate system, the velocity vector $\vec{v}$ in "broken down" into three components

$$\vec{v} = (u, v, w), \tag{4.16}$$

where u is the speed of the parcel in the x direction, v the speed in the y direction, and w the speed in the z direction. The convention used in this manuscript is that the positive x direction point directly east, the positive y direction points directly north, and the positive z direction points directly "up." With this notation, $\Delta\vec{v} = (\Delta u, \Delta v, \Delta w)$. Note that the Δ "operator" is distributed to each of the vector components. Including the Δt factor results in

$$\frac{\Delta\vec{v}}{\Delta t} = \left(\frac{\Delta u}{\Delta t}, \frac{\Delta u}{\Delta t}, \frac{\Delta w}{\Delta t}\right) \tag{4.17}$$

The force vector is written as $\vec{F} = (F_x, F_y, F_z)$. Consequently, the vector form of Newton's second law is

$$m\frac{\Delta\vec{v}}{\Delta t} = \vec{F} \tag{4.18}$$

where $\vec{F}$ represents the net force. The component-wise forms of this equation are

$$m\left(\frac{\Delta u}{\Delta t}, \frac{\Delta u}{\Delta t}, \frac{\Delta w}{\Delta t}\right) = (F_x, F_y, F_z) \tag{4.19}$$

$$\left(m\frac{\Delta u}{\Delta t}, m\frac{\Delta u}{\Delta t}, m\frac{\Delta w}{\Delta t}\right) = (F_x, F_y, F_z) \tag{4.20}$$

Equating components gives three separate scalar equations.

$$m\frac{\Delta u}{\Delta t} = F_x \tag{4.21}$$

$$m\frac{\Delta v}{\Delta t} = F_y \tag{4.22}$$

$$m\frac{\Delta w}{\Delta t} = F_z \tag{4.23}$$

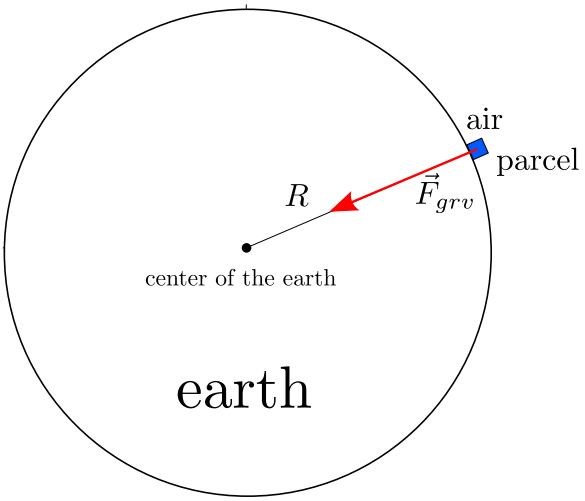

Figure 4.9: The gravitational force on an atmospheric parcel.

4.4 Atmospheric Forces

Newton's laws of motion pertain to reference frames that are fixed in space. Such frames are often referred to as **Newtonian**. In non-Newtonian reference frames, **apparent** forces will be identified so that Newton's laws will remain valid.

4.4.1 Gravitational Force: $\vec{F}_{grv}$

Two bodies of mass m_1 and m_2 attract each other with a force F_{grv} proportional to product of masses and inversely proportional to the square of the distance R between the centers of the bodies as shown in Equation 4.24

$$F_{grv} = G\frac{m_1 m_2}{R^2} \tag{4.24}$$

where G is the universal gravitational constant equal to 6.673×10^{-11} Nm^2/kg.

In most instances, the values for G, m_1 (the mass of the earth) and R are combined to give the constant value of $g = 9.8$ N/kg so that the gravitational force F_{grv} is given by

$$F_{grv} = -mg \tag{4.25}$$

where $m = m_2$, the mass of the object. In the instance of the earth's atmosphere, m is the mass of an atmospheric parcel. The minus sign is needed to indicate the *direction* of the force in *downward* (toward the earth's center and perpendicular to the surface at the point where parcel is located) because the positive direction for vertical motion is upward (away from the surface of the earth).

Applying Newton's second law of motion gives

$$m\frac{\Delta w}{\Delta t} = -mg \tag{4.26}$$

4.4.2 Horizontal Pressure Gradient Force: $\vec{F}_{hpg}$

The horizontal pressure gradient force is arguably the most important atmospheric force. Without this force, the Earth's atmosphere would not have motion. That is, there would be no wind. Pressure is the measure of a force per area. Its IS units are Newtons per square meter. One Newton per square meter is known as a **Pascal** (Pa).

Based on the definition of pressure, force due to pressure is calculated by multiplying pressure by the surface area of "action." Referring to Figure 4.10, the force on the left face of the cubicle air parcel is given as $P \cdot A$, where A is the area of the face. The direction of the pressure force is taken to be "inward" because it is an external pressure. The right face of the parcel has an external pressure represented by $P + \Delta P$, which is the pressure value at the left face modified by any change in pressure ΔP realized over the length of the parcel measured in the x direction, represented by Δx. Consequently, the force due to pressure on the parcel at its right face is given by $(P + \Delta P) \cdot A$. Notice that the direction of the external pressure force in pointing in the negative x direction. Therefore, the total force acting on the parcel in the x direction is given by $P \cdot A - (P + \Delta P) \cdot A = -\Delta P \cdot A$. Applying Newton's second law of motion gives

$$\begin{aligned} m\frac{\Delta u}{\Delta t} &= P \cdot A + -(P + \Delta P) \cdot A \\ &= P \cdot A - P \cdot A - \Delta P \cdot A \\ &= -\Delta P \cdot A \end{aligned} \tag{4.27}$$

where m is the mass of the parcel and u is the x-component of the velocity vector $\vec{v}$. If the density of the parcel is given by ρ, the parcel mass is expressed as $m = \rho V$, where $V = A \cdot \Delta x$ is the volume of the parcel. Substituting for m in Equation 4.27 results in

$$\begin{aligned} \rho A \Delta x \frac{\Delta u}{\Delta t} &= -\Delta P \cdot A \\ \rho \Delta x \frac{\Delta u}{\Delta t} &= -\Delta P \\ \frac{\Delta u}{\Delta t} &= -\frac{1}{\rho}\frac{\Delta P}{\Delta x} \\ \vec{F}_{hpg} &= -\frac{m}{\rho}\frac{\Delta P}{\Delta x} \end{aligned} \tag{4.28}$$

If the pressure P is decreasing in the positive x direction (Δx is positive), then ΔP and $\Delta P/\Delta x$ are negative, making $-\Delta P/\Delta x$ a positive quantity. Consequently, $\Delta u/\Delta t$ is positive, so the magnitude of u increases in a positive sense over a positive change in time Δt. That is, the parcel's velocity in the positive x direction increases.

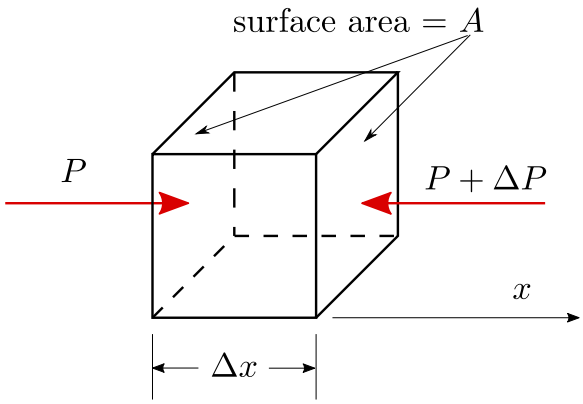

Figure 4.10: The pressure gradient force on an atmospheric parcel.

4.4.3 Vertical Pressure Gradient Force: $\vec{F}_{vpg}$

The pressure on an atmospheric parcel is proportional to the mass of the atmosphere in the column above the parcel. Therefore, the pressure on a parcel at the surface is maximum and the pressure on the parcels above the surface decreases to near zero at the top of the column. Consequently, the pressure gradient in the vertical, $\frac{\Delta P}{\Delta z}$, is negative ($p$ decreases as z increases).

$$\begin{aligned} \rho A \Delta z \frac{\Delta w}{\Delta t} &= -\Delta P \cdot A \\ \rho \Delta z \frac{\Delta w}{\Delta t} &= -\Delta P \\ \frac{\Delta w}{\Delta t} &= -\frac{1}{\rho}\frac{\Delta P}{\Delta z} \\ \vec{F}_{vpg} &= -\frac{m}{\rho}\frac{\Delta P}{\Delta z} \end{aligned} \tag{4.29}$$

The minus sign in Equation 4.29 is required to properly align the force so that its direction is upward (because the vertical pressure gradient is negative).

4.4.4 Hydrostatic Equation: Vertical Force Balance

The **hydrostatic condition** for an atmospheric state means that the forces of gravity and the vertical pressure gradient are in balance. Applying Newton's Second Law to the vertical

acceleration $\frac{\Delta w}{\Delta t}$, where w is the vertical velocity of an atmospheric parcel, gives

$$\begin{aligned} m\frac{\Delta w}{\Delta t} &= F_{vpg} + F_g \\ m\frac{\Delta w}{\Delta t} &= -\frac{m}{\rho}\frac{\Delta P}{\Delta z} - mg \\ \frac{\Delta w}{\Delta t} &= -\frac{1}{\rho}\frac{\Delta P}{\Delta z} - g \\ 0 &= -\frac{1}{\rho}\frac{\Delta P}{\Delta z} - g \\ \frac{\Delta P}{\Delta z} &= -\rho g \end{aligned} \tag{4.30}$$

The **hydrostatic equation**, shown in Equation 4.30, expresses the *reference state* of the atmospheric vertical motion where there is no vertical acceleration ($\Delta w = 0$). This does *not* mean there is no vertical motion. Rather, it means parcel speed in the vertical does not change under the assumption of **hydrostatic balance**. Parcels with zero vertical velocity remain motionless *in the vertical direction*. A non-zero vertical velocity w of a parcel will not change as well. Hydrostatic environments are often referred to as **hydrostatically stable**.

Portions of the atmosphere may not exhibit hydrostatic balance, or hydrostatic stability. A *non-hydrostatic* atmosphere implies the vertical velocity w of a parcel is changing. That is, parcels are experiencing vertical acceleration.

The environment within a thunderstorm is mostly, if not entirely, non-hydrostatic or unstable. Under certain conditions, the vertical velocity of parcels within a thunderstorm experience tremendous increase in their positive vertical motion. Strong, and increasing, positive vertical motion is a key component to severe thunderstorms that produce frequent lightning, large hail and tornadoes (under highly unstable thunderstorm environments).

Example 4.4.1 demonstrates how pressure at a certain elevation may be determined knowing the average density with the air column between the two given elevations z_1 and z_2, and the pressure value at one of the elevations.

Example 4.4.1. The average density in a column of air from the surface of the earth to an elevation of 3200 m is 0.95 kg $\cdot$ m^{-3}. Use the hydrostatic equation to calculate the pressure at 3200 m knowing the surface pressure is 1020 mb.

Solution:
Using the given information, the lowest level is $z_1 = 0$ (at the surface), and $z_2 = 3200$ m. Therefore $\Delta z = z_2 - z_1 = 3200$ m. The average density is given as $\bar{\rho} = 0.95$ kg $\cdot$ m^{-3}. The acceleration due to gravity is $g = 9.8$ m$\cdot$s^{-2}. The

resulting pressure change ΔP will be in units of Pascals, so that value must be divided by 100 to give pressure in mb. Therefore,

$$\frac{\Delta P}{\Delta z} = -\rho g \Rightarrow \Delta P = -\bar{\rho} g \Delta z = -0.95 \times 9.8 \times 3200 = -29792 \text{ Pascals} = -298 \text{ mb}$$

The decrease in column pressure is 298 mb, so the pressure at the top of the column is 1020 - 298 = $\boxed{722 \text{ mb}}$.

Example 4.4.2 shows how the hydrostatic equation may be used to determine the average density $\bar{\rho}$ with in an interval of an air column when the pressure is known at two difference levels within the column.

Example 4.4.2. Calculate the average density for the layer between 700 mb and 500 mb if the elevation of the 700 mb surface is 2898 m and the elevation of the 500 mb surface is 5370 m.

Solution:
The pressure in millibars is given at two known elevations, so ΔP and Δz may both be determined from known information. Remember that pressure must be given in Pascals in the hydrostatic equation. The value for g is a know constant of 9.8 m·s^{-2}.

Therefore, begin by rearranging the hydrostatic equation to solve for $\bar{\rho}$:

$$\frac{\Delta P}{\Delta z} = -\bar{\rho} g \Rightarrow \rho = -\frac{1}{g}\frac{\Delta P}{\Delta z}$$

Next, calculate the two differences:

$$\Delta P = 500 \text{ mb} - 700 \text{ mb} = -200 \text{ mb} = -20000 \text{ Pascals}$$

$$\Delta z = 5370 \text{ m} - 2898 \text{ m} = 2472 \text{ m}$$

Substitute the all know values in the equation for $\bar{\rho}$:

$$\bar{\rho} = -\frac{1}{9.8}\frac{-20000}{2472} = \boxed{0.83 \text{ kg} \cdot \text{m}^{-3}}$$

4.4.5 Frictional Force $\vec{F}_{frc}$

When an object such as an air parcel is moving relative to other objects, such as the earth's surface, buildings, or other air parcels, contact with these other objects will impede the motion of the air parcel. This is similar to the force you feel when you move your hand across a table's surface, for example. The magnitude of the force depends on the magnitude of the object's motion u and a frictional coefficient c_f that depends on the nature of the impeding object's surface.

$$\vec{F}_{frc} = c_f \cdot u^2 \left(-\frac{\vec{u}}{u}\right) \tag{4.31}$$

where $\frac{-\vec{u}}{u}$ is a vector of unit length pointing in the direction opposite the motion of the object.

The rougher the surface, the greater the coefficient in many cases. The direction of the force is exactly opposite the direction of the object's motion, as indicated in Figure 4.11.

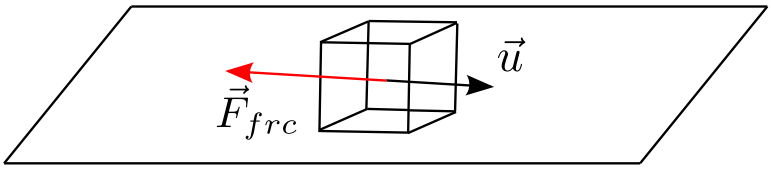

Figure 4.11: The frictional force on an object.

4.4.6 Centripetal Force $\vec{F}_{cen}$

An object that moves in a circular path, such as a mass on the end of a string, is accelerating. Consequently, it must be under the influence of a net non-zero force. Figure 4.12 shows an object rotating on the end of a string of length R, creating a circular path of radius R. The **angular speed** of the rotating object is given by ω, which is measured in radians per second. Recall there are 2π radians in a full circle. The circumference of the equatorial circle is equal to $2\pi R$, so the length of one radian is given by $2\pi R/2\pi = R$. Therefore, the tangential speed of the air parcel, shown as the red vector in Figure 4.12, is given by ωR.

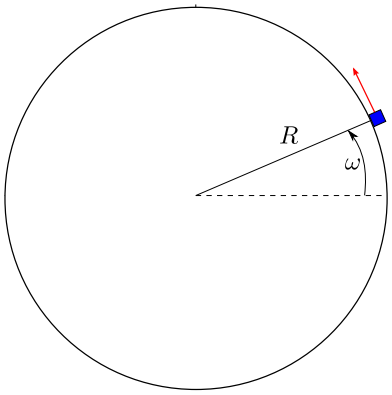

Figure 4.12: Rotating surface air parcel at rest at the earth's equator.

Example 4.4.3. An long-playing record rotates on a turntable at $33\frac{1}{3}$ revolutions per minute (RPMs). If the record has a radius of 6 inches, calculate the tangential speed, in meters per second, of a piece of dust stuck on the edge of the disk.

Solution:
Begin by converting RPMs into radians per second. One revolution $= 2\pi$ radians, so 33.33 RPMs equals $33.33 \cdot 2\pi = 66.66\pi$ rad/min.

$$\omega = 66.66\pi[\text{rad/min}] \cdot \frac{1}{60}[\text{min/sec}] = 3.487 \text{ rad/sec}$$

Next, convert the radius from inches to meters.

$$R = 6.0[\text{in}] \cdot \frac{1}{39.37}[\text{m/in}] = 0.1524 \text{ m}$$

so that

$$\text{tangential speed} = \omega \cdot R = 3.487 \cdot 0.1524 = 0.5314 \text{ m/sec}$$

The direction of the tangential speed of the mass is perpendicular to the radial direction. If the mass had zero net force acting on it, it would continue to move in the tangential

direction. The next objective is to identify the force that prevents the mass from remaining on its tangential vector path.

Figure 4.13a shows the mass at two locations on its circular path at times t and $t + \Delta t$. The magnitude of $\Delta\vec{V}$ is to be determined by knowing $\Delta\theta = \omega \cdot \Delta t$, the length of the tangential vector is given by $V = \omega R$ at both locations, and $\omega^2 = \frac{V^2}{R^2}$. Referring to Figure 4.13b and working with the right triangle created by having the angle $\Delta\theta$

$$\begin{aligned}
\Delta V &= 2\sin\left(\frac{\Delta\theta}{2}\right)\Delta V \\
&= 2\sin\left(\frac{\omega\Delta t}{2}\right)\omega R \\
&= \omega^2 \cdot R \cdot \Delta t \\
&= \frac{V^2}{R^2} \cdot R \cdot \Delta t \\
\frac{\Delta V}{\Delta t} &= \frac{V^2}{R}
\end{aligned}$$

If the mass of the object is given by m, the centripetal force is

$$\begin{aligned}
\vec{F}_{cen} &= m\left(\frac{V^2}{r}\right)\left(\frac{-\vec{r}}{r}\right) \\
&= -m\left(\frac{V^2}{r^2}\right)\vec{r} \qquad (4.32)
\end{aligned}$$

where $\frac{-\vec{r}}{r}$ is the inward, center-pointing vector with a length (magnitude) of one unit. Consequently, the magnitude of the centripetal acceleration is $\frac{V^2}{r}$, not $\frac{V^2}{r^2}$.

4.5 Apparent Forces

Atmospheric motions are calculated within a frame of reference that rotates in concert with the rotating earth. The rotating frame is non-Newtonian. Application of Newton's laws of motion are made valid by introducing **apparent forces**. Two apparent forces are described next.

4.5.1 Centrifugal Force F_{cfg}

Figure 4.14 shows an air parcel of mass m at rest on the surface of the earth at a northern latitude with angle θ measured from the equator. The origin of the reference frame is the center of the earth and is rotating with the same angular velocity ω as the earth. Consequently, the parcel is at rest in the reference frame. However the rotation of the parcel

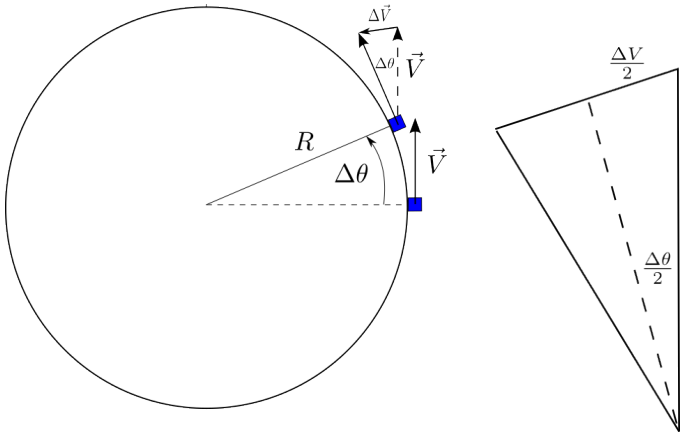

(a) Circular path of radius R. (b) Triangle.

Figure 4.13: Centripetal acceleration.

about the earth's north-south axis is a circular path of radius r resulting in a centripetal force of magnitude $m\left(\frac{V^2}{r}\right) = m\left(\frac{(\omega \cdot r)^2}{r}\right)$ with an inward direction given be the radius of the circle. If this is the singular force within this frame, the parcel should be accelerating. To validate Newton's law, the apparent **centrifugal force** of the same magnitude and opposite direction is applied to create a net zero force on the parcel in the frame of reference.

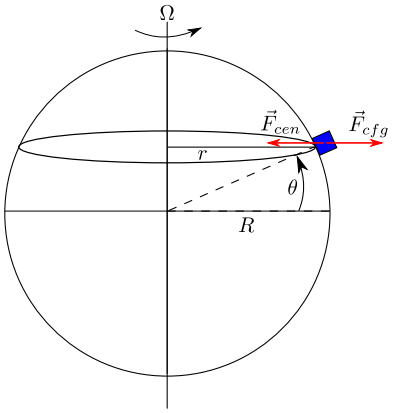

Figure 4.14: Air parcel at rest in a rotating frame.

4.5.2 Effective Gravity

The apparent centrifugal force introduced in Section 4.5.1 has a small but important effect on the gravitational force an object in the earth's atmosphere. The vector diagram shown in Figure 4.15 breaks down the centrifugal force into to components. One has a direction that is tangential to earth's surface, and is designated as $\vec{F}^T_{cfg}$. The other, represented by $\vec{F}^N_{cfg}$, is oriented in a direction opposite the gravitational force represented by $\vec{g}^*$. The later works to lessen the ultimate magnitude of the gravitational force. The magnitude of the reduction suggested by the vector lengths is exaggerated in the figure in order to more easily visualize the result of the apparent force. Regardless, the rotation of an object causes it to be "lighter" than it would normally be. The decrease in the gravitational force is greatest at the equator and reduces to zero at the poles where the centripetal force is zero.

The $\vec{F}^T_{cfg}$ component modifies the direction of the resulting gravitational force. Note that this direction change causes the effective gravitation force to lose its perpendicular orientation to the surface of the earth. If this were to remain true, a object, such as a ball on a flat portion of the surface would be accelerated in the equatorial direction. However, this is not what happens because the earth's profile shape changes from a sphere to an ellipse with a greater axial length at the equator than at the poles. The profile change results in the effective gravity $\vec{g}$ to point in an inward normal (downward) direction at the surface so that there is no equator-ward acceleration.

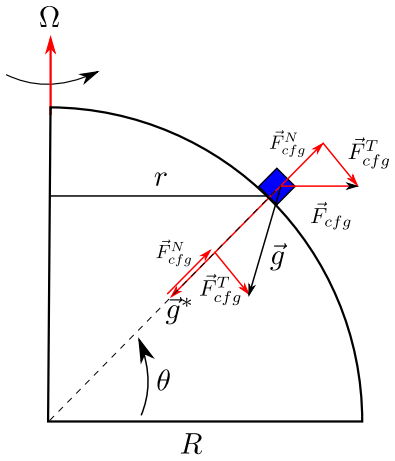

Figure 4.15: Effective gravity $\vec{g}$ as a result of the centrifugal force $\vec{F}_{cfg}$.

Example 4.5.1 shows just how small the actual change in the force of gravity is, even at the equator.

Example 4.5.1. Calculate the percentage reduction, associated with the effective gravity, a mass will experience when rotating with the earth at its equator.

Solution:
The centrifugal force has only a normal component at the earth's equator. Consequently, $|\vec{F}^N_{cfg}| = \Omega^2 Rm$. Using the values of $\Omega = 7.29 \times 10^{-5}$ sec^{-1}, $R =$ 6378 m, and $m = 1$ gives (use a mass of 1 because the percentage reduction is desired, not the actual reduction)

$$\begin{aligned}
\text{percentage reduction} &= \frac{\text{normal component of the centrifugal force}}{\text{gravitation force}} \times 100 \\
&= \frac{\Omega^2 R}{g} \times 100 \\
&= \frac{(7.29 \times 10^{-5})^2 \cdot 6378 \text{ N}}{9.8 \text{ N}} \times 100 \\
&= \frac{3.389 \times 10^{-5} \text{ N}}{9.8 \text{ N}} \times 100 \\
&= 3.458^{-4}\%
\end{aligned}$$

4.5.3 Coriolis Force: F_{cor}

The second apparent force arises when a parcel is moving relative to the rotating frame of the earth. To an observer in this frame, the object's path will appear to be curved unless the object is moving along the earth's equator. A more complete understanding of this apparent force will be achieved by first understanding why, and in what direction, the path appears to be curved. Secondly, the magnitude of the deflection from a straight-line path the object appears to undergo must be determined.

To understand the Coriolis deflection direction, refer to Figure 4.16 where an object will move relative to a rotating disk. The object is not fixed to the disk, and its path in an inertial (non-rotating, non-accelerating) frame is a straight line with constant speed, as is indicated by the uniform spacing between the black dots on the straight dotted line. The disk is rotating counter-clockwise with an angular speed of ω radians per second. An observer, represented by the enlarged eye icon, is rotating with the disk at the same angular speed. Without rotation, the observer would envision the object to move directly towards them. However, with the constant rotation the observer undergoes in the rotating frame, the object appears at a location further and further the observer's left as the observer

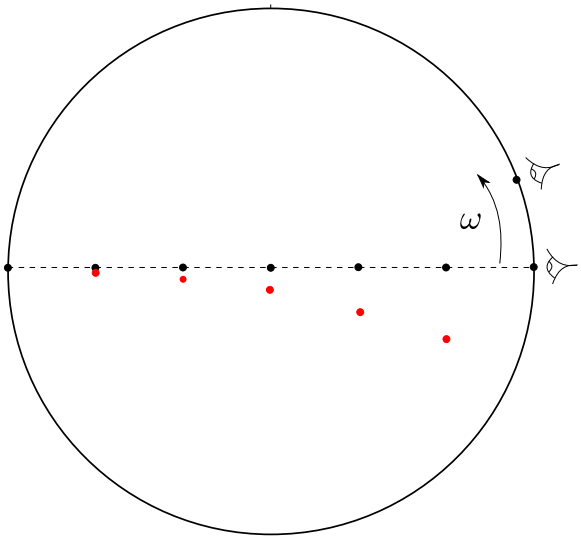

Figure 4.16: The apparent path to an observer in a rotating frame.

rotates counter-clockwise with the platform, creating the sense that the object's apparent path curves to the right of what the observer had expected it to be.

Objects, such as air parcels, that move relative to the earth's surface undergo a right-ward deflection in the northern hemisphere. It can be shown, using similar reason as in the last paragraph, that the Coriolis deflection for such movement in the southern hemisphere is left-ward. Next, the magnitude of the deflection will be determined using the understanding of the centrifugal force.

The expression for the northern hemisphere Coriolis deflection formula is established by first considered the motion of a 1 kilogram ($m = 1$) air parcel relative to the earth's surface on a eastward longitudinal path. The speed of the parcel is given by u, measured in meters per second. The radius of its circular path is given by r, so the increase in parcels angular speed in given by u/r. (Recall that the tangential speed u of an object a circular path of radius r and angular speed ω is $u = \omega r$, so $\omega = u/r$.) The horizontal motion of the parcel enhances the centripetal acceleration of the parcel so that the total centrifugal acceleration (in the opposite direction) is given by

$$\begin{aligned} \text{total centrifugal force} &= \left(\Omega + \frac{u}{r}\right)^2 \vec{r} \\ &= \Omega^2 \vec{r} + \frac{2\Omega u \vec{r}}{r} + \frac{u^2 \vec{r}}{r^2} \\ &= \left(\Omega^2 r + 2\Omega u + \frac{u^2}{r}\right) \frac{\vec{r}}{r} \end{aligned} \tag{4.33}$$

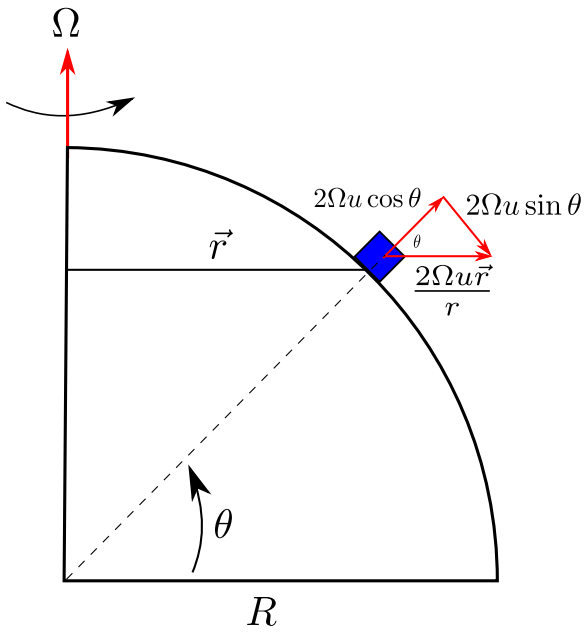

Figure 4.17: Coriolis component vectors associated with an eastward moving air parcel.

The direction of the acceleration is outward as indicated by $\vec{r}$. The expression $\frac{\vec{r}}{r}$ in a vector of unit length (magnitude = 1) pointing outward.

The first term on the right-hand side of Equation 4.33 is the "basic" centrifugal force that makes up a portion of the effective gravity. The third term is centrifugal force due to the tangential speed u. It is negligible because the magnitude of u is much, much less than that Ωr for large-scale atmospheric motions. This leaves the middle term, which is the Coriolis vector force on a one-kilogram air parcel in the direct of the outward point radius vector $\vec{r}$ as shown in Figure 4.17.

This resulting vector, with magnitude $2\Omega u$, is decomposed into two vectors, as shown in Figure 4.17. One is tangential to the surface of the earth. This is the north-south component, or the component in the "y"-direction. Right-triangle trigonometry gives the magnitude to be $2\Omega u \sin\theta$, where θ is the northern hemisphere latitude of the parcel's original path. The southerly direction of the resultant component results in a Coriolis force F_{cor} with southerly acceleration given by

$$\frac{\Delta v}{\Delta t} = -2\Omega u \sin\theta \tag{4.34}$$

where the minus sign indicates the deflection is southward due to the eastward motion of the atmospheric parcel.

The derivation of the Coriolis deflection was for an eastward moving parcel, so the sign

of u is positive, so the change in v given be Equation 4.34 is negative (the deflection is toward the equator). The sign of u is negative for a parcel moving in a westward direction. Consequently, Equation 4.34 results is a positive change for v, a northward deflection.

The Coriolis deflection has a vertical component with an acceleration given by

$$\frac{\Delta w}{\Delta t} = 2\Omega u \cos\theta \tag{4.35}$$

which means the parcel's motion along the latitude line will lessen its weight. The magnitude of the change is insignificant, so it will not be considered when analyzing the motion of atmospheric parcels.

The next step is to determine of the Coriolis deflection for an air parcel moving in a longitudinal direction. The derivation will be for a parcel moving equator-ward with a constant speed of v m·s^{-1}. In order to achieve the goal, the concept of **angular momentum** is introduced. Linear momentum is defined as $m\vec{v}$, the product of mass and speed. Momentum is the measure of the tendency for a body to remain in motion with the same speed and direction. The greater the body's momentum, the greater the required effort to change the body's speed or direction.

For objects with circular motion, three factors determine the momentum of the body. As in the case of linear momentum, the body's mass m and speed v are included. The speed is the tangential speed given by ωr, where ω is the magnitude of the angular speed measured in rad· sec^{-1}. The radius r plays an additional role, because the greater the radius, the more difficult it is to change the object's angular momentum. Consequently, the angular momentum is given by

$$\text{angular momentum} = m\vec{\omega}rr = m\vec{\omega}r^2 \tag{4.36}$$

The direction of the angular momentum vector is the same as the angular velocity vector $\vec{\omega}$. The angular momentum vector can be "felt" by a person who attempts to change the direction of a spinning bicycle, for example. The angular momentum points along the direction of the axle (the axis of rotation). For an air parcel, the direction of its angular momentum vector points in the direction of the earth's rotation vector Ω as shown in Figure 4.18.

The 1 kilogram ($m = 1$) parcel shown in Figure 4.18 is moving equator-ward with constant speed v. As it does, the radius of its rotation around the earth's north-south axis increases by the value of Δr. The angular momentum of the parcel is conserved as it moves. Therefore, the parcel must develop, or increase, its west-ward speed. That increase is represented by -Δu because a positive increase in u implies a deflection (deflection to the left) in the wrong direction. Equating the respective angular momentum expressions before

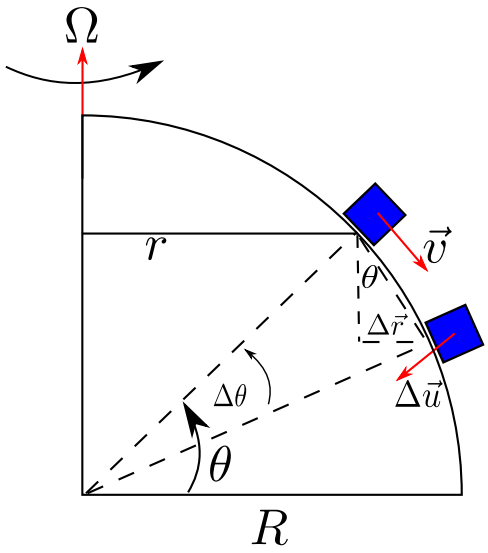

Figure 4.18: Coriolis deflection on a parcel moving equator-ward in the northern hemisphere.

and after a change in angle of Δt results in

$$\begin{aligned}
\Omega r^2 &= \left(\Omega - \frac{\Delta u}{r+\Delta r}\right)(r+\Delta r)^2 \\
\Omega r^2 &= \Omega\,(r+\Delta r)^2 - \Delta u \frac{(r+\Delta r)^2}{r+\Delta r} \\
\Omega r^2 &= \Omega r^2 + 2\Omega r\Delta r + \Omega(\Delta r)^2 - r\Delta u - \Delta r\Delta u \\
0 &= 2\Omega r\Delta r + -r\Delta u
\end{aligned} \tag{4.37}$$

The second-order change terms ($\Omega(\Delta r)^2$, $\Delta r\Delta u$) are negligible relative to the two other terms on the right hand side. Subtracting Ωr^2 from both sides and dividing the remaining two terms by r, solving for Δu gives

$$\Delta u = 2\Omega\Delta r \tag{4.38}$$

The magnitude of Δr is given by $R\Delta\theta\sin\theta$, as indicated in Figure 4.18. Substituting for Δr in Equation 4.38 and dividing by Δt gives

$$\frac{\Delta u}{\Delta t} = 2\Omega R\frac{\Delta\theta}{\Delta t}\sin\theta \tag{4.39}$$

With $R\Delta\theta/\Delta t = v$, the final expression for the rate of change of the latitudinal wind speed u is

$$\frac{\Delta u}{\Delta t} = 2\Omega v\sin\theta \tag{4.40}$$

A equator-ward motion of the parcel means that v is negative in Equation 4.40. Consequently, the change in u is negative, meaning that latitudinal speed of the parcel increases in a westward direction - deflection to the right of the original direction of motion.

A similar result holds for the case where the parcel is moving northward with a speed of v. In that instance, the northward motion means that v is in the positive y direction, so Equation 4.40 will result in positive (eastward) change for u. That is, a deflection to the right of the initial pole-ward motion.

So far, the magnitude and direction of the northern hemisphere Coriolis deflection has been identified for parcels moving in either a strictly east-west ($|\vec{u}| > 0$ and $|\vec{v}| = 0$) or north-south direction ($|\vec{u}| = 0$ and $|\vec{v}| > 0$). This is not as limiting as it might seem because a general direction of motion can be decomposed to its u and v components to which the resulting Coriolis deflection maybe determined. The following example shows how the Coriolis deflection results for strictly north-south and east-west moving parcels may be combined to determine the Coriolis deflection for a parcel moving in a general direction in the northern hemisphere.

Example 4.5.2. Suppose a 1 kilogram parcel is moving with a speed of 20 $\text{m}\cdot\text{s}^{-1}$ in the direction of 30 degrees east of north at the northern latitude of 60 degrees. Estimate the total Coriolis deflection, both in magnitude and direction, on the parcel over a one-minute interval.

Solution:

The first step is to determine the u and v magnitudes of the parcel's motion. Referring to Figure 4.19

$u = 20 \cdot \sin(30) = 10$ and $v = 20 \cdot \cos(30) = 17.32$.

Next use the formulas for $\Delta u/\Delta t$ (Equation 4.34) and $\Delta v/\Delta t$ (Equation 4.40) to calculate:

$$\frac{\Delta u}{\Delta t} = 2\Omega \cdot 17.32 \cdot \sin(30) = 2.1870 \times 10^{-3} \text{ m}\cdot\text{sec}^{-2}$$
$$\frac{\Delta u}{\Delta t} = -2\Omega \cdot 10.00 \cdot \sin(30) = -1.2626 \times 10^{-3} \text{ m}\cdot\text{sec}^{-2}$$

Next, these values will be multiplied by 60 sec/min to *estimate* the total change in the velocity components over the first minute. That is,

$$\Delta u = 60 \times 2.1870 \times 10^{-3} = 0.1312 \text{ m}\cdot\text{sec}^{-1}$$

and

$$\Delta v = 60 \times -1.2626 \times 10^{-3} = -0.0075 \text{ m·sec}^{-1}$$

Consequently, the parcels velocity vector after one minute will be, approximately,

$$\vec{v} = (u + \Delta u, v + \Delta v) = (10.0 + 0.1312, 17.32 + -0.0758) = (10.131, 17.3194)$$

which gives a new speed of 20.0648 m·sec^{-1}. The increase in speed results in order for the parcel to conserve its angular momentum as it moves (mostly) pole-ward and loses length from its radius of rotation.

The new direction of motion, measured as degrees east of north, is

$$\text{angle east of north} = \arctan(u/v) \cdot (180/\pi) = 30.33 \text{ degrees}$$

which indicates an eastward deflection as expected from its (mostly) pole-ward initial motion.

The exact Coriolis deflection of the air parcel in Example 4.5.2 is difficult to determine because once the parcel leaves its original position with original velocity, the initial Coriolis deflection will change the parcel's velocity vector which, in tern, changes the Coriolis deflection. Therefore, using the initial deflection as a representative over the first 1 minute of motion will only approximate the total change in the parcel's velocity vector of that time interval. Accurate expressions for the change in the parcel's velocity components requires the definite integral. That is

$$\Delta u = \int_{t_0}^{t_1} 2\Omega v(t) \sin(\theta(t)) dt \tag{4.41}$$

$$\Delta v = -\int_{t_0}^{t_1} 2\Omega u(t) \sin(\theta(t)) dt \tag{4.42}$$

4.6 Geostrophic Wind: V_{geo}

The first wind to consider is the geostrophic wind V_{geo}. It is a horizontal wind, which means it is comprised of air parcels moving on a path that has a constant height above the surface of the earth. Parcels in the geostrophic move at a constant speed along a straight path.

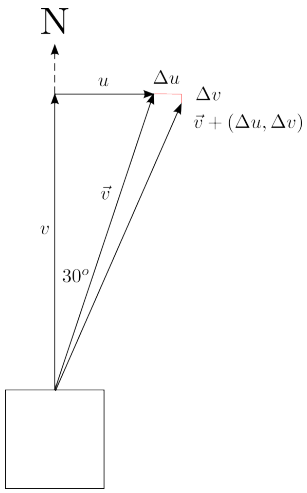

Figure 4.19: Coriolis deflection on a parcel with a general direction of motion in the northern hemisphere.

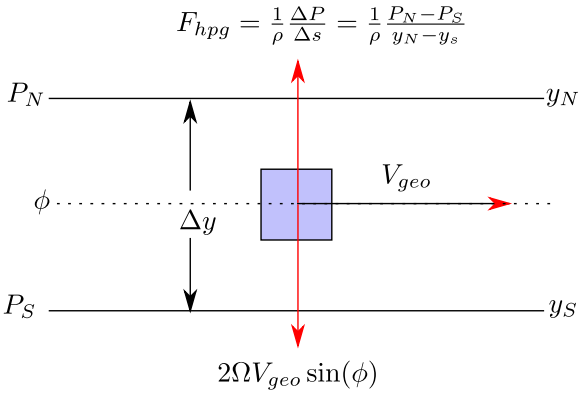

Figure 4.20: A parcel within geostrophic flow.

Consequently, the net force on the parcel is zero. The zero net force implies a *balance* of forces (equal in value and opposite in direction).

Figure 4.20 depicts a parcel in geostrophic balance moving directly west to east with a pressure gradient force pointing northward, and the southward balancing Coriolis force. Therefore, the parcels making up the wind are said to be in **geostrophic balance**. There are two forces acting on the parcel. One is the pressure gradient force, with magnitude $(1/\rho)(\Delta P)/\Delta y)$, and where Δy is the horizontal distance between two points used to calculate the pressure gradient. In this picture, the pressure at the northern location is represented by P_N, and the pressure at the southern point in represented by P_S. The other is the apparent force of the Coriolis deflection. Recall that any parcel in motion in the northern hemisphere, not at the equator, will experience a deflection to the right of its current direction of motion. The magnitude of the force is given by $2\Omega V_{geo}\sin(\phi)$, where V_{geo} is the geostrophic wind speed of the parcel and ϕ is the parcel's north latitude.

The direction of the parcel shown in Figure 4.20 is such that the velocity vector in the Cartesian coordinate system is $\vec{V}_{geo} = (u_{geo}, 0)$, with $u_{geo} > 0$. The pressure gradient term is such that $\Delta P/\Delta y < 0$ because the northern pressure contour value is less than the southern pressure contour value. Consequently, the geostrophic wind equation for u_{geo}, where u_{geo} is the u-component of the horizontal geostrophic wind vector, is determined by applying Newton's second law to the forces acting on the parcel in the y-direction. That is

$$\begin{aligned} m\frac{\Delta v}{\Delta t} &= -m\cdot 2\Omega u\sin\phi - \frac{m}{\rho}\frac{\Delta P}{\Delta y} && \text{(cancel the common } m\text{)} \\ 0 &= -2\Omega u_{geo}\sin\phi - \frac{1}{\rho}\frac{\Delta P}{\Delta y} && \text{(forces are balanced)} \\ 2\Omega u_{geo}\sin\phi &= -\frac{1}{\rho}\frac{\Delta P}{\Delta y} && (4.43) \end{aligned}$$

If a pressure pattern were such that $\Delta P/\Delta x > 0$, the resulting geostrophic wind would be southerly (from the south). Therefore, $\vec{V}_{geo} = (0, v_{geo})$ with $v_{geo} > 0$. Consequently, the geostrophic wind equation in this case is

$$2\Omega v_{geo}\sin\phi = \frac{1}{\rho}\frac{\Delta P}{\Delta x} \tag{4.44}$$

The following example shows how to calculate the geostrophic wind speed u_{geo} for a pressure gradient in the y direction.

Example 4.6.1. Referring to figure 4.20, suppose $P_N = 504$ mb, $P_S = 510$ mb, $y_N = 1000$ km, $y_S = 700$ km, $\phi = 45$ degrees, and $\rho = 0.91$ g/L. Calculate u_{geo} in m·s^{-1}.

Solution:

Begin by determining the pressure gradient force:

$$\begin{aligned} F_{hpg} &= \frac{1}{\rho}\frac{(P_N - P_S)\cdot 100}{(y_N - y_S)} \text{ (factor of 100 to convert to Pascals)} \\ &= \frac{1}{0.91}\frac{(504-510)\cdot 100}{(1000-700)} \\ &= -2.1978 \times 10^{-3} N \end{aligned}$$

Next, equate the pressure gradient force and the Coriolis force and solve for u_{geo}

$$\begin{aligned} 2\Omega u_{geo}\sin\phi &= -\frac{1}{\rho}\frac{\Delta P}{\Delta y} \\ 2\Omega u_{geo}\sin(45) &= 2.1978 \times 10^{-3} \\ 0.0001458 \cdot u_{geo} \cdot 0.707 &= 0.0021978 \\ u_{geo} &= \frac{0.0021978}{0.0001458 \cdot 0.707} \\ &= 21.31 \text{ m}\cdot\text{s}^{-1} \end{aligned}$$

The geostrophic wind can be thought of as a "reference" state of horizontal motion. It is the one instance when horizontal forces are in balance on a parcel so that it is not accelerating. The next several winds to be considered are such where the horizontal forces are not in balance. That is, there is a non-zero net horizontal force on the parcels so that their speed or direction of motion is changing. These winds are known as **ageostrophic** .

The geostrophic wind develops as parcels react to a horizontal pressure force. Figure 4.21 shows a pressure gradient associated with straight, uniformly spaced isobars between a high pressure region to the south and a low pressure region to the north. A parcel at rest (position number 1) near the bottom of the figure has an initial velocity vector (shown in black) that points directly north in response to the constant pressure force.

If this were the only force acting on the parcel, its velocity vector would increase in magnitude, but not change direction as the parcel migrates northward. However, the rotating frame in which the parcel moves will cause a Coriolis deflection in a rightward direction immediately after the parcel begins to move. The magnitude of the deflection vector (shown in blue in the figure at position 1) is initially small because it is proportional to the magnitude of the parcels speed, which is initially small.

The eastward pointing Coriolis force will cause the parcel to move slightly eastward as it moves from position 1 to position 2. The speed of the parcel increases as it moves northward due to the pressure gradient, whose magnitude at this time is greater than that

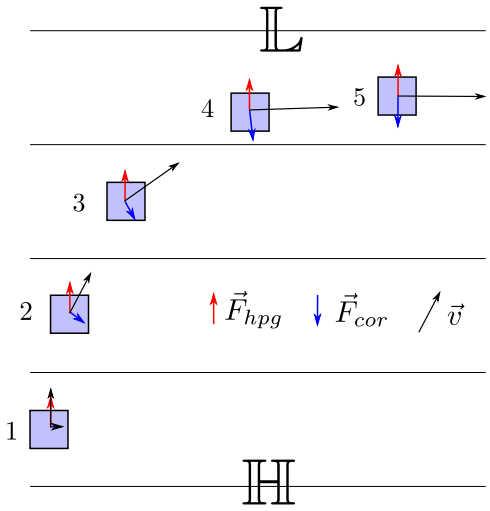

Figure 4.21: Developing geostrophic flow.

of the Coriolis deflection. However, the increased speed of the parcel means the Coriolis deflection increases in magnitude, as indicated with a greater length of the Coriolis vector shown in position 2 when compared to the length of the Coriolis vector in position 1.

A similar scenario is in place as the parcel moves from position 2 to 3. Note that the path of the parcel has a more eastward component as the Coriolis force increases, as indicated with a greater length of the blue Coriolis vector. By the time the parcel reaches position 4, the Coriolis vector has increased in length and its clockwise change in direction is such that it is almost equal and opposite to the constant pressure gradient vector.

When the parcel has reached position 5, the gradual increase in length and clockwise rotation of the Coriolis vector have lead to it being exactly equal in length, and opposite in direction, to the constant pressure gradient vector. At this instance the net force on the parcel is zero, so it will continue to move in a straight eastward direction with a constant speed unless, and until, another force disturbs the force balance.

The eventual and sustained eastward parcel path in this development means the parcel will move along a path that is parallel to the isobars that initiated its motion. Parcel trajectories that run parallel to isobars are observed in the earth's atmosphere when friction is negligible, that is for winds at a sufficiently high altitude. This is true for both balances flows, such as the geostrophic wind, as well as those that are subject to an imbalance of forces. The next wind to be considered is one in which there is a non-zero net force.

4.7 Gradient Wind: V_{gra}

Parcels making up winds that follow curved paths are know as **gradient winds**. An example of a parcel within a gradient wind is shown in Figure 4.22, where the parcel's path is indicated as a dashed curve. The sold contour are isobars located between the high and low pressure areas denoted as $\mathbb{H}$ and $\mathbb{L}$, respectively.

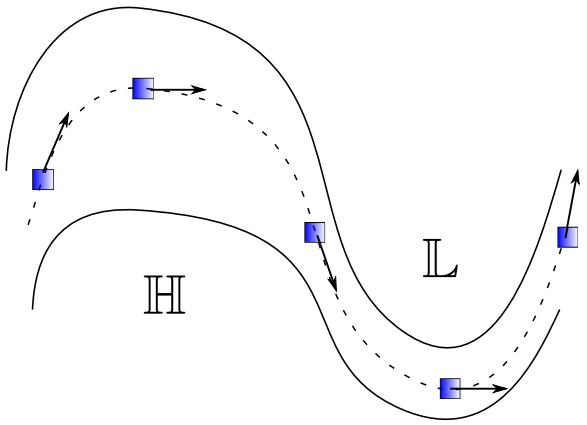

Figure 4.22: Gradient atmospheric flow associated with curved isobars.

4.7.1 Sub-geostrophic Wind: V_{geo}^{-}

The force analysis on a parcel undergoing curved flow is done in a polar coordinate system because the parcel's circular path at the moment of analysis naturally lends itself to an (r, θ) location. To that end, a parcel is shown in a polar system in Figure 4.23 on a circular path with tangential velocity vector $\vec{v}$ whose magnitude is given by v. At the moment of consideration, the circular path has a radius of r_0. As the parcel follows its path along the curved isobars, the circular radius of the path may change from one moment to another.

In the polar system, the forces on the one-kilogram mass are

- pressure gradient: $\vec{F}_{hpg} = -\frac{1}{\rho}\frac{\Delta P}{\Delta r}$ (inward direction because $\frac{\Delta P}{\Delta r} > 0$)
- Coriolis: $\vec{F}_{cor} = 2\Omega v \sin(\phi)$ (outward direction, the Coriolis deflect is to the right)
- centripetal: $\vec{F}_{cen} = -\frac{v^2}{r_o}$ (net force is inward ($-\vec{r}$ direction), so the negative sign is needed)

where v is the tangential wind speed, so $v > 0$.

Recall that for a one-kilogram mass, the formulas for the parcel forces are the same as those for the parcel accelerations. The terms on the left-hand-side of Equation 4.45 are the

two terms found in the geostrophic wind equation. The pressure gradient term is negative because the pressure increases with increasing radius r. The Coriolis term is positive because it deflects the parcel to the right (in the direction of positive r) is it moves northward. The negative net centripetal force implies the Coriolis deflection is less than it would be under geostrophic balance with the same pressure gradient magnitude. Consequently, $v_{gra} < v_{geo}$, so v_{gra} in this event is **sub-geostrophic** wind.

$$\frac{-1}{\rho}\frac{\Delta P}{\Delta r} + 2\Omega v \sin(\phi) = -\frac{v^2}{r_0} \tag{4.45}$$

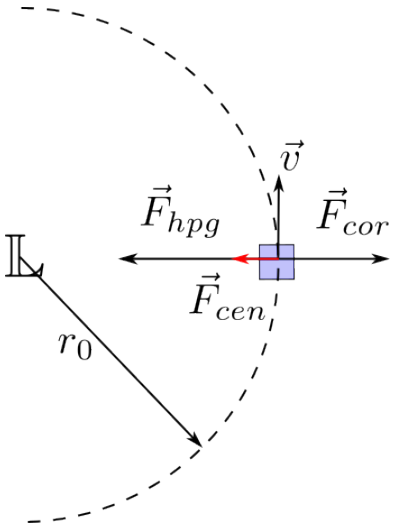

Figure 4.23: Gradient flow associated with a low pressure region.

Example 4.7.1. Under the influence of a pressure gradient force of 2.0×10^{-3} Newtons, a one gram per liter air parcel located at 45 degrees north follows a curved path of radius 300 km around a low pressure center. Calculate the gradient wind speed of the parcel in $\mathrm{m{\cdot}s^{-1}}$. Next, calculate and compare the gradient wind speed to the speed the parcel would attain if its flow were geostrophic with the same pressure gradient magnitude.

Solution:

Begin by rearranging Equation 4.45 as

$$\frac{v^2}{r_0} + 2\Omega v \sin(\phi) - \frac{1}{\rho}\frac{\Delta P}{\Delta r} = 0$$

$$v^2 + r_0 \cdot 2\Omega v \sin(\phi) - \frac{r_0}{\rho}\frac{\Delta P}{\Delta r} = 0 \tag{4.46}$$

Equation 4.46 is a quadratic equation in v ($av^2 + bv + c = 0$). Therefore

$$v = \frac{-b \pm \sqrt{b^2 - 4ac}}{2a} = \frac{-r_0 \cdot 2\Omega \sin(\phi) \pm \sqrt{(r_0 \cdot 2\Omega \sin(\phi))^2 - 4 \cdot 1 \cdot -\frac{r_0}{\rho}\frac{\Delta P}{\Delta r}}}{2 \cdot 1} \tag{4.47}$$

With $r_0 = 300 \times 1000$, $2\Omega \sin(45) = 1.0309 \times 10^{-4}$, and $-\frac{1}{\rho}\frac{\Delta P}{\Delta r} = -2.0000 \times 10^{-3}$, Equation 4.47 becomes

$$v = \frac{-300000 \cdot 1.0309 \times 10^{-4} \pm \sqrt{(300000 \cdot 1.0309 \times 10^{-4})^2 + 4 \cdot 6.0000 \times 10^2}}{2} \tag{4.48}$$

$$v = \frac{-30.93 \pm \sqrt{956.7 + 2400}}{2} = \frac{-30.93 \pm 57.93}{2} = 13.5 \text{ m·s}^{-1} \tag{4.49}$$

The positive square root is used in Equation 4.49 because the tangential speed of the parcel is positive.

Next, calculate the geostrophic wind speed for this same pressure gradient magnitude.

$$2\Omega \sin(45) V_{geo} = \frac{1}{\rho}\frac{\Delta P}{\Delta r} \tag{4.50}$$

$$V_{geo} = \frac{\frac{1}{\rho}\frac{\Delta P}{\Delta r}}{2\Omega \sin(45)} = \frac{2.0 \times 10^{-3}}{1.031 \times 10^{-4}} = 19.40 \text{ m·s}^{-1} \tag{4.51}$$

The result shown in Equation 4.51 confirms the gradient wind speed for this same pressure gradient force is less than geostrophic wind it would produce.

4.7.2 Super-Geostrophic Wind: V_{geo}^{+}

The next step is to complete a force analysis on an air parcel as it flows a curved path where the dominate pressure feature is a high pressure region, as shown in Figure 4.24. The motion of the parcel relative to the high pressure center is clockwise in the northern hemisphere.

Letting v be the tangential speed of the parcel (so $v > 0$), and knowing $\frac{\Delta P}{\Delta r} < 0$ The forces acting on the parcel are:

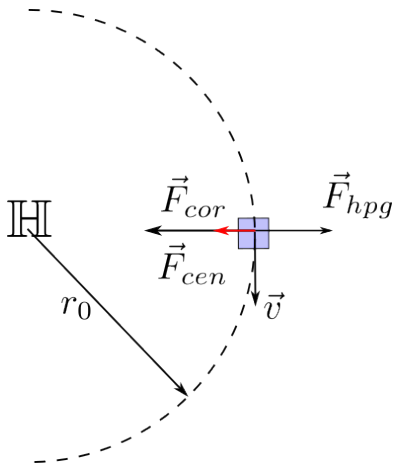

Figure 4.24: Gradient flow associated with a high pressure region.

- pressure gradient: $\vec{F}_{hpg} = -\frac{1}{\rho}\frac{\Delta P}{\Delta r}$ (outward direction because $\frac{\Delta P}{\Delta r} < 0$)
- Coriolis: $\vec{F}_{cor} = -2\Omega v \sin(\phi)$ ($v > 0$ is the tangential speed, so the Coriolis deflect is to the right, or in the $-\vec{r}$ direction)
- centripetal: $\vec{F}_{cen} = -\frac{v^2}{r_o}$ (net force is inward ($-\vec{r}$ direction) in circular motion)

The forces are arranged in Equation 4.52 with the negative net force shown on the right-hand-side. The usual geostrophic wind terms are the left-hand-side of the equation. The pressure gradient term is positive and the Coriolis term is negative. The fact that the net force is negative means the Coriolis magnitude is greater than the pressure gradient term. Consequently, the magnitude of v is greater than it would be if the two right-hand side terms were in balance. That is, $v_{gra} > v_{geo}$ for the same pressure gradient magnitude. The gradient flow is said to be **super geostrophic**.

$$\frac{-1}{\rho}\frac{\Delta P}{\Delta r} - 2\Omega v \sin(\phi) = -\frac{v^2}{r_0} \qquad \left(\frac{\Delta P}{\Delta r} < 0 \text{ and } v > 0\right) \tag{4.52}$$

Example 4.7.2. Under the influence of a pressure gradient force of -2.0 $\times$ 10^{-3} Newtons, a one gram per liter air parcel located at 45 degrees north follows a curved path of radius 300 km around a high pressure center. Calculate the gradient wind speed of the parcel in m·s^{-1}. Next, calculate and compare the gradient wind speed to the speed the parcel would attain if its flow were geostrophic with the same pressure gradient magnitude.

Solution:

Begin by rearranging Equation 4.52 as

$$\frac{v^2}{r_0} - 2\Omega v \sin(\phi) - \frac{1}{\rho}\frac{\Delta P}{\Delta r} = 0$$
$$v^2 - r_0 \cdot 2\Omega v \sin(\phi) - \frac{r_0}{\rho}\frac{\Delta P}{\Delta r} = 0 \tag{4.53}$$

Equation 4.53 is a quadratic equation in v ($av^2 + bv + c = 0$). Therefore

$$v = \frac{-b \pm \sqrt{b^2 - 4ac}}{2a} = \frac{r_0 \cdot 2\Omega \sin(\phi) \pm \sqrt{(r_0 \cdot 2\Omega \sin(\phi))^2 - 4 \cdot 1 \cdot -\frac{r_0}{\rho}\frac{\Delta P}{\Delta r}}}{2 \cdot 1} \tag{4.54}$$

With $r_0 = 300 \times 1000$, $2\Omega \sin(45) = 1.0309 \times 10^{-4}$, and $\frac{1}{\rho}\frac{\Delta P}{\Delta r} = -2.0000 \times 10^{-3}$, Equation 4.54 becomes

$$v = \frac{300000 \cdot 1.0309 \times 10^{-4} \pm \sqrt{(300000 \cdot 1.0309 \times 10^{-4})^2 + 4 \cdot 6 \times 10^2}}{2} \tag{4.55}$$
$$v = \frac{30.93 \pm \sqrt{956.7 + 2400}}{2} = \frac{30.93 + 57.93}{2} = 44.43 \text{ m·s}^{-1} \tag{4.56}$$

The positive square root is used in Equation 4.56 because the tangential speed of the parcel is positive.

Next, calculate the geostrophic wind speed for this same pressure gradient magnitude.

$$2\Omega \sin(45) V_{geo} = \frac{1}{\rho}\frac{\Delta P}{\Delta r} \tag{4.57}$$
$$V_{geo} = \frac{\frac{1}{\rho}\frac{\Delta P}{\Delta r}}{2\Omega \sin(45)} = \frac{2.0 \times 10^{-3}}{1.031 \times 10^{-4}} = 19.40 \text{ m·s}^{-1} \tag{4.58}$$

The result shown in Equation 4.58 confirms the gradient wind speed for this same pressure gradient force is greater than geostrophic wind it would produce.

It is important to note that winds around a high pressure center no faster than winds around a low pressure center. The comparisons made in the section are relative to the speed of a geostrophic wind in response to a given pressure gradient magnitude. In fact, observations show that wind speeds around high pressure centers are generally less in magnitude than those around low centers because the pressure gradient magnitudes associated with high pressure centers are significantly less than those associated with low centers.

4.8 Surface Winds: V_{sfc}

The winds considered up to this point exist at sufficiently high elevations so that friction is assumed to be inconsequential. The vertical structure of the earth's atmosphere can be differentiated into a friction and friction-free layers. The friction layer begins at the surface, of course, and extends to an elevation of between 1000 and 3000 meters. The actual elevation varies as a function of the time of day among other factors. It is usually lower in the evening than it is during the daylight hours.

Obviously, surface winds are in the friction layer, so the force of friction must be taken into account when analyzing wind forces. Figure 4.25 show the relevant forces on the parcel situated between regions of high and low pressure. The "new" force is that due to friction, designated as $\vec{F}_{frc}$ in the figure. The direction of the force is directly opposite the direction of the parcel's velocity. The magnitude of the force is proportional to the parcel speed, so the friction force is represented as $\vec{F}_{frc} = \alpha\vec{v}$, where α is the **coefficient of friction**. The frictional force slows the speed of the parcel and, therefore, the magnitude of the Coriolis force. Consequently, the pressure gradient force magnitude exceeds that of the Coriolis force and the net force is "pulls" the parcel toward the low pressure region and away from the region of higher pressure.

The angular magnitude of the friction-caused parcel deflection across the isobars is approximately 30 degrees. If an observer's back is to the wind, the direction to the surface low pressure center is determined by the observer turning 30 degrees clockwise. If the observer's arms are extended so that they and the torso form a "cross," the left arm points to the low pressure center. This relationship between surface pressure and wind direction is often called **Buys-Ballot's Law** after the Dutch meteorologist Christoph Buys-Ballot.

A near-surface parcel's longer-term trajectory near a low pressure center in shown in Figure 4.26. Instead of exhibiting gradient flow based on the curved shaped of the isobars, the parcel follows a winding path around the low as it slowly moves closer to the center of the low because the pressure gradient force (pointing towards the low center) is greater than the Coriolis force whose magnitude is decreased by the loss of wind speed due to friction.

4.9 Height Gradient

Although it seems natural to use elevation as the vertical measure in a three-dimensional coordinate system for the earth's atmosphere, it is often more common for pressure to be used. Consequently, constant pressure surfaces are used instead of constant height surfaces. As a result, the pressure gradient term (for example, $\Delta P/\Delta x$) in the equations for atmospheric winds is replaced by a height gradient (for example, $\Delta z/\Delta x$). The hydrostatic equation provides a means of making the translation from one type of gradient to the other.

The relationship between the horizontal pressure gradient on a constant height surface and the horizontal height gradient on a constant pressure surface is revealed with the aid of Figure 4.27. Two constant height and constant pressure surfaces are shown. Referring to

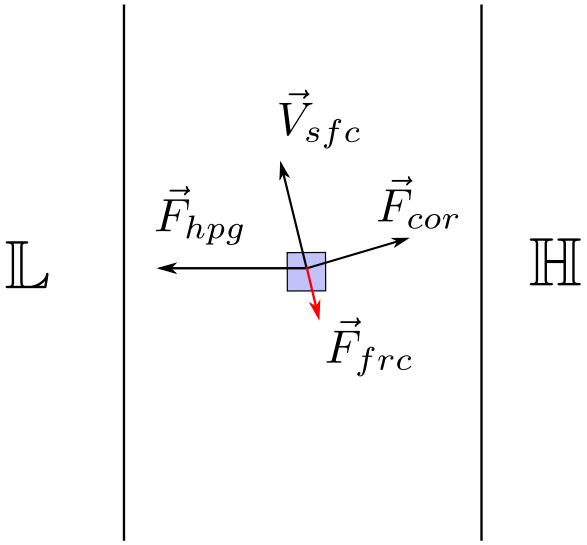

Figure 4.25: The relevant forces acting on a near-surface air parcel.

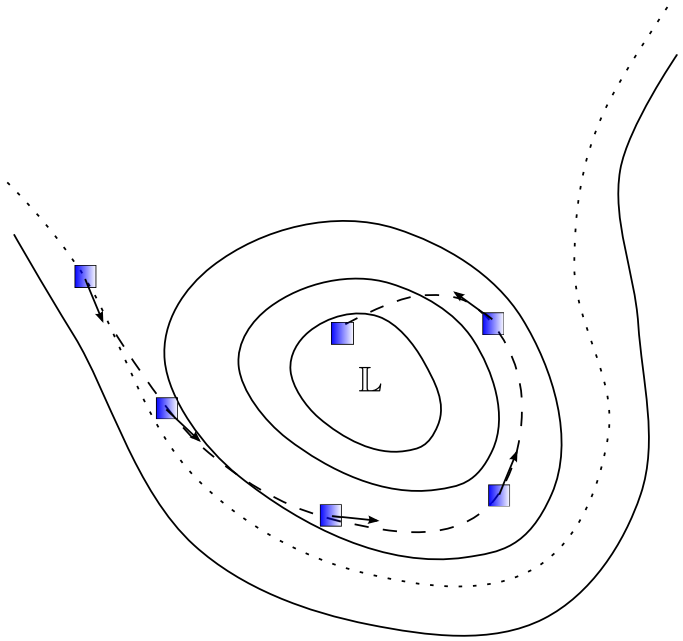

Figure 4.26: Friction flow associated with a low pressure region.

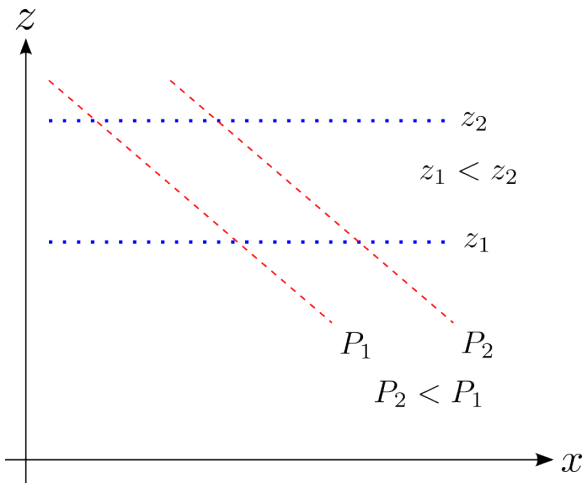

Figure 4.27: Height and pressure surfaces and the relationship of horizontal pressure and height gradients.

the figure, if a constant height surface is followed in the direction of increasing x, it is noted that $\Delta P/\Delta x < 0$ because $\Delta x > 0$ and $\Delta P < 0$. Similarly, if a constant pressure surface is traversed in the direction of increasing x, $\Delta z < 0$, so $\Delta z/\Delta x < 0$. If the pressure surfaces are titled "upwards" in Figure 4.27, it follows that both $\Delta P/\Delta x$ and $\Delta z/\Delta x$ are positive.

Therefore, it has been established that the two gradients have the same sign (either both positive or both negative). Additionally, the relationship reveals that high pressure and "high" heights are directly correlated. That is, if a location is know to be associated with high pressure, then the height at which that pressure is attained is relative high as well.

Now, using the magnitudes of the terms in the hydrostatic equation

$$\frac{\Delta p}{\Delta z} = \rho g \tag{4.59}$$

$$\frac{1}{\rho}\frac{\Delta p}{\Delta z} = g \tag{4.60}$$

$$\frac{1}{\rho}\Delta p = g\Delta z \tag{4.61}$$

$$\frac{1}{\rho}\frac{\Delta p}{\Delta x} = g\frac{\Delta z}{\Delta x} \tag{4.62}$$

The height gradient - pressure gradient relationship shown in Equation 4.62 can be substituted in the geostrophic wind Equations 4.43 and 4.44 to give

$$2\Omega u_{geo} \sin\phi = -g\frac{\Delta z}{\Delta y} \tag{4.63}$$

$$2\Omega v_{geo} \sin\phi = g\frac{\Delta z}{\Delta x} \tag{4.64}$$

isoheight contours are constant height contours. A benefit of isoheights is that they provide an intuitive sense of where a parcel wants to move. Just as a ball wants to roll downhill, an air parcel want to move from a greater to a lesser isoheight contour. That is, it want to move "downhill."

4.10 High-Low-High Pattern

With a general understanding of a few of the atmosphere's fundamental winds, and their associated forces, an understanding of a basic circulation pattern may be attained. This pattern is associated with a typical high-low-high pressure sequence in the earth's atmosphere. Figure 4.28 shows the heights associated with the 500 mb surface on January 9, 2022. Two height ridges are present - both identified with dashed red lines. One has an axis over the west coast of the US. The other axis ridge is situated along the east coast of the US. The trough (low heights) axis runs north-south through the Midwest (right through eastern Iowa) is shown as a blue dashed line.

The contours of the 500 mb surface on the friction-free surface have regions of curvature (situated around the ridge and trough axes) as well as straight contour lines. Therefore, the associated wind fields range from subgeostrophic (around the trough axis) to geostrophic (within the red rectangular regions) to supergeostrophic (situated around the ridge axes). Assuming the pressure height gradients (pressure gradients) associated with the flow are approximately equal, the relative speeds of parcels flowing in this pattern are known from the geostrophic and ageostrophic (sub- or supergeostrophic) wind pattern. These relative sizes are depicted in Figure

A schematic view of the atmospheric structure is shown in Figure 4.29. The upper air height pattern of high-low-high is results in the sequence of atmospheric winds: supergeostrophic $\rightarrow$ geostrophic $\rightarrow$ subgeostrophic $\rightarrow$ geostrophic $\rightarrow$ supergeostrophic. The air vertical columns are depicted as the region between the vertical dashed lines. The column on the left has a high pressure center at its base (at the surface of the earth). This high center develop because more air parcels are entering the column at the top than are leaving because the supergeostrophic air parcels feeding into the column are more numerous than those leaving the column at the subgeostrophic speed. More parcels in than out results in an increase of mass in the column. The increase in mass in the column results in an increase in pressure at the surface.

An atmospheric column situated downstream from the upper air low (and upstream) from the upper air high will lose mass because the supergeostrophic wind down stream is

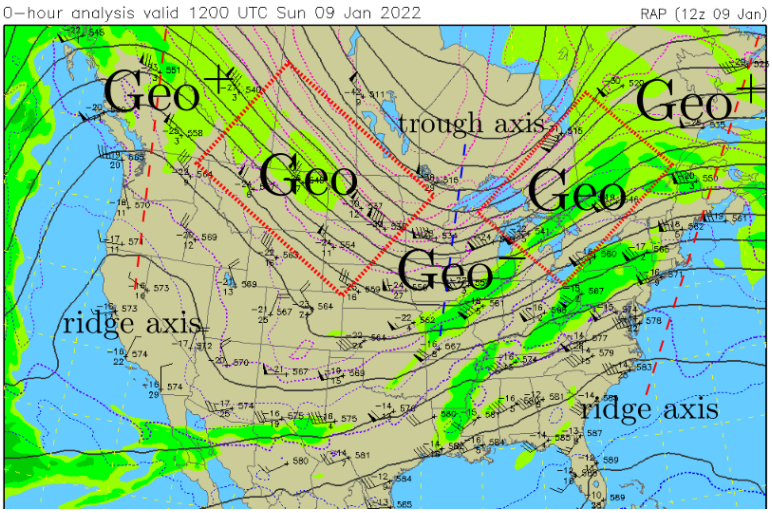

Figure 4.28: High-low-high pressure (height) sequence at 500 mb. Wind types in geostrophic (Geo) with in the rectangular regions outline in red, super geostrophic (Geo^{+}), and sub-geostrophic (Geo^{-}).

greater than the upstream subgeostrophic wind. This loss of mass results in a developing low pressure area at the surface.

Once the high and low pressure centers have developed at the surface, a pressure gradient will accelerate parcels from the high pressure to the low pressure. This pattern depicts how the pressure (height) surfaces at higher elevations create and connect to pressure patterns at the surface and instigate the results winds. An understanding of how the high and low pressure regions develop in the upper reaches of the atmosphere will be developed in subsequent section of the book.

Clear skies associated with the surface high pressure system and the due to the sinking air above, as shown in Figure 4.30. The surface low pressure system is coincides with the cloudy region due to the rising air parcels in the column(s) above the low. Why is this so? The complete answer to this question requires an understanding of moisture and thermodynamic principles of atmospheric parcels as they move vertically in the atmosphere. These are topics covered later in the text. There, the *what* and *why* that will be learned is that as parcels sink, they warm. As parcels warm, the condensed water portion of the parcel evaporates so any cloudiness is likely to dissipate to leave clear blue skies. The opposite is true for rising air parcels: they rise, they cool, and moisture is likely to condense to form clouds.

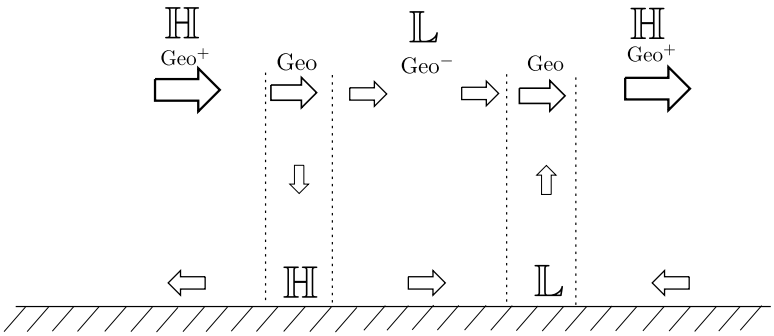

Figure 4.29: High-low-high pressure (height) sequence at 500 mb. Wind types in geostrophic (Geo) with in the rectangular regions outline in red, super geostrophic (Geo^+), and sub-geostrophic (Geo^-).

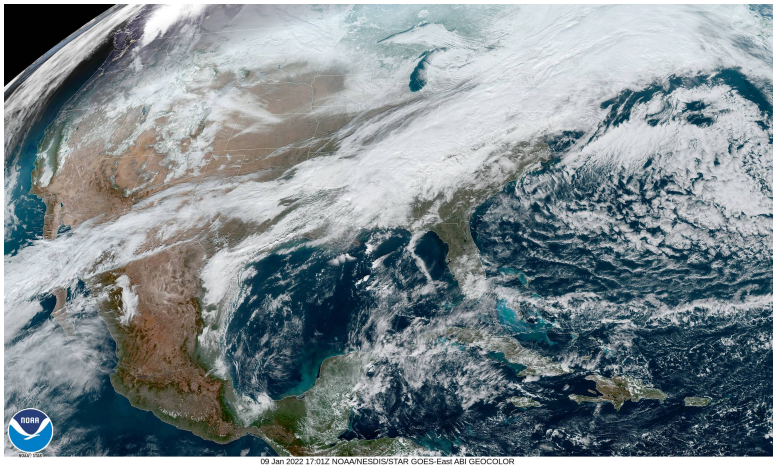

Figure 4.30: Satellite imagery for the same time period of the 500 mb height pattern (roughly).

Chapter 4 Exercises

4.1 Suppose a 2 kg parcel of air near the surface of the earth has a velocity vector $\vec{v}_0 = (5, 10)$ at time $t_1 = 0$, and at time $t_2 = 1$ hour the parcel has a velocity vector of $\vec{v}_2 = (7, 3)$. The component speeds u and v of the velocity vectors $\vec{v} = (u, v)$ are in meters per second.

(a) Calculate the speed s ($s(t) = \|\vec{v}\| = \sqrt{u^2 + v^2}$) of the parcel at both times t_1 and t_2.

(b) Find the change in velocity vector $\Delta\vec{v} = (\Delta u, \Delta v)$.

(c) Find the the acceleration vector $\vec{a} = (a_x, a_y)$ in m·sec^{-2}.

(d) Calculate the magnitude of the components of the force vector $\vec{F} = (F_x, F_y)$

4.2 Figure 4.31 shows surface pressure in the northern hemisphere with isobars drawn every 4 mb. Answer the following questions by referring to the figure.

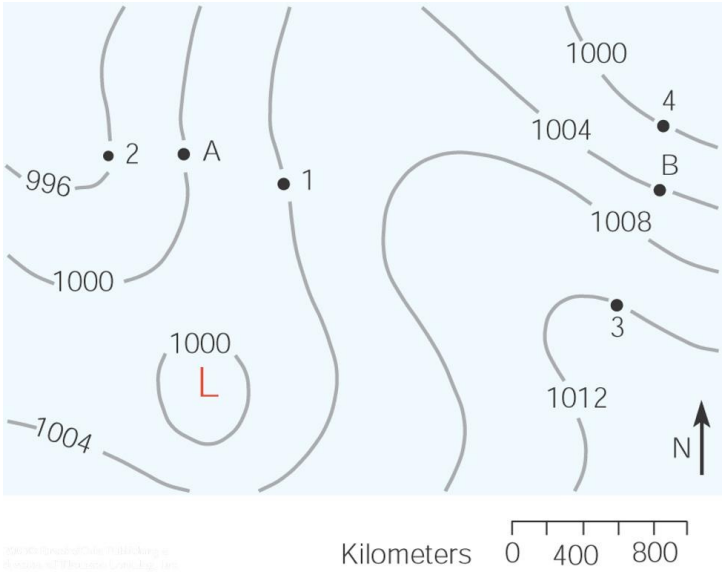

Figure 4.31: Sea-level pressure chart.

(a) Draw a solid line through the ridge and a dotted line through the trough.

(b) Draw an arrow to represent the wind direction at point A. Do the same for point B. (NOTE: This motion at the surface, so include the force due to friction and consider Buys-Ballot's law.)

(c) Compute the pressure gradient, in N/m^2/m, between points 1 and 2, and between points 3 and 4.

(c) Of the two locations A and B, which would have the greater wind speed? Explain why? (HINT: Consider the relative sizes of the pressure gradients calculated above.)

(d) Suppose points A and B are located at 41° N, and the density of air is 1.2 kg/m^3. Use the geostrophic wind equation to compute the geostrophic wind, in m/sec, at points A and B.

(e) Would the actual wind speed at points A and B be less than, equal to, or greater than the speed you calculated in part 4.2? Explain.

4.3 Suppose a 3 kg parcel of air near the surface of the earth has a velocity vector $\vec{v}_0 = (-1, 8)$ at time $t_1 = 0$, and at time $t_2 = 1$ hour the parcel has a velocity vector of $\vec{v}_2 = (4, 3)$. The component speeds u and v of the velocity vectors $\vec{v} = (u, v)$ are in meters per second.

(a) Calculate the speed s ($s(t) = \|\vec{v}\| = \sqrt{u^2 + v^2}$) of the parcel at both times t_0 and t_1.

(b) Find the change in velocity vector $\Delta\vec{v} = (\Delta u, \Delta v)$.

(c) Find the the acceleration vector $\vec{a} = (a_x, a_y)$ in m·sec^{-2}.

(d) Calculate the magnitude of the components of the force vector $\vec{F} = (F_x, F_y)$

4.4 Suppose the atmospheric pressure at the bottom of a deep air column 5.6 km thick is 1000 mb.

(a) If the average air density of the column is 0.91 kg/m^3, and the acceleration of gravity is 9.8 m/sec^2, use the hydrostatic equation to estimate the pressure at the top of the column.

(b) If the air in the column of problem (a) becomes much colder than average, would the atmospheric pressure at the top of the 5.6 km tall column be greater than, less than, or equal to the pressure computed in problem (a)? Use the hydrostatic equation to justify your answer.

(c) Determine the atmospheric pressure at the top of the 5.6 km tall column in part (a) if the column is quite cold and has an average density of 0.97 kg/m^3.

4.5 Suppose points A and B lie on the 40° N latitude line, with point B 100 km east of point A. At a point midway between A and B there is a southerly geostrophic wind blowing with a speed of 10 m/sec. If the surface pressure at point B is 1000 mb, determine the surface pressure at point A. The surface density is 1.2 g/L.

4.6 In this exercise you will calculate the speed of the gradient wind around a low pressure system. The pressure gradient force on the parcel is the same as that in the geostrophic wind example shown in the handout (0.0017 Nm^{-2}/m) as well as the latitude (45°north) and the parcel density (1.22 kg/m^3). The radius of curvature of flow is r=200 km = 200,000 m. Calculate the speed of the parcel and compare it with that of geostrophic case with the same pressure gradient. Recall the equation for the speed of the gradient wind around a low is

$$\frac{v^2}{r} + 2\Omega v \sin\phi - \frac{1}{\rho}\frac{\Delta P}{\Delta r} = 0$$

(NOTE: You will need to use the quadratic formula to find the speed v. By design, the speed must be positive. Use this as a means of determining which of the values to use as a result of the quadratic formula.)

4.7 Atmospheric mathematical modeling is frequently done using atmospheric pressure as a vertical coordinate instead of elevation. Consequently, vertical motion (speed) is given in units of microbars per second (μb/sec). Suppose an air parcel is moving in such a way that its speed is given as -50 μb/sec. Determine the parcel's vertical speed in meters per second and miles per hour. Is the parcel rising of falling? Explain. (Hint : Use the hydrostatic approximation to equate pressure change to height change. Assume the parcel is located at a pressure level of 850 mb.)

4.8 A 1 kg parcel, with a density of 0.845 gm / L, is moving with a speed of 15 $\mathrm{m{\cdot}s^{-1}}$in the direction of 40 degrees east of south. Calculate the total Coriolis deflection vector on the parcel over a 2-minute interval.

Chapter 5

Atmospheric Circulations

5.1 Overview

Atmospheric motions, or circulations, are frequently categorized by their scale - both by their longest horizontal length and their usual life-span (length in time). Figure 5.1 provides a graphical view of several categories and their intervals on the length and time scales. There are three primary categories for atmospheric motion scale: macro (Ma), meso (Me), and micro (Mi). The **planetary** (PL) and **synoptic** (SY) scales are distinguishable sub-categories within macro scale. The figure shows the strong positive correlation between length and time scales for atmospheric phenomena. Scales of motion are not, necessarily, independent from one another. Mesoscale circulation types may be part of a larger synoptic scale feature.

The focus of this chapter will be planetary scale circulations. Subsequent chapters will cover important atmospheric motions of smaller scale, with a sequence of presentation from larger to smaller scale. Understanding any atmospheric circulation requires an understanding of its energy (source and forms), force, and moisture features. Some of theses features are common to all circulations, while others are unique or more prominent, in others.

5.2 Single-Cell Model

The single-cell model of planetary motion is based on an idealized non-rotating planet with a homogeneous surface. That is, a surface with no variation in makeup such as a water surface on a potion of the planet, and land surface on the remaining portion.

If the planet has a uniformly heated surface, the isobars (lines of constant pressure) distributed through a vertical plane extending from the equator to the pole run parallel to the planet's surface. In such a simple, idealized situation, there would be no net force on any atmospheric air parcel, as shown in Figure 5.2. Consequently, the planet's atmosphere would be calm.

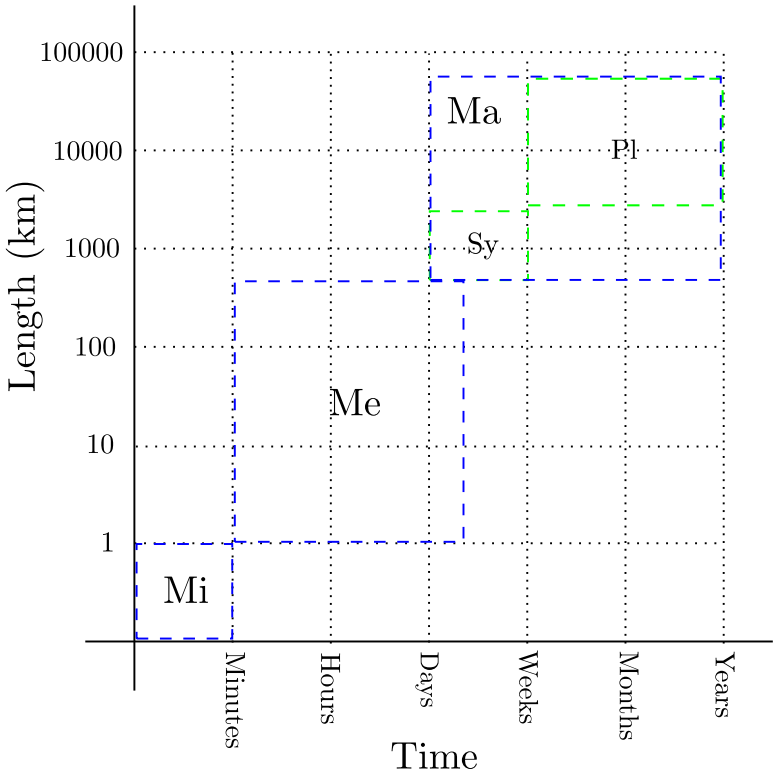

Figure 5.1: Various atmospheric phenomena scales.

In the case of a spherical planet heated by a single sun, as is the case with the Earth, differential surface heating results in a warm equatorial region and cool polar region. A surface temperature gradient results. Additionally, the air columns expand vertically over the warm surface while the vertical air columns contract over the cool surface. As a result, the isobars tilt "downward" as they extend from the equator to the pole, as shown in Figure 5.3. The tilting of the isobars creates a pressure gradient, with higher pressure on the equatorial side. Consequently, air parcels are accelerated pole-ward provided the pressure gradient force represents the net force on the parcel.

The pole-ward moving parcels result in a mass decrease in the upper reaches of the equatorial air columns. Low-level parcels with the column rise to fill the void resulting in a pressure decrease at the surface. The upper-air parcels travel to the polar region. Their added mass in the polar columns result in a pressure increase at the polar surface. The equatorial low pressure region, in conjunction with the polar high pressure region create a surface pressure gradient that, as a net force on the surface parcels, causes them to accelerate equator-ward. Thus a single rotational cell in the vertical plane is created.

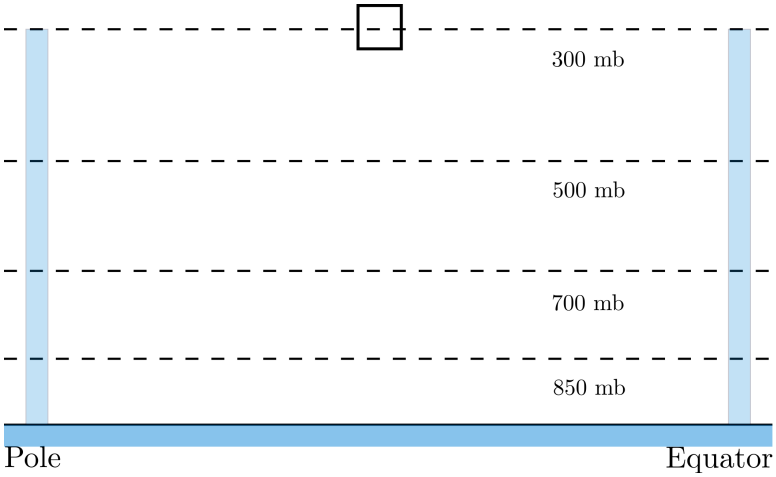

Figure 5.2: Uniformly heated surface.

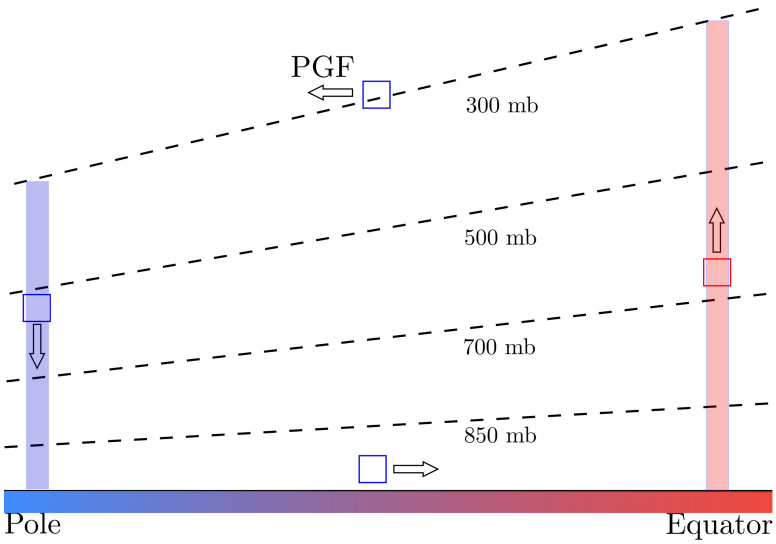

Figure 5.3: Non-uniformly heated surface.

With the equatorial region on the right side of the vertical plane, the counter clockwise rotating single cell exhibits rising air parcels in the equatorial region and sinking parcels over the polar region. Surface high pressure results at the pole due to the accumulating parcels above. Departing upper air equatorial parcels result in an equatorial surface low. Consequently, surface winds would be northerly from pole to equator. Upper-level winds

would be southerly from equator to pole.

A more realistic Earth-based circulation model would have the planet rotate on its pole to pole axis in a counter clockwise direction with the north pole on the "up side" of the sphere. Rotation introduces the apparent Coriolis force. The Coriolis force, in conjunction with the pressure gradient force, causes a right-ward path deflection for the moving atmospheric parcels in the northern hemisphere. Consequently, surface winds would be easterly, while upper air winds would be westerly.

The easterly surface winds from pole to equator do not match the observed surface wind pattern. Generally, surface winds are easterly near the pole and equator, but westerly in the mid-latitudes. For this and other reasons, the simple one-cell model is "rejected" as a viable explanation of the Earth's observed planetary scale motions.

5.3 Three-Cell Model

As elucidated in the previous section, the one-cell model fails to explain the observed surface wind pattern, especially the westerly pattern of the northern hemisphere mid-latitudes (Similarly, the easterly mid-latitude winds in the southern hemisphere). Further, this alternating surface wind direction pattern suggests the existence of three rotating vertical-plane cells.

Even though the one-cell model fails in some aspects, its thermal and physical underpinnings are not ill-founded. That is, the differential surface heating creates a pressure gradient that accelerates equatorial parcels pole-ward. A surface low pressure area develops in the equatorial region. Surface air is accelerated to the low. The northerly wind is deflected right-ward creating the surface easterlies as observed. However, the northbound upper air parcels do not complete the trek to the north pole. Rather, they begin to sink around the 30 degree north latitude.

There are various reasons why the upper air, polar-bound parcels sink. The relatively warm parcels, having risen from the surface, cool by radiation heat loss to the extent that they lose their relative buoyancy. Additionally, the Earth's rotation destabilizes the one larger cell that is expected to develop.

The sinking parcels reach the surface of the Earth and diverge. Some move equator-ward, others pole-ward. When the equatorial bound parcels reach their destination, a single, smaller cell has developed, stretching from the equator to the 30 degree north latitude. This cell is known as the **Hadley cell** after the English lawyer George Hadley, who was intent on finding a reason for the direction of the surface tropical winds.

The pole-bound surface parcels are part of the mid-latitude **Ferrel cell** that develops and rotates in a clockwise fashion. The parcels do not reach the pole, however. Instead, they meet the equatorial-bound parcels that are associated with the initial one-cell model. In theory, the meeting point is the 60 degree north latitude. Here, the converging parcels create a rising column of air parcels that splits at the top of the atmosphere. Some are

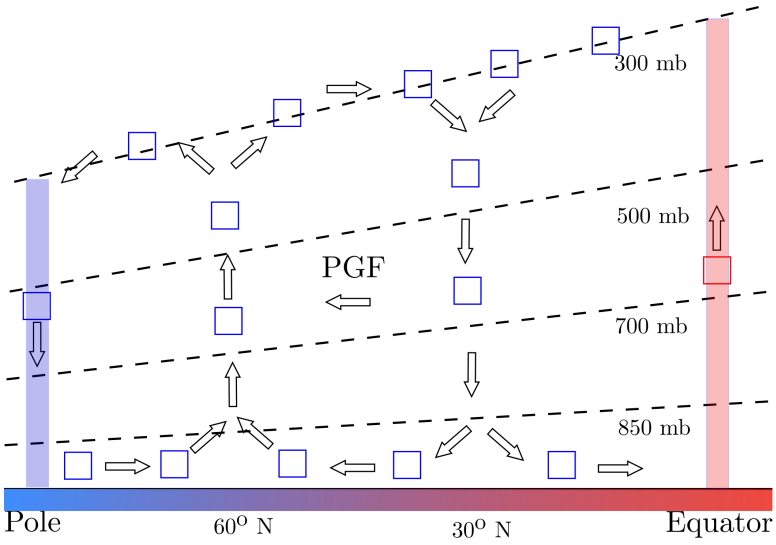

Figure 5.4: Cross-sectional view of the idealized three-cell model.

equator-bound as part of the mid-latitude cell. The others are pole-bound and belong to the **Polar cell** in the model. The resulting three cells are shown in Figure 5.4.

The three cells extend continuously in such a way that they circumvent to globe. The view in Figure 5.4 is that resulting from a vertical "slice" reaching from the pole to the equator. Additionally, the phenomenological cell and pressure patterns shown for the northern hemisphere is replicated as a mirror image for the southern hemisphere. This is partially due to the fact that the apparent deflection of parcel motion in the southern hemisphere is to the left of its current path instead of the right as it is in the northern hemisphere.

The Hadley and Polar cells are thermally direct cells because the warm air parcels are rising and the cooler air parcels are falling. The opposite is true with the Ferrel. The warmer parcels near 30° N are sinking while the relatively cooler parcels near 60° are rising. This is counter to what would be expected based on the concept of buoyancy. That is, warm parcel are less dense, so they would tend to rise while the cooler, denser parcels would like be sinking in their environment. Consequently, the Ferrel cell is a thermally indirect rotation and, therefore, is weaker that expected, especially at the higher altitudes.

5.3.1 Pressure Bands

The existence of the three cells give rise to three northern hemisphere pressure bands as shown in Figure 5.5. The rising, diverging parcels in air columns over the equator create a low pressure band that circumvents the globe creating what is known as the **inter-tropical convergence zone** (ITCZ). Figure 5.6 shows a satellite imagery of the intertropical con-

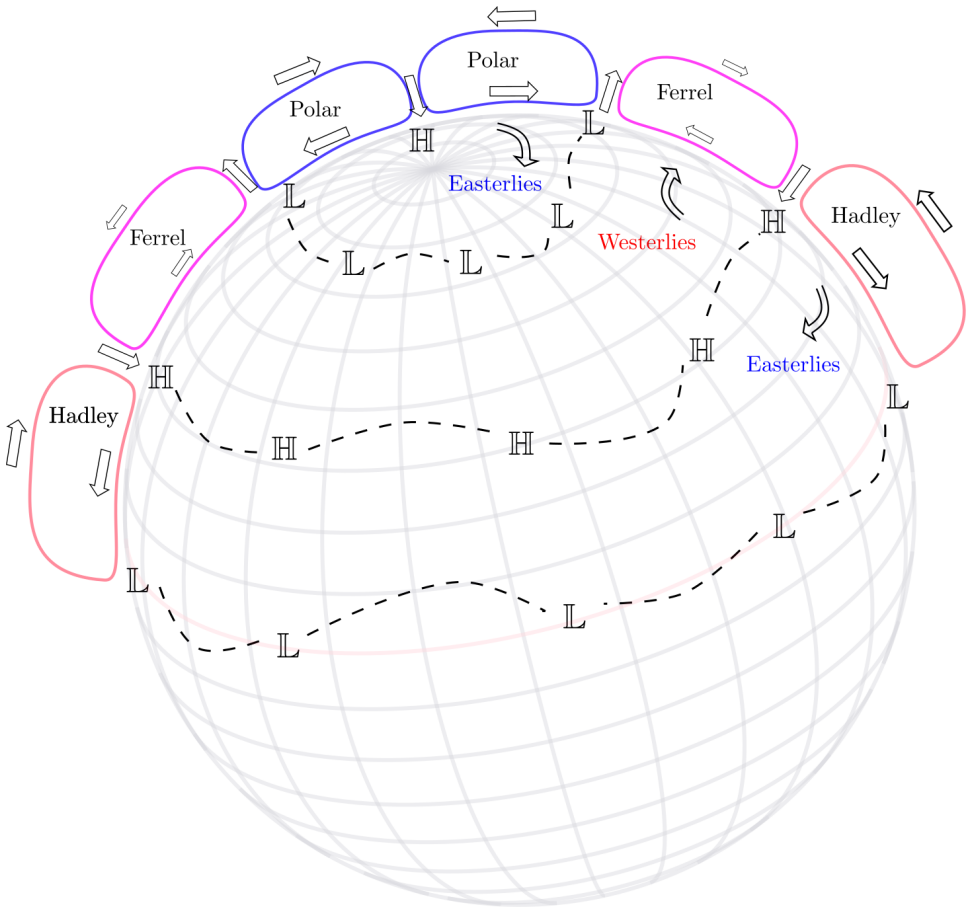

Figure 5.5: Three-dimensional view of the idealized three-cell model.

vergence zone identified by the horizontal band of cloudiness. The rising, moist air parcels cool as they ascend. The cooling of the air parcels condenses some of the water vapor to create clouds and perhaps, precipitation.

Converging parcels in the upper atmosphere over the 30° north latitude increase the pressure in atmospheric columns in this vicinity. The sinking parcels eventually diverge at the surface. As they sink, the increase in the pressure on the parcels warms them and endorses evaporation of condensed water content. Consequently, this high pressure band circumventing the globe is a region of relatively sunny and dry weather giving rise to many desert regions.

The Ferrel and Polar cells butt up against each other at the 60 degree north latitude.

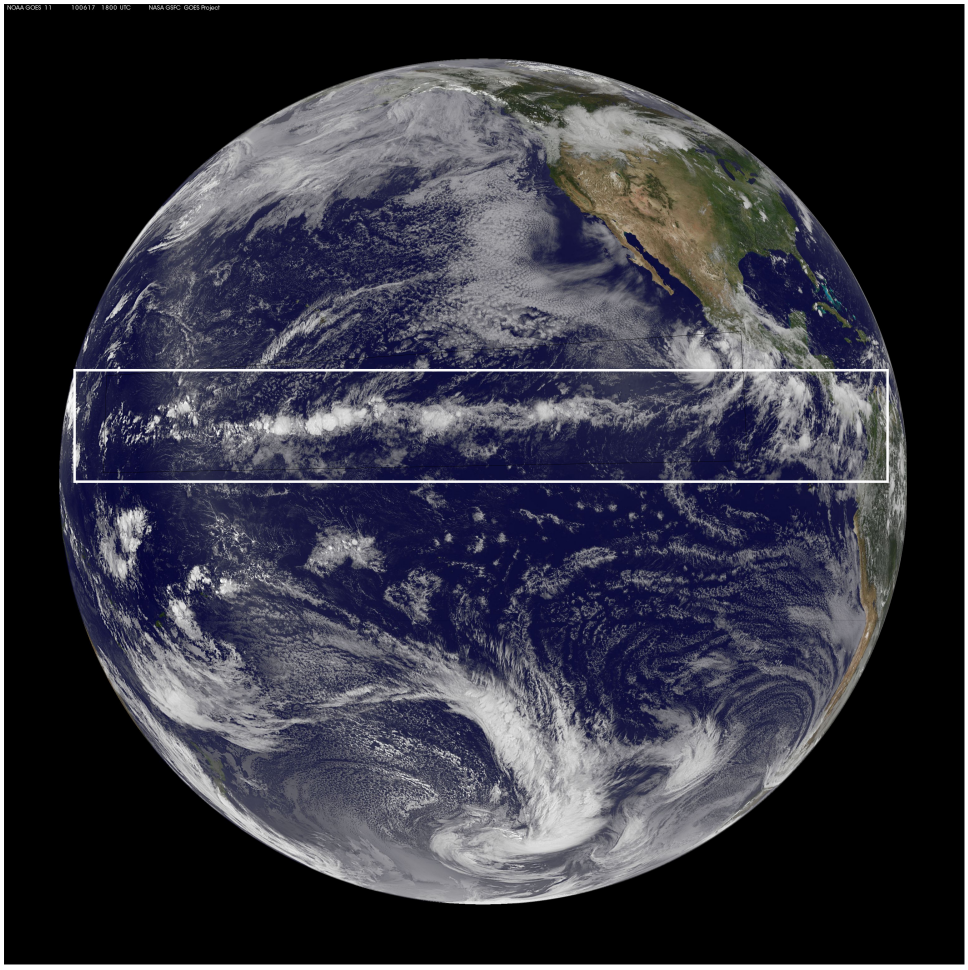

Figure 5.6: Satellite imagery showing the intertropical convergence zone cloud band within the white rectangle.

The rising parcels diverge at the top of the atmosphere to create a band of surface low pressure. Similar to the ITCZ, this band is a "trough" of low pressure that is characterized by cloudiness and precipitation.

5.3.2 Polar Front

The circulations associated with the Polar and Ferrel cells create a surface region, located approximately 60° north latitude, where parcels converge. The north-bound parcels bring warmer air north while the south-bound parcels from the polar region bring cooler air to the

region. The converging air, with associated temperature advection, create the **polar front**. The polar front is characterized by a steep temperature gradient, a discernible change in surface wind direction, and a change in atmospheric moisture along lines that cross the front perpendicularly.

5.3.3 Prevailing Surface Winds

The surface high and low pressure bands that result in the idealized three-cell model generate the observed surface wind pattern as shown in Figure 5.5. The surface pressure gradients that develop between the pressure bands accelerate surface air parcels from high pressure to low pressure. The motion time-scale associated with the general circulation is long enough so that the Coriolis rightward deflection eventually increases to balance the pressure gradient force (pressure gradient force + Coriolis deflection = 0).

Consequently, parcels moving from the polar high towards the subpolar low pressure band associated with the surface polar front follow a curved path, eventually creating the easterly surface winds.

Parcels moving northward from the subtropical high toward the subpolar low (the surface polar front) eventually reach a equilibrium state, resulting in the mid-latitude westerlies, as depicted in Figure 5.5.

The pressure gradient created by the subtropical high and the ITCZ accelerate surface parcels equatorward, only to bend into a westward direction (creating an easterly wind) once the Coriolis deflection balances the pressure gradient force.

5.3.4 Polar Vortex

The three-dimensional view of the northern hemisphere three-cell circulation shown in Figure 5.5 shows the existence of a surface high pressure region at the north pole. An upper air low pressure region is associated with the surface high. The upper air low accelerates air parcels pole-ward. The Coriolis effect deflects the parcel to the right resulting in a counter-clockwise rotation known as the **polar vortex**. This spinning mass of cold air is responsible for dramatic outbreaks of exceptionally cold air that plunges southward, sometime reaching the Midwestern and Northeastern portions of the United States. The cold mass of air can linger for several days creating an extended period of record, or near-record, low temperatures.

5.4 Jet Streams

Planetary and synoptic circulation patterns have time and spatial dimensions that are longer than other types of atmospheric circulations in the meso and micro scales. Although it would be reasonable to assume macro circulation patterns are rather homogeneous in space and time, there are instances where this is not the case.

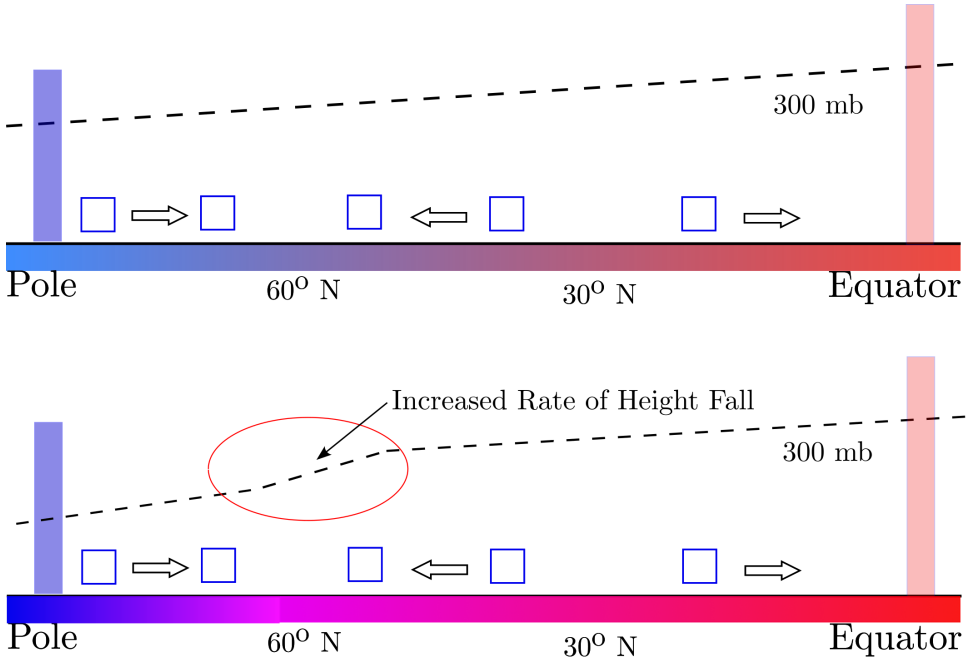

Figure 5.7: The surface polar front forms where the surface parcels converge near 60° north latitude.

An example of heterogeneous flow is a **jet stream**. This feature is characterized by narrow horizontal bands of increased wind speed embedded in the general flow. An increase in wind speed is typically due to an increase in the pressure gradient force on air parcels. Once a jet stream is observed, the explanation of its origin usually involves identifying the cause for a steeper pressure gradient.

Three **jets streams**, or *jets*, are explored in this section. The first two, the **polar jet** and **sub-tropical jet**, are global phenomena. The third is the **low-level jet** that is specific to the middle portion of the 48 contiguous United States.

5.4.1 Polar Jet

The polar jet is an upper level, fast moving stream embedded in the planetary circulation flow. Generally, it exists between the 500 and 200 mb levels. Is is associated with the surface polar front. The development of the polar front enhances the rate of height fall above the front, as shown in Figure 5.7. Recalling the height gradients are directly related to pressure gradients, the increase in the westerly wind speed is understood to be the result of the strengthened surface temperature gradient that enhances the height gradient above.

In theory, the polar jet develops as a continuous, single stream of higher velocity air

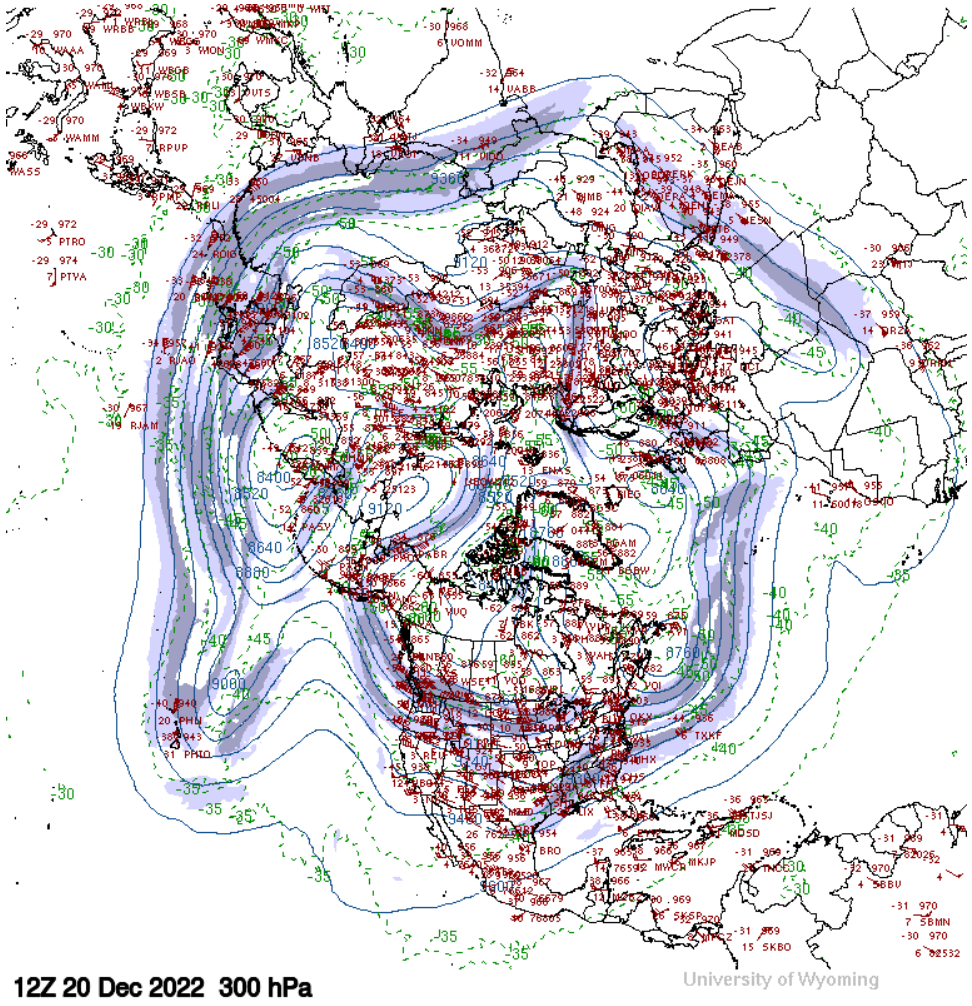

Figure 5.8: The northern hemisphere polar jet on December 19, 2022.

parcels traveling at the same speed as they encircle the globe in a perfectly circular path. In actuality, the polar jet rarely embodies either of these characteristics. Figure 5.8 shows the 300 mb surface over the northern hemisphere on December 20, 2022. It's characteristics are common to many instances of the phenomenon. The polar jet is identified by the closely packed height contours (solid lines) and the regions of dark gray shading. The instance of the polar jet is not a perfect circular steam of constant, higher speed parcels. Further, another common feature of the polar jet include its wavy pattern, the causes of which will be discussed later.

Figure 5.9 shows the flow at the 300 mb level on December 19, 2022 over the contiguous

United States. The polar jet is identified by the pink and red shading in the figure. Notice that in regions with this shading, the 300 mb height contours (shown as solid black contours) are packed more closely than in other regions in the figure. Additionally, note that the jet stream is not shown as a single continuous flow. Rather, it is split into two regions; a northerly branch over the northwestern states of Idaho and Montana, and a southerly branch flowing over the state of Texas. The two branches do eventually meet up again to form a single stream over the eastern portion of the United States. The polar jet with this structure is said to have a **split flow**.

The non-uniform speed feature of the polar jet gives rise to the existence of **jet streaks**. These are regions of increased speed, and often appear oval in shape, as indicated in Figure 5.9. The significance of jet streaks will be explored later in Chapter 7. Jet stream speed variation is due, in part, to sea and land surface thermal response to solar radiation heating. The north-south temperature gradient is generally greater over land than water. Consequently, the surface polar front packing of the isotherms is more extreme over land than water. This leads to a steeper height fall in the upper elevations over the surface polar front. The steeper height-fall (height gradient), in turn, results in a faster jet.

5.4.2 Sub-Tropical Jet

The sub-tropical jet stream forms in the upper atmosphere where the Hadley and Ferrel cells meet. The converging parcels enhance the north-south thermal gradient in much the same ways as the converging surface parcels do in the formation of the polar jet. In this instance, the frontal boundary exists at a higher altitude (as indicated in Figure 5.10), and is less prominent than the polar front because of the weaker circulation associated with the thermally indirect Ferrel cell. Never the less, there is an enhanced height gradient that ultimately enhances the speed of the parcels flowing northward towards the elevated front. The time-scale is long enough for the parcels to react to the right-ward deflection of the Coriolis force. Consequently, a west-to-east flowing jet stream develops at about 30 degrees north latitude.

$$L = m \cdot u \cdot r \tag{5.1}$$

The conservation of angular momentum is another factor that is responsible for the increased speed associated with the subtropical jet. The angular momentum L of an object is determined as the product of its mass m, the radius r of its circular path r, and its tangential velocity u, as shown in Equation 5.1. The tangential velocity of an air parcel on a circular path about the Earth is its east-west component of its velocity vector. The radius of the circular path an atmospheric parcel decreases as it travels pole-ward. For L to remain constant for an object of constant mass m, the tangential speed speed u must increase to compensate for the decrease in radius, as shown in Figure 5.11. This results in an acceleration of the parcel in an eastward direction.

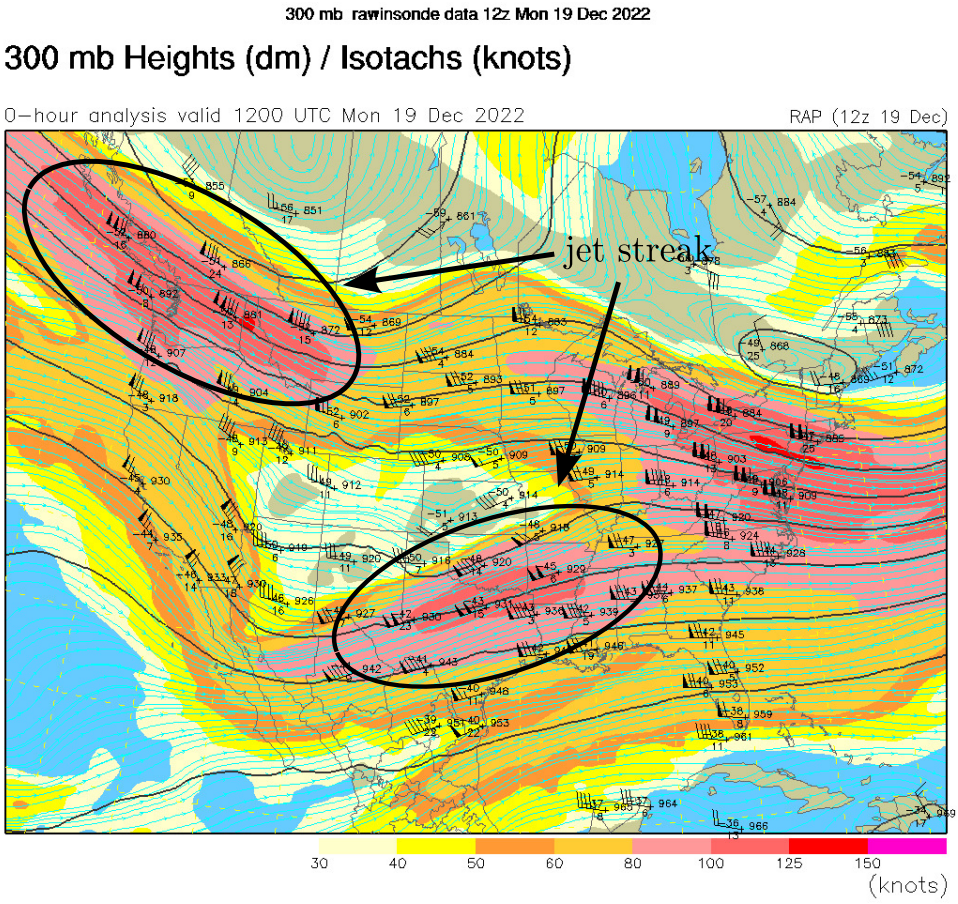

Figure 5.9: The polar jet over North America on December 19, 2022.

Example 5.4.1. A 2.0 kg parcel near the equator has an eastward velocity component of 10 ms^{-1} moves from the equator to 30 degrees north at the 300 mb level. Calculate the increase in its eastward speed due to the conservation of angular momentum

Solution:

Let $L_1 = m_1 \cdot u_1 \cdot r_1$ and $L_2 = m_2 \cdot u_2 \cdot r_2$ represent the parcel's angular momentum at the equator and 30 degrees north, respectively. Using the fact that $L_2 = L_1$

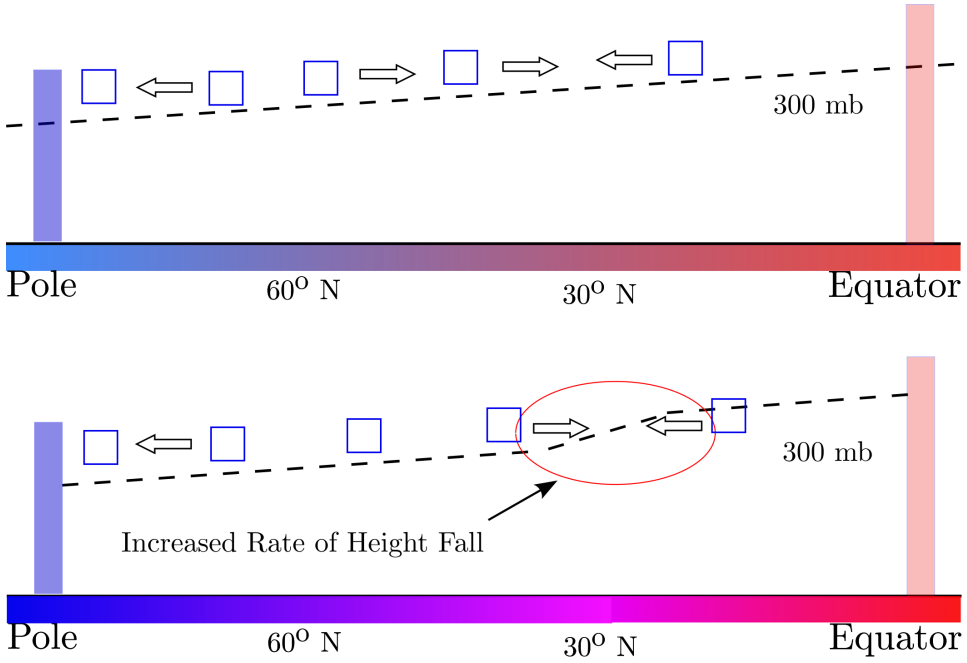

Figure 5.10: The subtropical upper-level front forms where the upper air parcels converge near 30° north latitude.

and $m_2 = m_1$, it follows

$$\begin{aligned} L_2 &= L_1 \\ u_2 \cdot r_2 &= u_1 \cdot r_1 \\ u_2 &= u_1 \cdot \frac{r_1}{r_2} \\ &= u_1 \cdot \frac{r_1}{\cos 30 \cdot r_1} \\ &= u_1 \cdot \frac{1}{\cos 30} \\ &= u_1 \cdot \frac{2}{\sqrt{3}} \\ &= u_1 \cdot 1.155 \\ &= u_1 + 0.155 \cdot u_1 \end{aligned}$$

The last line of the calculation indicates an increase of $0.155 \cdot 2 = 0.31$ ms^{-1}. Note that the factor of 0.155 is independent of the speed u_1. Consequently, this may be interpreted as a 15.5% increase in the eastward speed of a parcel.

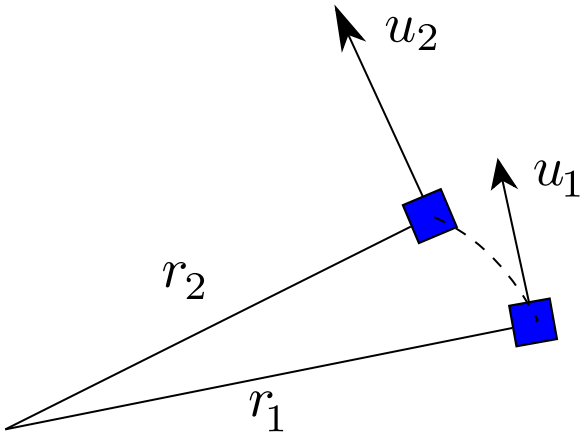

Figure 5.11: The conservation of angular momentum contributes to the acceleration of parcels that make up the subtropical jet.

5.4.3 Low-Level Jet

Unlike the polar and sub-tropical jets exist on a planetary scale and on a continual time basis, the low-level jet described in this section is an occasional feature of large-scale flow over the central portion of the United states. Although its time and length scales are much less than the polar and sub-tropical jets, the low-level jet plays a significant role in the weather, especially concerning precipitation for the mid section of the North American continent.

This jet develops due to a pressure gradient force between relative high pressure over the southeastern portion of the U.S. and low pressure over the central Rocky mountains, as depicted in Figure 5.12. Atmospheric parcels are initially accelerated westward by the pressure gradient force. The time scale for the phenomena is long enough for the Coriolis effect to deflect the parcel and eventually create a geostrophic southerly wind a low atmospheric levels just above planetary friction layer. The southerly wind transports moisture from the gulf of Mexico northward where it may provide needed, or enhanced, moisture and latent heat for precipitation events.

A surface or low-level low pressure area over the southern Rockies has the potential to create a low-level jet. Another frequent cause for the jet to develop is the differential heating between the southeastern US and the Rocky Mountains. The rocky surface of the mountains warms during the day. The evening radiational cooling causes pressure heights

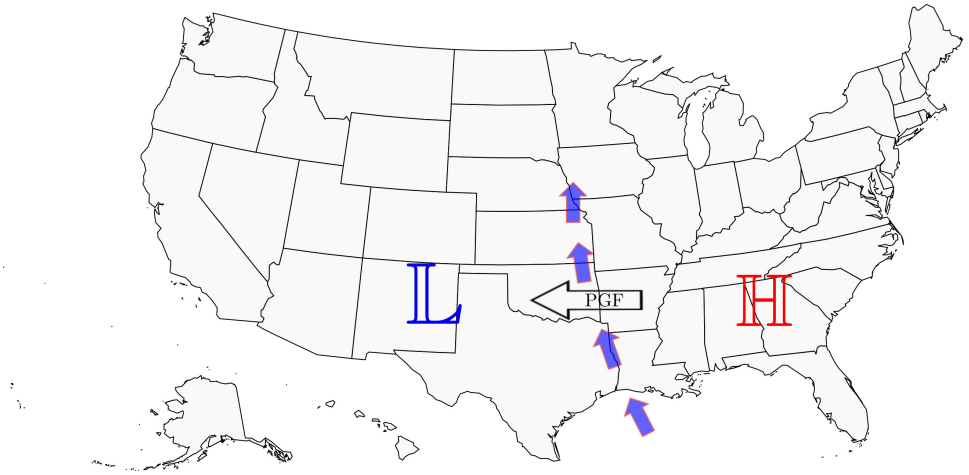

Figure 5.12: The low-level jet.

to fall relatively more than those over the southeastern U.S. causing a nocturnal pressure gradient. Additionally, the heat loss due to radiational cooling is greater for the dry air over the western portion of the United States Therefore, low-level jets that form due to this phenomena are called **nocturnal low-level jets**. The nocturnal jet reaches its maximum intensity in the hours around sunrise. As the sun continues to warm the Earth's surface the differential heating causing the pressure gradient diminishes. The strongest wind speeds, reaching a maximum magnitude between 40 and 70 knots, are typically located around the 850 mb level.

The low level jet intensity may be strengthened through its coupling with the occurrence of jet streaks embedded in the polar jet stream. Jet streak are regions of higher intensity pressure gradient which lead to pockets of increased wind speed associated with the jet stream. Regions of high altitude convergence and divergence develop in relation to the jet streaks. Divergence aloft will, in many instances, lead to pressure falls near the Earth's surface. When this happens, a north-south pressure gradient develops that enhances the pull of warm, moist air parcels near the Gulf of Mexico northward.

Chapter 5 Exercises

5.1 The solar radiation imbalance between the north pole and the equator is compensated by at least three energy transport mechanisms. Identify and describe these mechanisms. Include an indication of the latitudinal dependence of each mechanism. That is, for what northern hemisphere latitudinal interval, or intervals, is each of the mechanisms prominent.

5.2 One cell, three cell ... Explain why it is reasonable to conclude that any planetary scale

circulation model would have an odd number of vertical plane circulation cells in a given hemisphere.

5.3 The three cell theory for the northern hemisphere has surface high or low pressure "bands" that encircle the globe at certain latitudes in perfect, unbroken circles. With the aid of a sketch, indicate where (what latitude), what type (high or low pressure), and why the pressure bands develop as projected by the theory. Observation reveals the bands are not perfectly circular and unbroken, and the summer pattern is different than the winter pattern, especially for the northern hemisphere. Explain what factors account for the differences in model projections and observation.

5.4 Compare and contrast the polar and the subtropical jet streams in the northern hemisphere in terms of genesis, location, structure, and speed.

5.5 Explain how and why the pattern of land and water surfaces alters seasonal average surface pressure at 30° and 60° in the northern hemisphere (a) summer, and (b) winter.

5.6 Identify three jet streams relative to the United States. Describe the origin and characteristics of each. Discuss the impact, if any, each has on "weather" in the Midwest.

5.7 Explain where (latitude-wise) and why deserts generally exist in the northern hemisphere.

5.8 Explain where (latitude-wise) and how the surface polar front develops.

5.9 Explain the reason why a "general circulation" develops within the Earth's atmosphere.

5.10 Explain the impact of surface variation (land versus water) on the Earth's planetary-scale circulations.

5.11 Identify the different scales of motion within the Earth's atmosphere.

Chapter 6

Air Masses & Fronts

6.1 Overview

This chapter provides a superficial introduction to the planetary scale features of air masses and fronts. It describes how air masses develop their distinctive characteristics. At any time, the earth's surface has multiple, identifiable air masses. The boundary between these masses are referred to as "**fronts**." These boundaries become especially indefinable and important when the movement of air masses causes one type to collide with another. The collision sharpens the boundary, and in many instances create atmospheric conditions conducive to weather "events." These events can be severe in some cases.

6.2 Air Masses

The most basic characteristics of an atmospheric parcel include its temperature and moisture content. In fact, they are used almost exclusively classify air masses. There are broad categories within each. Temperature is classified as warm, polar, or arctic, with arctic being the coldest of the three. These categories are defined on a relative basis. That is, there is no specific temperature interval assigned to a given category.

Moisture content of a specific air mass is classified as either moist or dry. As with parcel temperature, the distinction is made in a relative way with no set interval of moisture measurement assigned to a given category.

Air masses types develop in-regions of high pressure. High pressure regions have weaker pressure gradients, so the winds associated with theses systems are slower. Slower moving air parcels near the earth's surface take on the characteristics of the surface over which they reside.

The high pressure bands associated with the three-cell planetary scale circulation model are primary locations for air mass development. Cold air masses (arctic and polar) develop in relation to the polar high pressure region. The warmer tropical air masses develop in the

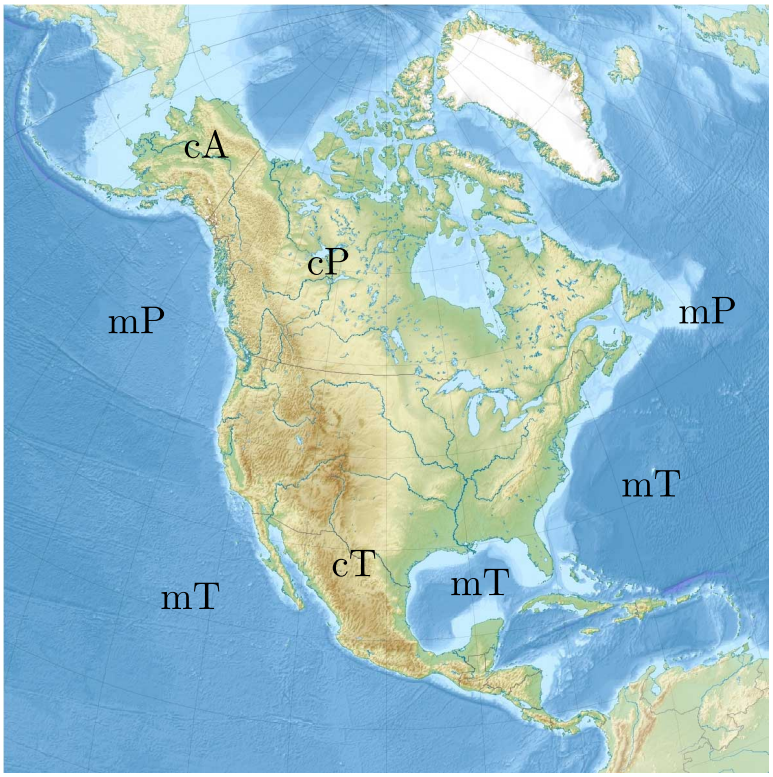

Figure 6.1: Origination regions of prominent North American air masses.

lower latitudes of the southern Unites States. Figure 6.1 shows the regions near the north American continent where air masses develop.

Air masses are identified using a two-letter system. The first letter is either a lowercase "m" for a maritime origin or "c" for a continental origin. Maritime air is relatively moist. Continental air is relative dry.

The second letter is uppercase and it roughly corresponds to the latitude of air mass origination. Tropical air masses are relatively warm and use the letter "T." Colder air masses that originate over Canada are designated with the letter "P" for **polar**. The coldest air masses have an Arctic origin so an "A" is used as the temperature identifier. Table 6.1 summarizes the identifiers and characteristics of the primary air masses for the North American continent.

Although low wind conditions facilitate the development of air mass characteristics, upper atmospheric winds are a primary reason air masses migrate. General circulation patterns, as explained in Chapter 5, include such features a the polar front, the boundary between arctic air to the north and tropical air to the south.

		Arctic (A) coldest	Polar (P) cold	Tropical (T) warm
Continental	dry	cA	cP	cT
Maritime	moist	mA	mP	mT

Table 6.1: Classification of the primary North American air masses.

Chapter 7 focuses on mid-latitude cyclones (MLCs) that frequently develop along the polar front. MLCs are just one type of cyclone. In the norther hemisphere, cyclones create counter-clockwise circular flow around their centers. This surface flow is another factor that causes frontal stationary frontal boundaries to migrate. MLC centers will be denoted using the letter "$\mathbb{L}$" in the text that follows.

The boundaries between the air masses become more explicit as one air mass replaces another. Theses frontal boundaries are the next focus of this chapter.

6.3 Fronts

Surface weather charts provide an abundance of meteorological information and analysis. The depiction of frontal boundaries provides vital information for observers and forecasters. There are four primary fronts that are marked on a surface chart. The types and symbolism used to show the location of frontal boundaries are shown in Figure 6.2.

Stationary fronts are indicated using alternating red and blue lines. The blue sections have triangular barbs and the red sections of red semicircular lobes. The rationale for these markings will be understood once the differential characteristics of the various fronts are disclosed later in this chapter. **Warm fronts** are marked entirely in red. **Cold fronts** are marked entirely in blue. **Occluded fronts** have a purple color with alternating triangular barbs and semicircular lobes.

Figure 6.3 show data and analysis of surface weather data collected on March 03 of 2020. There are a number of fronts marked on the chart. The longest one, stretching from Arizona in the southwest, to Maine in the northeast, is the polar front feature of the three-cell global atmospheric circulation. As seen on this chart, portions of the front are identified as stationary, warm, or cold fronts.

As stated above, temperature and atmospheric moisture content are the primary factors that distinguish air mass form one another. Frontal boundaries are where these characteristic change rather abruptly. Another important factor associated with fronts are the surface and near-surface winds. They may change in speed and direction across the frontal boundary.

Generally, frontal boundaries are regions of lower pressure because they are regions of converging surface parcels, especially when frontal boundaries are moving. As the parcels

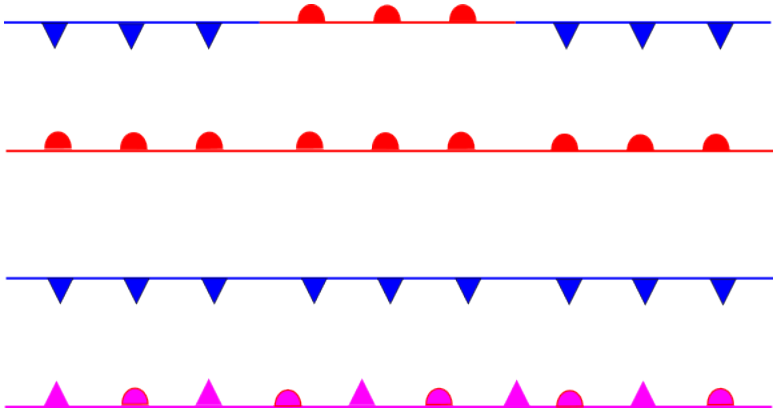

Figure 6.2: Frontal notations on weather charts. From top to bottom: stationary front, warm front, cold front, and occluded front.

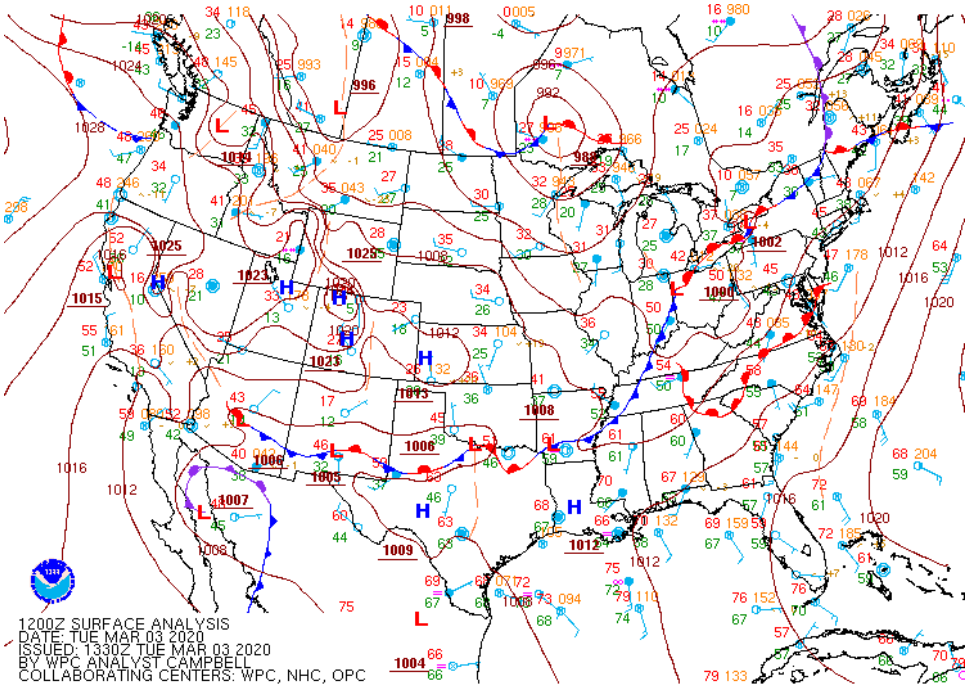

Figure 6.3: Frontal boundary depiction on a surface chart.

converge at the surface, they rise in the air column above the front and eventually diverge aloft. Lesser friction aloft results in greater parcel speed and, therefore, a divergence magnitude greater than its counterpart of surface convergence. Net loss of column mass results is a lower surface pressure. The characteristics that differentiate these various types of fronts are discussed next.

6.3.1 Stationary Front

Air masses are moved mostly by upper level winds. A *stationary front* results when upper-level winds are weak or flow in a directions parallel to the front. Surface winds blow parallel to, or slightly towards, the front. Frequently, the flow is in opposite direction on the two sided of the front. The result a boundary between air masses with characteristics like those shown if Figure 6.4.

Figure 6.4a shows the typical surface characteristics of a mid-latitude stationary front. A continental polar air mass rests to the north of the front and maritime tropical air to the south of the boundary. Higher pressure to the north of the front results in anti-cyclonic flow parallel to the front in an east-to-west direction. Lower pressure to the south results in parallel winds blowing west-to-east along the southern edge of the front.

Figure 6.4b is a vertical cross-sectional view of the front. Weak rising motion is associated with the stationary front as small-magnitude convergence exists along the front. Consequently, broken cloud cover with little precipitation is commonly associated with a stationary front.

Stationary fronts are usually not the focus of significant precipitation. The one exception to is during the summer months when the front acts like a track or trough for a series of thunderstorms to follow. Training cells in this scenario can result in significant rainfall along the frontal boundary.

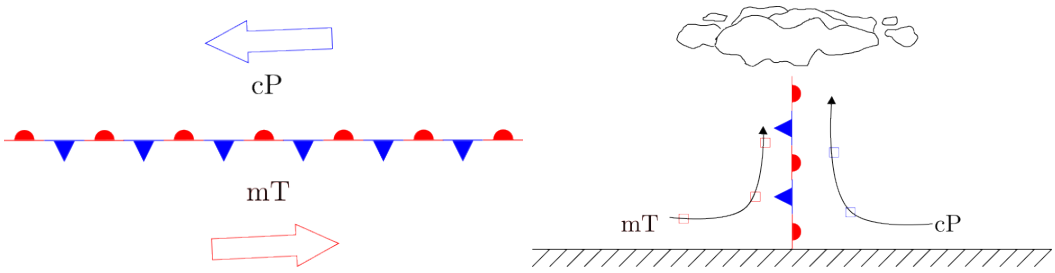

(a) Stationary front at the surface.

(b) Vertical cross-section of the stationary front.

Figure 6.4: Two views of a stationary front.

6.3.2 Warm Front

The wind characteristics associated with a stationary front may change in such a way that the perpendicular component on the warmer mT side becomes stronger than its counterpart on the cP side, as seen in Figure 6.5a. Consequently, a **warm front** develops with the warmer and more moist air mass advancing to replace the colder, dryer air mass. However, the warmer air parcels are more buoyant than the colder parcels so that they ride up and over the cooler parcels, as shown in Figure 6.5b.

The warm parcels cool as they rise due to the drop in pressure. Eventually, the cooling is sufficient to cause condensation within the parcel and the formation of clouds. The cloud cover further down-stream from the surface frontal location is higher. The much colder environment means the higher elevation clouds are entirely composed of ice crystals.

The slope of the warm front is given by $\frac{\Delta z}{\Delta s}$, where $\delta z =$ the change in elevation and $\delta s =$ the change in horizontal position, is about 1 km per 300 km. This is a rather "shallow" slope compared to other vertical cross-section slopes. Another frontal characteristic is the average speed at which the surface-based boundary moves. For a warm front, this speed averages about about 10 miles per hour. The movement is, in many instances, not continuous. Rather, the movement can stall out at times, and then jump ahead rather quickly.

The precipitation associated with a warm front is, generally, not heavy or intense and can vary in type, especially in the colder months. The precipitation far 'ahead of" the surface boundary can be frozen, either snow or sleet. As the warm front approaches a region, the precipitation may change to freezing rain. This happens because the frozen hydrometeors may pass through a significant vertical stretch of warmer air enabling them to melt. However, the melted particles may be below 32°F. If so, the liquid water will freeze on contact with surfaces such as tree branches and power lines. Road and walk-way surfaces can become slick as well.

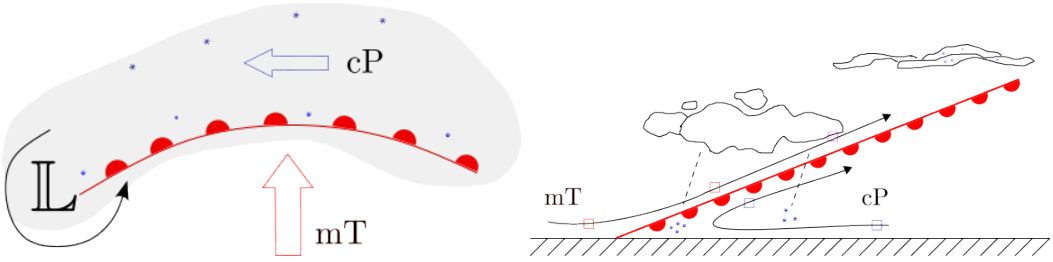

(a) Warm front at the surface. (b) Vertical cross-section of the warm front.

Figure 6.5: Two views of a warm front.

6.3.3 Cold Front

A **cold front** develops when the winds on the cold side of the frontal boundary are stronger than those on the warm side, as indicated in Figure 6.6a. In this scenario, colder and drier air replaces warm, moist air at the surface. The vertical cross-section of the idealized cold front is shown in Figure 6.6b. The cold front profile is more "vertical" than the case of the warm front.

The slope ($\frac{\Delta z}{\Delta s}$) of an average cold front is 1 km per 50 km, or roughly 6 times steeper than a warm front. Cold front surface speed averages about 15 to 25 mph, as much as three times as fast as the average speed of a warm front. One reason for the faster forward motion of the front is the downward motion of the colder parcels, as shown in Figure 6.6b. Colder parcels are more dense that the warmer parcels, so they "fall" from higher altitudes to the surface, picking speed as they descend and potential energy is converted to kinetic energy.

The warmer parcels on the mT side rise more quickly than in the case of warm fronts. This faster ascent results in clouds that grow faster and deeper into the upper atmosphere. In the warmer months, this process enhances the potential development of severe thunderstorms with intense rainfall and gusty winds. In the colder portions of the year, cold front usually do not generate thunderstorm growth. Instead, snow squalls and blowing of fallen snow are common characteristics of cold front passage.

Figure 6.6b depicts a type of cold front known as a **katafront**. In this case, the dominant line of precipitation develops slightly ahead of, or above, the surface front. An **anafront** is characterized by a precipitation band that forms behind the surface front. Further, the precipitation is less intense, more like the precipitation associated with a warm front.

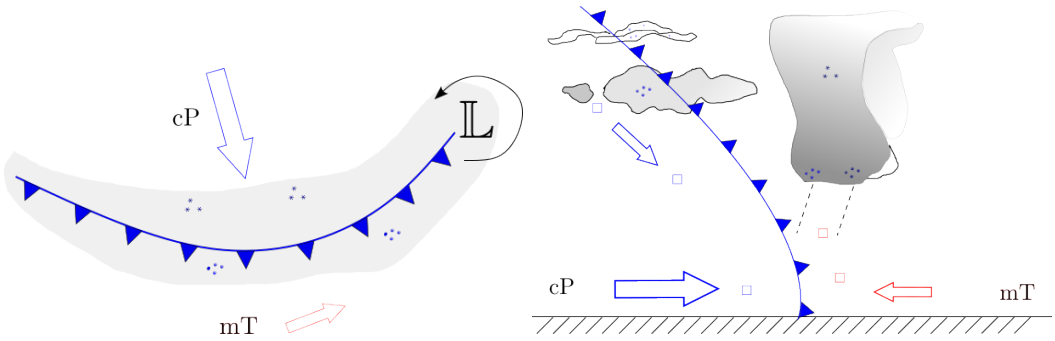

(a) Cold front at the surface.

(b) Vertical cross-section of the cold front.

Figure 6.6: Two views of a cold front.

6.3.4 Occluded Front

Warm and cold fronts develop when a stationary front begins to move. Chapter 7 is devoted to understanding the development and life cycle of the **mid-latitude cyclone.** The associated cyclonic flow results in a warm front developing to the east of the cyclone, and a cold front developing to the west of the cyclone. Much like hands on a clock, these fronts rotate around the center of the cyclone in a counter-clockwise direction.

As the cyclone circular rotation continues, the faster moving cold front may eventually "catch up" to the warm front. If so, the result is the development of an **occluded front**, as depicted in Figure 6.7a. The purple color of an occluded on the weather chart indicates that it is a mixture of warm and cold air. The barbs and semicircular lobes of the cold and warm front, respectively, point in the same direction, unlike the case of a stationary front.

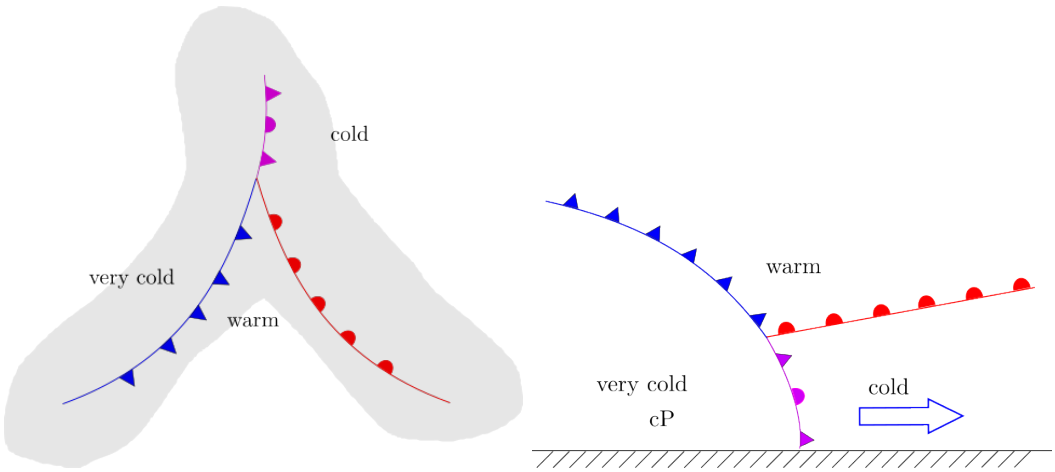

(a) Occluded front at the surface.

(b) Vertical cross-section of an occluded front.

Figure 6.7: Two views of an occluded front.

The vertical structure of an occluded front is depicted in Figure 6.7b. The coldest air mass is behind the front. The air ahead of the front is generally not as cold as that behind the front due to mixing of warm and cold parcels.

The location where the three types of fronts meet is called the **triple-point**. The relatively warm sector exists above the triple-point between the cold and warm frontal boundaries aloft, as shown in Figure 6.7b. The triple point is also a surface feature shown in Figure 6.7a. This point is a preferred location for the development of a subsequent low pressure center.

Chapter 6 Exercises

6.1 Explain why a cold front moves faster than a warm front.

6.2 Describe ways in which warm and cold fronts are similar, and ways in which they are dissimilar.

6.3 Explain how an occluded front develops. Sketch a vertical cross-section of atmosphere associated with an occluded front. Be sure to identify regions of relative cold air and warm air.

6.4 Approximately how far would and average warm front and an average cold front move in 24 hours?

6.5 If the warm and cold fronts associated with a mid-latitude cyclone move at their average speeds, approximately how long would it take for an occluded front to develop?

6.6 Explain why any frontal boundary can be the location for cloudiness and precipitation.

6.7 Describe where and why air masses are formed.

6.8 Identify to two primary characteristics that differentiate air masses.

Chapter 7

Mid-latitude Cyclones

7.1 Overview

The midlatitude cyclone (MLC) is one of the more important synoptic-scale features of North American weather. This feature is prominent in other regions on the Earth as well, and play a significant role in the dynamics of weather for the continental Unites States and North America. This chapter explains where and how these cyclones develop.

Generally speaking, midlatitude cyclones exist due to strong differences of surface temperatures in the northern hemisphere middle latitudes (the polar front) and the relative strength of the Coriolis force. Large horizontal- and time-scale cyclones require the Coriolis effect for their development. Although tropical cyclones exist, such as hurricanes or typhoons, they develop far enough north of the equator for sufficient Coriolis deflection. And, these water-born cyclones have the ocean surface heat as their primary energy source.

In terms of development, two important atmospheric flow characteristics of **mass divergence** and **vorticity** are studied in this chapter in order to understand the physical means of MLC development. Both flow-related characteristics have various forms with associated mathematical formulas. Additionally, they are intrinsically related in certain types of atmospheric conditions.

Significant attention is given to the **Norwegian Cyclone Model** that describes the life cycle of a typical MLC. This model has stood the test of time even though it was proposed in the early part of the twentieth century when current robust means of atmospheric data collection, such as Doppler radar and satellite imagery, were not available. However, the concept of the cold conveyor belt (one tweak of the model) is presented in this chapter. Even with a smaller than global scale, MLCs play a significant role in the global energy budget as explained near the end of the chapter.

7.2 Where and How MLCs Develop

To observers on the surface of the Earth, midlatitude cyclones exhibit horizontal, counterclockwise circular flow in the northern hemisphere. This circulation develops on a smaller horizontal scale than the larger scale planetary motion that does not exhibit horizontally-based circular motion.

The development of cyclonic flow is known as **cyclogenesis**. Common locations for cyclogenesis include regions where surface low pressure exists as part of the general, planetary-scale pressure patterns or where significant temperature gradients exist. A horizontal temperature gradient is temperature change with a change in horizontal position. The greater the change in temperature with respect to position, the greater the temperature gradient. The mathematical definition of a temperature gradient is given in Equation 7.1, where ΔT is the magnitude of temperature change, and Δs is the magnitude of position change.

$$\text{temperature gradient} = \frac{\Delta T}{\Delta s} \tag{7.1}$$

In terms of "standing" low pressure regions, the polar front associated with the general, planetary-scale circulation is a band of low pressure that, in theory, encircles the globe at a northern latitude of approximately 60 degrees. This band is a "trough" of low pressure. There is no circular flow, per se, associated with the trough. Wind direction does change "across" front, with a westerly wind to the south and an easterly wind to the north.

With respect to the continental United States, large temperature gradients naturally exist along the polar front (a predominant feature of the three cell general circulation model) and along land-water boundaries of significant length. Generally, that means boundaries associated with large water area such as the Gulf of Alaska, the Gulf of Mexico, and the eastern sea board. Please refer to Figure 7.1 for these various preferred locations. The figure also includes a typical path a cyclone will follow if it develops in one of these location.

In addition to a region of standing low pressure or a strong temperature gradient, cyclogenesis requires a mechanism that will decrease surface pressure. Pressure drop mechanisms such as mass divergence and vorticity advection will be described next.

7.3 Divergence: Loss of Mass

Figure 7.2 depicts a column of air in the Earth's atmosphere that is loosing mass due to **divergence**. An arbitrary horizontal cross-section of the column is shown with each side of the cross-section in a different color. The cross-section is replicated to the right of the atmospheric column, but shown from the perspective of look "down" through the column. The boundary colors of this replication correspond to the boundary colors of the cross-section shown in the atmospheric column.

There are two possible types of divergence that may exist in the flow field of atmospheric parcels. Referring to Figure 7.2, parcels numbered 1 and 2 depict **path divergence**. In

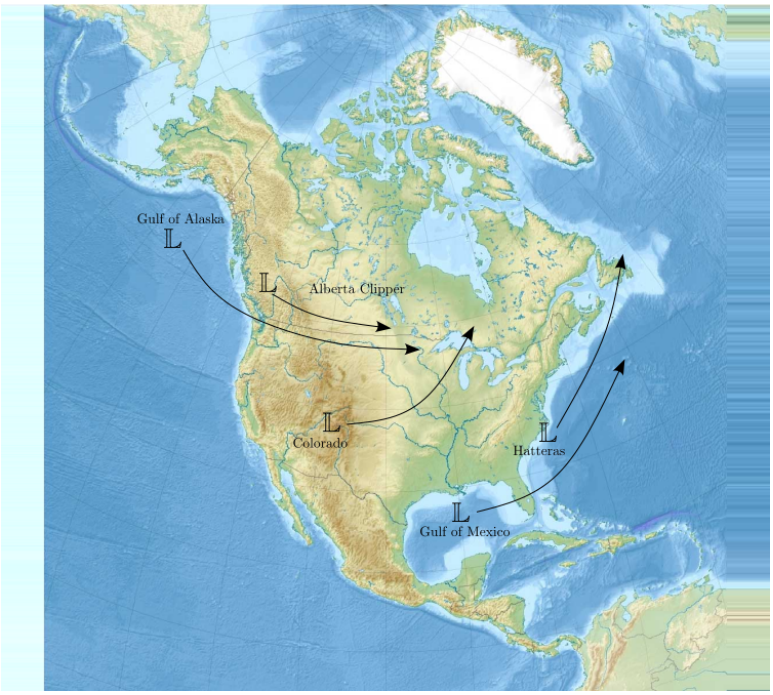

Figure 7.1: Preferred locations for the development of midlatitude cyclones.

this case the paths of the parcels, as shown with the curved arrows, spread further apart as the parcels enter and leave the column.

A second type of divergence, depicted by parcel numbers 3 and 4 in Figure 7.2, is **speed divergence**. In this instance, the parcels' paths are in the same direction, but their speeds are such that the distance between the parcels increase because the speed of parcel 4 is greater than the speed of parcel 3.

The increase in the distance between parcels results in a decrease in air density for the same area (or volume, assuming a cross-sectional thickness of one meter) of the parcel. Recalling that mass = volume $\times$ density, a decrease in density with a constant volume results in a decrease in mass. Further, the pressure at the base of the column is given by the mass of air in the column divided by the cross-sectional area of the column. A constant cross-sectional and a decrease in column mass results in a decrease in pressure at the base of the column (the Earth's surface), as indicated by the "$\mathbb{L}$" symbol in the figure.

A mathematical formula for **divergence** is given in Equation 7.2. The horizontal wind field is specified as a vector $\vec{v}$ with components u and v. Any vector, wind or otherwise, has both magnitude and direction. The vector's magnitude is the "length" of the vector, given

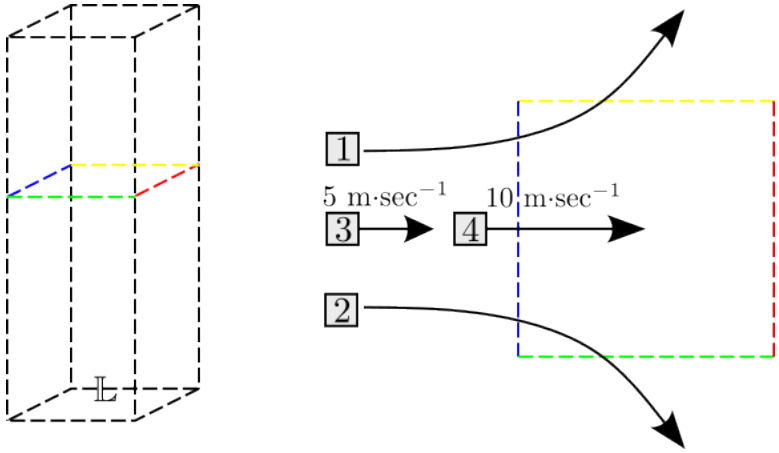

Figure 7.2: Loss of mass from an atmospheric column.

by the formula

$$\text{vector magnitude} = \sqrt{u^2 + v^2}$$

The direction is determined by the positive or negative signs of the two components. In this vector "structure," u is the wind speed in the x-direction and v is the wind speed in the direction of y, typically measured in m·s^{-1}. Referring to Figure 7.3, a positive u value indicates the wind has an x component in the positive x direction. A negative u value indicates the speed in the x-direction points in the negative x direction. The same is true for the value of v.

$$\text{divergence} = \text{div} = \frac{\Delta u}{\Delta x} + \frac{\Delta v}{\Delta y} \tag{7.2}$$

All terms in Equation 7.2 are "changes" (signified by the "Δ" symbol), so values for a given variable must be known at two locations. The change in u is associated with the change in x because the u flow direction is perpendicular to the west and east "faces" (oriented north to south) of the rectangular region shown in Figure 7.4. For a similar reason, the change in v is taken between the north and south faces of the region because the v flow is parallel to the y direction, therefore perpendicular to the east-west orientation of the north and south faces. A further understanding of the how the divergence is calculated is gained by considering Example 7.3.1.

Example 7.3.1. Use the velocity field information given by Figure 7.4 and the definition of divergence given by Equation 7.2 to determine the divergence at location "$\mathbb{X}$" in the figure.

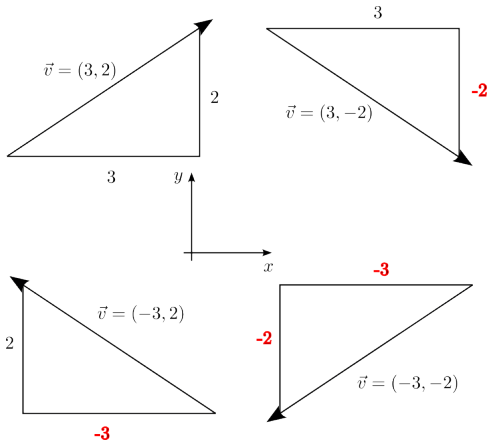

Figure 7.3: Wind vector examples.

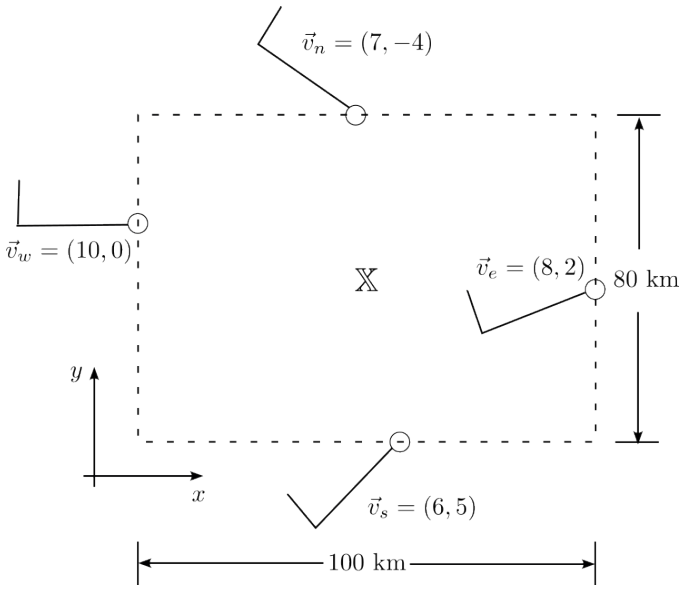

Figure 7.4: Example velocity field. The subscripts e, w, n, and s are used to identify on which "face" of the rectangular region the value resides.

Solution:

Using the $x - y$ coordinate orientation in the figure, $\Delta x = 100$ km, and $\Delta y = 80$ km. However, these value must be converted to lengths in meters, so $\Delta x =$

100 km × 1000 m per km = 100,000 m, and Δy = 80 km × 1000 m per km = 80,000 m.
Next, calculate Δu using the vectors $\vec{v}_e$ and $\vec{v}_w$.

$$\Delta u = u_e - u_w = 8 - 10 = -2 \text{ m·s}^{-1}$$

Note that u_e is used as the first value because it is associated with the greatest x-location. Now, calculate Δv in a similar way:

$$\Delta v = v_n - v_s = -4 - 5 = -9 \text{ m·s}^{-1}$$

With all Δ values known

$$\begin{aligned} \text{div} &= \frac{\Delta u}{\Delta x} + \frac{\Delta v}{\Delta y} \\ &= \frac{-2}{100000} + \frac{-9}{80000} \\ &= -0.00002 - 0.0001125 = -0.0001325 \\ &= -13.25 \times 10^{-5} \text{s}^{-1} \end{aligned}$$

The negative value for div means that at location $\mathbb{X}$, mass is accumulating. That is, a negative divergence value implies mass is "converging"(increasing) at that point. Consequently, the surface pressure at the base of the column of air with the cross-section used here increases.

Although the calculation of divergence is straight-forward using a mathematical equation and gridded wind field data as shown in Example 7.3.1, it is somewhat more difficult to discern divergence in visual analysis of atmospheric data charts. In the next section, an alternative means for locating regions of divergence of weather charts is introduced.

7.4 Vorticity

Vorticity is a measure of the rotation in the motion of an object. After describing the various forms of vorticity and defining it mathematically for sake of computational purposes, a relationship between divergence and vorticity is established at the end of the section.

7.4.1 Planetary Vorticity

The Earth may be thought of as a solid sphere that is rotating on its north-south axis with an angular speed of $\Omega = 2\pi$ radians per 24 hours $\approx 7.272 \times 10^{-5}$ radians per second. Based on the physics of a rotating body, the resulting vorticity of an object on the surface of the

Earth is given by $2 \times \Omega \approx 14.54 \times 10^{-5}$. The axis of rotation in this case is aligned with the Ω vector, shown in red in Figure 7.5.

For an atmospheric parcel, the important component of its rotation is that which aligns with its "upward-pointing" direction as shown by the black arrow on each of the parcels in Figure 7.5. (This is in the direction of a positive z value in the three-dimensional coordinate system where the parcel's position is given by the ordered triple $(x, y, z.)$ For a parcel at the equator, the red and black vectors are perpendicular to each other, so there is no parcel rotation relative to the z direction.

If the parcel is sitting at the north pole, its "upward" z-direction aligns with the Earth's axis of rotation, so its vorticity magnitude is 2Ω, the same as the Earth's.

For parcels between the equator and north pole, some portion of the Earth's rotation vector aligns with the parcel's z vector, and there exists $x - y$-plane rotation of the parcel. The magnitude of the vector alignment is given by $\sin\theta$, where θ is the angle between the Earth's equator and the z vector. Consequently, the vorticity of the parcel due to the Earth's rotation is $f = 2\Omega \sin\theta$.

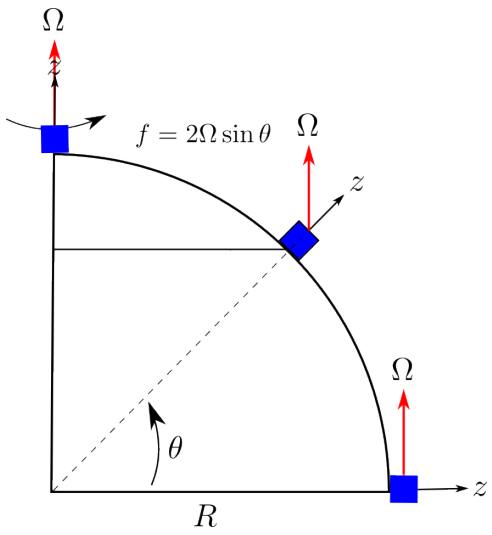

Figure 7.5: Parcel vorticity as a result of the Earth's rotation about its axis is $f = 2\Omega \sin\theta$.

7.4.2 Relative and Absolute Vorticity

The velocity vector field $\vec{v} = (u, v, w)$ of fluid motions, such as air parcels in the Earth's atmosphere, may cause parcels to rotate independently from the rotation of the Earth. The mathematical definition of vorticity is

$$\text{vorticity} = \nabla \times \vec{v} = (\partial v/\partial z - \partial w/\partial y,\ \partial u/\partial z - \partial w/\partial x,\ \partial v/\partial x - \partial u/\partial y) \tag{7.3}$$

The result on the right-hand side of Equation 7.3 is a vector. The third component of the result represents the vorticity (rotation) of a parcel with respect to its z direction. This orientation represents rotation of the parcel in the horizontal $(x - y)$ plane, and will be designated using the Greek letter "ζ" (zeta). Therefore, the mathematical definition for parcel rotation due to its motion in the atmosphere is

$$\zeta = \frac{\partial v}{\partial x} - \frac{\partial u}{\partial y} \qquad \text{(differential)} \tag{7.4}$$

$$= \frac{\Delta v}{\Delta x} - \frac{\Delta u}{\Delta y} \qquad \text{(discrete)} \tag{7.5}$$

where the **differential** definition for "change of," represented by the "∂" symbol in Equation 7.4, is replaced the **discrete** definition of "change of" represented by the Δ symbol in Equation 7.5.

The rotation represented by ζ is the result of the parcel's motion relative to the Earth's surface. If the parcel did not move relative to the Earth, then its rotation would be only that given by f, the Earth's rotation. Consequently, ζ is called the **relative vorticity**.

The sum of the planetary vorticity (f) and relative vorticity (ζ) is known as the **absolute vorticity** of the parcel.

$$\text{absolute vorticity} = \text{planetary vorticity} + \text{relative vorticity} = f + \zeta \tag{7.6}$$

Example 7.4.1. Use the velocity field information given by Figure 7.4 and the definition of relative vorticity given by Equation 7.5 to determine the vorticity at location "$\mathbb{X}$" in the figure.

Solution:

Using the $x - y$ coordinate orientation in the figure, $\Delta x = 100$ km, and $\Delta y = 80$ km. However, these value must be converted to lengths in meters, so $\Delta x = 100$ km $\times$ 1000 m per km = 100,000 m, and $\Delta y = 80$ km $\times$ 1000 m per km = 80,000 m.
Next, calculate Δu using the vectors $\vec{v}_e$ and $\vec{v}_w$.

$$\Delta u = u_e - u_w = 8 - 10 = -2 \text{ m·s}^{-1}$$

Note that u_e is used as the first value because it is associated with the greatest

x-location. Now, calculate Δv in a similar way:

$$\Delta v = v_n - v_s = -4 - 5 = -9 \text{ m}\cdot\text{s}^{-1}$$

With all Δ values known

$$\begin{aligned}\zeta &= \frac{\Delta v}{\Delta x} - \frac{\Delta u}{\Delta y} \\ &= \frac{-9}{100000} - \frac{-2}{80000} \\ &= -0.00009 - -0.000025 = -0.000065 \\ &= \boxed{\text{-6.5 } \times 10^{-5} \text{ sec}^{-1}}\end{aligned}$$

7.4.3 Curvature and Shear Vorticity

Relative vorticity ζ has two sub-types that can be found on weather charts without making direct mathematical calculations.

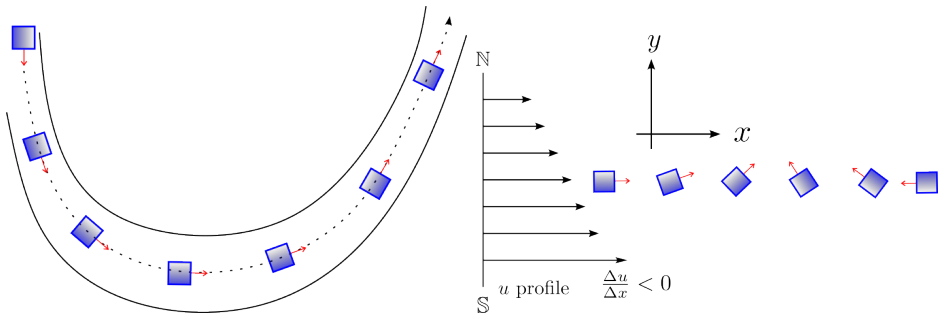

(a) Curvature Vorticity (b) Shear Vorticity

Figure 7.6: Two types of relative vorticity.

Curvature vorticity occurs when parcels follow a curved trajectory as shown in Figure 7.6a. The black curves represent constant height or pressure contours that the parcel will follow in the absence of a frictional force. The contours bend to the left in a counter-clockwise (ccw) fashion, so the parcel will also rotate in the same direction as it moves between the contours. This ccw rotation is visualized by observing how the red arrow on the forward "face" of the parcel rotates - in a ccw direction.

When the parcel is approaching the "bottom" of the trough as depicted in Figure 7.6a, its north-south motion aligned with the y-axis is negative, so the speed $v_1 < 0$ at a location (x_1, y_1). Once it has passed through the bottom of the trough and begins to move back north, its speed v_2 is positive at a location given by (x_2, y_2). Therefore $\Delta v = v_2 - v_1 > 0$. The value of x_2 is greater than x_1 because x_2 is further east of x_1, so $\Delta x = x_2 - x_1 > 0$.

Therefore $\frac{\Delta v}{\Delta x} > 0$, and this term in Equation 7.5 represents the **curvature vorticity** in the horizontal flow field.

Referring to Figure 7.6b, the u velocity magnitude (the length of the horizontal vectors, or arrows) decreases with increasing y value. This is an example of **wind shear**. As in the curvature case, the resulting rotation of the parcel is determined by noting the red arrow on the parcel is rotating in a ccw direction. The decreasing magnitude of u in the direction of increasing y implies $\frac{\Delta u}{\Delta y} < 0$, Consequently, the second term in Equation 7.5, and the preceding minus sign, generate a positive vorticity value (ccw rotation). The term $-\frac{\Delta u}{\Delta y}$ in Equation 7.5 represents the magnitude of the **shear vorticity** in the horizontal flow field.

The weather chart shown in Figure 7.7 exhibits both types of relative vorticities. The blue dashed box surrounds a region where curvature vorticity exists. The red dashed line identifies a decreasing speed profile as the the y direction increases. The wind speed at the lower end is approximately 125 knots. A station further up and along the line has a wind speed of approximately 75 knots. A third station on the line reported a speed of 50 knots. This indicates the existence of shear vorticity at this level in the atmosphere.

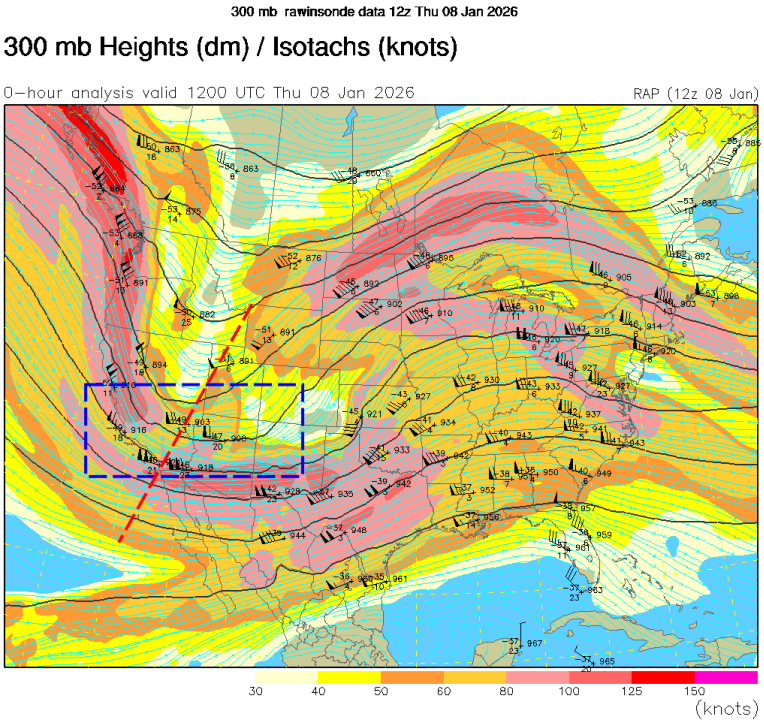

Figure 7.7: Upper air flow pattern with curvature and shear vorticity. The blue box shows a region of curvature vorticity. The red dashed line is provides evidence of shear vorticity.

7.4.4 Vorticity and Divergence Relationship

Isentropic atmospheric flows are those that are adiabatic and have no loss of energy due to friction or other means of irreversible energy loss. For such flows, a relationship between absolute vorticity ($\zeta + f$) and horizontal divergence exists as shown in Equation 7.7.

$$\frac{\Delta(\zeta + f)}{\Delta t} = -(\zeta + f)\left(\frac{\Delta u}{\Delta x} + \frac{\Delta v}{\Delta y}\right) \tag{7.7}$$

Careful examination of this equation reveals an important connection between vorticity change and divergence. Through this equations, it is understood that vorticity will change if horizontal divergence is not zero. That is, if vorticity changes, divergence or convergence (negative divergence) must exist.

Further aspects of this relationship are summarized in Table 7.1. Looking at the first row of the table, when the absolute vorticity is positive and the absolute vorticity increases, the column undergoes convergence (mass increases) and a surface pressure increase results. Row two of the table indicates when the absolute vorticity is positive and it is decreasing, the column experiences divergence (mass decrease) and a surface pressure decrease results. These relationships are one important feature for the development and intensification of midlatitude cyclones.

$\zeta + f$	$\Delta(\zeta + f)$	$-(\zeta + f)$	divergence or convergence
+	+	-	convergence
+	-	-	divergence
-	+	+	divergence
-	-	+	convergence

Table 7.1: Change in vorticity versus divergence.

7.5 Waves

The northern hemisphere polar jet stream associated with the three-cell general circulation model encircles the globe at a north latitude of approximately 60°. Observation shows that its path is not a perfect circle. Rather, it encircles the globe with a wavy pattern as shown at the 500 mb level in Figure 7.8. The genesis of this wavy pattern is explored in this section.

7.5.1 Wave Characteristics

Waves in the Earth's atmosphere, and waves in general, are characterized by such values as their wavelength, amplitude, and speed. A general wave form is shown in Figure 7.9. The **wave length** λ is the distance between consecutive wave peaks. The **amplitude** A is

Figure 7.8: Planetary-scale 500mb waves in the northern hemisphere.

the length of the space between the wave peak and the base line. Waves can be stationary

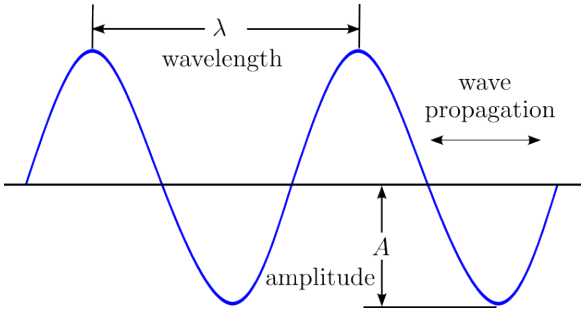

Figure 7.9: General wave characteristics.

in space, or they can propagate in a direction that is generally aligned with the reference or baseline as shown in Figure 7.9. The wave's speed may depend on such factors as the medium in which it resides and its wavelength.

Referring to Figure 7.8, the dashed lines identify the low pressure troughs, which can also be seen as the wave peaks. Then, the wave length of a given wave is the distance from its first peak to its second peak. Additionally, these dashed lines allow an easy count of the **wave number** of a given jet stream pattern. Here, there are five waves, so the wave

number is "five." The wave number for the jet stream may range from as few as three to as many as 11.

7.6 Atmospheric Waves and Change in Vorticity

The change in absolute or potential vorticity are major sources for the creation of atmospheric long waves. The process of wave creation related to vorticity and changes in vorticity is explained in this section.

7.6.1 Conservation of Absolute Vorticity

Recall that the sum of relative vorticity ζ and planetary vorticity f is defined to be the absolute vorticity of a parcel. The relative vorticity is separated into curvature (ζ_c) and shear vorticity (ζ_s). Consequently, absolute vorticity may be expressed as

$$\zeta_a = \zeta_c + \zeta_s + f \tag{7.8}$$

Vorticity is a measure of rotation. In the three-dimensional atmosphere, the measure can be taken to be rotation of cylinder, with a cross-section of area A and and height $\Delta z = H$. If the height of the cylinder is constant, then the absolute vorticity associated with the cylinder is conserved over time even if the cylinder's position in the atmosphere changes. In mathematical notation, this means

$$\frac{\Delta\zeta_a}{\Delta t} = \frac{\Delta\zeta_c + \Delta\zeta_s + \Delta f}{\Delta t} = 0. \tag{7.9}$$

It is important to note that Equation 7.9 does not mean all components of ζ_a do not change over time under conservation of ζ_a. For example, it could be that if f increases over time, there must be an equal, and opposite change in the sum of $\Delta\zeta_c$ and $\Delta\zeta_s$ over the same time change to cancel Δf.

7.6.2 Potential Vorticity

Potential vorticity is defined as

$$\zeta_p = \frac{\zeta + f}{H} \tag{7.10}$$

In Equation 7.10, ζ_p represents potential vorticity and it is the absolute vorticity (sum of ζ and f) divided by H, where $H = \Delta z$, the thickness of an atmospheric column having the associated value of absolute vorticity. Potential vorticity is conserved in isentropic flows. Mathematically, this implies

$$\frac{\zeta + f}{H} = \text{constant} \tag{7.11}$$

Isentropic atmospheric flows are those for which the potential temperature of a parcel does not change as it moves through the atmosphere. In an isentropic atmosphere, parcels stay on their isentropic level in the atmosphere. As a result of this fact, parcels that move northward in the northern hemisphere generally have an upward motion because the isentropic surfaces slant upward from the equator to the north pole.

As in the case of absolute vorticity, potential vorticity is often taken to represent the rotation of a vertical cylinder of air in the atmosphere with radius A and height H. The atmospheric consequence of Equation 7.11 is that if H changes (either increases or decreases) as the cylinder changes position, the absolute vorticity (the numerator) must change in equal magnitude to preserve the value of ζ_p.

7.7 Rossby Waves: Barotropic Development

7.7.1 Barotropic Wave Development

A **barotropic** atmosphere is one in which the parcel streamlines (parcel paths) run parallel to the temperature contours. As explained in Chapter 4, upper air flows experience insignificant friction. Consequently, parcel streamlines run parallel to pressure contours (isobars). As explained in Chapter 2, if parcel paths (that is, isobars) cross temperature contours, thermal advection (a form of heat or energy transfer) occurs. Consequently, a barotropic atmosphere is one in which there is no temperature advection (pressure contours and temperature contours do not intersect).

Another consequence of barotropic motion is that vertical cylinders of rotation, as introduced in Section 7.6.1, do not experience a change in column depth H as they move. Rotating cylinders do conserve absolute vorticity.

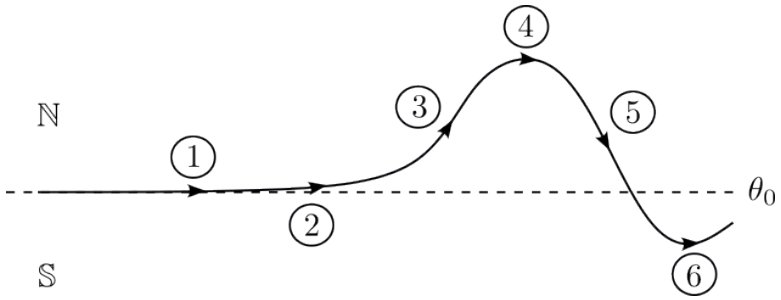

Figure 7.10: Development of a barotropic wave due to the conservation of absolute vorticity.

Referring to Figure 7.10, a parcel path (streamline) is shown as the curved path with arrows depicting the tangential direction of flow at various points. The dotted line represents angle θ_0 of the northern latitude of an initially unperturbed flow. If left unperturbed, the

parcel's flow streamline would continue along the dotted path. Such a strict west-to-east flow in the northern hemisphere is referred to as **zonal flow**.

At location 1, the absolute vorticity ζ_a is given entirely by planetary vorticity ($\zeta_c = \zeta_s = 0$) with a value $f_0 = 2\Omega \sin\theta_0$. suppose at this point, the flow is perturbed by some means and the path begins to bend northward.

At location 2, the northward path perturbation is evident as its north latitude is evidently (slightly) greater than θ_0. The increase in θ results in an increase in f. As f increases ($\Delta f > 0$), the principle of conservation of absolute vorticity results in ζ_c dropping from a value of zero to a negative value ($\Delta\zeta_c$) to counteractive the positive increase in absolute vorticity f.

When parcels reach point 3 in the path, the planetary vorticity has increased further due to the increase in angle θ as the parcels move further north. The conservation of absolute vorticity will require an even more negative ζ_c to counteract the additional increase in f. At this point, the more negative value of ζ_c is sufficient to eliminate the counter-clockwise bend in the streamline. Shortly after leaving point 3, the absolute vorticity ($f + \zeta_c$) is negative enough to initiate a clockwise (anti-cyclonic) bend in the path.

When parcels reach location 4, the negative value of ζ_c has acted long enough to change the trajectory to a southward direction as the parcels continue to move. Because the path has a southerly component, the value of planetary vorticity decreases (it is still positive, as always) as the air parcels move further south. In response to the decrease in f, the value of ζ_c begins to increase from in lowest negative value.

At point 5, the increase in ζ_c is great enough so that the path no longer has an anti-cyclonic curvature. The parcels continue their southward migration with enough momentum to push them further south than their original latitude angle of θ_0. Once south of the θ_0 angle, the value of planetary vorticity f is less than its original value f_0. This further decrease in f requires a further increase in ζ_c to a positive value.

By the time parcels reach point 6, the positive curvature vorticity ζ_c has acted long enough so that the streamline has lost its southerly component and the parcels begin to move back north. Moving northward, the parcels planetary vorticity increases, so the curvature vorticity must decrease in obedience to the conservation of absolute vorticity.

After leaving point 6, the magnitude of the northerly wind component causes the parcels to over-shoot their original θ_0 latitude, and the sequence of changes in f and ζ_c that began at point 3 will repeat, and the wavy pattern is repeated in the eastward direction.

7.7.2 Rossby Waves

Rossby waves are upper atmospheric waves with very long wavelengths often created in barotropic atmospheric environments. The streamline follows the value of $y(x)$ given in Equation 7.12, where $(x, y(x))$ gives the path's east and north coordinates, respectively. The

typical wavelength λ and amplitude A of a Rossby wave 6000 km and 1665 km, respectively.

$$y = A\cos\left[2\pi\left(\frac{x-ct}{\lambda}\right)\right] \tag{7.12}$$

The term c in Equation 7.12 is the **phase speed** of the crest of the wave.

The development of a Rossby wave requires the variability of planetary vorticity f with latitude θ. The parameter β is defined by

$$\beta = \frac{\Delta f}{\Delta y} = \frac{\Delta 2\Omega\sin\theta}{\Delta y} = \frac{2\Omega\cos\theta}{R} \tag{7.13}$$

where R is the radius of the Earth. It is common to assign a constant value to β by setting θ to a representative value such as 45°. In that case, $\beta = 1.616 \times 10^{-11}$ m^{-1} $\cdot$ sec^{-1}.

With β determined, the next step in calculating the value of c in Equation 7.12 is to use Equation 7.14 to calculate the **intrinsic wave speed** c_0.

$$c_0 = -\beta\left(\frac{\lambda}{2\pi}\right)^2 \tag{7.14}$$

The negative sign in Equation 7.14 indicates that the intrinsic speed direction is westward, opposite the typical planetary wind in the mid-latitudes. The westward movement is referred to as **retrograde** motion. Additionally, the longer the wave length λ, the faster the westward movement.

Finally, the wave phase speed c relative to the ground will depend on the eastward speed U_0 of the general circulation. The resulting phase speed c of the long wave is given by Equation 7.15. Note that if the c_0 has a greater magnitude than U_0, the long wave will be a **retrograde wave**.

$$c = U_0 + c_0 = U_0 - \beta\left(\frac{\lambda}{2\pi}\right)^2 \tag{7.15}$$

Example 7.7.1. Calculate the phase speed of an atmospheric wave of wavelength 6500 km if the general flow speed $U_0 = 30$ m$\cdot$s^{-1}.

Solution:

Use Equation 7.14 to calculate c_0 where λ is in meters:

$$\begin{aligned} c_0 &= -1.616 \times 10^{-11} \cdot \left(\frac{6500 \times 1000}{2 \times 3.1415} \right)^2 \\ &= -1.616 \times 10^{-11} \cdot \left(\frac{6.5 \times 10^6}{6.28} \right)^2 \\ &= -1.616 \times 10^{-11} \cdot \left(\frac{6.5^2 \times 10^{12}}{39.43} \right) \\ &= -1.616 \times 10^{-11} \times 1.071 \times 10^{12} \\ &= -1.616 \times 1.071 \times 10 \\ &= -17.30 \text{ m}\cdot\text{s}^{-1} \end{aligned}$$

Next, use Equation 7.15:

$$c = U_0 + c_0 = 30 - 17.30 = \boxed{12.70 \text{ m}\cdot\text{s}^{-1} = 27.9 \text{ mi} \cdot \text{s}^{-1}}$$

Atmospheric waves exist over a range of wave lengths. Those with shorter wave lengths are referred to as **short waves**. Short waves frequently develop as a cold pool of air that breaks away from the main circular flow of a strong upper air low pressure center.

Short waves move faster than long waves. Consequently, if a short wave is upstream from a long wave, its greater speed may result in it "catching up" to the long wave. If so, the short wave's dip in pressure or altitude will enhance the dip in the long wave's contours.

The time it takes a short wave to catch the long wave depends on the relative speeds of the two waves and the distance between the two waves. The difference in the intrinsic speed of the waves is the relative speed of the short wave with respect to the long wave. Example 7.7.2 shows how the time to catch up can be determined.

Example 7.7.2. An atmospheric wave of wavelength 6500 km is 1000 km downwind of a short wave with wave length of 2000 km. The general flow speed U_0 = 30 m·s^{-1}. Calculate how long it will take for the short wave to catch the long wave.

Solution:

The intrinsic speed of the long wave was calculated to be -17.30 m·s^{-1}in Example 7.7.1. The intrinsic wave speed of the short wave is calculated next:

Use Equation 7.14 to calculate c_0 where λ is in meters:

$$\begin{aligned} c_0 &= -1.616 \times 10^{-11} \cdot \left(\frac{2000 \times 1000}{2 \times 3.1415} \right)^2 \\ &= -1.616 \times 10^{-11} \cdot \left(\frac{2 \times 10^6}{6.28} \right)^2 \\ &= -1.616 \times 10^{-11} \cdot \left(\frac{2^2 \times 10^{12}}{39.43} \right) \\ &= -1.616 \times 10^{-11} \times 1.01 \times 10^{11} \\ &= -1.639 \text{ m}\cdot\text{s}^{-1} \end{aligned}$$

The relative speed of the short wave with respect to the long wave is -1.639 - -17.30 = 15.7 $\text{m}\cdot\text{s}^{-1}$.

The time required is found by dividing the distance between the waves by the relative speed of the short wave.

$$\text{time} = \frac{1000 \times 1000}{15.7} = 6.36 \times 10^4 \text{ sec} = \boxed{17.8 \text{ hrs}}$$

7.8 Mountain Waves

Rossby waves are initiated by some means of perturbation. One common perturbation source is a prominent mountain range such as the Rocky Mountain in the western portion of the United States. The development of such a wave perturbation is understood through the conservation of potential vorticity ζ_p under the assumption of isentropic flow.

Figure 7.11 illustrates the passage of a rotating cylinder of air parcels as it moves eastward over a mountain range. The top of the cylinder follows an isentropic surface with constant elevation. The cylinder's lower surface will follow the Earth's surface as it travels over the mountain range. Consequently, the height of the cylinder decreases from H_1 to H_2 as the cylinder moves from point 1 to point 2, and then increases back to the value of H_1 once it passes over the mountain and reaches point 5. As a consequence of the change in H and the conservation of potential vorticity ζ_p, the cylinder's wavy path is shown in Figure 7.11.

At point 1, the depth H begins to decrease, resulting in a decrease in vorticity under the obedience of conservation of ζ_p and a subsequent southward deflection which causes a decrease in planetary vorticity f. As the cylinder continues to move southward, the decrease in planetary vorticity over compensates for the decrease in H as H begins to increase.

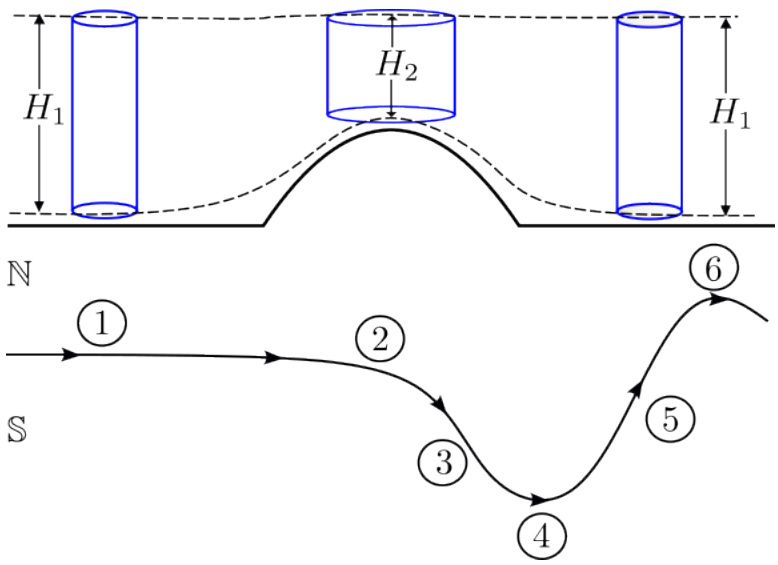

Figure 7.11: Development of a wave through conservation of potential vorticity in the flow over a mountain range.

At point 3, positive curvature vorticity ζ_c compensates for the over-shooting loss in planetary vorticity f. By the time the cylinder reaches point 4, the curvature vorticity increase has acted long enough to begin moving the cylinder back north.

By point 5, the northward migration increases the positive planetary vorticity enough that the curvature vorticity decreases to a nearly zero value.

However, the momentum of the cylinder's motion pushes it beyond its original latitude angle, and the planetary vorticity increase now has to be counteracted by a negative curvature vorticity, so the cylinder's path begins to bend in a anti-cyclonic direction (clockwise).

By the time the cylinder reaches point 6, the negative curvature vorticity has halted its northward movement, and turns the path southward. Now, the cylinder moves south and overshoots the original northern angle θ_0. The resulting drop in planetary vorticity will be compensated with increasing curvature vorticity. The cycle of rising/falling f compensated with falling-to-negative/rising-to-positive ζ_c is repeated to create the wavy pattern.

7.9 Baroclinic Waves

A baroclinic atmosphere is one in which the streamlines of the parcel motion cross isotherm contours. Figure 7.12 depicts such a situation where a cold "wedge" of air sits underneath a warmer air mass. The colder surface air is north of the warmer surface air to the south.

A cylinder of air with height H_1 migrates along a path oriented southwest-to-northeast.

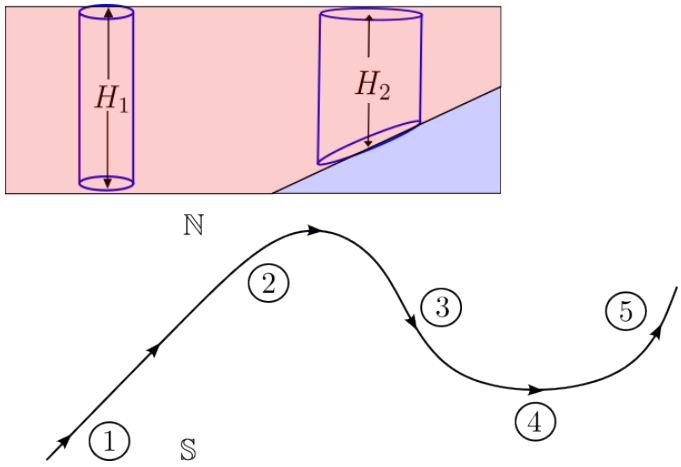

Figure 7.12: Development of a wave through conservation of potential vorticity in a baroclinic atmosphere.

At point 1 the absolute vorticity ($\zeta_a = f + \zeta_c + \zeta_s$) of the cylinder is equal to f only for the straight-line path.

As it meets the colder surface air at point 2 in its path, the base of the cylinder rides up the boundary of the differing air masses. The top of the cylinder remains at it original elevation, so the cylinder's depth decreases to H_2 in depth. In obedience to the conservation of potential vorticity, this decrease in depth must be matched by a decrease in absolute vorticity of equal magnitude. The northward component of the cylinders path results in an increase in planetary vorticity f, so the required decrease in ζ_a must be through a decrease in curvature vorticity ζ_c from it's initial zero value.

Between points 2 and 3, the increase in anti-cyclonic rotation due to the negative ζ_c results in the cylinder's path turning to a southeasterly direction. As the cylinder move further south on this path, the planetary vorticity decreases as the northern latitude of the cylinder decreases.

The southerly component of the path results in a increase in H prompting an increase in absolute vorticity ζ_a in accordance with the conservation of potential vorticity. This increase is supplied by an increase in curvature vorticity ζ_c. The increase results in a positive net absolute vorticity, so between points 3 and 4, the path becomes cyclonic (counter-clockwise)

The northward component of the path between points 4 and 5 results in an increase in planetary vorticity. It also results in a decrease in H, requiring a decrease in ζ_a. As before, the curvature vorticity ζ_c must become negative for the potential vorticity ζ_p to return to its original value. The cycle of increase/decrease in f and an associated decrease-to-negative/increase-to-positive in ζ_c results in a wavy flow pattern.

The resulting wavelength of a baroclinic waves is generally less than that of a barotropic

Rossby wave. They average between 3000 km to 4000 km. The shorter wavelengths result in a slower intrinsic wave speed c, so baroclinic waves are less likely to have retrograde propagation.

7.10 Norwegian Cyclone Model

The Norwegian Cyclone Model framework was developed in the early decades of the 1900s at the Bergen School of Meteorology. The individuals who played roles in the development of the model include physicist Vilhelm Bjerknes (the founder of the Bergen School), Vilhelm's son Jacob, Halvor Solberg, the Swedish meteorologist Tor Bergeron, and the student Carl-Gustaf Rossby. Remarkably, the development of this model was done solely on the basis of surface data and cloud observations and without upper air data. Even so, the model remains the cornerstone of mid-latitude cyclone understanding.

7.10.1 Cyclone Life Cycle

The life cycle (birth, development, and decay) of a midlatitude cyclone model (MLC) has distinct stages, and will be outlined in this section.

Stationary Frontal Stage

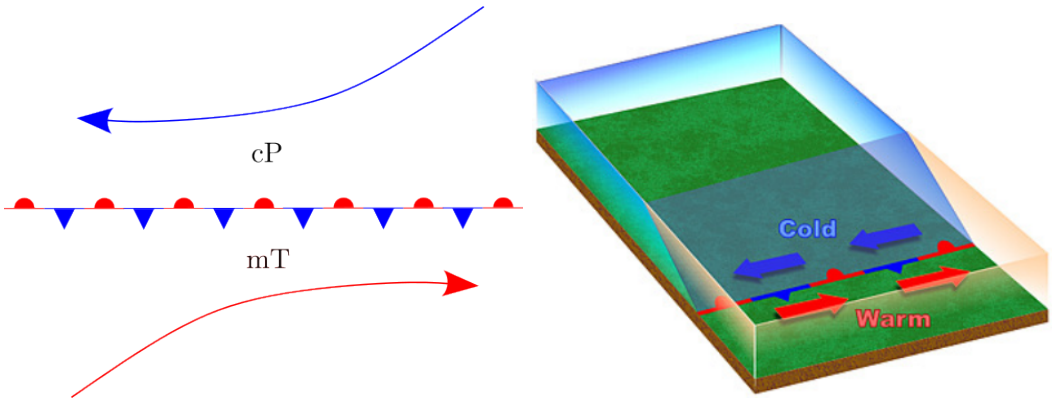

Figure 7.13: Birth of a midlatitude cyclone occurs along the stationary polar front.

The polar front feature of the three-cell general circulation model is a common location for the birth of a mid-latitude cyclone. When the front is stationary, as depicted in Figure 7.13, winds on the equatorial side are predominantly westerly, while those on the polar side are easterly. This wind pattern is "close to" cyclonic flow. Additionally, the polar front

is a trough of low pressure, a natural area for the birth of the low pressure center of a mid-latitude cyclone.

Wave Cyclogenesis

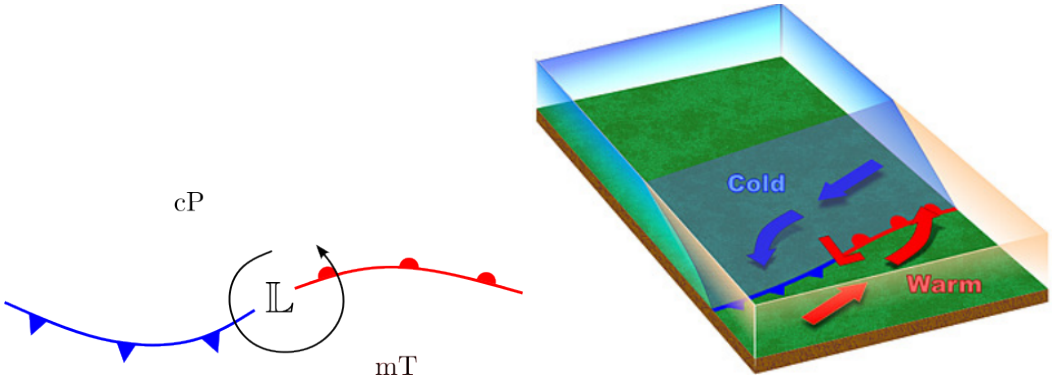

Figure 7.14: Cyclogenesis begins as a low center forms and counter-clockwise circulation creates a warm and cold front.

The center of the low will form when upper air divergence of mass is triggered by an event to be discussed in Section 7.11. This cyclogenesis is characterized by circulation around the low pressure center, denoted by $\mathbb{L}$ in Figure 7.14. As a result, the stationary front becomes a warm front to the east of the low, and it becomes a cold front to the west.

Open Wave Stage

The open wave stage of the mid-latitude life cycle is characterized by a more clearly defined low center with closed isobars the envelop the center. The strengthening low has an increased pressure gradient force that powers the cyclonic flow around the low with associated strong advection of mT air from the south and cP air from the north. The-cold front, with its faster progression than the warm front, closes the gap between the two. The region south of the warm front and ahead of the faster moving cold front is the **warm sector** of the storm. In many instances, the skies over this region are clear or have very thin cloud cover with no precipitation.

The warm front to the east of the low is a trough of low pressure. The low center's track usually follows the warm front as the low progresses east-northeast guided by the upper air flow as well.

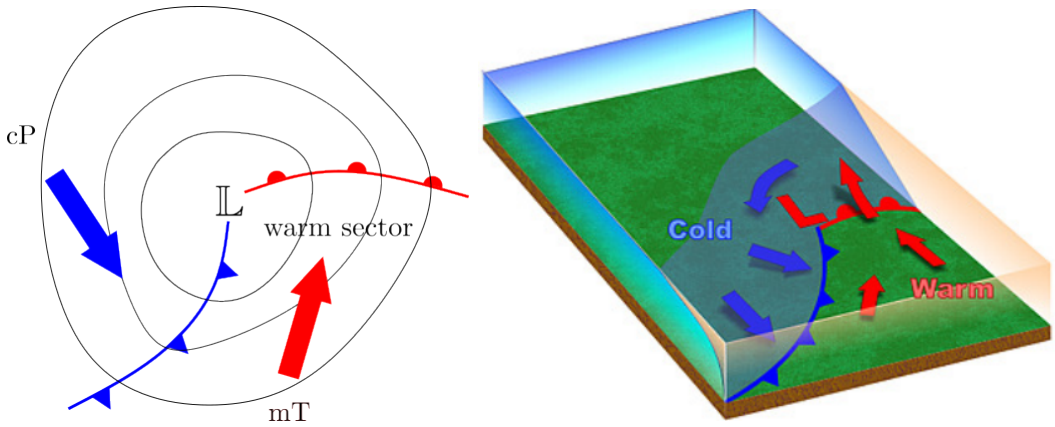

Figure 7.15: An open wave develops with multiple closed isobars and strengthening winds creating strong warm and cold temperature advection.

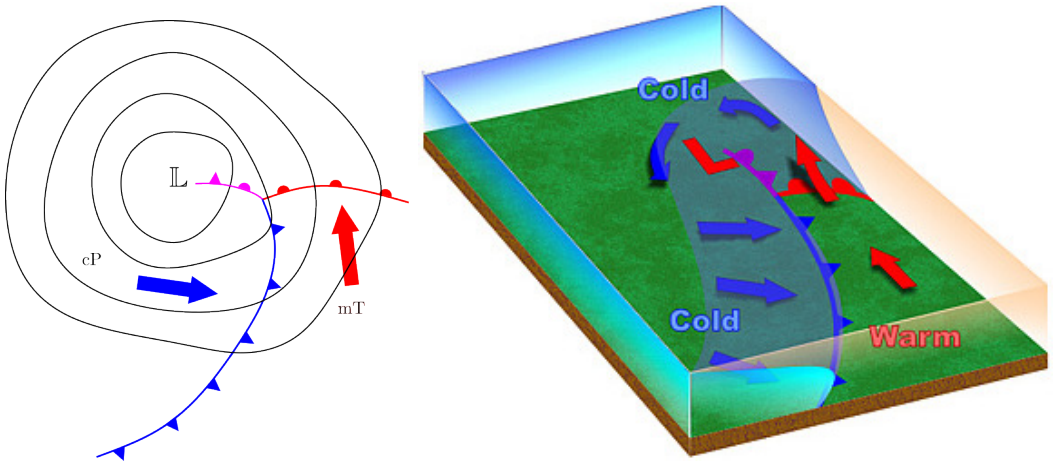

Figure 7.16: The cold front has overtaken the warm front to give rise to an occupied front in the mature stage of the cyclone's life cycle.

Mature Stage: Occlusion

Figure 7.16 shows the structure of the cyclone in its mature stage, where the faster moving cold front has caught up with the warm front to form the purple-colored occluded front. All three fronts meet at the **triple point**. In many cases, this is the location where a new low center will form. The cyclone is at its peak strength usually accompanied by wide spread precipitation at this time in its life-cycle.

Separation & Decay

The decay of the cycle occurs when the low is separated from the polar front and its associated polar jet that supplies the energy to power the storm, as shown in Figure 7.17. Once the low loses the mechanisms that sustain the upper air divergence, there is a net convergence of mass into the center of the low, and the surface pressure at the center and surrounding area begins to rise. At this stage, the low is said to be "**filling**" and is likened to the filling of a hole.

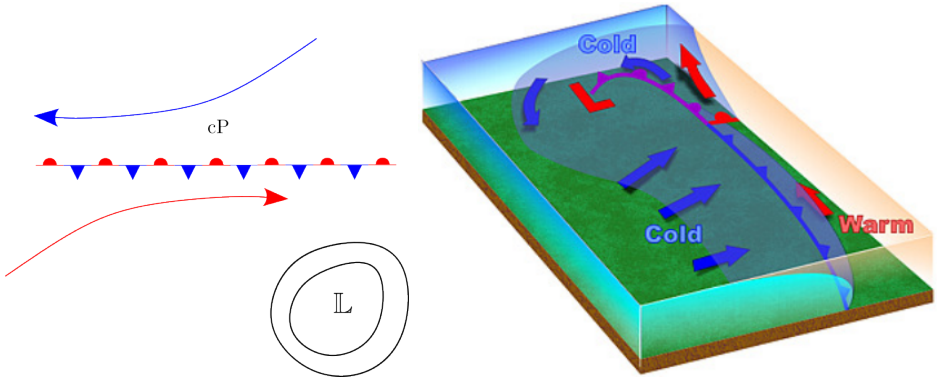

Figure 7.17: The low center has become detached from the original polar front, losing its access to the polar jet winds that energizes the storm.

7.10.2 Conveyor Belt Model

Atmospheric scientists developed the concept of MLC associated conveyor belts in the middle of the 20th century as data and observations of upper air motions was more readily available. Developed in different stages, conveyor belts are thought to be distinct steams moving parcels with different characteristics (temperature and moisture) from one portion of the atmosphere to another, much like convey belts in a factory will move objects from one place to another.

Figure 7.18 depicts three distinct belts associated with an idealized mid-latitude cyclone: the dry conveyor belt (introduced in 1964), the warm conveyor belt (introduced in 1973), and a comprehensive frame for conveyor belts, including the cold conveyor belt, in 1980.

The warm conveyor belt approached from the south. In addition to its warmth, it has a higher moisture content the the other air masses associated with the midlatitude cyclone. The warm parcels begin to rise as they approach the warm front. They continue to rise forming a broad area of cloudiness and precipitation. The rising belt does not offer an additional push of the warm front at the surface. Consequently, the warm front does not move as quickly as the cold front that trails to west northwest. As the flow reaches high

enough in the atmosphere, the parcels are swept eastward by the strong prevailing winds aloft.

The dry conveyor belt is made up of the cold and dry parcels from the continental polar air mass. As they approach the low behind the cold front at the surface, they descend creating an additional push on the surface cold front. The dry parcel add little moisture to the cyclone. Therefore, the main precipitation region is usually located ahead of the advancing cold front in a narrow, but frequently intense line of precipitation. In the warmer months, this precipitation can be made up of strong thunderstorms. In the winter, the result might be short-lived but intense snow squalls.

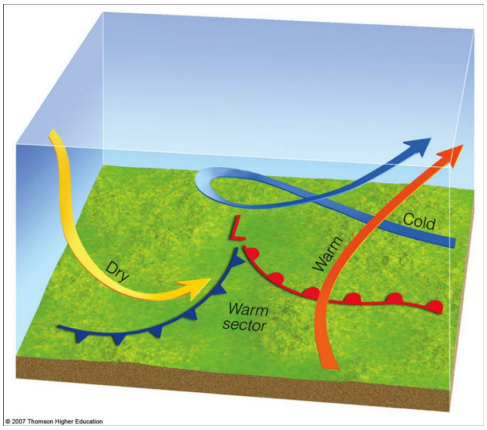

Figure 7.18: The idealized three conveyor belt model for midlatitude cyclones.

The cold conveyor belt originates to the east of the cyclone, perhaps bringing moisture from the Atlantic ocean. Consequently, it may result in significant precipitation area to the north of the advancing warm front. The cooler temperatures of the cold belt parcels mean that the belt flows beneath the warm belt. However, as the parcel move closer to the region above the surface low, they are drawn upwards and eventual turn back to the east, as depicted in figure 7.18.

7.11 Upper Air Support Mechanisms

The initiation and intensification of the surface low of a mid-latitude cyclone are the result of loss of mass from the column of air above the surface feature. This mass loss is due to divergent motion at elevations above the low.

7.11.1 Vorticity Advection

Figure 7.19 shows a deep 500 mb trough and the winds speed, relative to the geostrophic wind speeds, as the air parcels flow through the trough. Recall that upper atmospheric winds (friction free) are geostrophic when blowing parallel to straight isobars or height contours. Gradient winds are friction-free winds that follow curved contours. Wind speeds associated with cyclonic flow (around low centers or pressure troughs) have sub-geostrophic speeds (speeds less than geostrophic). Winds associated with anti-cyclonic flows (flows around high pressure centers or ridges) have super-geostrophic speeds.

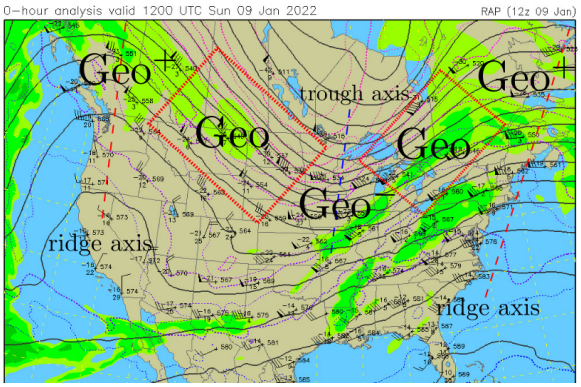

Figure 7.19: Upper atmospheric wind speed relative to geostrophic wind associated with a wave trough.

The relative wind speed of parcels approaching and flowing through the deep trough in Figure 7.19 are show in Figure 7.20. Parcel position along the wave pattern are denoted by numbers 1-5. The wind speeds at these locations are indicated by the vectors below the wave pattern in the figure. Ridge positions 1 and 5 along the wave have super geostrophic wind speed denoted by G^+. Wind speed at positions 2 and 4 is geostrophic (G). The wind speed at the trough axis, position 3, is sub-geostrophic and denoted by G^-.

The light blue rectangle in the figure indicates a region of convergence because the wind speed into the rectangle is less than the exiting speed. The light read rectangle indicates a region of divergence because the wind speed into the region is less than that exiting the region.

The light green region centered on the trough axis in the figure a the location of the relative curvature vorticity (ζ_c) maximum along the path. The region between, highlighted in yellow, is where positive vorticity advection (PVA) is very large, just after the positive vorticity maximum. Therefore, divergence occurs just downstream of the positive vorticity maximum.

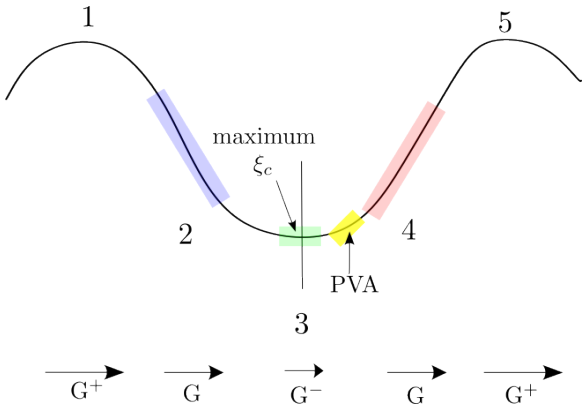

Figure 7.20: Upper atmospheric wind speed relative to geostrophic wind associated with a wave trough.

7.11.2 Baroclinic Instability

Figure 7.21 depicts the vertical structure of a baroclinic atmosphere showing regions of cold air advection (cold conveyor belt) and warm air advection (warm conveyor belt) relative to the 700 mb wave.

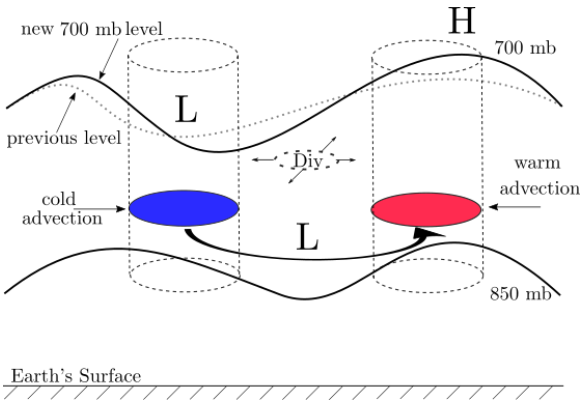

Figure 7.21: Vertical cross-section of baroclinic wave amplification.

When the flow around a low center or trough becomes baroclinic (velocity vectors cross temperature contours) the resulting regions of warm air advection (waa) and cold air advection (caa) in the downstream and upstream columns, respectively, cause the downstream column to expand and the upstream column to contract in the vertical direction. The warming and cooling of these columns cause the heights of the upper pressure surface to

rise and fall, respectively. Consequently, the trough and ridge pattern at the upper level is amplified. Referring to Figure 7.21, the original wave at 700 mb is depicted by the dotted curve. The amplified wave is shown in the solid curve.

The"digging" of the upper level trough enhances the curvature vorticity in the upper air height contour pattern. When parcels pass through, and downstream from, this enhanced vorticity maximum, they move into a region of enhanced divergence (as vorticity decreases, divergence increases). If the region of divergence is situated over the low at 850 mb, the low will deepen.

The increased pressure gradient associated with the low will cause an increase in the speed of the winds rotating counter-clockwise around the 850 mb trough of low center. As a result, the warm and cold temperature advection is increased which will further enhance the trough - ridge pattern above. This is an example of a "positive feed-back loop." Baroclinic instabilities often result in quickly strengthening storms because of these favorable, repetitive chain of events in the loop.

The parcels in the warm advection region also experience rising motion. These parcels generally originate near the Gulf of Mexico, so they likely have sufficient mixing ratios to create cloudy skies and areas of precipitation as they rise through the atmosphere experiencing a decrease in pressure, expansion of volume, and cooling as an end result. With sufficient cooling, the change of phase (vapor to liquid and liquid to ice) releases latent heat that may significantly warm the column more, creating additional amplification of the upper level wave pattern. These phenomena are often associated with an advancing warm front at the surface of the Earth with the frontal boundary extending vertically to the 850 mb level.

Example 7.11.1 show how the magnitude of thermal advection (either warm or cold) can be calculated.

Example 7.11.1. The weather recording station is shown in Figure 7.22 on a horizontal grid with uniform spacing of 100 km. Isotherms for 45°F and 55°F are shown. (i) Calculate the temperature gradient

$$\frac{\Delta T}{\Delta x}$$

for the station. (ii) If the station is reporting a wind vector of $\vec{v} = (5, 5)$ m·s^{-1}, calculate the total change in temperature the station will experience in the next hour.

Solution:

(i) Use grid locations 4b and 2b to determine the change in temperature and location. ΔT = 55 - 45 = 10°F. $\Delta x = 2 \times 100$ km $= 200 \times 1000 = 2 \times 10^5$

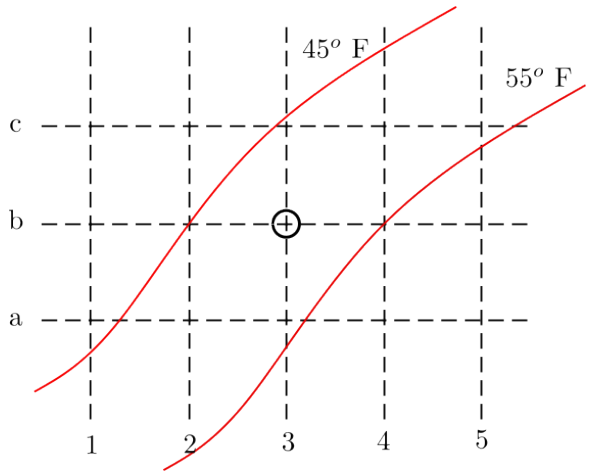

Figure 7.22: Calculating the magnitude of thermal advection.

meters. Then

$$\frac{\Delta T}{\Delta x} = \frac{10}{2 \times 10^5} = 5 \times 10^{-5} \text{ °F m}^{-1}$$

.
The temperature gradient is a vector, and in this example it is pointing in the positive x direction.

(ii) The total temperature change over a six-hour period is determined by calculating how much magnitude of the station's wind vector lines up with the temperature gradient. If they line up exactly, then the angle between the vectors is 0°. If they are perpendicular (in this case, that would mean the wind is southerly or northerly), the angle between the vectors is 90°(if southerly) or 270°if northerly. In these cases, the wind will not result in a temperature change at the station. To capture the alignment of the vectors and match the temperature change outcome, the total change in temperature is found using the formula given in Equation 7.16

$$\Delta T = -\cos(\alpha)\|\vec{v}\| \times \frac{\Delta T}{\Delta x} \times \text{the number of seconds} \tag{7.16}$$

Subbing the values for this case:

$$\begin{aligned}
\Delta T &= -\cos(\alpha)\|\vec{v}\| \times \frac{\Delta T}{\Delta x} \times \text{the number of seconds} \\
&= -\cos(45°)\sqrt{5^2+5^2} \times 5 \times 10^{-5}\ °\text{F m}^{-1} \times 60 \times 60 \\
&\approx -0.707 \times \sqrt{50} \times 5 \times 10^{-5} \times 3600 \\
&= -0.707 \times \sqrt{50} \times 5 \times 36 \times 10^2 \times 10^{-5} \\
&\approx -0.707 \times 7.07 \times 1.8 \times 10^2 \times 10^2 \times 10^{-5} \\
&= -9.0 \times 10^{-1} \\
&= \boxed{\text{-0.9 °F}}
\end{aligned}$$

7.11.3 Jet Steaks

Figure 7.23 shows an idealized pressure (height) contour pattern associated with a **jet streak**. The pressure contours are shown as solid lines. Pressure contours P_1, P_3, and P_5 are straight lines. The curved contours P_2 and P_4 "pinch" together to create a pressure gradient maximum on the P_3 contour at the center of the pattern.

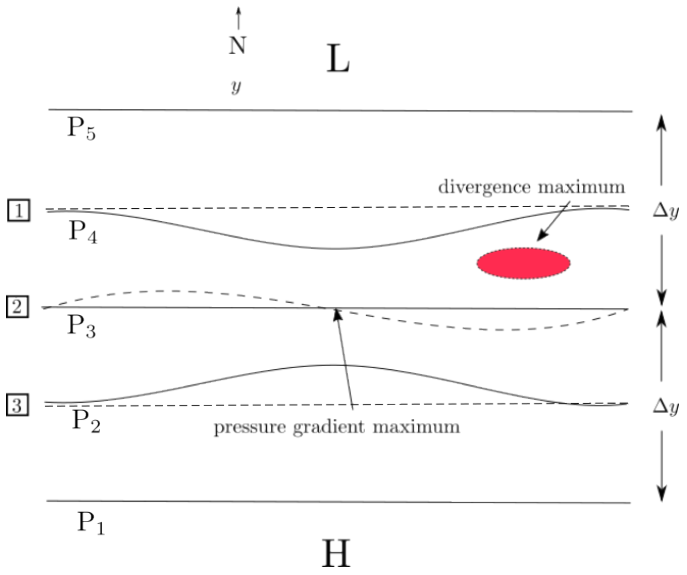

Figure 7.23: Vertical cross-section of baroclinic wave amplification.

Three parcels, numbered 1, 2, and 3 in the boxes, are entering the pressure field on the left-hand side. The parcel paths are indicated as dashed lines. The primary forces acting

on all parcels are the pressure gradient force and the Coriolis deflection. As they enter the field at the left-hand side, the two forces are equal in magnitude and opposite in direction - the pressure gradient force points in the y-direction (from high to low pressure), and the Coriolis deflection points in the negative y direction (to the right of the parcel's path).

Parcels 1 and 3 will follow straight line contours because the effective pressure gradient on them does not change. For example, the pressure gradient on parcel 1 is $\frac{-(P_5-P_3)}{\Delta y}$ throughout its shown path. A constant pressure gradient force means that the equal and opposite Coriolis deflection is constant as well. The same analysis and result applies to parcel 3.

However, parcel 2 will follow the dashed-line path, deviating from the path determined by pressure contour (indicated by the solid line). Upon entering the jet streak, parcel 2 experiences an increasing pressure gradient as it enters. This increase in pressure gradient force will, initially, exceed the right-ward Coriolis deflection causing the parcel to veer slightly to the left, down the pressure gradient and towards the low. The increasing pressure gradient force will eventually cause an increase in the parcel's speed that increases the Coriolis deflection. Additionally, the northward change in path increases the Coriolis deflection even more than what the increase in speed will create. However, once the parcel passes the point of maximum pressure gradient and the pressure gradient force on the parcel begins to decrease, the Coriolis deflection is now greater than the pressure gradient force and the parcel will deflect to the right of its gradient or geostrophic path. This occurs in the region of "natural" path divergence, so the over-reaction of the Coriolis deflection down stream from the pressure gradient maximum adds to the already present path divergence. This combined effect creates a region of enhanced divergence in the left exit flank of the jet streak.

7.12 Vertical Structure: Tilted and Stacked

A developing mid-latitude cyclone benefits greatly from a westward-tilting low or wave alignment that is shown in Figure 7.24a. The regions shaded in red in the figure are locations where mass divergence is occurring due to the wave dynamics explained in Section 7.11.1. Note that divergence regions, shaded in red, are positioned above the trough on the next lower level. The divergence aloft results in a deepening of the trough below. The blue-shaded region are the locations at which convergence occurs. Consequently, they lead to an increase in pressure at that location on the level below. The combine effect of the divergence-convergence pattern is to increase the amplitude of the wave below.

The vectors in Figure 7.24a indicate the speed of the features at the various levels. Generally speaking, the higher the elevation, the greater the speed. The result of this increasing speed with height is an eventual vertical stacking of the low centers or troughs, as shown in Figure 7.24b.

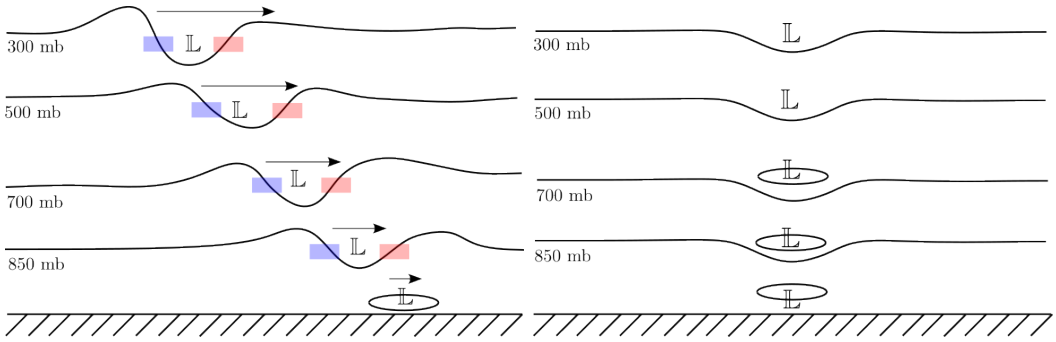

(a) Tilted lows. (b) Stacked lows.

Figure 7.24: Vertical cross-section of tilted and stacked lows.

7.13 MLC's Role in the Energy Budget

The global energy budget and transport mechanisms were introduced in Chapter 2. Recall that there is a surplus of incoming solar radiation in the equatorial region, and a deficit at the north and south poles. Without large-scale energy transport mechanisms, the equatorial region would become increasing warm, and the poles increasing cold.

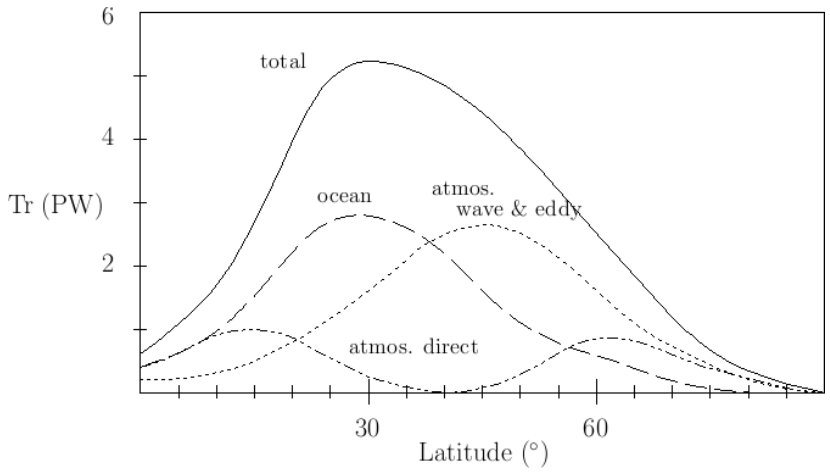

Figure 7.25: South-to-north energy transport in the northern hemisphere in response to the radiation energy imbalance (radiative forcing). Units of energy are petawatts = 10^{15} watts.

Figure 7.25 shows the strength of the various transport mechanisms responsible for creating a stable average temperature for Earth's latitudes.

The weakest component is that associated with the thermally direct Hadley and polar

cells. Ocean currents and atmospheric waves and eddies have approximately equal mitigation magnitudes. Ocean currents play a larger role in the lower latitudes.

Atmospheric circulations, made up of long wave pressure patterns and cyclonic midlatitude storms dominate in the midlatitudes, as indicated by the "wave & eddy" curve in Figure 7.25. The midlatitude cyclone, created by the north-south temperature gradient due to radiation imbalances, is one example of an "eddy." Consequently, they play and important role as a mechanism to partially alleviate the energy equator-pole solar radiation input imbalance.

Chapter 7 Exercises

7.1 Figure 7.26a shows station locations on a spatial grid. The distance between grid lines is a uniform 100 km in both the x (horizontal) and y (vertical) directions. The velocity vector $\vec{v}$ at each station is shown with its component magnitudes (units are m·sec^{-1}) as the ordered pair (u, v). Calculate the (a) divergence and, (b) vorticity for the location at the center (marked by "X") of the four stations. **Report your answer in units of** 10^{-5} **sec^{-1}.**

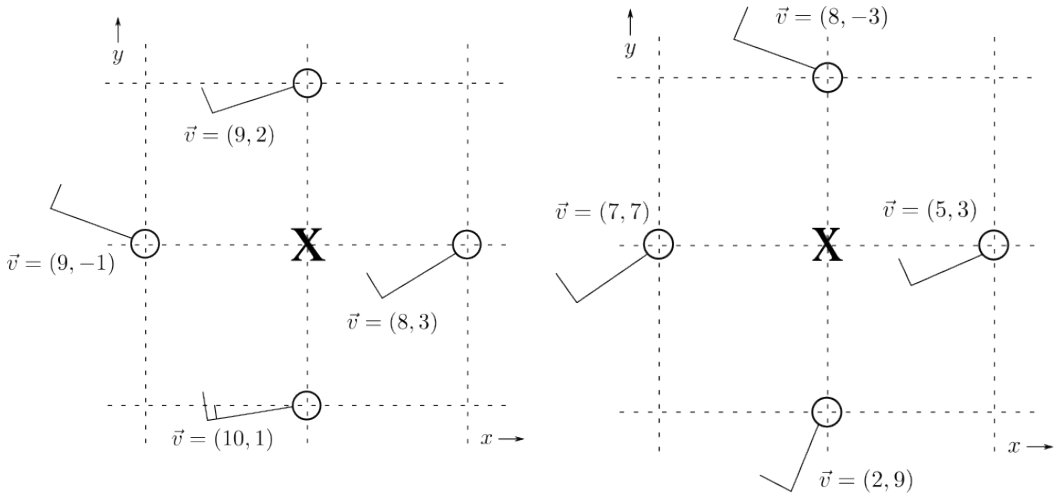

(a) Case 1. (b) Case 2.

Figure 7.26: Velocity vectors for station 1 and 2.

7.2 Figure 7.26b shows station locations on a spatial grid. The distance between grid lines is a uniform 100 km in both the x (horizontal) and y (vertical) directions. The velocity vector $\vec{v}$ at each station is shown with its component magnitudes (units are m·sec^{-1}) as the ordered pair (u, v). Calculate the (a) divergence and, (b) vorticity for the location at the center (marked by "X") of the four stations. **Report your answer in units of** 10^{-5} **sec^{-1}.**

7.3 Calculate the speed of a Rossby wave if the wind speed is 55 m·s^{-1}, the wavelength λ = 6000 km and the latitude is 45°N.

7.4 Calculate the speed of a Rossby wave if the wind speed is 60 m·s^{-1}, the wavelength λ = 3000 km and the latitude is 45°N.

7.5 Suppose the 300 mb jet stream has a wave number of 4. Calculate the average wavelength if the latitude is 45°N.

7.6 Suppose the 500 mb jet stream has a wave number of 5. Calculate the average wavelength if the latitude is 45°N.

7.7 The length of one 500 mb wave is 6000 km, and a short wave has a wavelength of 200 km. If the short wave trough is 400 km behind the long wave trough, how long will it be before their trough axes are aligned if the 500 mb wind speed is 55 m·s^{-1}? Assume angle ϕ = 45°.

7.8 The length of one 500 mb wave is 3000 km, and a short wave has a wavelength of 200 km. If the short wave trough is 300 km behind the long wave trough, how long will it be before their trough axes are aligned if the 500 mb wind speed is 60 m·s^{-1}? Assume angle ϕ = 45°.

Figure 7.27 shows surface temperature contours (solid lines, in degrees F) on a spatial grid. The distance between grid lines (dotted) is a uniform 100 km in both the x (horizontal) and y (vertical) directions. Station locations, numbered 1 - 4, are shown.

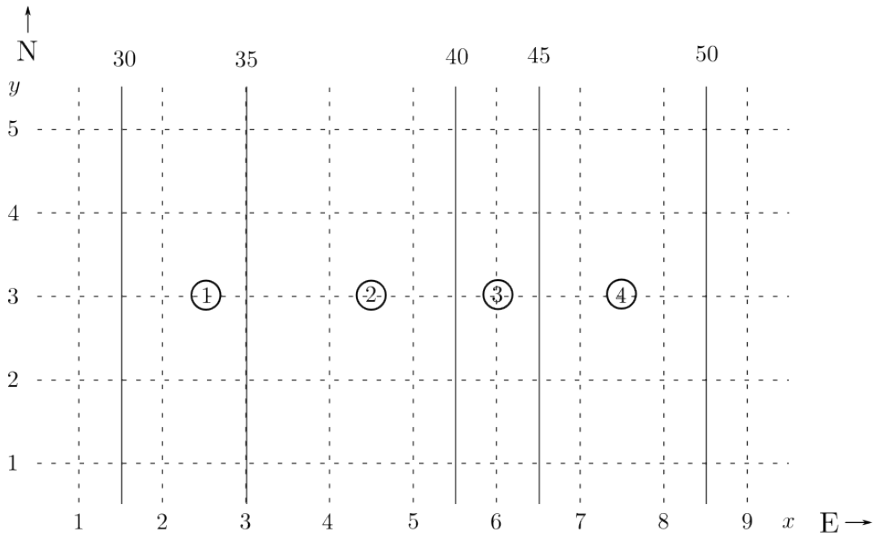

Figure 7.27: Spatial grid with temperature contours (in degrees Fahrenheit).

7.9 Calculate the temperature gradient $\frac{\Delta T}{\Delta x}$ (in 10^{-5} °F/meter) for station 1.

7.10 Calculate the temperature gradient $\frac{\Delta T}{\Delta x}$ (in 10^{-5} °F/meter) for station 2.

7.11 Calculate the temperature gradient $\frac{\Delta T}{\Delta x}$ (in 10^{-5} °F/meter) for station 3.

7.12 Calculate the temperature gradient $\frac{\Delta T}{\Delta x}$ (in 10^{-5} °F/meter) for station 4.

7.13 Station 1 has a westerly wind with a speed of 10 m·s^{-1}(the wind vector is $\vec{v} = (10, 0)$). Calculate the magnitude of the thermal advection at station 1 in °F/hour.

7.14 Station 2 has a westerly wind vector $\vec{v} = (15, 0)$. Calculate the magnitude of the thermal advection in °F/hour.

7.15 Station 3 has a westerly wind vector $\vec{v} = (10, 10)$. Calculate the magnitude of the thermal advection in °F/hour.

7.16 Station 4 has a southeasterly wind vector $\vec{v} = (-10, 10)$. Calculate the magnitude of the thermal advection in °F/hour.

7.17 If the wind speed doubles, then the magnitude of the temperature advection will _____. Explain.

7.18 If the magnitude of the temperature gradient doubles, then the magnitude of the temperature advection will _____. Explain.

7.19 Explain why the magnitude of thermal advection is zero if the wind blows parallel to the isotherms.

7.20 Identify and describe atmospheric features, or mechanisms, by which a midlatitude cyclone may develop or intensify during its lifetime.

7.21 Suppose a midlatitude cyclone is in the "open-wave" stage with very well-defined warm and cold fronts. Make a sketch of the low center and the relative locations of the two fronts. Next, compare and contrast characteristics such as frontal slope, frontal speed, type and nature of precipitation, etc., of the fronts.

7.22 Explain how a baroclinic atmosphere, in which warm and cold advection is taking place at the level of 850 mb, may result in a "positive feed back loop" from which a midlatitude cyclone will quickly strengthen. Provide supporting sketches.

7.23 Identify and describe, in the proper time sequence, the various stages in the life cycle of a midlatitude cyclone based on the Norwegian Cyclone Model. Provide a sketch for each stage.

7.24 Identify and describe flow patterns or mechanisms in the upper-level wind flow pattern (at levels of 850 mb or above) that can enhance the development and movement of a midlatitude cyclone.

7.25 Suppose a midlatitude cyclone is in the "open-wave" stage with very well-defined warm and cold fronts. Make a sketch of the low center and the relative locations of the two fronts. Next, compare and contrast characteristics such as frontal slope, frontal speed, type and nature of precipitation, etc., of the fronts.

7.26 Define "divergence" in meteorological terms, and how it is calculated. Explain why it is such an important factor in the theory of MLCs.

7.27 Define "vorticity" in meteorological terms, and why it is such an important factor in theory of MLCs.

7.28 Explain the connection between divergence and vorticity in the context of a 500 mb wave.

7.29 Define what a short wave is in meteorological terms and how they may contribute to the initiation or the deepening of an MLC.

7.30 A westward tilted vertical profile of low pressure troughs with respect to elevation z is conducive to MLC strengthening. Explain why this is.

7.31 Explain how warm and cold air advection contribute to the strengthening of an MLC.

7.32 Explain how warm and cold air advection is identified on a weather chart.

7.33 Explainthe role MLCs play in the planetary energy transport budget.

Chapter 8

Moisture Measures

8.1 Overview

The importance of water in the earth's atmosphere can not be overstated. Apart from serving as precipitation in weather phenomena, its enormous role in the Earth's energy budget through latent heat transfer must be understood. Therefore, accurate measurement of water, especially in its vapor state, is crucial. This chapter defines numerous ways atmospheric water vapor is measured and establishes the connections between the various measures.

8.2 Partial Pressure

The pressure on a parcel of air is the measure of the gravitational force per area of the atmospheric mass above the parcel. In a steady state, the volume of the parcel is not changing. Consequently, the pressure inside the parcel is equal and opposite in direction to the external pressure of the mass above. The internal pressure of the parcel is created by the movement of the parcel's gaseous constituents; primarily N_2, O_2, Ar and H_2O. If P_T is the total internal pressure, or simply pressure, of the parcel, then

$$P_T = \sum_i P_i = P_{N_2} + P_{O_2} + P_{AR} + ... + P_{H_2O} \tag{8.1}$$

where P_i is the parcel's partial pressure due to the gaseous constituent given by index i. The partial pressure of water vapor P_{H_2O} is typically represented by e. We shall refer to the water vapor pressure e as simply "vapor pressure."

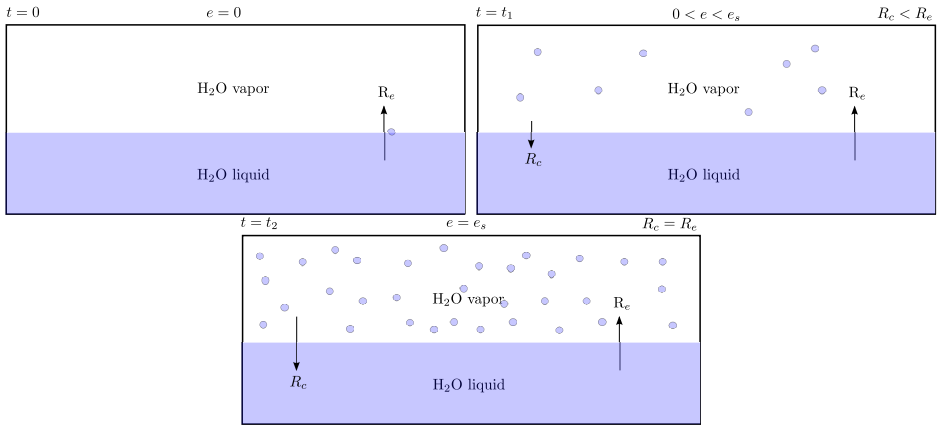

Figure 8.1: Water molecules evaporate into the air chamber until there is a sufficient number of them so that the rate of condensation, R_c matches the rate of evaporation R_e.

8.3 Saturation Vapor Pressure

The **saturation vapor pressure** e_s of a parcel is defined next. To do so, an idealized situation is imagined where a mass of liquid water partially fills a closed container, as shown in Figure 8.1. The air above the water mass is initially void of water vapor, so $e = 0$, as indicated for the case $t = 0$ in the figure.

The water and air above have the same temperatures T_w and T_a, respectively. Recall that temperature T is a measure of the average kinetic energy of the constituents making up the mass of a body, such as the mass of the water and the mass of the air situated above the water.

Typically, the various speeds of the constituents are distributed in a "normal" fashion about the mean, or average, speed $\bar{v}$. In a normal distribution, as shown in Figure 8.2, there are as many molecules with above average speeds as those with below average speeds, so the speed distribution on either side of the mean value creates a mirror image. Some molecules having higher than average speeds may have sufficient kinetic energy to "escape" the water mass and emerge as vapor.

The portion of the molecules with sufficient speed to escape the water and increase the number of vapor molecules is indicated in the shaded region of Figure 8.2. These are molecules that have a speed (kinetic energy) greater the required minimum speed, denoted by v_{min} in the figure. Note that as the temperature of the water increases, the average speed of the molecules increases, as indicated by the lower distribution curve in Figure 8.2, where the average speed is $\bar{v}_2 > \bar{v}_1$.

The rate at which molecules change from liquid to vapor state is denoted by R_e, the **rate of evaporation**. The vapor pressure e of the air above increases as more water molecules

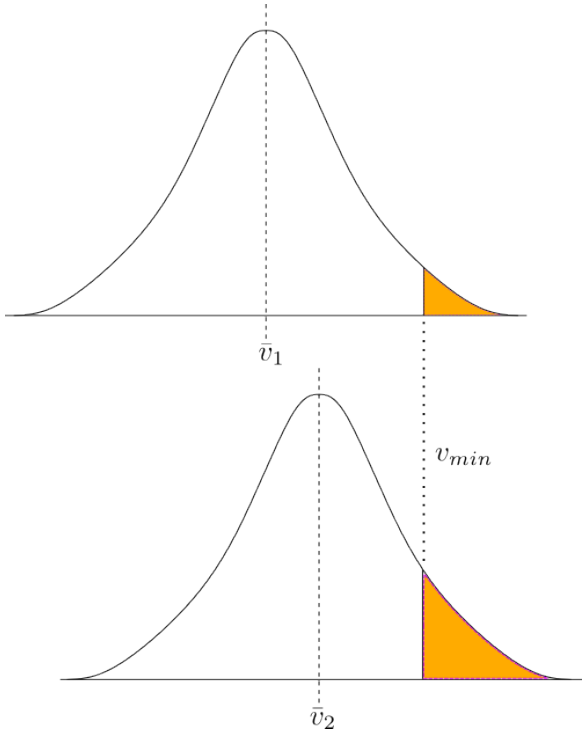

Figure 8.2: Normal distribution of liquid water molecule speeds.

evaporate. The **rate of condensation** R_c measures the magnitude at which the vapor molecules return to liquid state. Initially, the rate of evaporation is greater than the rate of condensation ($R_e > R_c$) so there is a net gain of vapor molecules, as indicated in Figure 8.1 for time $t = t_1$.

The speeds of the vapor molecules also follow a normal distribution. Eventually, the number of vapor molecules with deficient energy to remain in a vapor state is sufficient to produce a rate of condensation that is equal to the rate of evaporation ($R_e = R_c$). When these rates are equal, the vapor pressure e is equal to the saturation vapor pressure e_s. That is, $e = e_s$ when $R_e = R_c$. This situation is shown for time $t = t_2$ in Figure 8.1. Saturation vapor pressure is often referred to as **equilibrium vapor pressure** because the rates R_e and R_c are in equilibrium.

Saturation vapor pressure e_s is a function of the water temperature T_w. As T_w increases, the number of water molecules with sufficient energy to transition into the vapor phase increases. Consequently, the rate of evaporation R_e is greater. In order for R_c to be equal to R_e, more vapor molecules must collect in the air space. Consequently, $e_s(T2_w) > e_s(T1_w)$ when $T2_w > T1_w$.

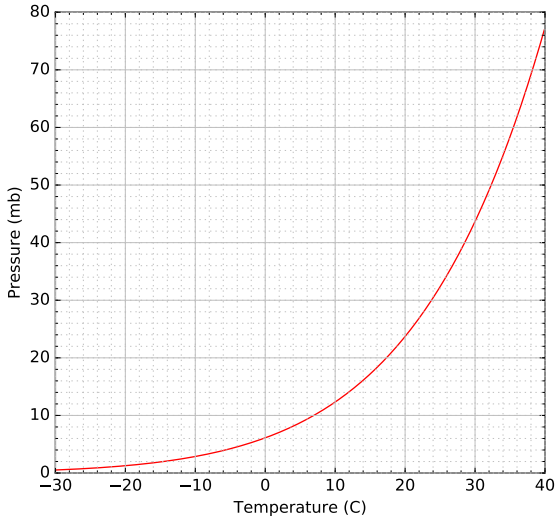

Figure 8.3: Plot of the Clausius-Clapeyron equation curve for a water surface.

The functional relationship between saturation vapor pressure and temperature is give by the **Clausius-Clapeyron** Equation 8.2.

$$e_s(T) = e_0 \cdot \exp\left(\left[\frac{L}{R_v}\left(\frac{1}{T_0} - \frac{1}{T}\right)\right]\right) \tag{8.2}$$

where $L = 2.50 \times 10^6$ J $\cdot$ kg^{-1} is the heat of vaporization (over a water surface,) or $L = 2.83 \times 10^6$ J $\cdot$ kg^{-1} is the heat of sublimation (over an ice surface), $R_v = 461$ J $\cdot$ K^{-1} $\cdot$ kg^{-1} is the gas constant for water vapor, $T_0 = 273$K, and $e_0 = 6.11$ mb is the saturation vapor pressure for $T = 273$K. Interestingly, saturation vapor pressure is not dependent on the system pressure P.

The saturation vapor pressure over an ice surface is generally less than that over a water surface when both have the same temperature T. Although the difference is slight, the implications are great. To understand why this is so, it is good to first consider the graph of the difference $e_s^w(T) - e_s^i(T)$ as shown in Figure 8.4. The maximum difference occurs at the temperature T of around -11°C. Even though this temperature is below freezing, the lower pressure environment of many clouds make it possible for all three phases of water to exist simultaneously within the cloud. The important result of this difference is the migration of water mass from liquid cloud droplets to cloud ice constituents. The air around the water droplets might be in an unsaturated state, so there is a net migration of water molecules from the droplets to the air. Concurrently, that same air may present itself

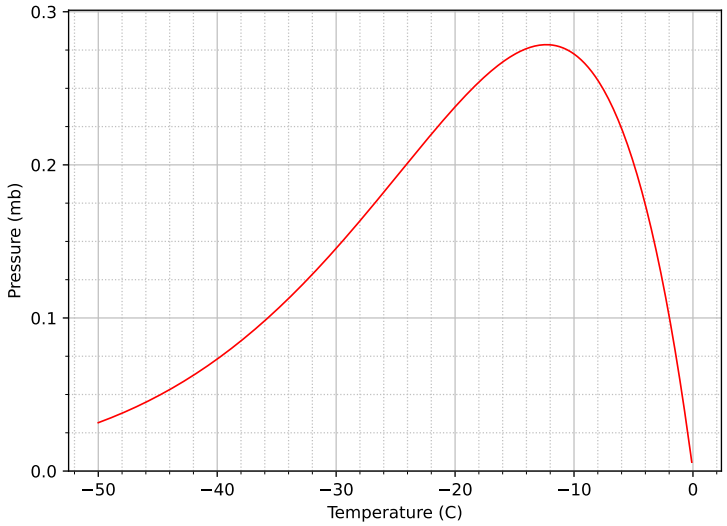

Figure 8.4: Plot of the difference in saturation vapor pressure for a water surface versus an ice surface.

as super saturated to the ice surface so that there is a net increase in water mass on the ice particles because $R_d(T) > R_s(T)$.

8.4 Measures of Moisture

The development of various atmospheric moisture measurements is done to suit particular needs. For example, one moisture measurement may give the mass of water vapor while another may provide information regarding the actual moisture content relative to the moisture capacity of a given parcel. The details of the various measures follow.

Mixing Ratio

The mixing ratio (MR) is defined as

$$MR = \frac{\text{mass of water vapor}}{\text{mass of dry air}} = \frac{\epsilon \cdot e}{P - e} \tag{8.3}$$

where P is the total pressure on the parcel, e is the vapor pressure, and ϵ is the ratio of R_d, the specific gas constant for dry air, and R_v, the specific gas constant for water vapor. The values for these constants are 287 $\text{J} \cdot \text{kg}^{-1} \cdot \text{K}^{-1}$and 461.5 $\text{J} \cdot \text{kg}^{-1} \cdot \text{K}^{-1}$, respectively. Therefore, the value for ϵ is 0.622, and is given in units of grams of water per kilograms of

air (not grams per gram nor kilograms per kilograms) because the ratio of kilograms per kilograms is a very small number.

Specific Humidity

The specific humidity (SH) is defined as

$$SH = \frac{\text{mass of water vapor}}{\text{mass of air}} = \frac{\epsilon \cdot e}{P - (1 - \epsilon)e} \tag{8.4}$$

and is given in units of grams of water per kilograms of air. Specific humidity is useful in weather forecasting to predict phenomena like dew, fog, and rainfall.

Absolute Humidity

The absolute humidity (AH) is defined as

$$AH = \frac{\text{mass of water vapor}}{\text{parcel volume}} = \frac{e}{R_v \cdot T} \tag{8.5}$$

where the temperature T is the absolute temperature measured in Kelvin, K.

Relative Humidity

The relative humidity (RH) is defined as

$$RH = \frac{\text{vapor pressure}}{\text{saturation vapor pressure}} \times 100 = \frac{e}{e_s} \times 100 = \frac{MR}{MR_s} \times 100 \tag{8.6}$$

where e_s and MR_s are the saturation vapor pressure and saturation mixing ratio, respectively.

Relative humidity is perhaps the most commonly used moisture measure. However, as it will be shown in the next section, the *relative* nature of RH means it can change with changing parcel temperature without a change in the vapor content of a parcel. Therefore, the ratio may not be very useful unless the temperature of the parcel is known. For example, a relative humidity of 40% for a parcel temperature of 45° has a very different feel for a human as opposed to a 40% RH with a parcel temperature of 85°.

8.5 Dew Point Temperature

As pointed out in the previous section, relative humidity may not be a very useful moisture measure without also knowing the air temperature (parcel temperature). The value of **dew point temperature** is a more complete indication of moisture content and is often preferred by meteorologists more so than relative humidity.

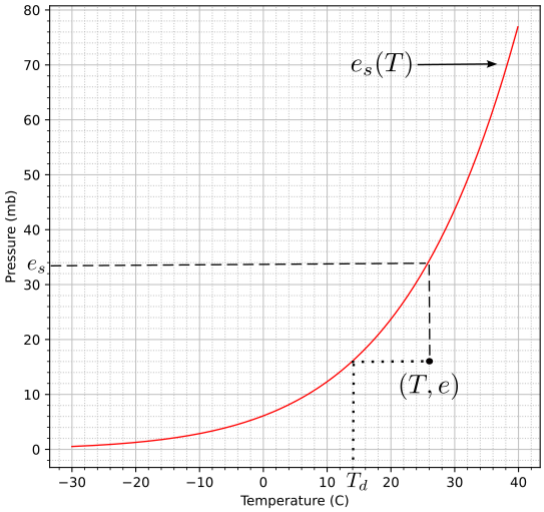

Figure 8.5: Plot of the saturation vapor pressure e_s as a function of temperature. Temperature T_d is the **dew point temperature**.

The saturation vapor pressure curve in Figure 8.5 shows the relationship between parcel temperature T and the saturation, or equilibrium, vapor pressure e_s. Most parcels have a temperature T and vapor pressure e that result in the parcel being "unsaturated." That is, the parcel's vapor pressure is lower than the vapor pressure needed for the rate of condensation R_c to match the rate of evaporation R_e ($e < e_s \Rightarrow R_c < R_e$). In this case, we cannot "see" the moisture in the parcel - the parcel is not part of any dew or cloud formation.

The temperature for which the parcel's vapor pressure e would is equal to the equilibrium vapor pressure e_s is known as the **dew point temperature** T_d. The dotted lines on Figure 8.5 show the direct connection between e and dew point temperature T_d for an air parcel, as well as the direct connection between parcel temperature T and equilibrium vapor pressure e_s.

For dew or cloud formation, the vapor pressure e of the parcel must be equal to its saturation vapor pressure e_s (In some situations, fog and cloud formation will begin for vapor pressure slightly less than e_s.) If the vapor pressure of a parcel is well below the requisite equilibrium vapor pressure, in order for dew or a cloud to exist, one of the following must occur:

(a) the temperature of the parcel must decrease (cool) to its dew point temperature T_d,

(b) the vapor pressure e of the parcel must increase to e_s by the addition of more vapor,

or

(c) some combination of temperature decrease and vapor pressure increase must occur so that the vapor pressure is "close" to the equilibrium value.

Instead of using the graph in Figure 8.5 to determine the relationship between T, e, T_d and e_s, a table of values is used. Such a table is given at the end of the exercise set. The table gives values saturation vapor pressures for discrete values of temperature, measured in degrees Celsius, in the range of -20 to 40. The approximate Fahrenheit temperature is listed as well as mixing ratios as a function of temperature and pressure for several pressure values.

For temperatures between -20°C and 40°C and not shown on the table, use the closest temperature value in the table for determining the approximate saturation vapor pressure or mixing ratio.

Example 8.5.1 shows how to calculate the dew point temperature and relative humidity when its temperature and vapor pressure is known.

Example 8.5.1. Suppose a parcel has a temperature of 70° and a vapor pressure of 15 mb. Calculate the dew point temperature and the relative humidity of the parcel.

Solution:

The dew point is the temperature the parcel needs to have for it to be saturated. Use the saturation table given at the end of the exercise set to determine the parcel's dew point T_d

For a vapor pressure of 15 mb, use the table entry for SVP of 15.1 mb. Then, the saturation temperature is approximately 55 F. Therefore, $\boxed{T_d = 55°.}$

To determine the RH of the parcel, use Equation 8.6. We have e=15 mb. Use the table to determine e_s for 70°: it is approximately 25.3 mb. Therefore, $\boxed{RH = 100 \times \frac{15}{25.3} = 63.8\%}$

The next example shows how dew point temperature and vapor pressure can be determined if the temperature and relative humidity of the parcel are known.

Example 8.5.2. Suppose the temperature T and RH of a parcel are 75° and 50%, respectively. Determine the parcel's vapor pressure and dew point temperature.

Solution:

First, we use the RH formula to determine e of the parcel.

$$RH = 100 \times \frac{e}{e_s} \Rightarrow \frac{e}{e_s} = \frac{RH}{100} \Rightarrow e = \frac{RH}{100} \times e_s \tag{8.7}$$

From the table, e_s for $T = 75^\circ$ is 30 mb. Using the know quantities in the equation above gives $\boxed{e_s = 50/100\times \text{ 30 mb} = 15 \text{ mb.}}$

Next, use the parcel's vapor pressure of 15 mb and the table to find $\boxed{T_d \approx= 55^\circ \text{ F}}$

Temperature		SVP (e_s)	Saturation Mixing Ratio (g/kg)			
°C	°F	mb	1000 mb	850 mb	700 mb	500 mb
-20	-4.0	1.3	0.8	0.9	1.1	1.6
-19	-2.2	1.4	0.9	1.0	1.2	1.7
-18	-0.4	1.5	0.9	1.1	1.3	1.9
-17	1.4	1.6	1.0	1.2	1.5	2.0
-16	3.2	1.8	1.1	1.3	1.6	2.2
-15	5.0	1.9	1.2	1.4	1.7	2.4
-14	6.8	2.1	1.3	1.5	1.9	2.6
-13	8.6	2.3	1.4	1.7	2.0	2.8
-12	10.4	2.5	1.5	1.8	2.2	3.1
-11	12.2	2.7	1.7	1.9	2.4	3.3
-10	14.0	2.9	1.8	2.1	2.6	3.6
-9	15.8	3.1	1.9	2.3	2.8	3.9
-8	17.6	3.4	2.1	2.5	3.0	4.2
-7	19.4	3.6	2.3	2.7	3.2	4.5
-6	21.2	3.9	2.4	2.9	3.5	4.9
-5	23.0	4.2	2.6	3.1	3.8	5.3
-4	24.8	4.5	2.8	3.3	4.1	5.7
-3	26.6	4.9	3.1	3.6	4.4	6.2
-2	28.4	5.3	3.3	3.9	4.7	6.6
-1	30.2	5.7	3.6	4.2	5.1	7.1
0	32.0	6.1	3.8	4.5	5.5	7.7
1	33.8	6.6	4.1	4.8	5.9	8.3
2	35.6	7.1	4.4	5.2	6.3	8.9
3	37.4	7.6	4.8	5.6	6.8	9.6
4	39.2	8.1	5.1	6.0	7.3	10.3
5	41.0	8.7	5.5	6.5	7.9	11.1
6	42.8	9.4	5.9	6.9	8.4	11.9
7	44.6	10.0	6.3	7.4	9.1	12.7
8	46.4	10.8	6.8	8.0	9.7	13.7
9	48.2	11.5	7.2	8.5	10.4	14.7
10	50.0	12.3	7.8	9.2	11.2	15.7
11	51.8	13.2	8.3	9.8	11.9	16.9
12	53.6	14.1	8.9	10.5	12.8	18.1
13	55.4	15.1	9.5	11.2	13.7	19.3
14	57.2	16.1	10.2	12.0	14.6	20.7
15	59.0	17.2	10.9	12.8	15.7	22.2
16	60.8	18.4	11.6	13.7	16.7	23.7
17	62.6	19.6	12.4	14.7	17.9	25.3
18	64.4	20.9	13.3	15.7	19.1	27.1
19	66.2	22.3	14.2	16.7	20.4	29.0
20	68.0	23.7	15.1	17.8	21.8	31.0
21	69.8	25.2	16.1	19.0	23.3	33.1
22	71.6	26.9	17.2	20.3	24.8	35.3
23	73.4	28.6	18.3	21.7	26.5	37.7
24	75.2	30.4	19.5	23.1	28.3	40.3
25	77.0	32.3	20.8	24.6	30.1	43.0
26	78.8	34.4	22.1	26.2	32.1	45.9
27	80.6	36.5	23.6	27.9	34.2	49.0
28	82.4	38.8	25.1	29.7	36.5	52.3
29	84.2	41.2	26.7	31.7	38.9	55.8
30	86.0	43.7	28.4	33.7	41.4	59.5
31	87.8	46.3	30.2	35.8	44.1	63.5
32	89.6	49.1	32.1	38.1	46.9	67.7
33	91.4	52.0	34.2	40.6	50.0	72.3
34	93.2	55.1	36.3	43.1	53.2	77.1
35	95.0	58.4	38.6	45.9	56.6	82.3
36	96.8	61.8	41.0	48.8	60.3	87.8
37	98.6	65.4	43.5	51.9	64.1	93.6
38	100.4	69.2	46.2	55.1	68.2	99.9
39	102.2	73.2	49.1	58.6	72.6	106.7
40	104.0	77.4	52.2	62.3	77.3	113.9

Exercises

8.1 Calculate the mixing ratio (MR) for a parcel with a temperature of 15° C, pressure of 1000 mb that is

(a) 1% water vapor

(b) 4% water vapor.

8.2 Calculate the mixing ratio (MR) for a parcel with a temperature of 0° C, pressure of 850 mb that is

(a) 1% water vapor

(b) 4% water vapor.

8.3 A parcel at the surface of the earth, where pressure is 1020 mb, has a mixing ratio of 10 g/kg.

(a) Calculate the vapor partial pressure of the parcel.

(b) Suppose the parcel is lifted to the 700 mb pressure level. Assuming the parcel's mixing ratio is conserved, calculate the vapor partial pressure at the parcel's new height.

8.4 A parcel at the surface of the earth, where pressure is 1000 mb, has a mixing ratio of 20 g/kg.

(a) Calculate the vapor partial pressure of the parcel.

(b) Suppose the parcel is lifted to the 850 mb pressure level. Assuming the parcel's mixing ratio is conserved, calculate the vapor partial pressure at the parcel's new height.

8.5 Given that a parcel of air has a temperature of 15° C, determine the saturation vapor pressure relative to a water surface.

8.6 A parcel of air has a saturation vapor pressure of 15 mb. Determine the parcel's temperature in °C.

8.7 Suppose a parcel's saturation vapor pressure is 12 mb. Determine the parcel's temperature in °C.

8.8 A parcel of air has a saturation vapor pressure of 2 mb (relative to a water surface). Determine the parcel's temperature in °F.

8.9 A parcel has temperature of 25° C and a vapor pressure of 10 mb.

(a) Calculate the relative humidity of the parcel.

(b) Determine the dew point of the parcel.

8.10 Suppose a parcel at the surface of the earth has a relative humidity of 90% and a temperature of 50° F. Determine the mixing ratio of the parcel.

8.11 Suppose a surface parcel (so pressure is 1000 mb) has a relative humidity of 70% and a temperature of 90° F. Determine the mixing ratio of the parcel.

8.12 A parcel of air has a temperature of 60° F and a dew point of 45° F. Determine the relative humidity of the parcel.

8.13 A parcel of air has a temperature of 80° F and a dew point of 35° F. Determine the relative humidity of the parcel.

8.14 Suppose a parcel of air has a temperature of 75° F and a relative humidity of 50%. Determine the parcel's dew point temperature.

8.15 Suppose a parcel of air has a temperature of 45° F and a relative humidity of 80%. Determine the parcel's dew point temperature.

8.16 A air parcel near the surface of the earth has a dew point temperature of 10° C and a relative humidity of 90%. Determine the parcel's temperature.

8.17 A air parcel near the surface of the earth has a dew point temperature of 20° C and a relative humidity of 70%. Determine the parcel's temperature.

8.18 Why does saturation vapor pressure increase with increasing temperature? What effect, if any, does a decrease in atmospheric pressure have on saturation vapor pressure?

8.19 Suppose the moisture content, in terms of vapor pressure, remains constant for a given parcel of air from sunrise to sunset. The temperature of the parcel as a function of time of day is shown in Figure 8.6 below. When is the relative humidity of the parcel minimum? maximum? Provide an explanation. When is the dew point of the parcel maximum? minimum? Provide an explanation.

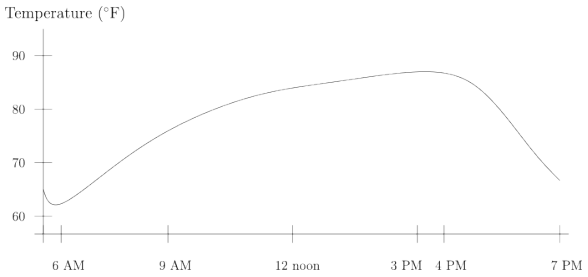

Figure 8.6: Temperature as a function of time.

8.20 Explain the relationship between saturation vapor pressure, the rate of evaporation, and the rate of condensation.

Chapter 9

Atmospheric Stability & Clouds

9.1 Overview

This chapter begins with a brief section on cloud classification. It is followed by a section on atmospheric stability. Next, mechanical cloud formation processes are introduced. The chapter concludes by covering the important aspects of cloud formation by convection. This includes an introduction to the use of thermodynamic charts for determining the stability of the atmosphere. The resulting analysis provides vital information on the requirements for thunderstorm development and determining the potential for severe storm development.

9.2 Formation & Classification

9.2.1 General Cloud Formation

An atmospheric parcel must reach its saturation dew point in order for its moisture to be visible. If a multitude of parcels have visible moisture, a cloud is formed, either above or at the Earth's surface. A cloud at the surface is known as **fog**. For an unsaturated parcel to reach saturation, its temperature must cool to its dew point temperature, or water vapor must be added to the parcel, or a combination of both.

In terms of decreasing the parcel temperature to its dew point temperature, the predominant method is by lifting the parcel. Any upward movement of a parcel results in a pressure decrease on the parcel. A pressure decrease results in parcel expansion. Parcel expansion results in the decrease in parcel temperature. This processed is visualized in Figure 9.1.

Assuming the parcel lifting is an adiabatic process, no energy (heat) is exchanged between the parcel and the surrounding **environmental parcels**. Therefore, the parcel's potential temperature θ is conserved. That is, $\Delta\theta = 0$. As P decreases, the quotient $\frac{1000}{P}$ increases, so a decrease in T must follow to so that $\Delta\theta = 0$ is true.

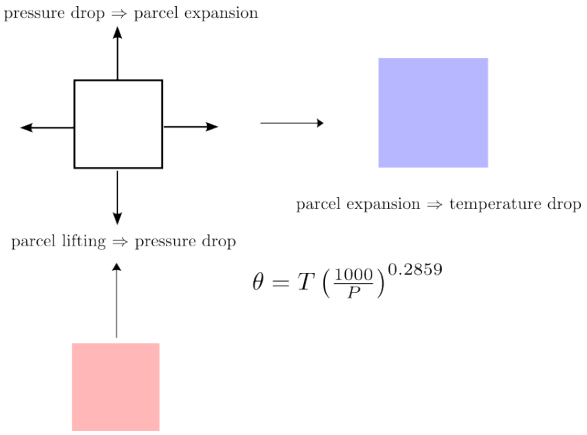

Figure 9.1: Adiabatic lifting results in parcel cooling.

9.2.2 General Cloud Classification

In a simplified way, cloud formation can be separated into mechanical and thermal mechanisms. Mechanical mechanisms are predominantly horizontal motions that result in broader and flatter clouds. This general cloud type is known as **stratus clouds**.

Thermally based mechanisms, especially by convective means, result in clouds that have a longer vertical extend than horizontal. This general cloud type is known as **cumulus clouds**. Cumulus clouds are typically "puffy" in appearance.

Cloud type differentiation also includes cloud elevation. Mid-level clouds are often prefixed with **alto**, and higher elevation clouds are prefixed with **cirrus**. As a result, middle-level flatter clouds are called **alto-stratus**, and the puffy convection driven clouds are called **alto-cumulus**. Similar nomenclature is used for high level clouds. Lower level clouds are generally not prefixed. That is, there is no general prefix for low clouds.

Clouds that result in precipitation are typically classified as **nimbus**. An alto-stratus-nimbus cloud is a mid-level, flat cloud, precipitating cloud. A precipitating cumulus cloud is typically tall in nature, so it extends from low to high altitudes, so it is typically referred to as a **cumulo-nimbus** cloud with no altitude specification.

9.3 Atmospheric Stability

9.3.1 Lapse Rates

The term **temperature lapse rate** refers to how quickly the temperature changes as altitude increases. Mathematically, it is defined as

$$\text{lapse rate} = \Gamma = -\frac{\Delta T}{\Delta z} \tag{9.1}$$

With very few exceptions, a lapse rate is a positive number. That is, environmental temperature T_e almost always decreases ($\Delta T < 0$) as altitude z increases ($\Delta z > 0$). This means that the rate of change of T with respect to z is referred to as a **lapse rate**.

Classifying atmospheric stability is based on comparing two temperature lapse rates: the environmental lapse rate Γ_e and the lapse rate of a rising atmospheric parcel. A parcel rises as a dry parcel or moist parcel. A dry parcel means that no vapor condensation is occurring as the parcel rises. In this case, the parcel's lapse rate is represented by Γ_d, the **dry adiabatic lapse rate**. Alternatively, the temperature of the rising, cooling parcel may reach its dew point temperature so that condensation will occur. Condensation results in latent heat release. This lapse rate is known as the **moist adiabatic lapse rate** and is represented by Γ_m. In summary:

- Γ_e = the environmental lapse rate
- Γ_d = the dry parcel lapse rate
- Γ_m = the moist parcel lapse rate

Figure 9.2 depicts two atmospheric parcels that are lifted from altitude z_0 to z_1. Altitude z increases upward. Locations z_0 and z_1 are arbitrary altitudes. The environmental temperature T_e is scaled on the right side of the figure. The temperature T_e^1 is less than temperature T_e^2. At level z_0, the parcel's temperature T^0, for both the dry and moist cases, is equal to the environmental temperature T_e^0.

The parcel on the left will experience a temperature drop at the **dry adiabatic rate** as it is lifted to level z_1 because its temperature throughout the elevation rise is greater than its dew point temperature. Therefore, no moisture will condense as it rises to the z_1 altitude. Its temperature will decrease to T_d^1.

The parcel on the right in Figure 9.2 is moist, which means its temperature T_m^0 is equal to its dew point temperature as it rises to level z_1 resulting in condensation and latent heat release. The adiabatic process means all the latent heat is used to warm the parcel, so its temperature will decrease to $T_m^1 > T_d^1$.

The following atmospheric stability types result from the three possible relative values of T_e^1, T_d^1, and T_m^1. Note that in all scenarios, $T_d^1 < T_m^1$.

1: stable: $T_d^1 < T_m^1 < T_e^1 \Rightarrow \Gamma_e < \Gamma_m < \Gamma_d$

2: conditionally stable: $T_d^1 < T_e^1 < T_m^1 \Rightarrow \Gamma_m < \Gamma_e < \Gamma_d$

3: unstable: $T_e^1 < T_d^1 < T_m^1 \Rightarrow \Gamma_m < \Gamma_d < \Gamma_e$

If the parcel's temperature T^1 at level z_1 is greater than the environmental temperature T_e^1, then the parcel's density ρ_1 is less than that of the surrounding environmental parcels. This conclusion is established by the following:

$$P = 2.87 \cdot \rho T \Rightarrow \rho = \frac{P}{2.87 \cdot T}$$

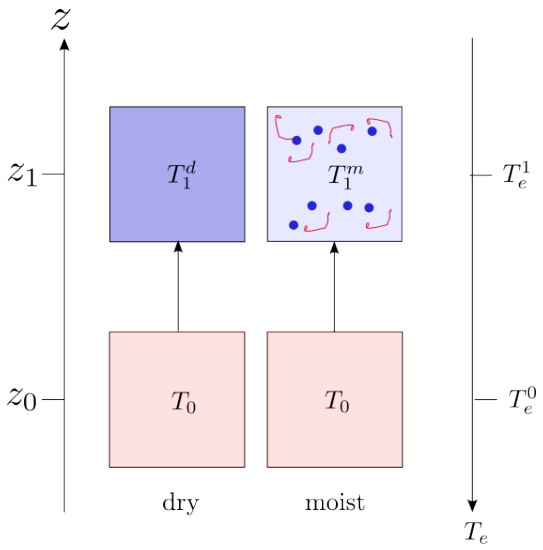

Figure 9.2: Stable Environment.

If $T_1 > T_e^1$, then

$$\rho_1 = \frac{P}{2.87 \cdot T_1} < \rho_e^1 = \frac{P}{2.87 \cdot T_e^1}$$

Recall that P is the atmospheric pressure. If two side-by-side parcels are at the same altitude z, they are under the same pressure P.

The warmer parcel, with a temperature greater than the environmental temperature, will rise for the same reason a hot air balloon rises - a positive **buoyant force** pushes the parcel in the positive z direction. In fact, the parcel will continue to rise until it reaches a level z where its temperature is equal to the environmental temperature T_e.

9.3.2 Atmospheric Stability

Atmospheric stability is determined by comparing the environmental lapse rate Γ_e and the rising parcel's lapse rate, either Γ_d or Γ_m. As a means of reference, averages for these three lapse rates are

- $\bar{\Gamma}_e = 6.5°\text{C}$ per 1000 m
- $\bar{\Gamma}_d = 10°\text{C}$ per 1000 m
- $\bar{\Gamma}_m = 6°\text{C}$ per 1000 m

which means, on average, both dry and moist parcels cool faster than the environment in the z direction. If so, then as the parcel rises from a level where its temperature is less than

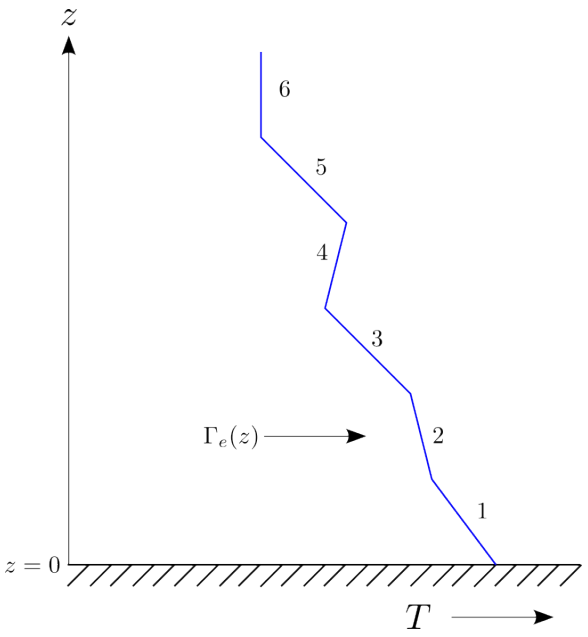

Figure 9.3: An environmental temperature profile with a variable lapse rate Γ_e.

or equal to the environmental temperature ($T_p^0 \leq T_e^0$), its new temperature T_p^1 is less than the environmental temperature T_e^1 at the higher altitude. Further, this would mean that the environment is always stable.

It is important to emphasize that the stated environmental lapse rate of 6.5°C per 1000 m is an average value. The environmental lapse rate can change with time or position. Therefore, the relative magnitude of Γ_e versus Γ_d and Γ_m may vary over time and space resulting in three types of atmospheric stability shown below.

In reality, the atmospheric stability can change within an atmospheric column. Figure 9.3 depicts the environmental temperature as a function of altitude z. Temperature increases to the right, as indicated in the figure below the surface position where $z = 0$. This type of graph is referred to as a **temperature profile**. The environmental lapse rate Γ_e is the ***negative*** slope of the profile.

The profile is made up by six straight-line segments, numbered 1-6, each with a constant value for Γ_e. Remember, a positive lapse rate means temperature is decreasing with increasing z. The greatest lapse rate (the most positive value) is that of segments 3 and 5. The temperature over segment 4 is actually increasing, so $\Gamma_e < 0$. A negative lapse rate (that is, an increase in temperature with altitude) identifies a **temperature inversion** in the profile. Note that segment 6 is a vertical line, so the environmental temperature T_e is constant of this length, meaning $\Gamma_e = 0$. Segment 6 is likely associated with the region of

the atmosphere known as the stratosphere (strato means "straight") which is situated just above the troposphere.

The type of atmospheric stability is determined be the relative magnitude of Γ_e versus dry and moist adiabatic lapse rate Γ_d and Γ_m, respectively. Therefore, each segment will have a particular stability type. The likely stability types, as a function profile segment number are listed below:

1: conditionally stable: $\Gamma_m < \Gamma_e < \Gamma_d$

2: stable: $\Gamma_e < \Gamma_m < \Gamma_d$

3: unstable: $\Gamma_m < \Gamma_d < \Gamma_e$

4: stable: $\Gamma_e < \Gamma_m < \Gamma_d$

5: unstable: $\Gamma_m < \Gamma_d < \Gamma_e$

6: stable: $\Gamma_e < \Gamma_m < \Gamma_d$

The fact that different layers of the atmosphere may have different lapses rates, with some being more unstable than others, is one reason clouds may exist at one level but not others. Looking at the environmental profile shown in Figure 9.3, the segments, or levels, of the atmosphere where cloud development is likely would be numbers 3 and 5. Level 1 may see cloud development provided there is sufficient surface-based lifting.

9.4 Cloud Formation

This section outlines various cloud formation processes. There are a variety of means by which a cloud is formed. Often more than one is involved to create, grow, and sustain the cloud's existence. The responsible process may depend on the temperature of a cloud region, which generally depends on altitude. Additionally, processes may change over the lifetime of a cloud.

Cloud formation requires dry parcels to become saturated. A parcel can become saturated by cooling its temperature to the dew point value or by increasing the vapor content to increase the parcel's dew point temperature. The former is more likely the means by which clouds are formed. And cooling by lifting the parcel is the most common process for do so.

9.4.1 Destabilizing Processes

As mentioned in the previous section, cooling a parcel by lifting is a predominant means of cloud development. This process is made made easier if the atmosphere is not strongly stable. Therefore, the first step is to explore how the atmosphere becomes more conducive to cloud grow by decreasing, or destabilizing, the environment.

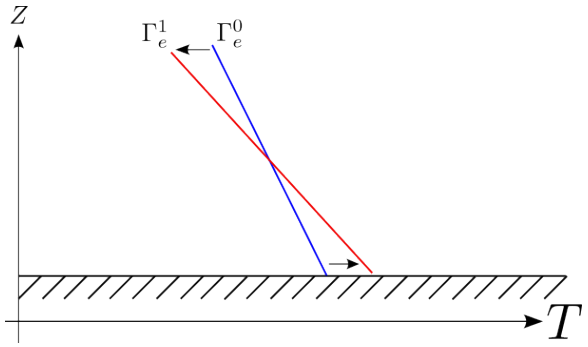

Figure 9.4: Destabilizing the environment by tilting the temperature profile.

The environmental lapse rate is a variable that depends on time and elevation. The greater the rate, the more likely the environment becomes conditionally stable and more conducive to rising motion and cooling parcels. Referring to Figure 9.4, suppose the initial rate is Γ_e^0, represented by the blue profile in the figure. The red profile of represents an environmental profile with a greater lapse rate of Γ_e^1. The arrows indicate that the new profile is created by warming (pushing the profile) to the right at the surface (or a lower level), and pushing the profile to the left (cooling) at an upper elevation.

Warming at the surface occurs by warm advection. This is especially pronounced with strong warm fronts. The opposite is true with the cold advection associated with the passage of a cold front. In this case, the atmosphere typically becomes more stable once the cold front has moved through.

Another way the surface warms is in the 24-hour cycle of solar radiation, especially at the mid- to low-latitudes. On clear days, as the sun warms the surface, the heat is transferred to the adjacent surface parcels, pushing the profile to the right at the surface, and creating a greater value for Γ_e. The reverse is true after sunset, when the earth begins to cool and the lower end of the profile moves back to the left (declining T). Increased cloud cover in the warm seasons act to reduce surface solar heating, thereby stabilizing the lower atmosphere.

Cold advection aloft is a common way in which the local environment may become less stable. Short waves in the upper atmosphere are typically a pool of cooler air. As the short wave moves with the larger scale flow, the advected cold pool will tilt the environmental lapse to the left (decreasing T) and increasing Γ_e. The opposite is true with upper air warm advection. In this event, the profile become less steep, and the environment becomes more stable.

9.4.2 Convergence

Figure 9.5 depicts the case of parcel lift due to convergence. The focus of convergence is a surface low pressure trough associated with a stationary front or the center of a surface cyclone. The vertical component of the velocity vector is not strong, so the clouds are rather shallow (the horizontal length is greater than the vertical depth) and precipitation is not likely to fall from the clouds.

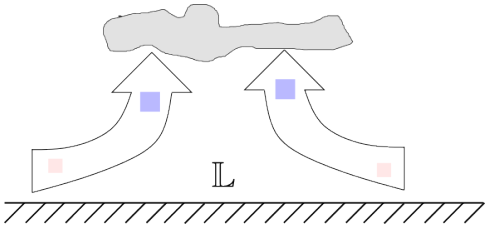

Figure 9.5: Cloud formation due to a low pressure convergence zone.

9.4.3 Frontal Lifting

The movement of fronts, either warm or cold, cause near-surface parcel to rise in the atmosphere. Sufficient gain in altitude results in sufficient cooling to dew point temperature. Figure 9.6 shows atmospheric cross-sections of an warm and cold front.

The gradual rise of parcels ahead of the slower moving warm front results in widespread, stratus cloud formation, both at the cirrus and alto levels ahead of the advancing warm front. Closer to the surface front, the clouds tend to be thicker and lower, especially as precipitation processes develop precipitable hydrometeors. Cumulus clouds can develop with the passing of a warm front in the warmer seasons because the atmosphere is less stable with warmer, more moist surface-based parcels, as it will be shown in Section 9.4.4.

The faster moving cold front, with a more vertical upper atmospheric frontal boundary, tends to push surface-based parcel more quickly into the upper atmosphere. In the warmer seasons when surface parcel mixing ratios are higher, cumulus clouds with extensive vertical development form slightly ahead of and near the front. Trailing clouds behind the front tend to be more stratus in nature. In the cooler seasons, the cumulus cloud formation is less likely because of a more stable environment with colder and drier surface parcels.

9.4.4 Convection

Convection occurs when parcels, more buoyant than their surrounding environment, rise and cool to their dew point temperature. Convection occurs more frequently in the warmer months when solar radiation greatly warms the surface of the earth causing a destabilization of the near-surface environment.

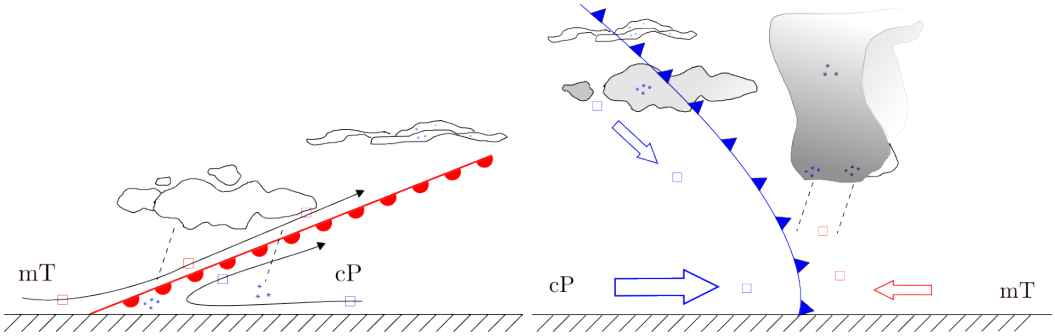

(a) Warm front lift and stratus clouds. (b) Cold front lift and cumulus clouds.

Figure 9.6: Cloud creation by frontal lifting.

As shown later in the text, strong and free convection may need a mechanical boost, such as the passing of a cold front, to initiate a broad area of convection that may, in some instances, develop into severe thunderstorms that are the result of the strong and deep convection.

Organized, circular regions of convection may form what is known as a mesocyclone, often a parent of destructive tornadoes as described in Chapter 11.

9.4.5 Isentropic Lift

An **isentropic surface** is a three-dimensional surface on which the potential temperature is constant. In an isentropic atmosphere, air parcel movement is on constant isentropic surfaces. In some instances, as shown in Figure 9.7, as a parcel moves along its constant isentropic path, that path will cross constant pressure surfaces. The figure shows a typical vertical structure in the south-to-north atmospheric cross section.

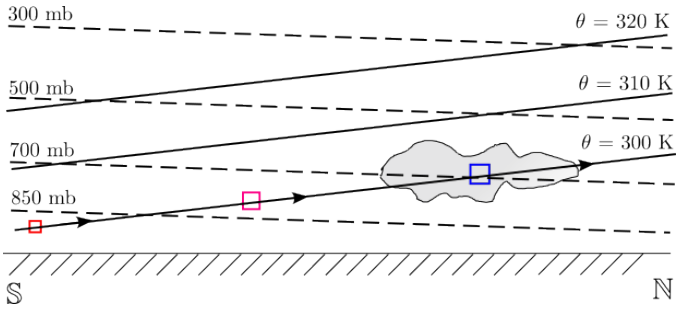

Figure 9.7: Cloud formation by isentropic lifting.

Constant pressure surfaces, depicted as dashed lines, slant downward from the equator

to the pole. The warm equatorial air "pushes" a given surface up (because of the increased overall depth of the warm air column) and the cold polar air causes the pressure surface to fall (because the cold air contracts the column's height). Constant θ surfaces, shown as solid lines, slant upward along south-to-north lines because of this temperature gradient as well.

Referring to Equation 9.2, as the parcel temperature T decreases (denoted by the $\downarrow$ symbol) on its north-bound path, the parcel must rise to a lower pressure P level to maintain a constant potential temperature, denoted by $\overleftrightarrow{\theta}$. (A decrease in P will increase the quotient $\frac{1000}{P}$ in Equation 9.2.) Thermodynamically, the decrease in parcel pressure leads to volume expansion and cooling. Sufficient cooling results in condensation and stratus-type cloud formation, as depicted in Figure 9.7.

$$\overleftrightarrow{\theta} = T(\downarrow)\left(\frac{1000}{P(\downarrow)}\right)^{0.2859} \tag{9.2}$$

9.4.6 Orographic Lift

Surface parcels are forced upward as the approach and cross over mountains with sufficient elevation, as shown in Figure 9.8. The parcels cool as they ascend the windward side of the mountain. Clouds may form at or near the top of the mountain if sufficient cooling results. On the lee, or downwind, side of the mountain, the parcels sink and warm to temperatures that are greater than the parcel's dew point temperature. This cloud formation is sometimes referred to mountain **cap clouds**.

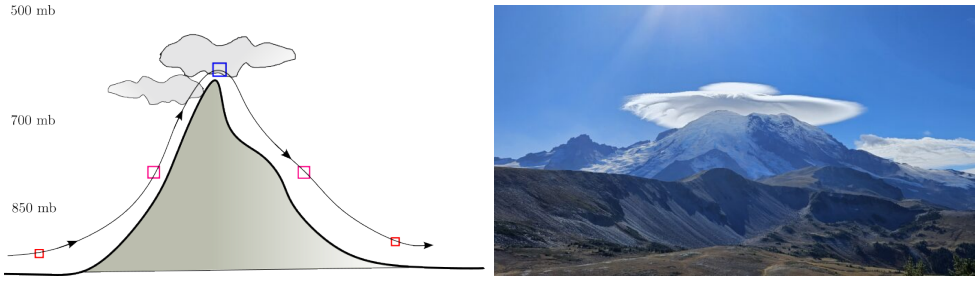

Figure 9.8: Cloud formation by orographic lifting.

9.4.7 Radiative Cooling

As explained in Chapter 2, all objects radiate energy when their temperature is above absolute zero. This includes an atmospheric parcel made up of gaseous molecules including water vapor. When the loss of energy by radiation exceeds energy gain by radiation or other

means, the temperature of the parcel will drop. This happens at high altitudes, where cirrus clouds form.

In Chapter 5, the role of radiative cooling in forming the Hadley cell of the three-cell general circulation model was described. This cooling results in the high altitude parcels sinking instead of continuing to migrate to the north. The radiative cooling in this instance can also enhance cloud formation in the Hadley cell the exists north of the equator in the northern hemisphere.

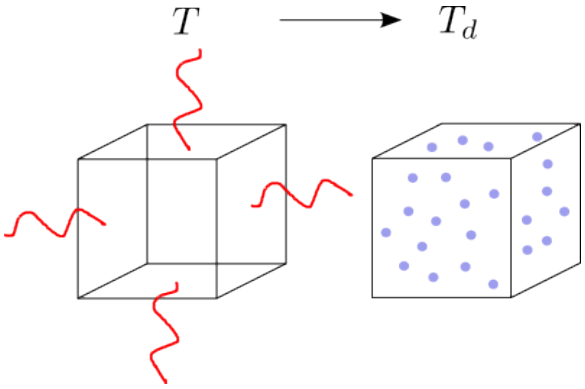

Figure 9.9: Radiational cooling of an atmospheric parcel to its dew point temperature.

However, radiational cooling is more commonly associated with fog formation, which is discussed in Section 9.5.

9.5 Fog Types

As mentioned, above, fog is actually a cloud that forms at the surface of the Earth. The mechanisms that create fog are similar to those that result in cloud formation.

An example of **advection fog** is shown in Figure 9.10. The fog that frequently forms over the bay of San Francisco results from the advection of the warmer, moisture laden air parcels that are advected over the cooler bay waters. Sufficient cooling reduces the advected parcel's temperature to their dew point temperature and fog forms.

In a similar way, fog will form near water-land boundaries such as along the shores of Lake Superior and Lake Michigan as the warmer air over the water is advected on-shore over the cooler land surfaces.

Advection fog sometimes occurs when a warm front passes over snow-covered surfaces. The warmer parcel behind the advancing front have vapor pressure near saturation. The cooling of the near-surface parcels will decrease the parcel temperature to dew point, and the saturated parcels will form fog. Additionally, the warm parcel may cause surface snow

Figure 9.10: Advection fog over the San Francisco Bay.

to melt, resulting in additional vapor pressure requiring less temperature decrease of the parcel to reach it's dew point.

Figure 9.11 shows **radiation fog** sitting in the Upper Iowa River valley upstream from Decorah, Iowa. As the sun sets for a clear and calm evening, the Earth's surface experiences a net loss of radiant energy. The lack of surface winds allow the parcels near the surface cool as well, including those with abundant water vapor resting over the river water. Eventually, the over-water parcels cool to their dew point temperature, forming condensation and fog. The Figure 9.11 photo was taken from an airplane just after sunrise before solar radiation warms the parcels sufficiently to evaporate the condensed parcel moisture.

Steam fog in shown in Figure 9.12 that formed on a very chilly early morning over the Upper Iowa River near the West Decorah Bridge. This fog is one of the few examples when condensation occurs by adding moisture to a parcel and not by cooling the parcel to its dew point temperature. On these very cold mornings, the temperature of the water is greater than that of the air pair parcel resting near the water on the calm morning.

The vapor escaping the water surface enters the relatively cold parcel and raises the parcel's vapor pressure e to the level of the parcel saturation vapor pressure e_s, and condensation occurs. Not only does condensation occur, but the release of latent heat will warm the parcel, and its higher temperature makes the parcel more buoyant than those above it, so the water-level parcel will rise creating the effect of steam.

Figure 9.11: Radiation fog in the Upper Iowa River valley.

Figure 9.12: Steam fog rising from the waters of the Upper Iowa River.

9.6 Skew T-log P Chart

Figure 9.13 show the **Skew T - log P** thermodynamic chart with labels for each of the contour, or lines, on the chart.

The chart contours are:

- **Temperature**, in degrees Celsius, are sold red lines that slant to the right (run askew).

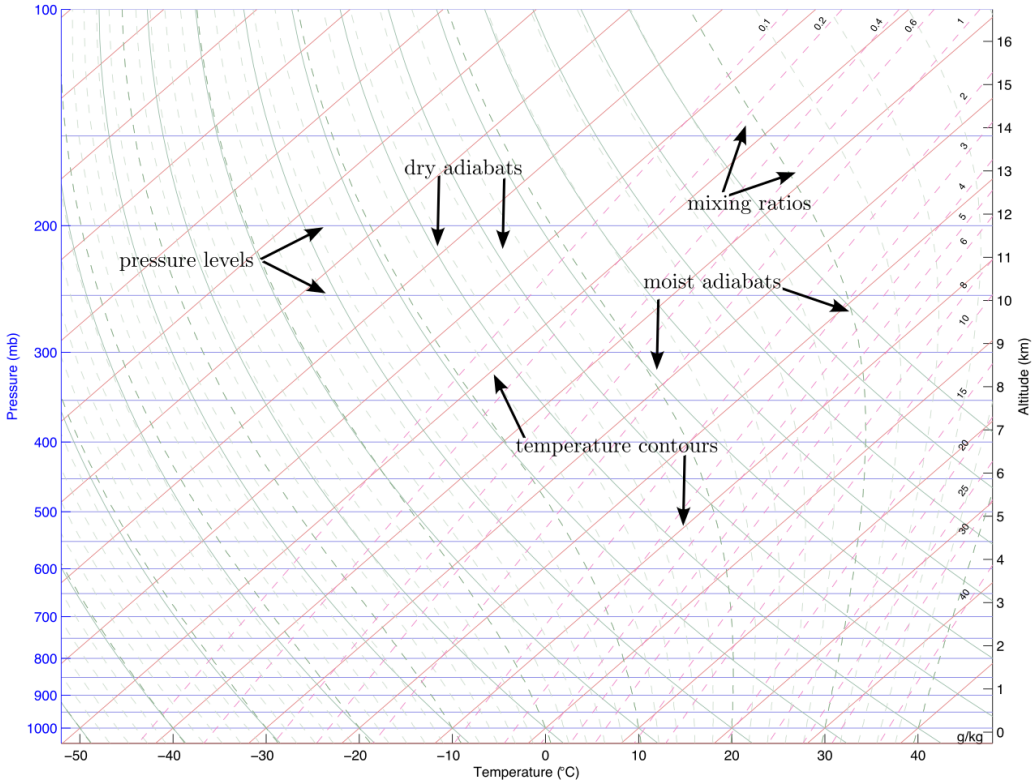

Figure 9.13: Skew T-log P chart with identified contours.

- **Pressure** are the solid blue lines that run horizontally across the chart. They have units of kilo-pascals, or mb. The pressure value increases by 100 mb between consecutive lines, but the spacing is not uniform as a function of altitude, given in km on the right-hand-side of the chart. Pressure decreases exponentially with height, so the spacing of the pressure lines is determined by the logarithm of the pressure. The further up in the atmosphere, the slower the decline in pressure, so a greater increase in altitude is required from the same change in pressure. That is why the chart is referred to as "log P."

- **Dry Adiabats** are the solid green lines. As a parcel moves up in the atmosphere without moisture condensation, it will follow a dry adiabat as a way to determine its temperature as it rises.

- **Moist Adiabats** are the dashed green lines. If a saturated (meaning "moist") parcel is lifted higher in the atmosphere, moisture will condense releasing latent heat, so the rate of temperature decrease is less than the case of parcel lifting without condensation

and latent heat release.

- **Mixing Ratio** are the dashed red lines and can be used to determine the mixing ratio and the saturation mixing ratio of a parcel.

Determining variables from the chart:

- **Lifting a parcel from the surface**. Suppose the parcel pressure (P), temperature (T), and dew point(T_d) are given quantities, with $P = 1000$ mb. The mixing ratio is the W contour through T_d. The saturation mixing ratio W_s in the W contour through T.

  Tracking these variables as the parcel is lifted: If $T_d < T$, T follows the dry adiabat. T_d follows the mixing ratio line until $T = T_d$. At this time, the parcel is "moist," so $T = T_d$ for the rest of the parcel ascension, and both follow the moist adiabat. The mixing ratio decreases because vapor moisture mass is deceasing in the parcel. Therefore the mixing ratio is that W contour through the temperature contour of the parcel.

- The **Mixing ratio** W for a parcel is the mixing ratio contour through the dew point temperature at the pressure level of interest.

- The **Saturation mixing ratio** W_s of a parcel is the mixing ratio contour through the parcel's temperature at the pressure level of interest.

- The **Potential Temperature** θ: If P = 1000 mb, $\theta = T$. If $P < 1000$ mb, follow the dry adiabat through T to the 1000 mb level. The temperature on the dry adiabat is θ.

- The **Equivalent Potential Temperature** θ_e is the temperature a parcel would have if it were moved (after lifting to a sufficient elevation) to the 1000 mb level and all of its vapor mass were to condense and warm the dry constituents of the parcel. The θ_e value of a parcel is determined from the skew-T chart in the following way: Identify the parcel's temperature and dew point at a given pressure level. Lift the parcel along the dry adiabat until it reaches saturation. After saturation, continue to lift the parcel along the moist adiabat until the moist and dry adiabats run parallel. The dry and moist adiabats run parallel when the parcel's vapor has been completely removed by condensation or deposition Now, follow the dry adiabat to determine the parcel temperature at 1000 mb. This is θ_e for the parcel.

- **Wet-bulb Temperature** θ_W The wet-bulb temperature of a parcel is the temperature that results after complete evaporational cooling at constant pressure. It is found on the chart by lifting the parcel along a dry adiabat until saturation. Next, the parcel is returned along the moist adiabat to its original pressure level.

- **Wet-bulb Potential Temperature** is found the same way as the wet-bulb temperature except the parcel is moved along the moist adiabat down to the 1000-mb level. Wet-bulb potential temperature standardizes wet-bulb temperature thus allowing for direct comparison of wet bulb temperature at different pressure levels.

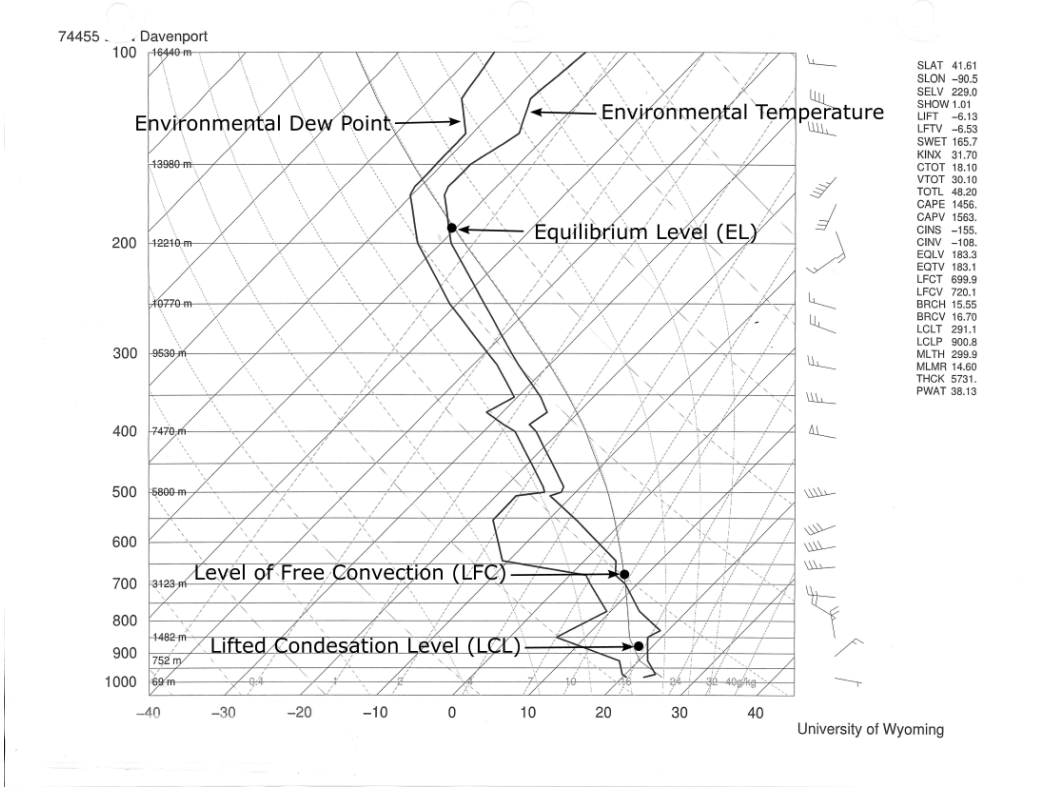

Figure 9.14: Skew T-log P chart with identified contours.

Figure 9.14 shows a data plot of the environmental temperature and dew point readings as a function of pressure (or elevation). Temperature is the darker curve to the right. The dew point profile is the sold curve on the left. The environmental dew point temperature is always less than or equal to the environmental temperature. The thinner curve represents the temperature a parcel will have as it rises through the atmosphere from the surface of the Earth.

There are three important points shown on the figure. The first is the **lifted condensation level** (LCL). This is the elevation at which the lifted parcel's temperature has cooled to its dew point temperature. Consequently, condensation occurs and the cloud base is

formed.

As the parcel continues to rise (not on its own accord), it reaches the **level of free convection** (LFC). At this level, the parcel's temperature meets, and then exceeds, the environmental temperature. Therefore, it is able to rise on its own accord because it is now less dense the its neighboring environmental parcels. The resulting positive buoyancy propels the parcel upward until it reaches the **equilibrium level**. Here,the cloud's vertical growth ends, so this level marks the top of the cloud.

Exercise 9.5 requires plotting similar environmental data and identifying these three important levels.

Exercises

9.1 Use the skew-T chart to determine the potential temperature θ, to the nearest degree C, of a parcel

(a) at 400 mb and T = -40 °C. θ = _____°C

(b) at 700 mb and T = 5 °C. θ = _____°C

(c) at 500 mb and T = -20 °C. θ = _____°C

9.2 Use a skew-T chart to determine the equivalent potential temperature θ_e, to the nearest degree K, for each of the following:

(a) A parcel with P = 1000 mb, T = 10°C, and T_d = 5°C θ_e = _____°C

(b) A parcel with P = 1000 mb, T = 20°C, and T_d = 10°C θ_e = _____°C

(c) A parcel with P = 1000 mb, T = 15°C, and T_d = 15°C θ_e = _____°C

9.3 Suppose a parcel at the surface (P = 1000 mb) has a temperature of 25 °C and a dew point temperature of 0 °C. Determine its dew point temperature and mixing ratio if it is lifted to the

(a) 800 mb level T_d = _____°C W = _____ g/kg

(b) 500 mb level T_d = _____°C W = _____ g/kg

9.4 Suppose a parcel at the surface (P = 1000 mb) has a temperature of 30 °C and a dew point temperature of 5 °C. Determine its dew point temperature and mixing ratio if it is lifted to the

(a) 800 mb level T_d = _____°C W = _____ g/kg

(b) 500 mb level T_d = _____°C W = _____ g/kg

9.5 Plot the temperature and dew point on the chart using the sounding data in Figure 9.15. The following pressure levels must be plotted: 980, 906.6, 850, 700, 608.8, 500, 400, 300, 250, 200, 150 mb. You may plot temperatures at other levels if you want, but you can answer the following questions without doing so. **Answer the following questions based on a surface (1000 mb) temperature of 30 °C and a dew point of 22 °C.**

9.6 Use your plot from Exercise 9.5 to determine the following:

(a) Determine the lifted condensation level (LCL) LCL = _____ mb

(b) Determine the level of free convection (LFC) LFC = _____ mb

(c) Determine the equilibrium level (EL) EL = _____ mb

9.7 The concept of lapse rate plays a crucial role in determining the stability of the atmosphere which in turn determines the likelihood of cloud formation.

(a) Define the lapse rate of the environment and the lapse rate(s) of a rising parcel.

(b) Identify the various types of atmospheric stability and how they are determined based on the environmental and rising parcel lapse rate.

9.8 Identify and explain at least two ways the atmosphere, or particular layers of the atmosphere, may become conducive to cloud formation.

9.9 Explain why a rising atmospheric parcel experiences a temperature drop using the definition of potential temperature. What assumption is made about the lifting process that allows a condition to be placed on the parcel's potential temperature?

9.10 Explain why the moist adiabatic lapse rate is always less than the dry adiabatic lapse rate.

9.11 Explain the process of steam fog formation. Why is it considered to be a relatively rare way for fog or clouds to form?

9.12 Explain how cap clouds form.

9.13 Explain how advection fog may form. Where or when is advection fog more likely to form?

soundingData.txt

PRES hPa	HGHT m	TEMP C	DWPT C	RELH %	MIXR g/kg	DRCT deg	SKNT knot	THTA K	THTE K	THTV K
1000.0	54									
980.0	229	24.4	21.7	85	16.99	210	4	299.3	349.1	302.3
971.6	305	24.6	21.1	81	16.46	215	8	300.2	348.7	303.2
958.0	429	25.0	20.0	74	15.62	221	13	301.8	348.1	304.6
938.5	610	24.1	19.3	74	15.24	230	21	302.7	348.1	305.5
931.0	681	23.8	19.0	75	15.09	233	20	303.1	348.0	305.8
925.0	738	24.2	15.2	57	11.88	235	19	304.1	339.7	306.2
919.0	795	24.6	11.6	44	9.42	237	19	305.0	333.6	306.8
906.6	914	23.7	10.4	43	8.81	240	19	305.3	332.1	306.9
882.0	1154	22.0	8.0	41	7.68	244	19	305.9	329.5	307.4
875.4	1219	22.8	4.8	31	6.18	245	19	307.4	326.6	308.6
869.0	1283	23.6	1.6	24	4.97	246	20	308.9	324.6	309.8
850.0	1475	22.4	-2.6	19	3.73	250	23	309.6	321.6	310.3
815.9	1829	20.7	-6.6	15	2.87	250	29	311.4	320.9	312.0
806.0	1934	20.2	-7.8	14	2.65	250	28	312.0	320.8	312.5
787.2	2134	18.6	-7.7	16	2.73	250	25	312.4	321.5	312.9
759.4	2438	16.2	-7.5	19	2.87	255	19	313.1	322.5	313.6
732.6	2743	13.8	-7.4	22	3.01	275	16	313.7	323.6	314.2
700.0	3128	10.8	-7.2	28	3.20	285	17	314.4	325.0	315.0
681.0	3353	8.7	-8.0	30	3.10	290	17	314.6	324.8	315.1
656.0	3658	5.8	-9.0	34	2.97	275	19	314.7	324.6	315.3
632.0	3962	3.0	-10.0	38	2.84	270	21	314.8	324.3	315.4
608.8	4267	0.1	-11.0	43	2.72	270	23	314.9	324.0	315.4
607.0	4291	-0.1	-11.1	43	2.71	270	24	314.9	323.9	315.4
563.6	4877	-4.9	-9.4	71	3.33	270	35	316.0	327.0	316.6
540.0	5215	-7.7	-8.5	94	3.75	275	44	316.6	328.9	317.3
521.4	5486	-9.1	-10.1	93	3.44	280	51	318.1	329.5	318.8
500.0	5810	-10.7	-11.9	91	3.09	285	51	319.9	330.3	320.5
481.4	6096	-12.6	-14.1	89	2.70	285	49	321.1	330.3	321.6
426.3	7010	-18.6	-20.9	82	1.71	280	49	324.8	330.9	325.1
400.0	7490	-21.7	-24.5	78	1.32	295	39	326.7	331.5	327.0
392.9	7620	-22.6	-25.4	78	1.24	295	37	327.2	331.7	327.4
376.7	7925	-24.8	-27.5	79	1.07	300	31	328.2	332.2	328.4
339.0	8691	-30.3	-32.7	79	0.73	288	25	330.8	333.6	330.9
317.8	9144	-34.0	-36.7	76	0.52	280	21	331.8	333.9	331.9
300.0	9550	-37.3	-40.3	73	0.38	280	19	332.7	334.2	332.8
254.2	10668	-46.9	-50.8	65	0.14	265	21	334.6	335.2	334.6
250.0	10780	-47.9	-51.8	64	0.13	265	21	334.7	335.3	334.8
242.6	10973	-49.5	-53.3	64	0.11	260	19	335.3	335.7	335.3
210.3	11887	-56.9	-60.5	64	0.05	230	29	337.6	337.9	337.6
200.0	12210	-59.5	-63.0	64	0.04	230	27	338.4	338.6	338.4
184.0	12730	-63.3	-67.1	60	0.02	230	25	340.4	340.5	340.4
181.9	12802	-63.7	-67.5	59	0.02	230	25	340.9	341.0	340.9
177.0	12970	-64.5	-68.5	58	0.02	240	31	342.2	342.3	342.2
157.0	13716	-60.7	-69.5	31	0.02	270	37	360.6	360.7	360.6
152.0	13917	-59.7	-69.7	26	0.02	274	36	365.6	365.8	365.6
150.0	14000	-60.3	-71.3	22	0.02	275	35	366.0	366.1	366.0
135.4	14630	-63.3	-74.9	20	0.01	280	23	371.5	371.6	371.5
124.0	15169	-65.9	-77.9	17	0.01	245	22	376.3	376.3	376.3
122.5	15240	-65.7	-77.9	17	0.01	240	21	377.9	378.0	377.9
116.6	15545	-64.8	-78.1	15	0.01	235	23	385.0	385.0	385.0
107.0	16067	-63.3	-78.3	11	0.01	226	18	397.4	397.4	397.4
100.3	16459	-65.4	-81.3	9	0.01	220	14	400.7	400.8	400.7
100.0	16480	-65.5	-81.5	9	0.01	220	14	400.9	400.9	400.9

Figure 9.15: Sounding data.

Chapter 10

Precipitation Processes

10.1 Overview

Precipitation occurs frequently in many parts of the world. The Midwestern portion of the United States records measurable precipitation, in the form of liquid or frozen hydrometeors, about 120 days a year. Although a nuisance to some people, it is essential to agricultural production.

As common and essential as precipitation is, the processes that form precipitation are not completely understood. However, there are at least two distinct steps involved in making a sufficiently humid air parcel reach the point of precipitation. In the case of a warm cloud environment, a small droplet with a radius on the order of one μ m (10^{-6} m) must grow to a raindrop of radius on the order of 1 mm (10^{-3} m). This means the mass of the droplet must increase by a factor of 10^9 (1 billion times!) because volume (mass) is proportional to the third-power of radius.

In basic and general terms, there are two steps that must be accomplished for precipitation to form. Parcels must first be transformed from having insufficient relative humidity (RH) to ones with sufficient RH so a cloud, made up of cloud droplets or ice crystals, may form. The second step involves growing the droplets or ice crystals to a sufficient mass so that they will be able to fall out of the cloud. The precipitable masses are technically known as **hydrometeors**. Processes that accomplish cloud formation are relatively distinct from those processes that create hydrometeors.

Obviously, liquid and frozen cloud constituents form in warm and cold cloud environments, respectively. The processes that create and grow the various liquid and frozen cloud constituents are typically too slow to create hydrometeors. Just as the creation of a liquid or frozen cloud constituent largely depends on the environment where it is created, so do the processes of growth of the constituent to hydrometeors. Therefore, one process is mostly a warm cloud mechanism, the other is a mixed cloud (cold cloud) mechanism.

10.2 Cooling Generalities

Precipitation generally requires atmospheric parcels to have a sufficient moisture content so that cooling of the parcel results in condensation or deposition. Cooling is generally caused by a pressure decrease that causes the parcel to expand, and the expansion leads to a temperature decease within the parcel. The pressure decrease is usually caused by a parcel being lifted higher to lower pressure levels.

The environmental pressure may decrease on the parcel as it travels northward. As parcels move horizontally, they generally follow levels of constant potential temperature θ or equivalent potential temperature θ_e. The constant θ contours can be thought of as constant density contours because if parcel density ρ is constant, then the parcel's temperature T and pressure P are constant, so its potential temperature remains constant.

Constant θ surfaces generally increase in height as they run south-to-north. Consequently, the "lifting" of the parcel is actually a result of the horizontal south-to-north motion with the parcel staying on its initial θ level. As the parcel moves northward, the environmental pressure will decrease, in most instances, because the pressure contours rarely increase in height in he south-to-north direction.

Lifting can be in response to horizontal motion such as when a parcel moves uphill or over a mountain. This lifting may be referred to as "orographic."

In some instances, parcels move almost "straight upwards" when their density decreases because the parcel warms, for instance. The most likely scenario for this occurrence pertains to parcel near the surface of the Earth warming by conductive heat transfer from the Earth's surface. When the parcel's density drops, it will rise to the level in the atmosphere at which the environmental density matches that of the parcel.

10.3 Cloud Constituents

The makeup of a cloud includes a number of constituents with a range of size from 0.1 μm (10^{-6} m) for aerosols on the small end of the spectrum, to 30 mm (10^{-3} m) for large snowflakes on the large end of the spectrum, as shown in Figure 10.1. The roles that constituents play in cloud and precipitation formation vary as well.

Aerosols are small and light enough so that they remain suspended particles within the cloud. Some aerosols provided a location on which cloud droplets or ice crystals begin to grow and are known as **condensation nuclei** or **deposition nuclei**.

Hydrometeors, such as rain drops, snow flakes, graupel, and hail are large (massive) enough to precipitate out of the cloud.

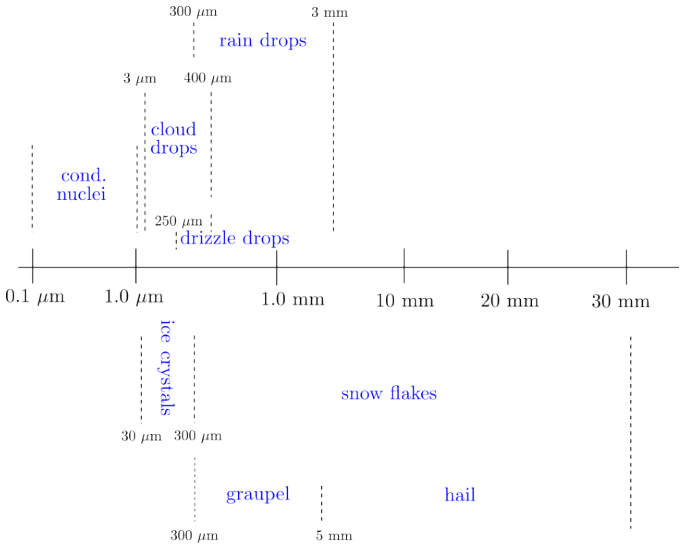

Figure 10.1: The range in hydrometeor radii. Constituent sizes are relatively small, so lengths are typically given in micrometers (μm), with 1 $\mu m = 10^{-6}$ meter and 1000 μm = 1 mm $= 10^{-3}$ meter.

10.4 Warm Clouds

This section focuses processes of cloud formation in a relatively warm environment. First, the theory and physics of cloud droplet creation is explained. Next, factors related to droplet growth are presented.

Warm clouds, or warm cloud regions, are those that are warm enough so that its water content includes visible constituents in liquid form. Surprisingly, the temperature for which this is true does not need to be warmer than 0°C. Figure 10.2 relates the all-water percentage make up of a cloud as a function of the cloud's environmental temperature. At lower pressures at higher altitude, a good percentage of the cloud is liquid water at temperatures below freezing (0°C) Such droplets are referred to as **super-cooled** cloud droplets.

10.4.1 Droplet Formation

Homogeneous Nucleation

Cloud droplets are small liquid water constituents. They are large enough to be seen, so they make all or part of the visible cloud. In theory, when the vapor pressure is at or above the level of saturation, droplets may form by molecules of water vapor randomly colliding and combining their masses to create a very small embryonic water droplet. This process of droplet formation is referred to as **homogeneous nucleation**.

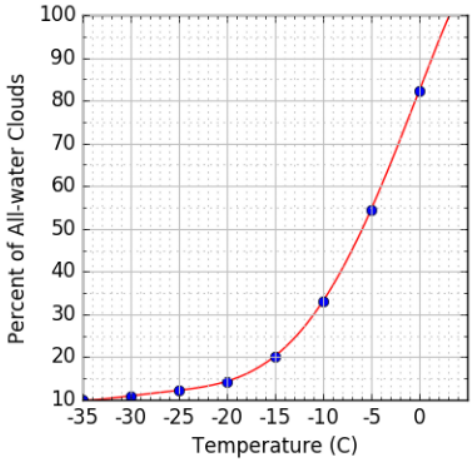

Figure 10.2: Percentage of all-water clouds as a function of ambient temperature.

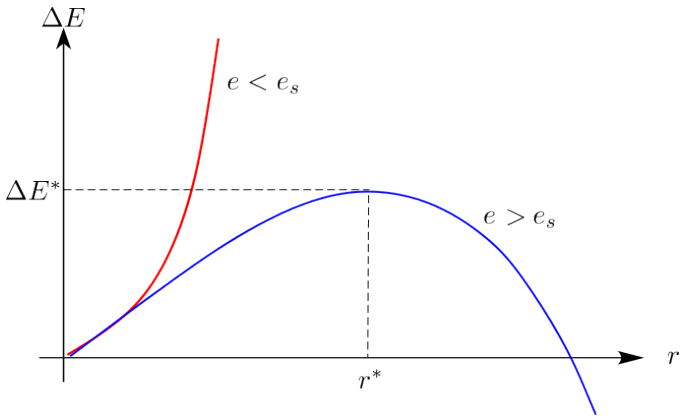

Figure 10.3: The change in energy required for homogeneous nucleation growth as a function of radius r.

Homogeneous nucleation may continue until enough mass is combined so that the liquid constituent is large enough to be seen (3 μm to 300 μm). However, the energy associated with this process is such that it rarely, if every happens. More specifically, homogeneous nucleation requires the small droplet to acquire a higher energy state that makes the process generally unstable. (Many physical systems naturally seek a lower, more stable, energy state.) The smaller the radius of a newly formed drop, the higher the energy state.

Figure 10.3 shows the change in energy ΔE required for a homogeneous nucleated embryo to grow as a function of its radius r. The red curve corresponds to the case where the cloud's vapor pressure e is less than the saturation vapor pressure e_s. There is a steep rise (exponential rise) in energy required for the embryo to grow. Consequently, homogeneous nucleation will require the parcel's vapor pressure to be at least as great as the parcel's saturation vapor pressure.

As Figure 10.3 shows, in a supersaturated cloud environment (the blue curve for $e > e_s$), the droplet requires less energy increase to grow. In fact, if the radius of the droplet reaches a critical value, designated as r^* on the graph, ΔE required for continual growth actually decreases for increasing r.

The value of r^*, derived from the associated energy consideration, is shown in Equation 10.1. This equation is attributed to Lord Kelvin who derived the result.

$$r^* = \frac{2\sigma}{nkT \ln \frac{e}{e_s}} \tag{10.1}$$

The symbol σ represents the work required to create a unit area of vapor-liquid interface, n is the number of water vapor molecules per unit volume, T is the temperature of the cloud environment, and k is the Boltzmann constant.

Consequently, very few droplets forming in this way reach a sufficiently large enough radius (a more stable energy state) to sustain themselves.

Heterogeneous Nucleation

Atmospheric aerosols, such as dust particles or liberated sea salt, provide a surface conducive for vapor condensation when the vapor pressure is at or near saturation. The formation of embryonic cloud droplets in this manner is call **heterogeneous nucleation**. The particles on which the vapor condenses are known as **cloud condensation nuclei** (CCN). This droplet creation process is accepted as the primary way cloud droplets are formed.

One major source of CCN is sulfate aerosol (SO_4^{2-}). These sulfate aerosols form partly from the dimethyl sulfide (DMS) produced by phytoplankton in the open ocean. Large algae blooms in ocean surface waters occur in a wide range of latitudes and contribute considerable DMS into the atmosphere to act as nuclei.

Regardless of homogeneous or heterogeneous nucleation, once a small cloud droplet is created, there are important factors, or effects, that are associated with the continued growth of the droplet. They will be described next.

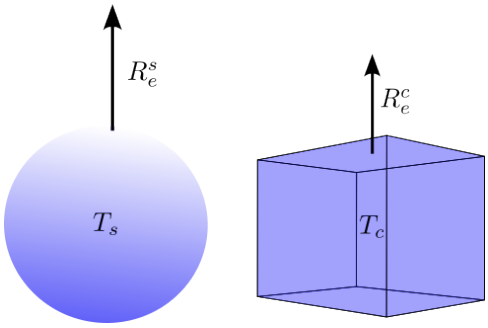

Figure 10.4: The difference in rates of evaporation: curved surface rate = R_e^s and the flat surface rate = R_e^c.

Curvature Effect

Saturation vapor pressure e_s as a function of temperature developed in a previous section is determined for flat water surfaces. Equilibrium vapor pressure over curved liquid surfaces is **greater** than that over a flat surface. Why this is true is explained using Figure 10.4. Pictured are two shapes for a liquid water constituents. The spherical shape represents one with a curved surface. The cubic shape represents one with flat surfaces. T_s and T_c are the liquid water temperature for the sphere and cube, respectively.

If a flat surface and a curved surface are associated with the same volume of water at the same temperature ($T_s = T_c$), the number of water molecules transforming from liquid to vapor phase is the same for both volumes. The lesser surface area of the sphere relative to the flat-surfaced cube results in a greater rate of evaporation R_e^s per unit surface for the sphere. That is $R_e^s > R_e^c$, as shown in Figure 10.4 with R_e^s associated with a vector with longer length.

The greater rate of evaporation R_e^s for the curved spherical surface will require a greater rate of condensation R_c^s for equality of the rates. Consequently, the vapor pressure must increase in order for the condensation rate R_c^s to increase to R_e^s for the curved surface.

The required increase in vapor pressure for the curved surface is quantified by the **Kelvin equation** 10.2

$$\ln\left(\frac{e}{e_0}\right) = \frac{2\gamma V_m}{rRT} \Rightarrow e = e_0 \exp\left(\frac{2\gamma V_m}{rRT}\right) \tag{10.2}$$

wherein e is the equilibrium vapor pressure over the curved surface, e_0 is the saturation vapor pressure over a flat surface, γ is the surface tension, V_m is the molar volume (the volume occupied by one mole of the a substance for a given temperature and pressure), r is the radius of the drop, R is the universal gas constant, and T is the temperature of the drop.

A cloud droplet within the water vapor of the cloud has a convex surface relative to the

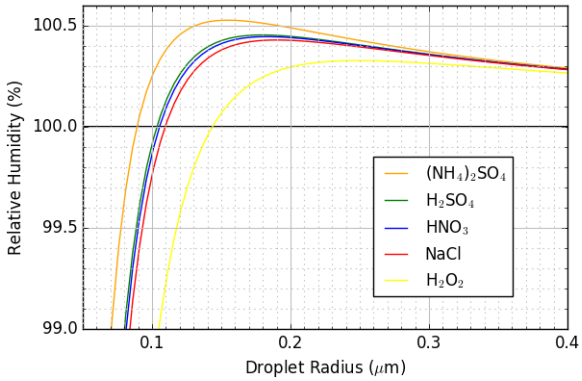

Figure 10.5: Kohler curves- the solute effect for various hygroscopic condensation nuclei.

vapor, so r is positive and the natural log of the vapor pressure ratio is positive implying the required vapor pressure e is greater than e_0. Holding all other quantities fixed, $\ln(e/e_0)$ becomes larger as r becomes smaller. That is, the smaller the drop radius, the greater the vapor pressure must be for $R_c = R_e$. In its exponential form, the relationship shows that the saturation vapor pressure e increases exponentially as the drop radius r goes to zero.

Solute Effect

Certain CCN will dissolve when water vapor condenses on the nuclei. The solution has few water molecules per volume than the pure cloud drop, so the rate of evaporation R_e per unit area is less. Additionally, the surface tension γ of the cloud drop is less in some instances because the pure water has one of the strongest values of surface tension of any molecule. Therefore, the equilibrium vapor pressure e is less than the saturation vapor pressure e_0 determined for a flat surface.

Hygroscopic CCN are those that attract water so that condensation may begin at relative humidities as low as 70%. Table salt (NaCl) is an example of a hygroscopic CCN. This is the reason salt grains will create a "pool" of condensation around them when sitting on a surface on a humid day.

Figure 10.5 shows how the solute effect for various hygroscopic condensation nuclei reduces the required relative humidity for droplet growth as a function of the droplet radius.

The solute effect is so strong for some CCN that it over powers the negative curvature effect. However, as additional water vapor condenses of the droplet, the solute concentration will decrease (the solute concentration is the ratio of the mass of the solute - that portion of the CCN that dissolves - divided by the volume or the water in the droplet) resulting in a decrease of the solute effect. Eventually the magnitude of the curvature effect will rival that of the decreasing solute effect and the droplet will require a supersaturated environment for

it to continue to grow.

The Kohler equation quantifies the competing curvature and solute effects.

10.4.2 Collision-Coalescence

The **collision-coalescence process** is thought to be the dominant precipitation making process within a warm cloud or warm region of a cloud. The collision-coalescence process is an efficient rain maker, and the greater the warm depth of the cloud, the greater the potential for substantial rainfall totals. Forecasting the amount of precipitation that will fall from clouds in a thunderstorm event often includes considering the depth of the warm sector of a cloud.

Cloud droplet formation results in a range of cloud droplet sizes as well as liquid constituents with radii large enough to be considered as a rain drop. The radius of a given constituent may be any value within the spectrum range. The larger the constituent, the greater the mass because the density of liquid water is constant, unlike an air parcel.

Cloud constituents with greater mass will have a greater force of gravity acting on them; great enough to overcome the lift the constituent experiences due to the updraft within the cloud. Consequently, the constituent will fall with a speed depending on its mass, or size. Table 10.1 lists the average fall speed of cloud constituents as a function of the radius.

Type	Radius (cm)	Fall Speed (cm/sec)
Small cloud droplets	0.0005	0.2778
Typical cloud droplets	0.001	1.1111
Large cloud droplets	0.0025	8.3333
Drizzle drops	0.025	194.44
Typical rain drops	0.1	638.89
Large rain drops	0.25	916.67

Table 10.1: Fall speed data from the Smithsonian Meteorological Tables.

The wide and continuous spectrum of constituent sizes results in a similarity wide and continuous spectrum of fall speeds. The different fall speeds result in constituents having relative motions. That is, larger constituents at higher elevations with catch up with smaller constituents at lower elevations. The resulting collision may cause the two masses to coalesce, creating single drop with a mass equal to the sum of the masses of the colliding spheres. The result is depicted in Figure 10.6a.

However, the surface tension of the spherical water droplets want to preserve the spheres, so they may not coalesce after they collide, as depicted in Figure 10.6b. Which of these two outcomes likely depends on how close the paths of the two colliding drops are. In the case

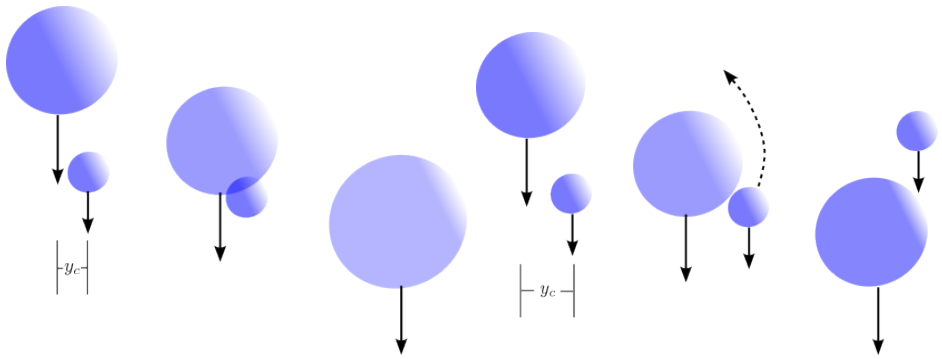

(a) Collision with coalescence (b) Collision without coalescence

Figure 10.6: Two types of relative vorticity.

of coalescence, the smaller drop may be closer to the downward path of the larger drop. The relative speed of the two drops may be a factor in the result.

Whatever factors may play a role in the outcome of the collision, the process has an efficiency, or probability, of coalescence ranging between 0.0 (no chance) and 1.0 (certainty) of coalescence after collision. The collision efficiency, E, for a pair of droplets with the collector radius r_1, and the collectee with radius r_2 is defined as [1]

$$E = 1 - \frac{\pi y_c^2}{\pi(r_1 + r_2)^2} = 1 - \frac{y_c}{r_1 + r_2} \tag{10.3}$$

where y_c is called the initial offset distance, the horizontal distance between the vertical lines running through the center of the drops.

If $y_c = 0$ (head-on collision), then the efficiency $E = 1$, so coalescence is guaranteed. If $y_c \geq (r_1 + r_2)$, the quotient $y_c/(r_1 + r_2) \geq 1$, so $E \leq 0$, and coalescence will not occur. Research indicates that coalescence generally occurs for $y_c/(r_1 + r_2) \leq 0.16$ to 0.20. Charge separation on and among droplets will increase the value of $y_c/(r_1 + r_2)$ (decrease the value of E) at which coalescence will occur.

10.5 Mixed Clouds

Warm clouds are more likely to exist in warmer regions of the planet such as near the tropics. At higher latitudes, clouds with great vertical extent may have warm lower elevation portions during warmer seasons. Otherwise, it is likely that clouds, or portions of clouds, are at temperatures and pressure levels where water exists in all three phases. Clouds of this type are known as **mixed clouds**.

[1] P. K. Wang, page 253

The temperature range for these mixed clouds, or regions within a mixed cloud, is -40°C to 0°C, so the liquid and vapor phases of H_2O are below freezing or **supercooled**. So the question arises "how can liquid cloud droplets exist at temperatures well below freezing?" The answer to this question hinges on the two ways it is believed frozen cloud constituents (ice crystals, primarily) are formed. One is by **homogeneous nucleation** - that is, pure water molecules coming together to form an ice crystal. The process is thought to begin by a number of cold water vapor molecules coming together to form and an **ice embryo**. The embryo has a difficult time surviving at warmer temperatures, of course. At temperatures below freezing, survival chances are diminished by the agitation it encounters inherent in the motion within the cloud. Agitation is less in colder regimes, so the ice embryo has a greater chance of surviving at much colder temperatures. Larger embryos are less susceptible to the agitation aspects as well. It has been determined that homogeneous nucleation is not very likely except in temperature regimes that approach -40°C and almost exclusively for very large crystals.

10.5.1 Deposition Nuclei

If homogeneous nucleation is an unlikely means of forming ice crystals, then mechanisms for ice crystal development likely involve something working in conjunction with water molecules. These processes are known as **heterogeneous nucleation**. Crystal growth more easily occurs when ice-like nuclei (or ice nuclei) are included in the cloud environment. Ice nuclei are physical cloud constituents other than H_2O molecules that have a structure similar to the of an ice crystal. They provide either a surface on which H_2O vapor deposits or serve as a catalyst - an instigator - for the deposition process.

Examples of atmospheric constituents with ice-like structure include clay mineral particles (kaolinite), decayed plant leaves, and plankton-rich sea water. The atmospheric concentration of such constituents is greater in the colder regions of the cloud. Additionally, the concentration of the various ice nuclei is much less than that of condensation nuclei - which is an important aspect of the predominance of ice crystal growth over water droplet growth as we shall see later.

Ice nuclei instigate crystal formation in a several ways. One is by deposition, the accumulation of water mass on the nucleus by vapor changing directly to its frozen phase. Alternatively, ice nuclei may become immersed in a supercooled droplet causing it to freeze. In this instance it acts more like a catalyst than a surface on which the ice crystal formation begins. Recent studies show that ice crystal formation is the result of the foreign constituent simply contacting a supercooled droplet without becoming immersed. Another possible means of crystal formation may entail a two-step process where condensation initially occurs on the nuclei and then the accumulated liquid water mass freezes.

10.5.2 Bergeron Process

The theory of the **Bergeron process** is associated with mixed clouds - those that have resident H_2O in all three phases. Consequently, it is sometimes referred to as the **three-phase process**.

The mixed cloud has liquid water droplets and ice crystals. Cloud air temperatures less than 0°C results in the cloud droplets being **supercooled**. The ice crystal are fewer in number per volume because the deposition nuclei are less abundant. It is estimated that the supercooled water droplets outnumber the ice crystals by a factor as high as one hundred thousand to 1 million.

The saturation vapor pressure over water, e_s^{water}, is greater than the saturation vapor pressure, e_s^{ice}, over a flatter ice surface. Figure 10.7 shows the magnitude of this difference as a function of temperature. The difference is near zero when the cloud environmental temperature is near 0°C. For temperatures less than 0°C, the difference in saturation vapor pressure grows until the temperature reaches -11°C. Thereafter, the difference declines and goes to zero as the cloud temperature continues to decrease.

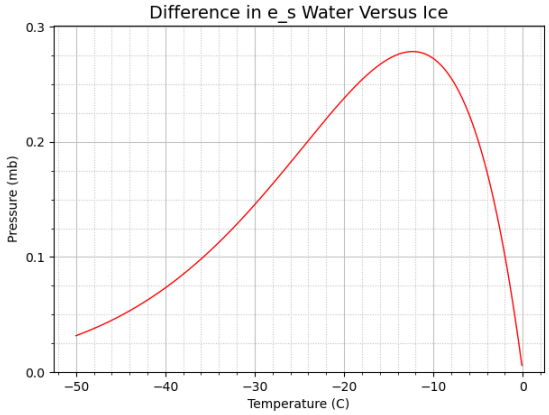

Figure 10.7: Saturation vapor pressure difference over water versus over ice..

Frequently, the environmental vapor pressure of the cloud e^{cloud} has a value such that $e_s^{water} > e^{cloud} > e_s^{ice}$. If so, the cloud environment is subsaturated relative to the water droplet, and supersaturated relative the the ice crystal. Consequently, there is a net loss of H_2O mass on the droplets by evaporation, and a net gain of H_2O mass for the ice crystals by the process of deposition. The fewer number of ice crystals than cloud droplets means the ice crystal gain more mass per crystal than the mass loss per droplets.

This migration of H_2O mass is depicted in Figure 10.8. The nature of this process, the migration of H_2O from the droplets to the ice crystals is often referred to as the **diffusion** step in frozen hydrometeor development.

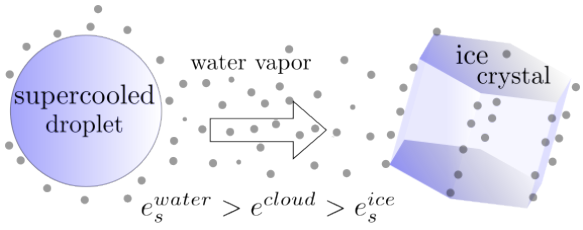

Figure 10.8: Saturation vapor pressure difference over water versus over ice.

The six-sided shape of the frozen particle results because it matches the crystalline shape of solid H_2O. The resultant particle has a range of related but different shapes. Their commonality is that they are all six-sided prisms, like the target crystal shown in Figure 10.8.

Other possible shapes that depend on the ambient cloud temperature are shown in Figure 10.9. This figure is based on the work of of Caltech professor of physics Kenneth Libbrecht.

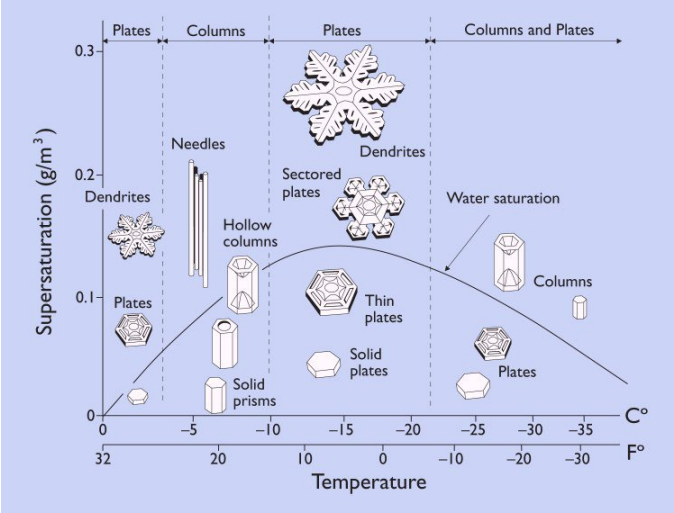

Figure 10.9: Crystal growth shapes a function of temperature. (Credit: Caltech/Libbrecht)

The diffusion of water vapor from liquid droplets, or the general cloud environment, to ice crystal will continue with the six corners being the preferred sites of deposition. Eventually, enough H_2O deposits on the corners to form six arms or branches. Depending on the cloud environment, facets can for on the tips of the newly form branches. Each of the facets can develop branches and so on until a snow flake is like the one pictured in

Figure 10.10: Snowflake.

Figure 10.10. The process is random enough that no two snowflakes have the same shape even though each of the branches of the flake are identical because they all form in the same environment as the move about by wind currents within the cloud.

Aggregation and Accretion

Continued grow of hydrometeors is accomplished by processes known as **aggregation** and **accretion**.

Aggregation occurs within the colder regions of a cloud when two snow or ice crystals collide and join to create a larger hydrometeor. An example of aggregated snowflakes is shown in Figure 10.11a. The process is more likely to occur in higher humidity cloud environments where liquid water on the surfaces of the crystals will freeze and weld the two frozen hydrometeors.

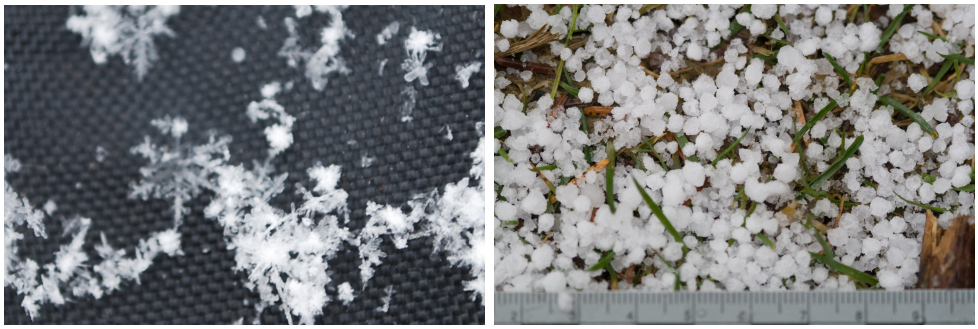

(a) Snowflake aggregation (b) Graupel

Figure 10.11: Aggregation and Accretion.

The process of accretion is more likely to occur in the warmer regions of the cloud. In this instance, supercooled cloud droplets strike a frozen hydrometeor and may freeze on contact to increase the frozen H_2O mass. In some instances, the liquid water does not freeze, and a mushy liquid surface form that surrounds the frozen center. This type of hydrometeor is known as **graupel** and is depicted in Figure 10.11b.

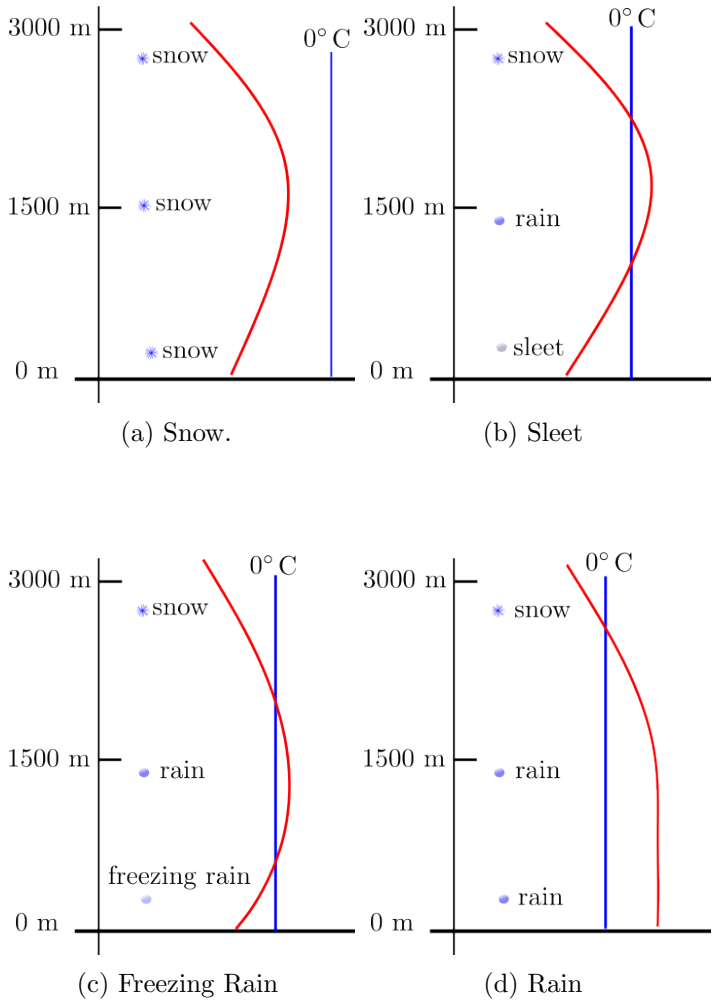

Figure 10.12: Temperature profiles for precipitation types.

10.6 Precipitation Profiles

The type of precipitation at the surface will depend on the vertical temperature profile. Profile for four precipitation types are shown in Figure 10.12.

Note that in all cases, the precipitation begins as snow at an elevation of 3000 m or greater. The profile for snow is shown in Figure 10.12a. In this case, the atmospheric temperature throughout the 3000 meter depth remains well below the freezing mark of 0°C.

Sleet forms when the original snowflake falls though a warm layer that is deep and warm enough to melt the snowflake to form a small rain drop. However, the atmospheric temperature profile closer to the surface of the Earth falls below freezing with a sufficient depth to freeze the droplet to form sleet before it reaches the surface. This type of profile is commonly associated with an advancing warm front of an MLC.

The freezing rain profile of Figure 10.12c has a near-surface layer that is below freezing but not sufficiently cold or thick enough to cause the rain droplet, formed in the above freezing layer, to completely freeze before reaching the round. The liquid droplets are frequently supercooled, and will freeze on contact with any surface. Freezing rain is part of an ice storm that causes slick driving and walking surfaces. Additionally, the ice buildup on power lines and tree branches can cause them to break and fall.

Exercises

10.1 Explain why it is unlikely for a cloud droplet to form in a homogeneous manner.

10.2 Why is it true that no two snowflakes are the same even if they originate in the same cloud.

10.3 Identify at least three different cloud constituents. Explain what characteristics differentiate them. Explain any similarities they may have.

10.4 Suppose two warm cloud droplets have radii of r_1 and r_2, respectively. Describe how these values determine the likelihood they will coalesce upon collision.

10.5 Explain why the saturation vapor pressure over mass of water with a curved surface is greater than the saturation vapor pressure of an equal volume of water at the same temperature but over a flat surface.

10.6 Explain how the solute process enhances the initiation of warm cloud droplet nucleation.

10.7 Explain two important aspects of the Bergeron Process.

10.8 Explain how the environmental vertical temperature profile contributes to the type of precipitation observed at the Earth's surface.

10.9 Explain why an advancing warm front may result in a sequence of changing precipitation type. What would be a typical order in the sequence of precipitation type?

10.10 Explain how the environmental vertical temperature profile contributes to the occurrence of an ice storm.

Chapter 11

Thunderstorms

11.1 Overview

Thunderstorms are convection-based storms with lightning and thunder. Convection is the result of warmer, less dense parcels rising above cooler, more dense parcels. Although there are characteristics that distinguish one type of thunderstorm from another, the predominant, common feature any variety is the convective thunderstorm **cell**.

Thunderstorm development requires an atmosphere that is, at least, conditionally unstable. Conditional instability requires moisture condensation. Consequently, thunderstorms develop in relatively moist atmospheres. However, even in a conditionally stable atmosphere, thunderstorm development may require a triggering feature such as warm or cold front movement, an orographic feature (such as a mountain), or an upper-level shortwave.

Severe Thunderstorms

Severe thunderstorms are characterized by at least one of the following:

- hail of at least three-quarter inches in diameter
- surface wind gusts of at least 50 $\text{mi} \cdot \text{hr}^{-1}$
- tornado development

Severe thunderstorm develop in an environment with significant **convective available potential energy** (CAPE) and **wind shear**, the change in wind speed or direction with a change in position. In the case of thunderstorms, vertical wind shear - the change in wind speed or direction with height is the important factor.

Convective Available Potential Energy

Convective available potential energy (CAPE) is, roughly, a measure of the difference in the the rising parcel's temperature and the environmental temperature, as indicated in

Figure 11.1a and the region labeled "CAPE area." Equation 11.1 provides the means for transforming the CAPE area from a sounding to a value for CAPE.

$$\begin{aligned} CAPE &= \frac{g}{T_e} \cdot \text{CAPE area} \\ &= \sum_{n=1}^{N} \frac{g}{T_e} (T_p - T_e)_n \cdot \Delta z_n \end{aligned} \tag{11.1}$$

In the equation, g is the acceleration due to gravity, T_p is the rising parcel's temperature, and T_e is the environmental temperature. Geometrically, the area between the T_p and T_e profiles in Figure 11.1a is calculated in N incremental steps with the area in each step given by the product of the width $(T_p - T_e)_n$ and height of Δz_n.

Equation 11.1 gives CAPE values with units of Joules per kg. The kinetic energy, in Joules, of a mass m moving with speed v is $\frac{1}{2}\text{m}\cdot\text{v}^2$. Equating $m \times$ CAPE with $\frac{1}{2}\text{m}\cdot\text{v}^2$ results in Equation 11.2 for the speed of the parcel when it reaches the equilibrium level (EL) as shown in Figure 11.1a

$$\begin{aligned} \frac{1}{2} \cdot m \cdot v^2 &= m \cdot CAPE \\ v^2 &= 2 \cdot CAPE \\ v &= \sqrt{2 \cdot CAPE} \\ \text{parcel speed at the EL} &= \sqrt{2 \cdot CAPE} \end{aligned} \tag{11.2}$$

One way to understand the significance of this measure is that the greater the difference in the temperatures, the greater the difference in parcel density. The greater the difference in density, the greater the buoyant force on the rising parcel. The greater the the buoyant force, the greater the speed of the rising parcels.

Vertical Wind Shear

Figure 11.1b shows the plot of wind speed and direction at elevations of 1-6 km with readings taken from a weather station sounding. The data show that both the wind speed (measured in $\text{m}\cdot\text{s}^{-1}$) and direction (measured in degrees in a counter-clockwise direction with the easterly direction have degree measure of zero) change with as the elevation changes from the surface of the Earth ($z = 0$). Not surprisingly, the wind speed increases with elevation.

11.2 Single Cell Life Cycle

The single cell thunderstorm is also known as an **ordinary thunderstorm**. The single cell has distinctive stages within its life cycle, and they are described in this section.

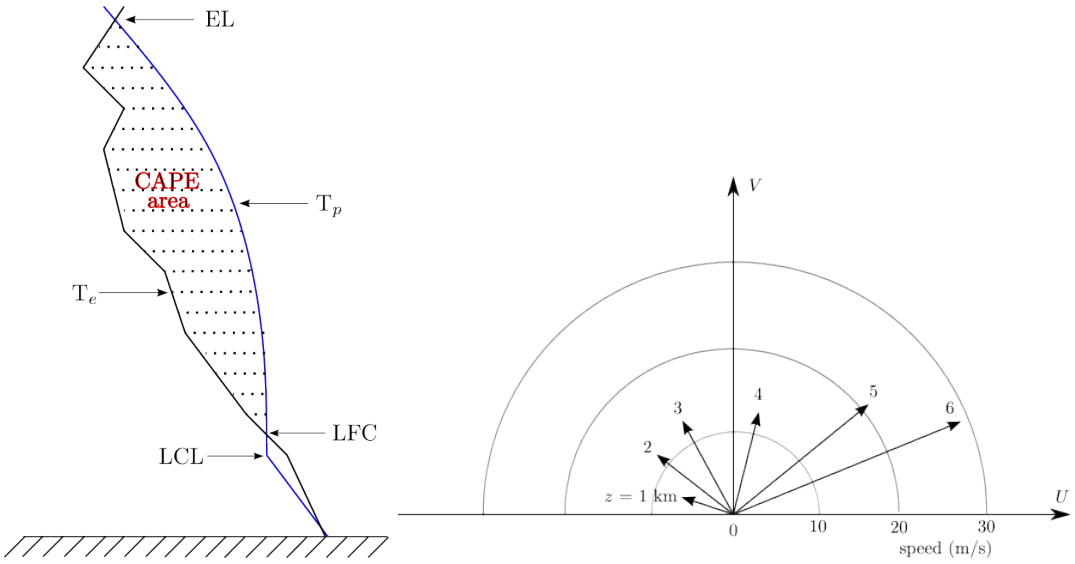

(a) The CAPE area. (b) Vertical wind shear.

Figure 11.1: Cape and Vertical wind shear.

11.2.1 Developing Stage

The development stage has moist air parcels lifted sufficiently high to reach a level where the parcel's temperature has cooled enough so that the H_2O vapor begins to condense and a shallow cumulus cloud is visible. (This cumulus cloud development is the reason this stage is also referred to as the **cumulus stage**.)

Entrainment of drier air parcels may inhibit the growth of the cumulus cloud as the parcels rise to higher levels. However, the earlier parcels attempts will moisten the vertical path for following parcels and the cloud will continue to increase its vertical extent.

As more latent heat is released by condensation, a significant updraft is formed within the cumulus cloud that powers the rising motion to altitudes with temperature as cold as -15°C. The warm updrafts of this stage are indicated by the red arrows in Figure 11.2a. The cold temperatures at this elevation means the cold has mixed environment where both supercooled cloud droplets exist with ice crystal an water vapor.

The strength of the warm updrafts create the clearly defined, firm edges of the cumulus cloud as depicted in Figure 11.2b. The cloud is said to have a cauliflower look created by the multiple and firm updraft turrets.

The vertical extend of the cloud now has the potential to harbor both the warmer region collision-coalescence process and the colder region Bergeron process. Consequently, both liquid and frozen hydrometeors will eventually gain enough mass so that the force of gravity will be stronger than the lift caused by the strong updraft(s). They will begin to

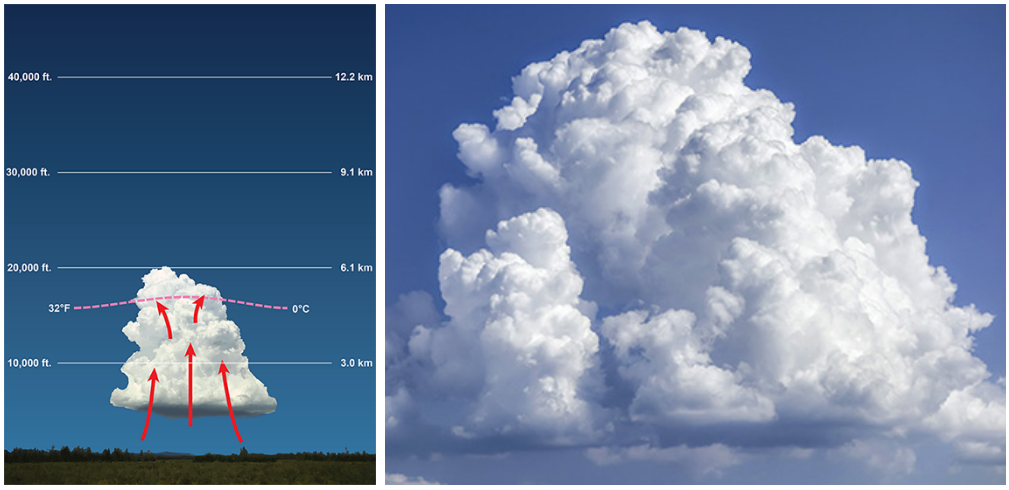

(a) Cross-section view. (b) Photograph.

Figure 11.2: Single cell in its development stage.

fall and create a downdraft, and that marks the time in the thunderstorm's life cycle when it transitions to its mature stage.

11.2.2 Mature Stage

The beginning of the single cell thunderstorm **mature stage** is marked be the beginning of the downdraft, as depicted by the blue arrows shown in Figure 11.3a. The **anvil top**, as shown in Figure 11.3b is another defining feature of this stage in the life cycle. Updraft(s) remain throughout the mature stage, ut it (they) weaken as the downdraft(s) begin and eventually dominate.

In addition to the anvil top, the upper portion of the cloud loses its firm edges (the cauliflower look) as the updraft(s) weakens. The weaker updrafts result in loss of warm air at the upper elevations and the cloud begin to glaciate (turn to ice), thus creating the fuzzier, wispier look.

The downdraft(s) that form may be powered by more than the force of gravity on the large hydrometeors. The relative low pressure created by the sinking motion, in conjunction with turbulent mixing, will entrain drier are within the down draft causing some of the liquid hydrometeors to evaporate. The heat of vaporization is drawn from the air in the downdraft, thus causing the parcel temperature to cool. The cooling leads to greater parcel density and negative buoyancy. Consequently, the entrainment of dry air will accelerate the downward speed of the downdraft parcels.

At the surface, the downdraft with ts cold air will create a localized cold front as shown in Figure 11.3a as the blue curve with the triangle pips. This is also referred to as the

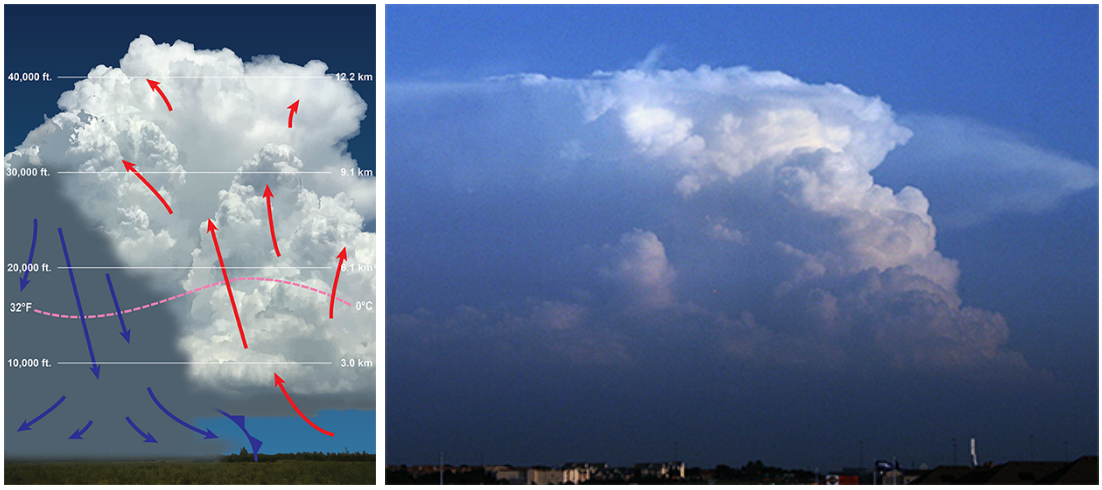

(a) Cross-section view. (b) Photograph.

Figure 11.3: Single cell in its mature stage.

thunderstorm **gust front**. The speed and strength of the front is determined by the relative coolness of the downdraft and its speed. Te straight-line winds can exceed 50 mi $\cdot$ hr^{-1}, therefore meeting the criteria of a severe thunderstorm.

In theory, the downdraft cold air (called the **cold pool**) will spread out in all directions once it reaches the Earth's surface. However, the greatest portion of the cold pool, as well as the greatest wind associated with the gust front, will be in the direction of motion of the thunderstorm. The precipitation that created the downdraft, that creates the gust front, will occur once the front has passed a given location.

11.2.3 Dissipating Stage

The **dissipating stage** begins when the thunderstorm no longer has a defined updraft. The updraft is the source of moisture and energy for the storm. As the gust front and its associated cold pool expand its reach on the Earth's surface, it will separate the cell from any updraft effectively cutting of the cells energy and moisture source.

The moderate to heavy rainfall means the cloud "rains out" and begins to shrink from the ground up. Eventually, the precipitation will cease and the cell's life cycle ends. The entire life cycle maybe time as short as an hour to as long as two hours.

Single cell thunderstorms exist in an environment of low vertical wind shear. That is, an environment where the wind speed does not significantly increase with an increase in altitude. Multicellular thunderstorms, ones with a series of cells that develop in time, develop in environments of moderate wind shear.

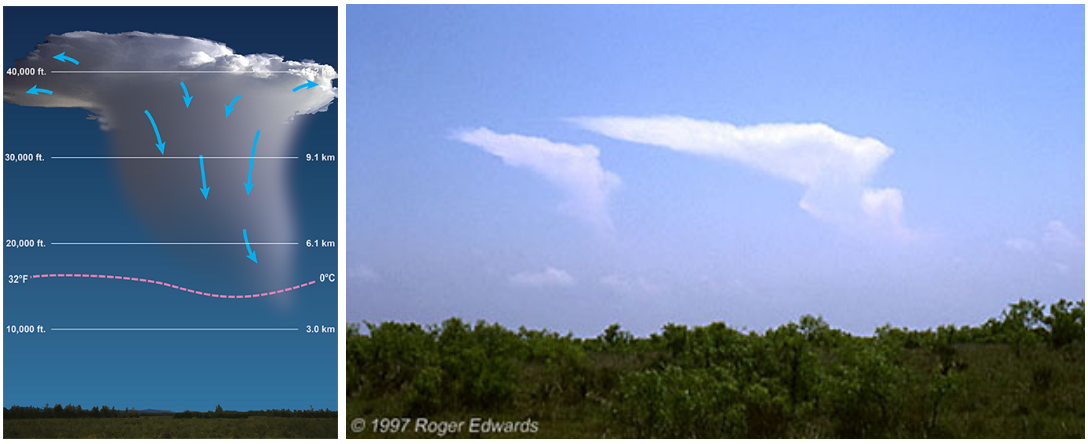

(a) Cross-section view. (b) Photograph.

Figure 11.4: Single cell in its dissipating stage.

11.3 Multicellular

Single cell thunderstorms exist in an environment of low vertical wind shear. That is, an environment where the wind speed does not significantly increase with an increase in altitude. Multicellular thunderstorms, ones with a series of cells that develop in time as shown in Figure 11.5, develop in environments of moderate wind shear.

Figure 11.5: Multicellular thunderstorm in the early evening.

Figure 11.6 diagrams the situation where the dissipating storm's cold pool may interact with the environmental vertical wind shear to successfully develop a subsequent thunder-

storm cell.

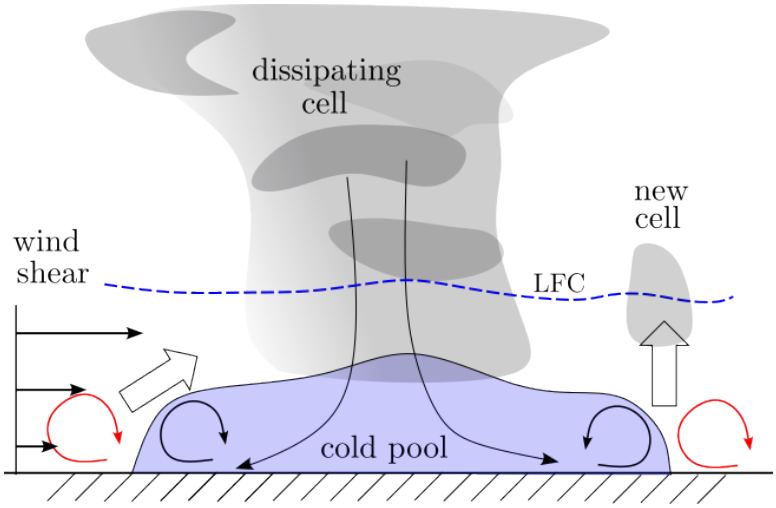

Figure 11.6: Cold pool interaction with vertical wind speed shear.

11.4 Supercells

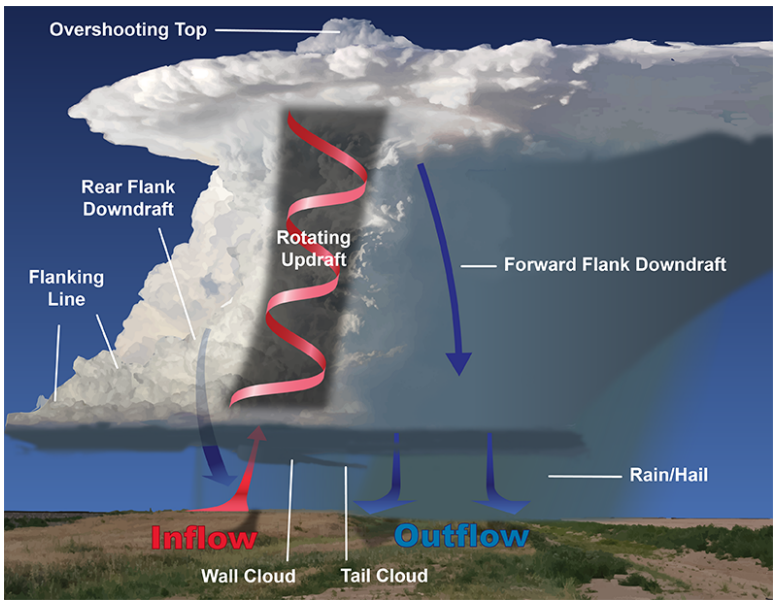

Figure 11.7: The gravitational force on an atmospheric parcel.

11.4.1 Mesocyclone

The two important radial forces that act on the parcel as it follows a circular path of constant radius R around the center of the mesocyclone (mesolow) are the outward-pointing centrifugal force and the inward-pointing pressure gradient force. These forces are shown in Figure 11.8a. The Coriolis effect is small in this scenario, so it is not included in the sum of forces.

The mesolow forms as the rotating air parcels are pulled outward from the center by the outward-pointing centrifugal force. In response, the inward pointing pressure gradient force increases until its magnitude is equal to that of the centrifugal force.

The outward direction is taken as positive in the polar coordinate system. The radial forces are in balance because the radius of the parcel's path is constant ($r = R$). Therefore,

$$\frac{1}{\rho}\frac{\Delta P}{\Delta r} = \frac{V^2}{R} \tag{11.3}$$

Equation 11.3 is known as the **cyclostrophic equation**, and the radial forces on the parcel are said to be in cyclostrophic balance. The angular speed of the parcel is denoted by V. The parcel's angular direction of motion can be either clockwise or counter-clockwise depending on the environmental circumstances that initiates the circular motion.

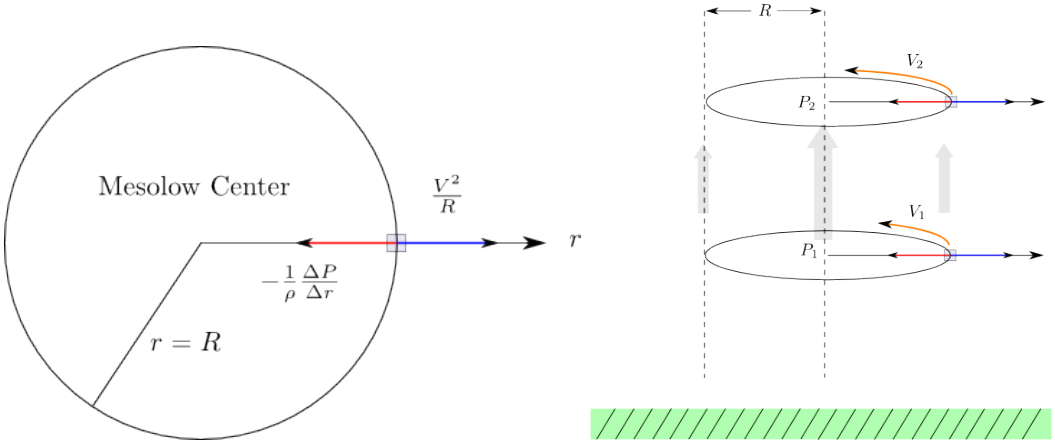

(a) Significant radial forces. (b) Circulation at different altitudes.

Figure 11.8: Supercell mesocyclone.

The dynamics of the mesolow work to enhance the updraft strength and longevity through the development of a vertical pressure gradient. The idealized, three-dimensional mesolow is depicted in Figure 11.8b with a uniform radius R throughout its depth. The lower level of the cylinder is closer to the surface and the increased friction influence will result in speed V_1 being less than V_2. The uniform cylinder radius means that $\frac{\Delta P_1}{\Delta R}$ is less

than $\frac{\Delta P_2}{\Delta R}$. A greater pressure gradient at level 2 means that the drop in central pressure P_2 at level 2 must be greater than the drop in central pressure P_1 at level 1. Consequently, the vertical drop in pressure at the center of the low is greater than the "normal" drop at the perimeter of the mesolow cylinder, creating an enhanced updraft at the center of the mesolow.

(a) Supercell shelf cloud. (b) Supercell overshooting top.

Figure 11.9: Supercell characteristic features.

Mesocyclone: Spinning Vortex Tube

A hodograph of wind data collected at a balloon launch site is made by first plotting the wind vectors at the elevations of 1,2,3,4,5, and 6 kilometers, as shown in Figure 11.10a. The wind at the 1 km height is from the east-southeast at about 5 m/sec. The wind at the 2 km elevation is from the southeast at a speed of approximately 11 m/sec. The wind at the 6 km elevation is southwesterly at a speed of approximately 28 m/sec. The vertical wind shear pattern depicted on this chart is typical for the Midwest during "thunderstorm season.". When the wind vectors turn clockwise with height as in this case, the wind is said to "veer" with height. If the wind vectors turn counterclockwise with height, they are said to "back" with height.

The next step in constructing the hodograph is the connect the tips of the wind vectors with a straight line segment as shown in red in Figure 11.10b. Connecting the tips of the vectors shows the clockwise bend to the wind vectors with height.

The storm direction is determined by the average velocity and is represented by the $\vec{u}'$ vector in Figure 11.10c. New coordinates are drawn to represent "storm relative coordinates." The blue vectors shown the storm relative environmental wind vectors at the elevations of 2, 3, 4, and 5 km. Vectors $\vec{v}_2$ and $\vec{v}_3$ are labeled because they are used to determine the magnitude of the storm relative vertical wind shear given by $\Delta u/\Delta z$ that

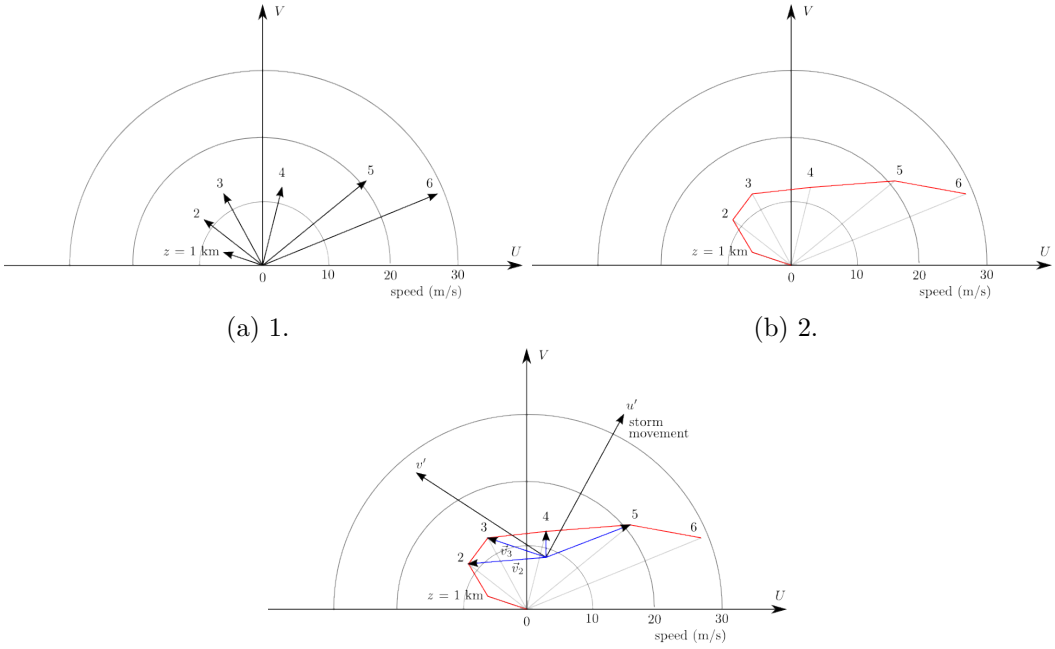

(a) 1.

(b) 2.

(c) 3.

Figure 11.10: Hodographs .

translates into the stream-wise vorticity with a horizontal axis aligned with the lower-level flow stream into the developing cell.

Figure 11.11 shows how the vertical wind shear given by vectors $\vec{v}_2$ and $\vec{v}_3$ generates vorticity in the vertical plane perpendicular to the horizontal inflow stream near the surface. If this stream is lifted by a convective cell, the horizontal vorticity axis is transformed into a vertical axis.

11.5 Tornadoes

Figure 11.12 depicts the relations between the supercell tornado and the forward and real flank downdrafts.

11.6 Cells in Clusters

11.7 Cells in Lines

The very thin line of thunderstorms in June of 2008 is shown in Figure 11.13.

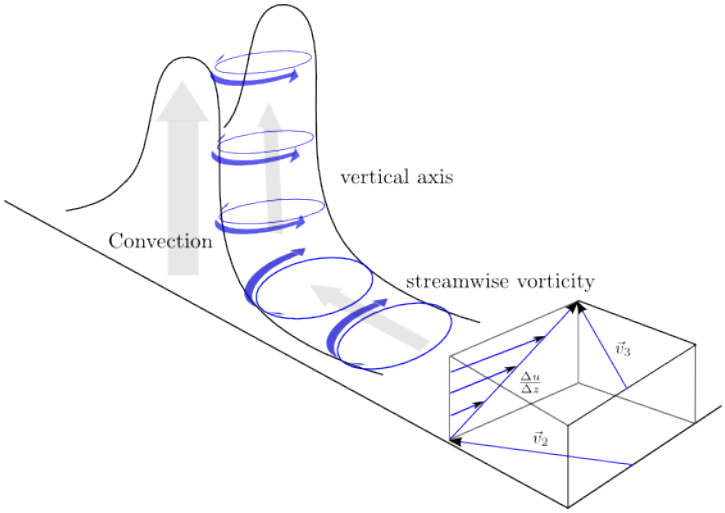

Figure 11.11: Vertical wind shear translates to stream-wise vorticity..

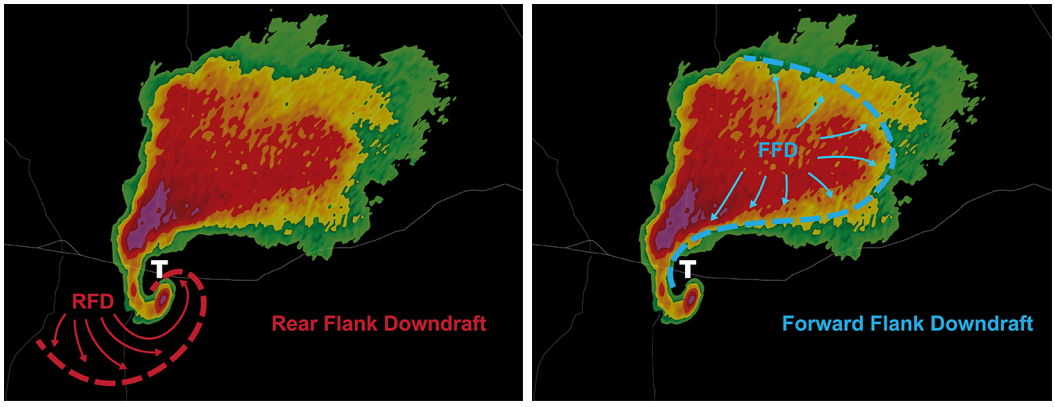

(a) Rear flank downdraft. (b) Forward flank downdraft.

Figure 11.12: Supercell tornadoes.

11.7.1 Bow Echo

Bookend vorticities are evident in Figure 11.15.

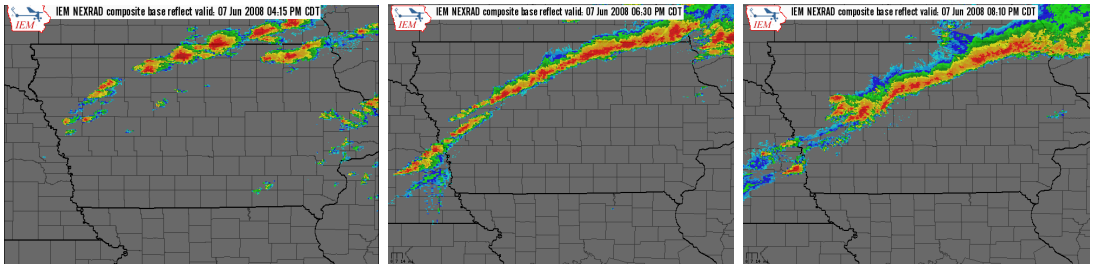

(a) 1. (b) 2. (c) 3.

Figure 11.13: North Iowa line of thunderstorms.

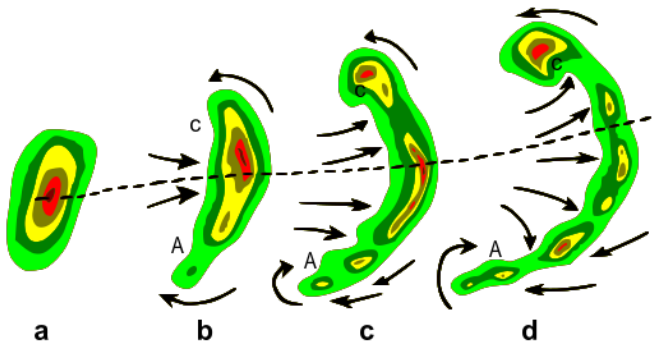

Figure 11.14: Bow echo evolution

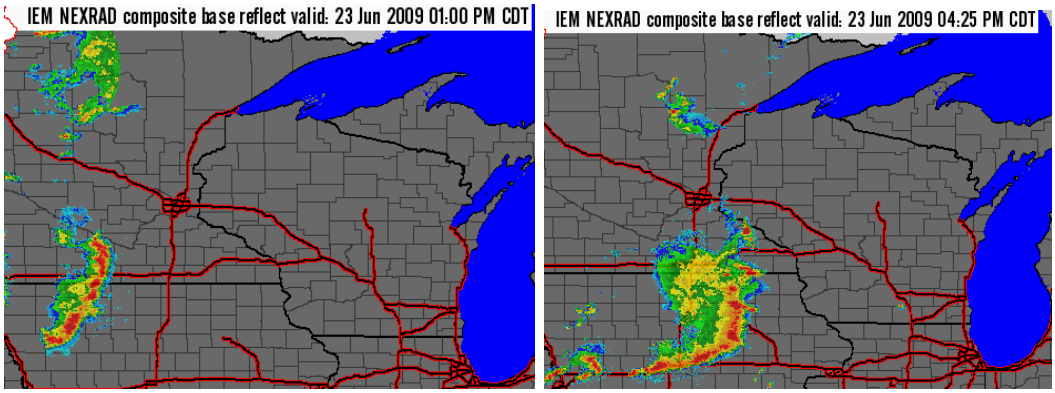

(a) 1. (b) 2.

Figure 11.15: Iowa bow echo.

11.8 Lightning & Thunder

11.8.1 Charge Separation

Convective Charging

The process of convective charging is illustrated in the panels of Figure 11.16.

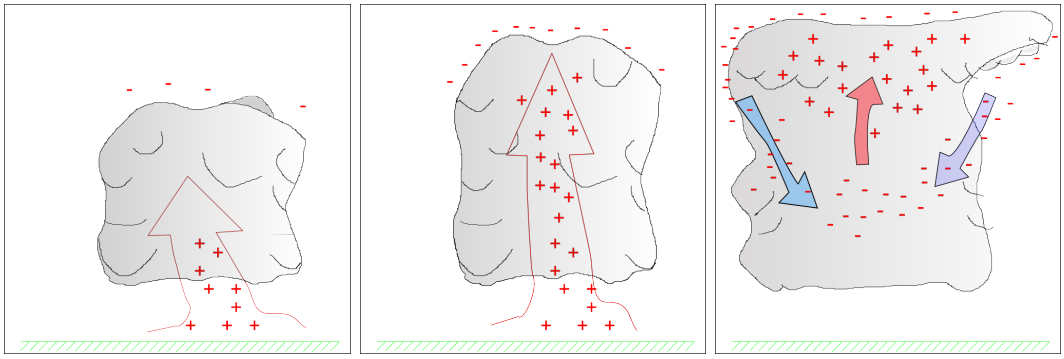

(a) 1. (b) 2. (c) 3.

Figure 11.16: Convective Charging.

positive ions are the predominant type near the earth's surface, the ratio of positive to negative ions is approximately 1.2, so the first panel shows a collection of positive ions (a net positive charge) near the surface of the earth that is swept up into the developing cumulus cloud in the early development stages

convective updraft carries the net positive charge into the forming cloud and, eventually, lifts the positive ions to the very top of the cloud

the positive area within the cloud's updraft causes a negative ion "curtain" to form on the top and side boundaries of the cumulus cloud, as shown in the second figure

entrainment of the net negatively charge environmental parcels form much of the cloud's downdraft, therefore creating the negatively charged lower portion of the cloud

many investigators have found qualitative and quantitative discrepancies between this theory and observation (Chiu and Klett, 1976; Latham, 1981; Williams ¡e¿et al.¡/e¿, 1989)

Inductive Charging: Ion Capture

The process of ion capture in inductive charging is illustrated in the panels of Figure 11.17.

earth electric field induces charge separation within the individual cloud constituents– negative on the top and positive on the bottom

as the cloud constituent falls through the cloud, it attracts free negative ions to the bottom surface, but positive ions can not "catch up" to the constituent to attach to the top

the net negatively charged cloud constituents migrate to the lower, warmer region of the cloud

removing the attached negative ions from the higher, colder region of the cloud leaves a net positive charge near the top of the cloud

theory produces the correct polarity, but is found to be effective only under weak electric fields, so is quantitatively unrealistic

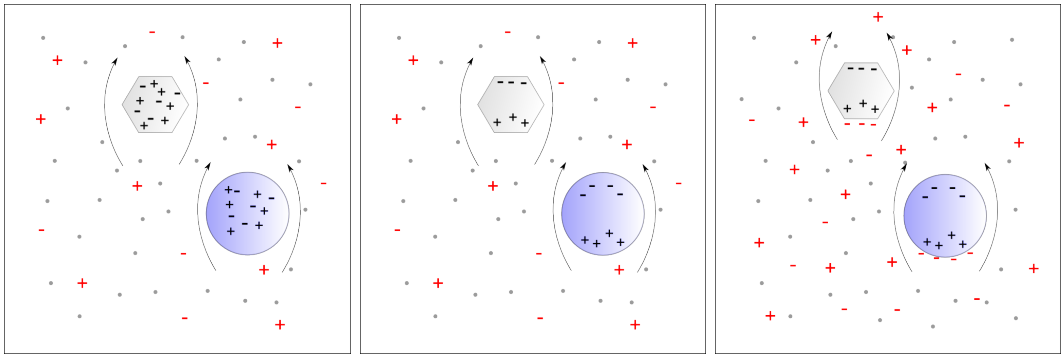

(a) 1. (b) 2. (c) 3.

Figure 11.17: Inductive charging: ion capture.

Inductive Charging: Particle Rebound

The process of particle rebound in inductive charging is illustrated in the panels of Figure 11.18.

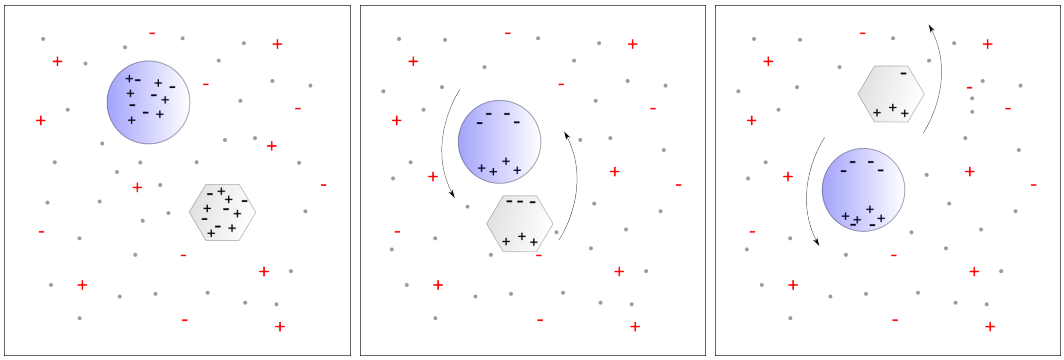

(a) 1. (b) 2. (c) 3.

Figure 11.18: Inductive charging: particle rebound.

charge separation by charge migration within individual cloud particles due to the earth's electric field

negative charge on the top, positive charge on the bottom

larger, faster falling particle and a smaller particle collide

net positive charge transferred to the smaller particle because the larger particle has greater surface area, net negative to the larger, warmer particle

¡li¿heavier, negative particle falls to the bottom of the cloud, positive, lighter particle is lifted to the top of the cloud

one problem (of several) with this theory is the assumption that the collision angle

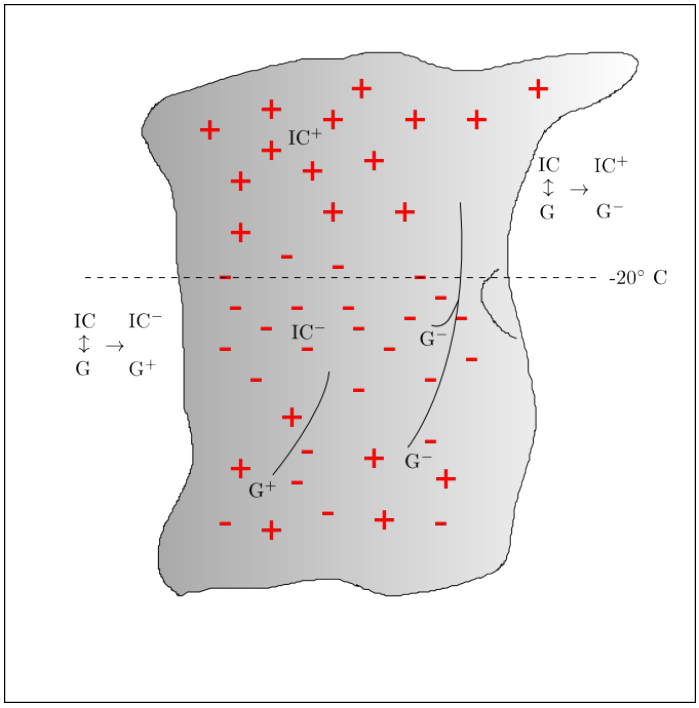

Figure 11.19: Riming electrification.

is such that positive and negative surface regions of the respective hydrometeors actually collide

Non-Inductive Charging: Thermometric Effect

laboratory experiments show that when a hail pellet collides with an ice crystal having a colder temperature, the hail/graupel becomes charged

caused by the temperature gradient at the point of contact

H+ ions travel faster in the ice lattice than the OH- ions, so a net positive charge transfer to the colder ice particle

this process requires impact velocities and temperature differences that are unlikely in cloud environments

Non-Inductive Charging: Riming Electrification

The process of riming electrification is depicted in Figure 11.19.

substantial electric charge can be deposited on riming graupel in a collision with an ice crystal in a cloud with super-cooled water vapor present

Magnitude and sign of the electrification are a function of temperature and cloud water content (CWC). Collision of graupel (G) and ice crystals (IC) at temperatures less than -20 degrees C results in a negative charge transfer to the graupel (G^-) that falls to lower regions of the cloud. The lighter, positive charged ice crystals (IC^+) remain in the higher reaches of the cloud. In warmer environments (middle cloud height), the collision of graupel and ice crystals result in a positive charge transfer to the graupel (G^+) that ultimately fall to lower levels in the cloud. The negatively charged ice crystals (IC^-) remain in the mid-altitude of the cloud to reinforce the overall negative cloud charge in this region. The lower portion of the cloud is populated by both positively and negatively charged graupel, thus explaining the tri-pole pattern observed in many electrified clouds.

The magnitude of charge transfer decreases in higher moisture environments. This explains why more heavily moisture-laden ocean based clouds seem to produce fewer lightning strokes

considered by many researchers to be the major charging mechanism

promising theory, but it is not known why the collisions between ice crystals and graupel result in the charging behavior characteristics

11.8.2 Lightning

11.8.3 Thunder

Chapter 11 Exercises

11.1 A cumulus cloud environment has an LFC is 1000m and an EL is 9000m. If a thunderstorm CAPE is 2000 J/kg, how long will it take for a cumulus cloud to grow from the LFC to the EL?

11.2 It takes 20 minutes for a developing cumulus cloud to grow from the LFC to the EL. Estimate the environmental cape.

11.3 Answer both of the following.

(a) First question

(b) Second question

Chapter 12

Tropical Cyclones

12.1 Overview

Chapter 13

Weather Forecasting

Index